Functional role of C1Q-TNF related peptide 8 (CTRP8)-binding RXFP1 in brain tumors

By

THATCHAWAN THANASUPAWAT

A Thesis submitted to the Faculty of Graduate Studies of
The University of Manitoba
in partial fulfillment of the requirements of the degree of

DOCTOR OF PHILOSOPHY

Department of Human Anatomy and Cell Science
University of Manitoba
Winnipeg, Manitoba
Canada

TABLE OF CONTENTS

ABSTRACT

Glioblastoma (GB) is the most common and highly aggressive form of primary brain cancer which is usually fatal. The GB invasive phenotype and the development of treatment resistance are major challenges and the underlying mechanisms remain poorly understood. I identified the presence of relaxin family peptide receptor1 (RXFP1) and its novel ligand C1q-tumor necrosis factor-related peptide8 (CTRP8) in human GB cells and elucidate the functional role of this novel receptor-ligand system in cell migration and chemoresistance.

Primary and established GB cells expressed RXFP1 and the novel RXFP1 ligand CTRP8. Similar to relaxin (RLN2), CTRP8 increased intracellular cAMP levels and activated PI3K-PKC, and STAT3 pathways. This coincided with enhanced motility and production/secretion of cathepsin B, a marker of GB invasion. The resistance to the chemotherapeutic drug temozolomide (TMZ) is a common occurrence and a major cause for fatal outcome. TMZ induces methyl purine adducts which are repaired by the base excision repair (BER) pathway. Failure to repair the resulting single strand DNA break results in double strand DNA (dsDNA) breaks which are detected by γH_2AX at damaged DNA sites. In this study, I have investigated the potential role of RXFP1 in chemoresistance to the commonly used TMZ in human GB. Upon TMZ treatment, CTRP8/RLN2 mediated activation of RXFP1 was able to protect human patient GB cells from DNA damage and enhanced their survival. Activation of RXFP1 resulted in STAT3 pathway activation and the RXFP1- and STAT3-dependent up-regulation of proteins and their activity deemed important for TMZ-induced DNA repair. I identified the BER member N-methylpurine-DNA glycosylase (MPG), and anti-apoptotic factors Bcl-2 and

Bcl-XL as CTRP8/RLN2-RXFP1-STAT3 targets to mitigate TMZ-induced DNA damage and to increase GB cell survival.

High Mobility Group AT-hook protein 2 (HMGA2) is a non-histone chromatin protein which is a BER member containing AP/dRP lyase activity. I showed increased HMGA2 protein expression upon CTRP8/RLN2-RXFP1-STAT3 pathway activation. I observed that the presence of HMGA2 reduced TMZ-induced DNA damage as detected by γH_2AX. The knockdown of HMGA2 sensitized GB cells to TMZ and increased apoptosis. Dovitinib, (DOV) is a FDA-approved DNA minor groove binder agent. DOV enhanced TMZ sensitivity by downregulating key factors in single strand DNA repair, including MPG, HMGA2, APE1, and MGMT. Moreover, DOV inhibited phospho-STAT3^{Tyr705}-LIN28A which are upstream regulators of HMGA2. HMGA2 played an importance role to promote TMZ chemoresistance in GB cells. The sequential treatment with DOV and TMZ decreased in cell viability in GB cells.

My results indicate a novel role for the CTRP8-RXFP1 ligand-receptor system in STAT3-dependent cell invasion, TMZ chemoresistance, and survival in patient GB cells. I applied DOV to sensitize GB cells to TMZ-induced DNA damage to provide a new and attractive therapeutic target to improve TMZ efficacy in GB patients.

ACKNOWLEDGEMENTS

First and foremost, I would like to express my deepest gratitude to my supervisor Dr. Thomas Klonisch, Professor and Head, Department of Human Anatomy and Cell Science, for giving me the great opportunity to be in Winnipeg, study and be a part of your research team. I am very grateful for your advice, encouragement, motivation, guidance, understanding, patience, kindness and supporting. Thank you for continuously believing in me and pushing me to my limit to complete my work. Thank you again for everything Tom! And I will never forget your motto "Never ever give up".

I sincerely express my gratitude to Dr. Sabine-Hombach Klonisch. I am very thankful for advice, discussion, help, listening in scientific topic and my personal life. Thank you Sabine for being a great mentor!

I would like to thank my committee members, Dr. Jerry Krcek, Dr. Marc Del Bigio, Dr. Hugo Bergen and Dr. Donald Miller for their advice, guidance and support throughout my studies. I would like to further thank to Dr. Laura Parry for being my external examiner and her valuable comments and suggestions.

I would like to thank neurosurgeons, Dr. Jerry Krcek and Dr. Jason Beiko, and neuropathologists, Dr. Marc Del Bigio, Dr. Sherry Krawitz, and Dr. Kant Matsuda for providing patient brain tumor samples and providing pathology diagnostic, and Dr. Marshall Pitz, neuro-oncologist, for doing clinical database management.

My heartfelt thanks to Dr. Aleksandra Glogowska for being a great partner. Thank you for your help for the experiments. Thank you for your valuable and continuous advice, and support. Thank you Aleks.

I extend my thank to my lab members. My special thanks to Dr. Suchitra Natarajan for helping me in HMGA2-related work. Thank you to past and present members, Adrain, Manoj, Dana, Farhana, Forouh, Idunnu, and Aditya for a great friendship. Thank you for a good team and making the lab fun and enjoyable. I have a great time and with you guys.

I would like to further thank you the Department of Human Anatomy and Cell Science, especially Jennifer Genest, Jacki Armstrong, Nadine Persaud, and Roberta Van Aertselaer for all their support and helping me through my studies.

My special thanks to Usakorn and Narisorn who came together with me from Thailand. Thank you for continuous supported, helped, and stayed together. It was a great time to have you with me here.

To my family, Mom and Dad, thank you for your warm love, support, understanding, listening, believing and always being with me. Thank you for your skype calling, seeing your faces makes me feel like I am home and never be lonely. To my brother, Chaiyos and my sister, Kankanit thank you for being good kids and taking care of Mom and Dad when I am far away from home.

To my extend family, thank you everyone for all your wonderful love, support and believing in me. Special thanks to my aunt, Wanpen for helping everything as I request.

To my Grandpa, this work is dedicated to you. I know you really wanted to see my degree. I am very sorry that I cannot bring it to show you. But now I believe you know that I did it and you are pround of me.

Finally, thank you everybody who helps and supports me throughout my studies.

LIST OF TABLES

LIST OF FIGURES

LIST OF ABBREVIATIONS

AAG	3-alkyladenine DNA glycosylase
AC5	adenylyl cyclase 5
AIC	4-amino-5-imidazole-carboxamide
AKAP79	a-kinase-anchoring protein 79
AKT	protein kinase B or serine/threonine kinase
ALDH	aldehyde dehydrogenase
aPKCs	atypical PKC isoforms
AP site	apurinic/apyrimidinic abasic site
APE1	apurinic/apyrimidinic (AP) endonuclease 1
APNG	alkylpurine-DNA-N-glycosylase
ASCL1	achaete-scute family bHLH transcription factor 1
ATM	ataxia Telangiectasia Mutated kinase
ATR	ataxia Telangiectasia and Rad3-related kinase
Bak	bcl-2 homologous antagonist/killer
Bax	bcl-2-associated X protein
BBB	blood brain barrier
Bcl-2	B-cell lymphoma 2
Bcl-Xl	B-cell lymphoma-extra large
BER	base excision repair
BRET	bioluminescence resonance energy transfer
BSA	bovine serum albumin
C/EBP β	CCAAT enhancer-binding protein beta
cAMP	cyclic 3′–5′ adenosine monophosphate
Cath	cathepsin
CBTRUS	Central Brain Tumor Registry of the United States
CDKN2A	cyclin dependent kinase inhibitor 2A
cDNA	complementary deoxyribonucleic acid
cGMP	cyclic guanosine monophosphate
CHI3-L	chitinase 3-like protein 1
CHK1	checkpoint Kinase1

CHO-K1	chinese hamster ovary cells
CI	cell index
CNS	central nervous system
cPKCs	conventional PKC isoforms
CRE	cAMP-response element
CRF	C1Q-related factor
CTNND2	catenin delta 2
CTRP	complement C1Q tumor necrosis factor (TNF) related protein
DAB	3,3'-Diaminobenzidine
DAPI	4',6-diamidino-2-phenylindole
DCX	doublecortin
DDR	DNA damage response
dI	deoxyinosine
DLL3	delta-like 3
DME/F12	Dulbecco's Modified Eagle's medium and F-12
DNA pol β	DNA polymerase beta
DNA	deoxyribonucleic acid
DOV	dovitinib
dRP	deoxyribose-1-phosphate
ECL	chemiluminescence substrate
ECL2	extracellular loop 2
ECM	extracellular matrix
EGFR	epidermal growth factor receptor
EGFRvIII	epidermal growth factor receptor variant III
eNOS	endothelial nitric oxide
ERK1/2	extracellular signal-regulated protein kinases 1 and 2
EXO1	exonuclease 1
FACS	fluorescence-activated cell sorting
FBS	fetal bovine serum
FDA	Food and Drug Administration
FGFR	fibroblast growth factor receptor

FHIT	fragile histidine triad
GABRA1	gamma-aminobutyric acid A receptor, alpha 1
GAPDH	glyceraldehyde 3-phosphate dehydrogenase
GB	glioblastoma
G-CIMP	glioma-CpG island methylator phenotype
GPCR	G-protein coupled receptor
HA	normal human astrocyte cells
HCC	hepatocellular carcinoma
HEI10	human enhancer of invasion 10
HEK293	human embryonic kidney cells 293
HeLa	human cervical cancer cells
HepG2	human liver cancer cells
HMG	high mobility group
HMGA	high mobility group AT-hook protein
HUVEC	human umbilical vein endothelial cells
IC_{50}	half maximal inhibitory concentration
ICL3	intracellular loop 3
IDH	isocitrate dehydrogenase
IGFBP2	insulin-like growth factor binding protein 2
IgG	immunoglobulin G
IL6	interleukin 6
iNOS	inducible nitric oxide synthase
INSL	insulin/relaxin-like peptides
JAK	janus kinase
LDL-A	low-density lipoprotein class A
LGR	leucine-rich repeat containing G protein-coupled receptor
LIN28A	lin-28 homolog A
LNCaP	human prostate adenocarcinoma cells
LOH	loss of heterozygosity
LPS	lipopolysaccharides
LRR	leucine-rich repeat

MAPK	mitogen activated kinase-like protein
MCF-7	human breast ER and PR positive cancer cells
MCl-1	myeloid leukemia cell 1
MDA-MB231	human breast triple negative cancer cells
MERTK	c-mer proto-oncogene tyrosine kinase
MET	MET proto-oncogene, receptor tyrosine kinase
MGMT	O^6-methylguanine-DNA methyltransferase
miRNA	micro RNA
MMP	matrix metalloproteinase
MMR	DNA mismatch repair
MMS	methyl methanesulfonate
MPG	N-methylpurine DNA glycosylase
MSH	mutS homolog 2
MT1-MMP	membrane type 1-matrix metalloproteinase 1
MTIC	5-(3-dimethyl-1-triazen) imidazole-4-carboxamide
MUC1	mucin 1, cell surface associated
MX	methoxyamine
N^3-MeA	N^3-methyladenine
N^7-MeG	N^7-methylguanine
NEFL	neurofilament, light polypeptide
NET	netropsin
NF-κB	nuclear factor kappa-light-chain-enhancer of activated B cells
NHE	normal human endometrial cells
NKX2-2	NK2 homeobox 2
NO	nitric oxide
nPKCs	novel PKC isoforms
NSCLC	non-small-cell lung carcinoma
O^6-BG	benzylguanine
O^6-MeG	O^6-methylguanine
OLIG2	oligodendrocyte transcription factor 2
OSM	oncostatin M

OVLT	organum vasculosum of the lamina terminals
PAR1	protease activated receptor 1
PAR-6	partitioning defective-6
PARP1	poly (ADP-ribose) polymerase 1
PB1	Phox and Bem 1 domain
PBS	phosphate buffered saline
PC3	human prostate cancer cells
PCR	polymerase chain reaction
PDE4D3	cyclic AMP-dependent phosphodiesterase type D, variant 3
PDGFR	platelet-derived growth factor receptor
PDGFRA	platelet-derived growth factor receptor, alpha polypeptide
PEN	pentamidine
PI	propidium iodine
PI3K	phosphatidyl inositol 3 kinase
PKA	protein kinase A
PKC	protein kinase C
PMS2	PMS2 postmeiotic segregation increased 2, mismatch repair endonuclease PMS2
pre-miRNA	precursor miRNA
PTEN	phosphatase and tensin homolog
qPCR	quantitative Polymerase chain reaction
RAD51L1	rad51 homolog B
RET	RET proto-oncogene, RET receptor tyrosine kinase
rhCTRP8	recombinant human CTRP8
RHPN2	rhophilin Rho GTPase binding protein 2
rhRLN2	recombinant relaxin 2
RLN	relaxin
RNA	ribonucleic acid
RT	room temperature
RT-PCR	reverse transcription polymerase chain reaction
RXFP	relaxin family peptide

S100A4	S100 calcium binding protein A4
S100P	S100 calcium binding protein P
S1PR1	sphingosine-1-phosphate receptor 1
SDS	sodium dodecyl sulfate
SDS-PAGE	sodium dodecyl sulfate polyacrylamide gel electrophoresis
SFO	subfornical organ
SHP-1	Src homology region 2 domain-containing phosphatase-1
siRNA	small interfering RNA
SLC12A5	solute carrier family 12 potassium-chloride transporter member 5
SLUG	snail family transcriptional repressor 2
SMAD	SMAD family member
SNAIL	snail family transcriptional repressor 2
SNPs	single nucleotide polymorphisms
SOX	SRY (sex determining region Y)
STAT3	signal transducer and activator of transcription
SVZ	subventricular zone
SYT1	synaptotagmin I
TAZ	transcriptional co-activator with PDZ-binding motif
TBS	tris buffered saline
TCF	transcription factor
TCGA	The Cancer Genome Atlas
TGF-β	transforming growth factor beta
THP-1	human monocytic cells
TM	transmembrane
TMZ	temozolomide
TNBC	triple negative breast cancer
TNF	*t*umor necrosis factor
TWIST	twist family BHLH transcription factor 1
U251	glioma cells
UTR	untranslated region
VEGF	vascular endothelial growth factor

VEGFR	vascular endothelial growth factor receptor
WHO	World Health Organization
XRCC1	x-ray repair cross-complementing group 1
γH2AX	histone H2AX phosphorylation

LIST OF COPYRIGHTED MATERIALS

1. Copies of the permission letter of the publications below are attached at the end of this thesis as an appendix.

1.1 Glogowska, A., et al., 2013. C1q-tumor necrosis factor-related protein 8 (CTRP8) is a novel interaction partner of relaxin receptor RXFP1 in human brain cancer cells. J Pathol 231(4): 466-479

1.2 Kern, A., and G. D. Bryant-Greenwood. 2009. Mechanisms of relaxin receptor (LGR7/RXFP1) expression and function. Annals of the New York Academy of Sciences 1160: 60-66.

1.3 Louis, D. N., A. Perry, G. Reifenberger, A. von Deimling, D. Figarella-Branger, W. K. Cavenee, H. Ohgaki, O. D. Wiestler, P. Kleihues, and D. W. Ellison. 2016. The 2016 World Health Organization Classification of Tumors of the Central Nervous System: a summary. Acta Neuropathol 131: 803-820.

1.4 Ohgaki, H., and P. Kleihues. 2013. The definition of primary and secondary glioblastoma. Clin Cancer Res 19: 764-772.

2. The following publications are an open-access articles distributed under the terms of the Creative Commons Attribution License (CC BY). The use, distribution or reproduction in other forums is permitted, provided the original author(s) or licensor are credited and that the original publication in this journal is cited, in accordance with accepted academic practice.

2.1 Ozturk, N., I. Singh, A. Mehta, T. Braun, and G. Barreto. 2014. HMGA proteins as modulators of chromatin structure during transcriptional activation. Front Cell Dev Biol 2: 5.

2.2 Ramirez, Y. P., J. L. Weatherbee, R. T. Wheelhouse, and A. H. Ross. 2013. Glioblastoma multiforme therapy and mechanisms of resistance. Pharmaceuticals (Basel) 6: 1475-1506.

2.3 Thanasupawat, T., et al., 2015. RXFP1 is targeted by complement C1q tumor necrosis factor-related factor 8 in brain cancer**.** Front Endocrinol (Lausanne) 6: 127.

2.4 Thanasupawat, T., et al., 2017. Dovitinib enhances temozolomide efficacy in glioblastoma cells. Mol Oncol 11(8): 1078-1098.

CHAPTER 1: INTRODUCTION

1.1 Relaxin family peptide receptors (RXFPs)

Relaxin Family peptide receptors (RXFPs) are G protein couple receptors (GPCRs). RXFPs bind to their ligands, relaxin family peptides including relaxin-1 (RLN1), relaxin (RLN2), relaxin-3 (RLN3) (also known as INSL7), insulin-like peptide 3 (INSL3), and INSL5. The RXFP family contains four members which can be classified into two groups based on their structures and signaling properties. RXFP1 and RXFP2 contain an extensive extracellular leucine-rich repeat (LRR) region, whereas the extracellular domains of RXFP3 and RXFP4 are small. RXFP1-4 were originally named leucine-rich G protein coupled receptor 7 (LGR7), LGR8, GPCR135 and GPCR142, respectively. RXFP1 binds to RLN2 with high affinity but can also interact with RLN1 and RLN3 to activate signaling pathways. INSL3 is a cognate ligand for RXFP2. RXFP3 is activated by RLN3 and RXFP4 binds to INSL5 (Bathgate et al. 2006, Kong et al. 2010, Bathgate et al. 2013).

1.2 Relaxin family peptide receptor 1 (RXFP1)

1.2.1 Structural features of RXFP1

The structure of RXFP1 consists of three major parts: (i) an extracellular domain, (ii) a 7 transmembrane (TM) domain and (iii) a cytoplasmic domain of C-terminal tail **(Figure 1.1)**. The extracellular domain is divided into 10 leucine rich repeats (LRR) domains and a unique low density lipoprotein receptor type A (LDL-A) domain at the N-terminus. A unique cysteine rich LDL-A module is a specific structure in RXFP1/2 not observed in other GPCRs.

Figure 1.1 Structure of RXFP1 receptor.

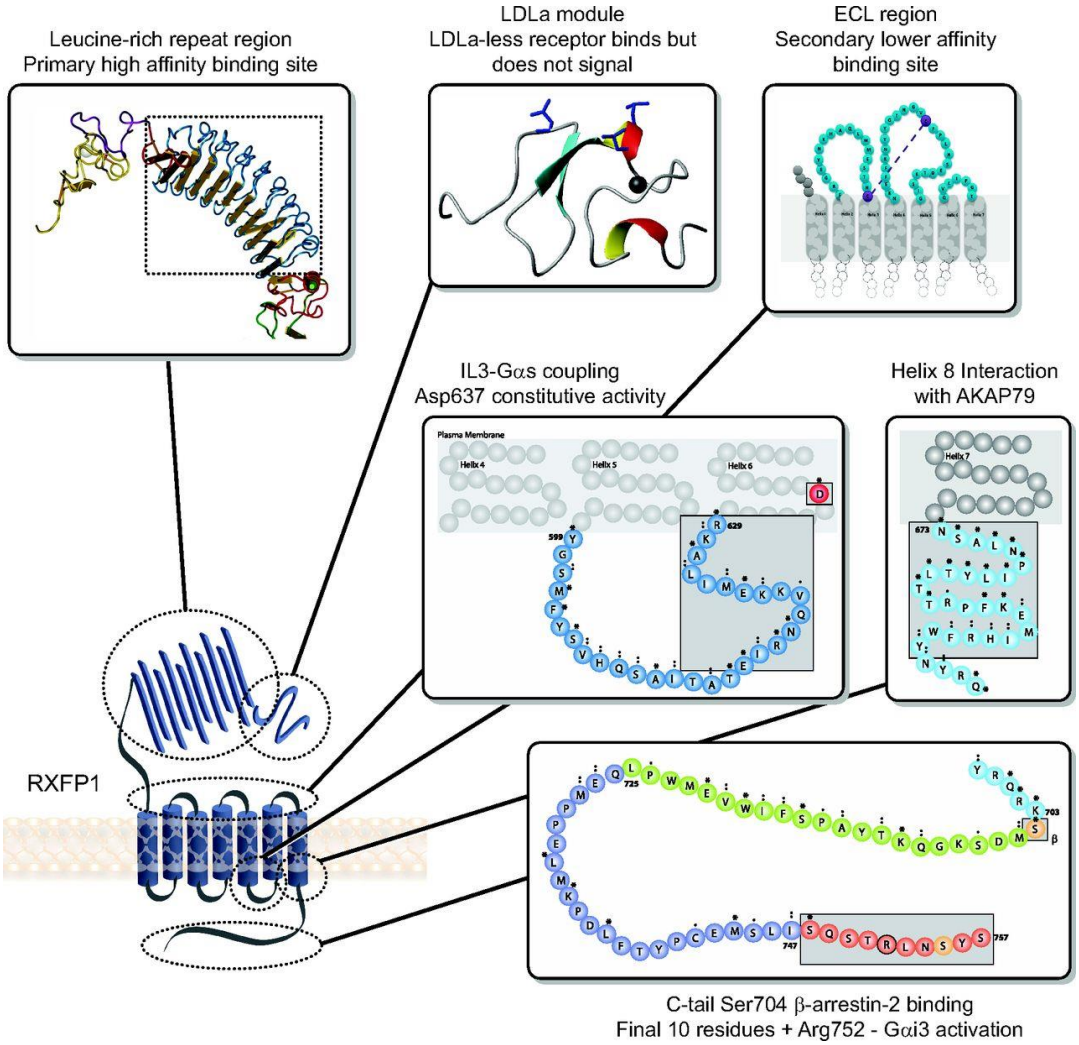

Figure 1.1 RXFP1 contains an extracellular domain with an unique LDLa module at N-terminus tail connects to LRR region and links to 7-TM domain. LRR region has a primary high-affinity binding site for RLN2 but the secondary low-affinity binding site is at ECL of TM domain. The LDL module and ICL are essential for signaling. C-terminal tail is important for protein-protein interaction in signalosome mechanism. Reprinted Bathgate, R. A., M. L. Halls, E. T. van der Westhuizen, G. E. Callander, M. Kocan, and R. J. Summers. 2013. Relaxin family peptides and their receptors. Physiol Rev 93: 405-480.

RLN2 can bind to RXFP1 with high affinity at two sites of the extracellular domain. The first binding site localizes at the LRR4-8 regions of RXFP1 and the second site is at the linker between LRR and LDL-A module. These binding sites stabilize and extend the helix conformation of the linker to allow both RLN2 and LDL-A module to bind to the extracellular loop 2 (ECL2) of the 7TM region in order to activate cell signaling (Sethi et al. 2016). The third intracellular loop (ICL3) couples to $G_{\alpha s}$ which increases cAMP accumulation. The constitutive active Asp637Tyr mutation in TM6 of RXFP1 results in ligand-independent signaling and increases cellular cAMP levels. The C-terminal tail domain is essential for signalosome formation which is specific to RXFP1. This domain also increases cAMP accumulation through the $G_{\alpha i3}$ signaling pathway. (Halls et al. 2006, Hopkins et al. 2007, Kern et al. 2007, Halls and Cooper 2010, Bathgate et al. 2013, Halls et al. 2015).

The RXFP1 gene is large and contains 18 exons and 17 introns. Hence, 29 variant splice forms have been described. Some variants are composed of only the extracellular or transmembrane domain (Scott et al. 2006, Kern et al. 2008). Some of these variants are expressed at the cell membrane but others are located in the ER (Muda et al. 2005, Scott et al. 2006). Most of these RXFP1 splice forms cannot bind to RLN2. The variants without LDL-A module are able to bind to RLN2 but cannot activate the signal (Scott et al. 2006) **(Table 1)**. Some variants function as antagonists to inhibit the activation of RXFP1 by RLN2 (Scott et al. 2005). There are three variants of RXFP1 that can form heterodimers with wild type RXFP1 and can activate cell signaling (Kern et al. 2008).

Construct of RXFP1	cAMP response	% of cell surface expression compared to WT RXFP1
WT	+	100
Deletion of LDL-A module	-	98±6.4
C47A/C53A (in LDL-A module)	-	102±17
D58E	-	96±9.1
LDL-A/LGR8	-	170±10.5
N36Q	+	37±7

Table 1. cAMP response and cell surface expression of RXFP1 splice variants.

Mechanisms of relaxin receptor (LGR7/RXFP1) expression and function. Annals of the New York Academy of Sciences 1160: 60-66. Adapted from Kern, A., and G. D. Bryant-Greenwood. 2009. Mechanisms of relaxin receptor (LGR7/RXFP1) expression and function. Annals of the New York Academy of Sciences 1160: 60-66, with permission from John Wiley and Sons

1.2.2 Ligands of RXFP1

The cognate ligand of RXFP1 is RLN2 which is a small 6 kDa peptide hormone. RLN2 is a member of insulin-like superfamily and is produced as pre-prohormone. The pre-prohormone contains a signal peptide, B-chain, C-chain, and a C-terminal A-chain. The signal peptide is cleaved and the resulting active prohormone has its C-chain cleaved to be fully processed to the 6 kDa relaxin peptide. The active RLN2 structure consists of an A- and B- chain linked with two disulfide bonds. The conserved amino acids motif $R^{13}xxR^{17}xxI^{20}/V$ motif in the B-chain is important for binding to the extracellular domain of RXFP1. The T16, K17, S19, and L20 residues of the A-chain of RLN2 are crucial for receptor binding and activation (Hossain et al. 2008, Park et al. 2008, Bathgate et al. 2013).

Recently, Glogowska et al. discovered CTRP8 as a novel ligand of RXFP1. The putative RXFP1 binding site of CTRP8 differs from RLN2. However, CTRP8 can still activate signal pathways and activates RXFP1 expressed in human glioblastoma cells. (Glogowska et al. 2013). CTRP8 will be described later in more detail.

1.2.3 Signal transduction pathways of RXFP1

Binding of RLN2 to RXFP1 triggers several pathways, including the cAMP signaling pathway, mitogen activated protein kinases (MAPKs), and the nitric oxide (NO) dependent pathways (**Figure 1.2).** The major pathway of RXFP1 activation is the accumulation of cAMP triggered by heterotrimeric G proteins. The ICL3 of RXFP1 couples to $G_{\alpha S}$ to activate cAMP production by adenylate cyclase (AC), whereas $G_{\alpha OB}$ inhibits this AC activity. RXFP1 coupled $G_{\alpha i3}$ via the βγ subunits stimulates phosphatidyl inositol 3 kinase (PI3K) and protein kinase C zeta (PKCζ) leading to the activation of adenylyl cyclase 5 (AC5) and the production of cAMP. Increasing cAMP levels further activate protein kinase A (PKA) which phosphorylates several downstream target proteins. $G_{\alpha i3}$ mediated PI3K-PKCζ-AC5 pathway is dependent on the last 10 amino acids, particularly Arg752, located within the C-terminal tail of RXFP1. The increase in cAMP through $G_{\alpha S}$ and $G_{\alpha OB}$ stimulates cAMP-response element (CRE)-mediated gene transcription. Another downstream target of $G_{\alpha i3}$ coupled signaling is the transcription factor nuclear factor kappa B (NF-κB) (Halls et al. 2006, Halls et al. 2009, Bathgate et al. 2013, Halls et al. 2015).

Figure 1.2 Canonical signaling pathway of RXFP1 activated by RLN2.

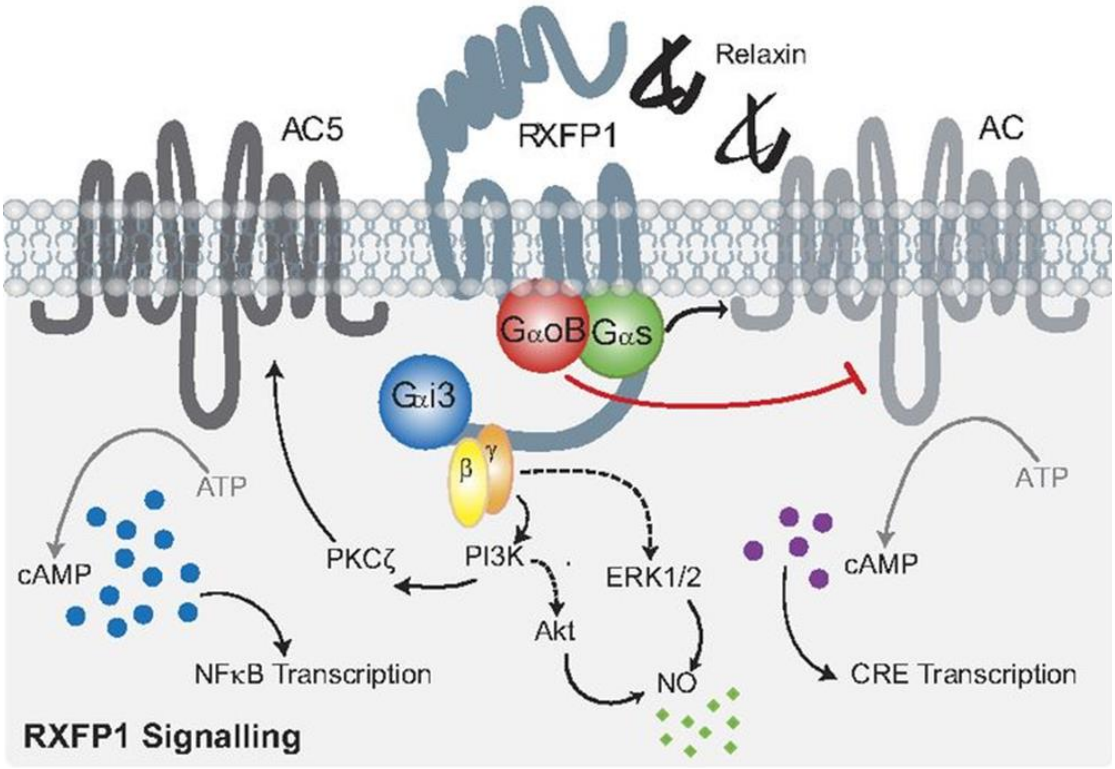

Figure 1.2 RLN2 binds to RXFP1 then the receptor couples to $G_{\alpha s}$ and $G_{\alpha oB}$ regulate cAMP level through AC. RXFP1 couples β and γ subunits of $G_{\alpha i3}$ to activate PI3 kinase subsequently PKCζ zeta translocate to activate AC5 to release cAMP. The subunits of $G_{\alpha i3}$ also activate MAP kinase signaling pathway to release NO. Reprinted from Bathgate, R. A., M. L. Halls, E. T. van der Westhuizen, G. E. Callander, M. Kocan, and R. J. Summers. 2013. Relaxin family peptides and their receptors. Physiol Rev 93: 405-480.

At attomolar RLN2 concentrations, RXFP1 is activated by a specific signalosome **(Figure 1.3)**. This signal is stimulated by the C-terminal tail of RXFP1 which couples to AC2 via A-kinase anchoring protein 79 (AKAP79) to facilitate βγ subunits of Gαs to stimulate AC2 to result in cAMP production. The signalosome activity is regulated by the binding of β-arrestin 2 and then recruits protein kinase A (PKA) and phosphodiesterase (PDE) 4D3 to form a complex at the C-terminal tail of RXFP1. The regulatory units of the signalosome (β-arrestin 2, PKA and PDE4D3) dissociate off the receptor when RXFP1 is

exposed to higher (> nanomolar) concentrations of RLN2. The signalosome pathway is a specific mechanism to AC2 which is preferentially expressed in lung, brain, heart, uterine myometrium, and skeletal muscle tissues (Halls and Cooper 2010, Bathgate et al. 2013, Halls et al. 2015). Therefore, signalosome signaling may be a specific to certain tissues.

Figure 1.3 Atypical RXFP1 signalosome mechanism.

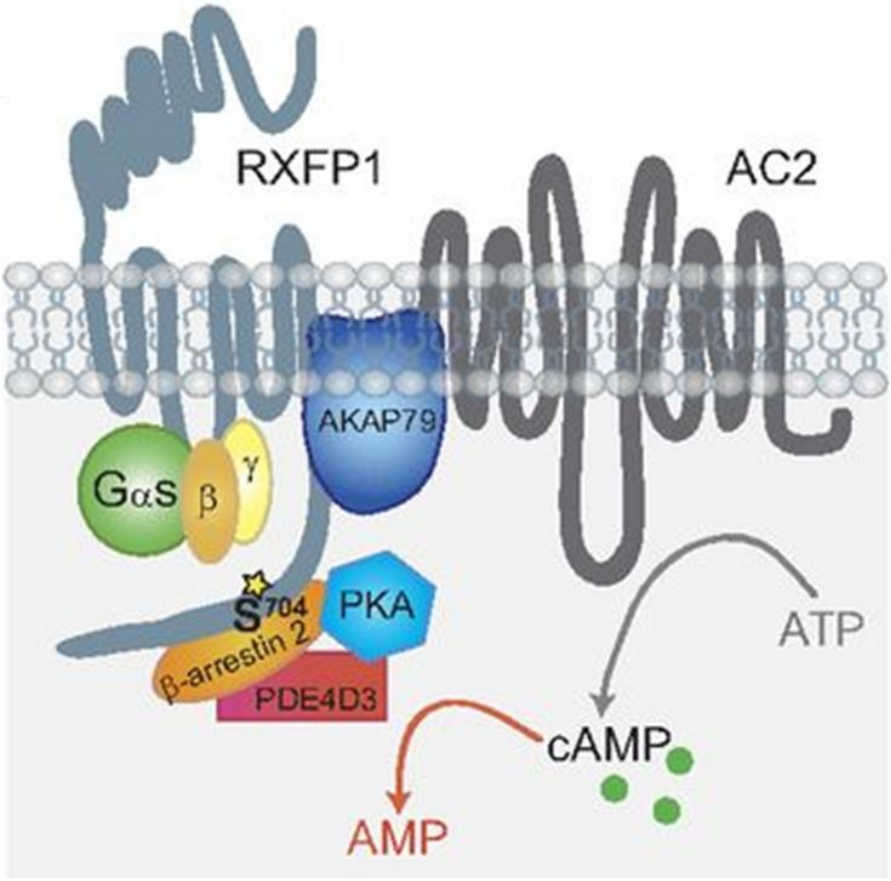

Figure 1.3 Signalosome complexes are formed between RXFP1, AKAP79, AC2, PKA, PDE4D3 and β-arrestin 2. Once the receptor receives attomolar concentration of RLN2, this signalosome complexes are activated to release cAMP. Reprinted from Bathgate, R. A., M. L. Halls, E. T. van der Westhuizen, G. E. Callander, M. Kocan, and R. J. Summers. 2013. Relaxin family peptides and their receptors. Physiol Rev 93: 405-480.

Apart from the cAMP signaling pathway, RXFP1 also stimulates the MAPK and NO pathway in specific cell types. In normal human endometrial cells (NHE cells), human cervical cancer cells (HeLa), and primary human umbilical vein endothelial cells (HUVECs) stimulation by RLN2 induces phosphorylation of ERK1/2 (Dschietzig et al. 2003). The activation of ERK1/2 in human monocytic cells (THP-1) and human coronary artery and pulmonary artery smooth muscle cells induces vascular endothelial growth factor (VEGF) expression (Zhang et al. 2002). The RXFP1 activation by RLN2 induces an increase in cellular NO levels through PI3K-Akt mediated activation of endothelial nitric oxide synthase (eNOS) activity (Nistri and Bani 2003). Inducible NOS (iNOS) activity is stimulated by cAMP-PKA-NFkB activation in HUVECs (Fei et al. 1990, Quattrone et al. 2004).

Bioluminescence resonance energy transfer (BRET) studies revealed the homo- and heterodimerization of RXFP1and showed that this dimerization is crucial for receptor signaling functions (Svendsen et al. 2008). Unlike other GPCRs, there is no receptor phosphorylation, desensitization, or internalization upon RXFP1 activation (Callander et al. 2009, Halls et al. 2015). Hence, RXFP1 can provide prolonged signaling upon interaction with its ligands.

1.2.4 Functional roles of the RLN2-RXFP1 system

This section will explain the function of the RLN2-RXFP1 ligand-receptor system.

1.2.4.1 RLN2-RXFP1 in the reproductive system and breast

RLN2 has long been known as a pregnancy hormone and has important functions in the reproductive system (Marshall et al. 2016). In women, RLN2 and RXFP1 are expressed in the follicles and corpus luteum of ovarian tissue where RLN2 is involved in

follicle development (Blankenship et al. 1994, Shirota et al. 2005, Anand-Ivell and Ivell 2014). RLN2 levels increase after ovulation and are highest in the late secretory phase of the menstrual cycle (Bryant-Greenwood et al. 1993). RLN2 and RXFP1 also present in the luminal and glandular epithelium of the endometrium during all menstrual cycle stages (Luna et al. 2004, Krusche et al. 2007). RLN2 is detected in decidualized stromal cells in the late secretory phase. It suggested that RLN2 acts as a paracrine hormone to prepare the uterus for pregnancy (Marshall et al. 2016).

During pregnancy, RLN2 levels differ between species. In women, the plasma RLN2 level is highest in the first trimester, likely to prepare the endometrium for embryo implantation and maintenance (Eddie et al. 1990, Stewart et al. 1990, Chen et al. 2003). In pregnant rats and pigs, the RLN2 levels peak in the last stage of pregnancy (Sherwood et al. 1980, Eldridge-White et al. 1989). RLN2 promotes vagina growth during pregnancy and its function on the cervix and pubic symphysis are crucial for proper delivery in mice and rats (Hall 1960, Zhao et al. 1996, Zhao et al. 2001). RLN2 signals through RXFP1 regulates pubic symphysis relaxation and collagen turnover in the cervix in mice (Kaftanovskaya et al. 2015). Moreover, RLN2-RXFP1 activates hyaluronan synthases and aquaporins expression to induce water recruitment into extracellular matrix for softening the collagen in the cervix in mice (Soh et al. 2012). In mice and rats, RLN2-RXFP1 induces proliferation and inhibits apoptosis of epithelial and stromal cells in the cervix and vagina (Lee et al. 2005a, Yao et al. 2008).

During the peri-implantation period in marmoset monkeys, both RXFP and RLN2 are highly expressed in the uterus where this ligand-receptor system is believed to play a role in the adaptive response to embryo implantation (Einspanier et al. 2009). There is no

evidence for a role of RLN2-RXFP1 in human embryo implantation. In rats, mice and pigs, RLN2 inhibits spontaneous myometrial contractions during early pregnancy in support of implantation. However, RLN2 does not have this contraction inhibitory effect in the human uterus (MacLennan et al. 1986, MacLennan and Grant 1991, Sherwood 2004, Bathgate et al. 2006). In marmoset monkeys, RLN2 induces cAMP production for decidualization which leads to increased endometrium angiogenesis and thickening in preparation for implantation (Einspanier et al. 2001, Bartsch et al. 2004, Goldsmith et al. 2004, Shirota et al. 2005).

In the male reproductive system, RLN2 is produced in the prostate and is secreted into the seminal fluid (Loumaye et al. 1980, Ivell et al. 2011). RXFP1 transcripts were detected in spermatid and Sertoli cells which are important for spermatogenesis (Filonzi et al. 2007). Many studies have associated RLN2-RXFP1 with enhances fertility by its ability to increase sperm motility, capacitation and acrosome reaction (Lessing et al. 1985, Carrell et al. 1995, Miah et al. 2015).

1.2.4.2 RLN2-RXFP1 in the central nervous system

RLN2-RXFP1 activation in the amygdala impairs fear-related memory consolidation in rats (Ma et al. 2005). RXFP1 is highly expressed in brain region associated with memory formation, including neocortex, hippocampus, thalamic nuclei, and supra-mammillary nucleus. However, there is currently no evidence to support a role for RXFP1 in memory (Halls et al. 2015). RXFP1 is also expressed in oxytocin containing cells of the paraventricular and supraoptic hypothalamic nuclei in rats. Intravenous injection of RLN2 increases plasma oxytocin and neuron activity (Way and Leng 1992, Burazin et al. 2005). RLN2-RXFP1 activates Fos expression in neurons of peripheral and dorsal segments of

the subfornical organ (SFO), the dorsal cap region of the organum vasculosum of the lamina terminals (OVLT) and in the supraoptic and paraventricular nuclei of the hypothalamus (McKinley et al. 1997, McKinley et al. 1998, Sunn et al. 2001, Sunn et al. 2002). Circulating RLN2 can penetrate to SFO and OVLT regions which lack a blood brain barrier (BBB) and causes the reduction in plasma osmolality in pregnant rats (Sunn et al. 2002). RXFP1 protein expression is detected in the postmortem human neocortex, including frontal, temporal, parietal, occipital regions and in the hippocampus. These regions of the brain are involved in depression, memory and emotional processing in Alzheimer's disease patients (Lee et al. 2016).

1.2.4.3 RLN2-RXFP1 in the cardiovascular system

RLN2 plays important roles in the heart and blood vessels. RLN2-RXFP1 functions as vasodilators by activating NOS, PKA, VEGF and MMPs to prevent the tightening of blood vessel walls and promote vascularization (Sarwar et al. 2016). RLN2 also increases the cardiac index (the amount of blood pumped by the heart [liters per minute] divided by the body surface area) and decreases vascular resistance, blood pressure and pulmonary pressure during pregnancy (Conrad 2004, Conrad and Novak 2004, Debrah et al. 2005, Debrah et al. 2006) and in chronic heart failure patients (Fisher et al. 2003, Dschietzig et al. 2009, Teichman et al. 2009). RXFP1 is expressed in human cardiac fibroblasts and cardiomyocytes (Sarwar et al. 2015). RLN2-RXFP1 has anti-apoptotic and anti-hypertrophic functions in neonatal rat cardiomyocytes and induces the growth and maturation of neonatal mouse cardiomyocytes (Moore et al. 2007, Yao et al. 2009, Samuel et al. 2011). RLN2 protects against myocardial injury in rats and pigs cardiomyocytes (Bani et al. 1998, Nistri et al. 2008). RLN2 inhibits apoptosis induced by oxidative stress through

the activation of Akt and ERK signaling pathways (Moore et al. 2007) and induces the Notch-1 signaling pathway after hypoxia to promote re-oxygenation (Boccalini et al. 2015). Clinically used RLN2 (Serelaxin) serves as promising new therapeutic drug in cardiovascular diseases and is used in phase III clinical trials for congestive and acute heart failure patients [clinical trial number: NCT00520806] (Grossman and Frishman 2010, Ponikowski et al. 2012, Castrini et al. 2015).

RLN2-RXFP1 activation impacts on the vascular system causing vasodilation of arteries, arterioles and capillaries in the reproductive system, heart, cecum and liver (Bigazzi et al. 1986, Bani et al. 1988, Bani-Sacchi et al. 1995, Bani et al. 1998). RXFP1 is expressed in the rat abdominal aorta, in uterine, mesenteric, femoral and renal arteries and is highly expressed in uterine arteries during early pregnancy. This implies a functional role of RLN2-RXFP1 in the regulation of vascular adaptations during pregnancy (Sarwar et al. 2016). This is supported by the fact that during the menstrual cycle and pregnancy RLN2-RXFP1 was shown to up-regulates VEGF by human uterine cells (Unemori et al. 1999, Bond et al. 2004).

1.2.4.4 RLN2-RXFP1 in extracellular matrix remodeling

RLN2-RXFP1 affects extracellular matrix (ECM) remodeling. RLN2 can stimulate collagen degradation, a major component in various connective body tissues. Fibrosis, the excessive of extracellular deposition of collagen in tissue, causes scarring and thickening of tissues affecting normal organs functions. Many studies have demonstrated that RLN2 can inhibit fibrosis and serves as anti-fibrotic agent (Zhou et al. 2015, Samuel et al. 2016, Tan et al. 2016). The overexpression of collagen observed in lung, kidney, liver, and heart is associated with a progressive tissue fibrosis (Bennett et al. 2009, Du et al. 2009, Tang et

al. 2009, Hewitson et al. 2010). RLN2 reduces fibrosis by antagonizing transforming growth factor β1 (TGF- β1) function, NO and down-regulating Smad signaling pathways that activate ECM synthesis and secretion (Heeg et al. 2005, Mookerjee et al. 2009). RLN2 reduces collagen expression and induces the expression of matrix degrading enzymes (Unemori and Amento 1990, Unemori et al. 1996). Matrix metalloproteinase (MMP) are protease enzymes capable of degrading components of the ECM and basement membrane which contributes to tissue remodeling and maintenance (Samuel et al. 2007). In fibro-chondrocytic cells, RLN2-RXFP1 has an important role in the regulation of airway ECM (Samuel et al. 2009) by activating the expression of MMP-9 (gelatinase B) and MMP-13 (collagenase 3) through PI3K, ERK, Akt and PKCζ signaling pathways (Ahmad et al. 2012). In a mouse model of bleomycin-induced pulmonary fibrosis, RLN2 inhibits lung fibrosis and prevents the increase in alveolar thickness (Unemori et al. 1996).

1.2.4.5 RXFP1 and cancers

This topic has been published in a review "**Thanasupawat, T**., et al., RXFP1 is targeted by complement C1q tumor necrosis factor-related factor 8 in brain cancer**.** Front Endocrinol (Lausanne), 2015. 6: p. 127".

Most of the cellular and molecular mechanisms involved in RXFP1-mediated cancer promotion have been established in breast, thyroid, and prostate cancer models. (Silvertown et al. 2003, Klonisch et al. 2007, Halls and Cooper 2010, Summers 2012, Halls et al. 2015). Increased expression of relaxin-like peptides, RLN2 and INSL3, has been detected in *breast cancer* (Tashima et al. 1994, Hombach-Klonisch et al. 2000). Using the ERα-positive human breast cancer cell line MCF-7, the group of Mario Bigazzi showed that highly purified porcine relaxin acted in a dose- and time-dependent manner and

promoted proliferation with short-term exposure at low concentrations. Long-term exposure of up to 7 days reduced proliferation and promoted differentiation of MCF-7 cells as demonstrated by the up-regulation of cell surface protein E-cadherin (Bigazzi et al. 1992, Sacchi et al. 1994). This was accompanied by an increase in inducible NO synthase activity and intracellular NO production (Bani et al. 1995). Inco-culture with myoepithelial cells, relaxin enhanced ultrastructural signs of MCF-7 cell differentiation (Bani et al. 1994). Exposure to human recombinant RLN2 for 24 h induced S100A4 expression and increased cell migration in ERα-negative MDA-MB231 triple-negative breast cancer cells, but exposure for more than 3 days downregulated S100A4 levels and reduced cell migration and invasiveness in the same cell model in an RXFP1-dependent manner, leading to reduced tumor xenograft growth *in vivo* (Radestock et al. 2008). In an *ex-vivo* brain metastasis model, RLN2 promoted the invasion of RXFP1-expressing MCF-7 human breast cancer cells into brain tissue slices (Binder et al. 2014). These data suggest concentration-, time-, and cell context-dependent actions of relaxin in breast cancer and an essential role for RXFP1 in mediating cell motility and invasion.

Increased expression of RLN2 and RXFP1 was also shown in *thyroid cancer*. RLN2-RXFP1 signaling promotes thyroid cancer motility and invasiveness. RXFP1 mediated the motility enhancing effect of RLN2, in part through the induction of S100A4 in human thyroid carcinoma cells and RLN2 enhanced thyroid xenograft angiogenesis (Radestock et al. 2010). RLN2-RXFP1 signaling increased the expression and secretion of the lysosomal proteinases, cathepsin-D (cath-D) and cathepsin-L (cath-L), This resulted in enhanced elastinolytic activity and cell invasion through elastin matrices (Hombach-Klonisch et al. 2006). RXFP1 activation by RLN2 in human thyroid cancer cells increased

cell migration and extracellular matrix invasion through enhanced collagenolytic activity due to the upregulation and increased secretion of MMP2 and enhanced membrane-anchored MT1-MMP/MMP14 (Bialek et al. 2011).

In *prostate cancer*, RLN2-RXFP1 signaling increased cell migration and proliferation in androgen-receptor (AR)-dependent LNCaP and AR-independent PC3 prostate cancer cells (Feng et al. 2009) and this promoted growth in xenografts derived of androgen-independent PC3 prostate cancer cells (Neschadim et al. 2014). The siRNA-mediated knockdown of RXFP1 prevented the RLN2-induced increase in prostate cancer cell proliferation and invasiveness and induced apoptosis (Feng et al. 2007). Injection of siRNA-loaded biodegradable nanoparticles into xenografts of AR-positive LNCaP cells and AR-negative PC3 cells downregulated RXFP1 and resulted in a significant reduction in tumor proliferation and metastasis, implicating RXFP1 as an important growth and survival factor in prostate cancer independent of androgen receptor expression (Feng et al. 2010). RXFP1-dependent and RLN2-induced proliferation of prostate carcinoma cells was mediated via a PI3K/Akt signaling pathway. In LNCaP cells, the simultaneous blocking of protein kinase A (PKA) and NF-κB signaling almost completely abolished RLN2-mediated proliferation and colony formation (Vinall et al. 2011). The extracellular LDL-A module of RXFP1 was shown to reduce S100A4, S100P, IGFBP2, and MUC1 expression and inhibit RXFP1-mediated proliferation and invasion of PC3 prostate cancer cells (Feng and Agoulnik 2011). Similar to RXFP1 knockdown in PC3 cells, LDL-A expression reduced $pAKT^{T308}$ and decreased cell proliferation and colony formation, suggesting that LDL-A module can block activation of endogenous RXFP1 in PC3 cells (Feng and Agoulnik 2011).

The established role of RXFP1 in cancer and other diseases has prompted attempts to identify specific agonists and antagonists of RXFP1. A recent large high-throughput screen of small molecule libraries yielded RXFP1 agonists (Chen et al. 2013, Xiao et al. 2013). The challenging search for RXFP1 antagonists has so far produced few promising candidates. The conversion of the two arginine residues (B13, B17) to lysine residues (ΔH2) within the receptor binding domain of the B-chain of human RLN2 ("GRELVR") was shown to reduce bioactivity and cAMP production in RXFP1-positive myelo-monocytic THP1 cells and RXFP1 expressing HEK293 cells. This ΔH2 mutant was able to bind to RXFP1 and function as a partial antagonist to functional RLN2 in an *in vivo* xenograft model of prostate cancer (Silvertown et al. 2007). In MCF-7 breast cancer cells and renal myofibroblasts with endogenous expression of relaxin, the ΔH2 analog blocked RXFP1 activation and significantly inhibited RLN2-induced MCF-7 cell migration (Hossain et al. 2010). When a chemically synthesized ΔH2 antagonist, named AT-001, was used alone or in combination with the anti-mitotic taxane drug docetaxel, xenografts derived from PC3 androgen-independent prostate cancer cells were reported to show a dramatic 60 and 90% reduction in growth (Neschadim et al. 2014). Although these are promising results, the vulnerability of peptide antagonists to proteolytic attack, size restrictions limiting their tissue penetration, and the difficulty in chemically synthesizing large amounts of ΔH2 derivatives remains challenges.

Our recent discovery of a novel RXFP1 ligand that is structurally distinct from relaxin-like peptides may provide new opportunities for developing RXFP1 antagonists. We identified C1q/tumor necrosis factor-related protein (CTRP) family member CTRP8 as a novel RXFP1 ligand. Importantly, a small competitor peptide derived from the closely

related C1Q tumor necrosis factor related factor 6 (CTRP6) was able to disrupt the CTRP8-induced and RXFP1-dependent migration of human glioma cells (Glogowska et al. 2013). This suggests a novel and as yet poorly understood regulatory network in which C1Q tumor necrosis factor-related factors, depending on the presence of resident secreting cells, can modulate RXFP1 functions in a tissue-dependent and tumor-specific manner.

1.3 Relaxin family peptide receptor 2 (RXFP2) and cancers

RXFP2 has a similar structure to RXFP1, containing LDL-A module at the N-terminal, 10 LRR domain, 7-TM, and C-terminal tail. INSL3 is a congnate ligand of RXFP2. INSL3 binds and activates RXFP2 by coupling to $G_{\alpha s}$ to activate AC which increase cAMP level, and coupling to $G_{\alpha oB}$ to inhibit AC to increase cAMP accumulation. RLN2 is able to bind RXFP2 at lower affinity than RXFP1 and can weakly activate RXFP2 to increase the level of cAMP in HEK293-RXFP2 (Halls et al. 2006, 2007). However, there is no evidence showing the activation of RXFP2 by RLN2 *in vivo*. The RXFP2-INSL3 system increases cell motility in PC-3 prostate cancer cells (Klonisch et al. 2005). In FTC-133 thyroid cancer cells, INSL3 activtaes RXFP2 to trigger the secretion of S100A4 and cathepsin L and ehnance cell motility (Hombach-Klonisch et al. 2010). High expression levels of RXFP2 promote cell invasion in hepatocellular carcinoma (Lin et al. 2011).

In my study, I found RXFP1 highly expresses in GB but there is no RXFP2 expression. Therefore, first, I focused on the function of RXFP1-RLN2 system in GB cell migration and invasion. I also studied how RXFP1 activation cam promote TMZ chemoresistance in human GB cells.

1.4 P59 and P74 peptides

Shemesh et. al identified peptide GPCR ligands using *in silico* computer methods and confirmed by *in vitro* analysis. They discovered two novel GPCR-activating peptides, P59 (CGEN-2510) and P74 (CGEN-25009) which can activate RXFP1 and RXFP2 (Shemesh et al. 2008). Both P59 and P74 are short linear peptides derived from the same precursor, complement C1Q tumor necrosis factor-related protein 8 (CTRP8), and share amino acid (aa) sequences with the collagen and C1Q domain of CTRP8. P59 contains 23 aa and P74 contains a duplication of a peptide motif of 10 aa in the C-terminal part of P59, therefore, P74 is 33 aa in length (**Figure 1.4**). Both peptides could activate cAMP production in both RXFP1- and RXFP2-transfected CHO-K1 cells but failed to activate RXFP3 (Shemesh et al. 2009).

P74 has been shown to have relaxin-like anti-inflammatory and anti-fibrotic activities. This peptide was able to decrease lung inflammation and injury in a bleomycin-induced pulmonary fibrosis mouse model (Pini et al. 2010, Tan et al. 2016). P74 requires RXFP1 to activate downstream signaling in human idiopathic pulmonary fibrosis to increase the sensitivity of anti-fibrotic activity (Tan et al. 2016) and triggers cAMP, cGMP, and NO signaling mediators in myelo-monocytic THP-1 cells (Pini et al. 2010).

Figure 1.4 Sequences of short linear peptides, P59 and P74.

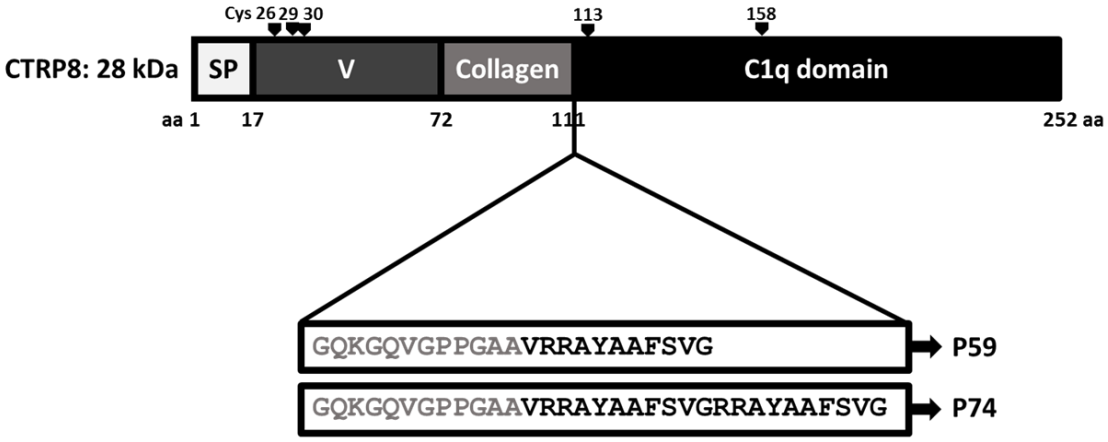

Figure 1.4 The sequences of P59 and P74 are derived from collagen-c1q domains of CTRP8. The structure of CTRP8 consists of 4 domains, signal peptide (SP), N-terminal, collagen, and c1q domains. P74 has a duplication of RRAYAAFSVG motif of c1q domain.

1.5 Tissue distribution and structure of CTRP family members

The family of complement C1QTNF-related peptides, in particular CTRP8, has been featured in a recent review "**Thanasupawat, T**., et al., RXFP1 is targeted by complement C1q tumor necrosis factor-related factor 8 in brain cancer**.** Front Endocrinol (Lausanne), 2015. 6: p. 127". The family of complement C1Q tumor necrosis factor-related proteins is composed of adiponectin and 16 CTRP members (CTRP19, 9B, 10−15). All CTRPs are secreted proteins that assemble into trimers and higher-order oligomers. In co-expression systems, CTRPs can also form heteromeric complexes (Wong et al. 2008, Peterson et al. 2009, Wong et al. 2009). The C-terminal globular domain of CTRPs shares close similarity with the 3D structure of the complement component C1q and the tumor necrosis factor (TNF) homology domain present in members of the TNF family (Shapiro and Scherer 1998, Kishore et al. 2004, Ghai et al. 2007). Unlike adiponectin, which is

produced at high level and almost exclusively by adipocytes, many CTRP members have broad expression profiles. CTRP members are expressed in various tissues and cell types (Hayward et al. 2003, Lee et al. 2005b, Wong et al. 2008). Of particular interest for my work is CTRP8, which is expressed in the human testis and lung tissues (Peterson et al. 2009).

The structure of CTRPs has been highly conserved during vertebrate evolution as determined by sequence comparison of orthologous CTRPs from zebrafish, frog, mouse, and human genomes (Seldin et al. 2014). All CTRPs share a common protein structure with adiponectin; CTRP9 shows the highest homology (54%) in the globular C1q domain with adiponectin (Wong et al. 2009). *Ctrp8* and *Ctrp9B* are both pseudogenes in the mouse genome (Peterson et al. 2009). The structure of CTRPs consists of four distinct domains (**Figure 1.5A**). The *N-terminal signal peptide* facilitates protein secretion and is followed by a *short variable region*. The variable region contains one or more conserved cysteine (Cys) residues, which create disulfide bonds to facilitate higher-order multimeric protein assembly and/or secretion (Wong et al. 2008, Wong et al. 2009, Wei et al. 2012, Wei et al. 2013, Seldin et al. 2014, Tu and Palczewski 2014). Next, a *collagen-like domain* contains a variable number of Gly-X–Y (where X and Y indicate any amino acid; often Y is a proline or hydroxyproline) repeats, which are essential for the formation of a left-handed coiled coil structure composed of three collagen-like chains. This collagen triple helix acts as a stabilizing stalk for the formation of CTRP trimers (**Figure 1.5B**) (Kishore et al. 2004). Located at the C-terminus of each collagen like domain is a *jelly-roll* β-*sandwich folded globular domain* with 3D structural homology to complement component C1q and the tumor necrosis factor ligand family, hence the name CTRP (Wong et al. 2004,

Wong et al. 2008, Schaffler and Buechler 2012, Seldin et al. 2014). Connected by the collagenous stalk, three such C1q like protomers form the globular head typical for CTRP members. The collagen domain not only facilitates trimer formation but also contributes to multimerization of CTRPs into bouquet-like quaternary structures (**Figure 1.5C**) (Kishore et al. 2004, Tu and Palczewski 2012). CTRP4 is unique among the secreted members of the C1qTNF family as it lacks the collagen domain but, instead, contains two tandem globular C1q domains connected by a short non-conserved 18 amino acid linker. CTRP4 protein is encoded by a single exon and its globular C1q domain shows highest homology (44%) to the CTRP member C1qDC1/Caprin-2 (Byerly et al. 2014). The crystal structure of CTRP5 identified residues Y_{152}, F_{230}, and V_{232} within the globular domain as important contributors to the trimer formation and these residues are highly conserved among C1q family proteins (Ghai et al. 2007, Peterson et al. 2009, Tu and Palczewski 2012). Exceptions are CTRP1^{Y230} and CTRP6^{H230} and CTRP8^{H230} where the phenylalanine residue F_{230} of CTRP5 is replaced by less hydrophobic His (H) or Tyr (Y) residues, suggesting potential differences in trimerization and complex stability (Tu and Palczewski 2012). In the context of RXFP1, this finding is intriguing for three reasons: (i) phylogenetic analysis of currently known C1q globular domains of C1q-like family members identified a close relationship of CTRP members 1, 6, and 8 (Innamorati et al. 2006, Ghai et al. 2007); (ii) CTRP1 and CTRP8 share an identical peptide sequence identified as a binding motif for the relaxin receptor RXFP1 (Shemesh et al. 2008, Shemesh et al. 2009), and (iii) we described CTRP8 as a novel ligand of RXFP1 (Glogowska et al. 2013).

Figure 1.5 Structure of CTRP family members.

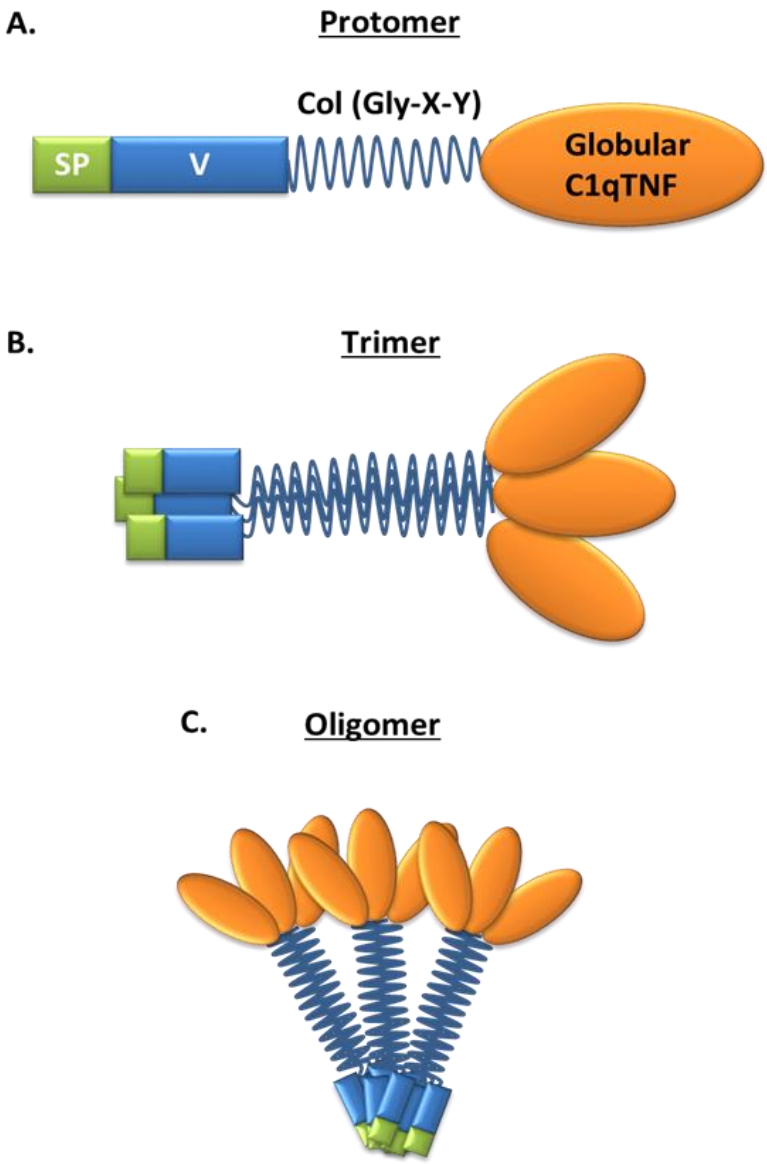

Figure 1.5 (A) Domain structure of a single CTRP protomer, which is composed of a signal peptide (SP), variable region (V), collagen domain (Col-Gly-X-Y), and globular C1q/TNF domain; **(B)** CTRP are secreted and form homotrimers; **(C)** trimers can form higher-order multimeric 3D structures composed of multiple trimers. Reprinted from Thanasupawat, T., A. Glogowska, M. Burg, G. W. Wong, C. Hoang-Vu, S. Hombach-Klonisch, and T. Klonisch. 2015. RXFP1 is Targeted by Complement C1q Tumor Necrosis Factor-Related Factor 8 in Brain Cancer. Frontiers in endocrinology 6: 127.

CTRPs are subjected to posttranslational modifications. This includes *N*-linked glycan modifications for CTRP1, CTRP2, CTRP6, CTRP12, and CTRP15, whereas CTRP3, CTRP5, CTRP9, CTRP10, CTRP11, and CTRP13 contain other carbohydrate moieties (Wong et al. 2004, Innamorati et al. 2006, Wong et al. 2008, Wong et al. 2009, Wei et al. 2011, Seldin et al. 2012, Wei et al. 2012, Wei et al. 2013, Seldin et al. 2014). However, glycosylation was not detected for CTRP8 (Peterson et al. 2009). Also, bacterially produced (non-glycosylated) recombinant proteins, CTRP1, CTRP6, and CTRP8, retain bioactivity, suggesting that posttranslational glycan modifications are not required for some of their biological effects. Adiponectin, CTRP2, CTRP3, CTRP4, CTRP7, CTRP9, CTRP10 contain Ca^{2+} binding sites, whereas CTRP1, CTRP5, CTRP6, and CTRP8 lack a Ca^{2+}binding element (Shapiro and Scherer 1998, Tu and Palczewski 2012, 2014). Ca^{2+} ions were reported to promote stable trimer formation and oligomerization of adiponectin (Banga et al. 2008, Min et al. 2012).

1.5.1 CTRP members in cancer

Research on the role of C1q-TNF-related proteins in cancer is an emerging field. So far CTRP3, CTRP4, and CTRP6 have been associated with tumor-promoting effects. Secreted *CTRP3/cartducin* plays a role in cartilage development. Elevated protein expression of CTRP3/cartducin in mouse osteosarcoma cell lines was shown to promote cell proliferation in a dose-dependent manner. The MAPK/ERK kinase 1/2 (MEK1/2) inhibitor, U0126, prevented this mitogenic effect indicating that CTRP3 induces cell proliferation via ERK1/2-signaling (Akiyama et al. 2009). CTRP3 was also shown to induce migration of mouse endothelial cells in an ERK1/2-dependent manner (Akiyama et al. 2009) suggesting a role in angiogenesis. The receptor mediating the effects of

CTRP3/cartducin is unknown. HeLa and HEK293 cells were used to show that *CTRP4* functions as tumor-promoting inflammatory regulator. CTRP4 overexpression increased NFκB activation in a dose-dependent manner and induced transcriptional activity of the NFκB target TNF-α. In human HepG2 hepatocarcinoma cells, secreted CTRP4 and recombinant CTRP4 caused enhanced $STAT3^{Tyr705}$ phosphorylation and increased IL6 and TNF-α secretion in a dose dependent manner. Interestingly, IL-6 exposure increased expression of CTRP4 indicating positive feedback regulation in these cancer cells (Li et al. 2011). Immunoreactive *CTRP6* was detected in human hepatocellular carcinoma tissue specimens and was localized to hepatocellular carcinoma cells and endothelial cells within the tumor. Recombinant CTRP6 increased Akt phosphorylation in isolated liver endothelial cells and this signaling was mediated via the C-terminal C1q domain of CTRP6. Indeed, HepG2 xenografts with exogenous expression of CTRP6 showed increased tumor angiogenesis and reduced necrosis (Takeuchi et al. 2011). Taken together, these results are consistent with C1q-TNF-related proteins in promoting tumorigenesis.

1.5.2 CTRP8 is a novel RXFP1 ligand in glioblastoma

CTRP8 is evolutionarily highly conserved and secreted as a homotrimer or a heterotrimer with the C1qTNF family member C1q-related factor (CRF) (Berube et al. 1999); the latter also forms heterotrimers with CTRP1, CTRP9, and CTRP10 when co-expressed in cells (Peterson et al. 2009). Until recently, CTRP8 was the least understood C1q-TNF-related protein member, in part, because Ctrp8 is a pseudogene in mice and PCR analysis revealed expression of CTRP8 in human restricted to lung and testis (Peterson et al. 2009). We recently identified CTRP8 as a novel ligand for RXFP1 in human glioblastoma cells (Glogowska et al. 2013). Human patient-derived glioblastoma(GB) cells

and established GB cell lines express RXFP1, but lack the classical RXFP1 ligands, RLN1 and RLN2. It was demonstrated that in human GB cells, CTRP8 is expressed and secreted and RXFP1 serves as a novel receptor for CTRP8 in these cells. CTRP8 and RLN2, as well as two biologically active peptides homologous to a peptide sequence within the N-terminal region of the C1q globular domain of human CTRP8, P59, and P74 (Shemesh et al. 2008, Shemesh et al. 2009), activated RXFP1 by increasing cAMP levels and PI3K–PKCζ/ PKCδ–ERK1/2 signaling. The RXFP1 negative U251 GB cell line and HEK293 cells devoid of RXFP1 with exogenous expression of the related receptor RXFP2, did not respond to CTRP8 with increased cAMP levels demonstrating a specific RXFP1-mediated signaling. Furthermore, CTRP8, P59, and P74 showed a dose–response increase in cell motility that was dependent on RXFP1. RXFP1 activation by CTRP8, P59, and P74 increased cathepsin-B (cath-B) protein production and secretion, which mediated the RXFP1-induced enhanced GB cell invasiveness through laminin matrices. In addition GB invasiveness was abolished by specific inhibitors for PKCζ, PKCδ, PI3K, and cath-B, as well as RNAi-mediated RXFP1 knockdown. An interaction between RXFP1 and CTRP8 was demonstrated by co-immunoprecipitation of epitope-tagged HA-RXFP1 and CTRP8-His in HEK293 cells. Our structural simulation studies predicted that the amino acid sequence "YAAFSVG" present in the P59 and P74 peptides and located within the N-terminal C1q globular domain of CTRP8 were likely interacting with the leucine-rich repeats (LRR) 7 and 8 of RXFP1 (Glogowska et al. 2013). We dismissed the possibility of the formation of CTRP8/CRF heterotrimers because GB cells are devoid of the CTRP8 hetero-oligomerization partner CRF (Peterson et al. 2009). Importantly, competitive binding assays demonstrated that a small peptide derived from the N-terminal region of the

globular C1q domain of human CTRP6 was able to successfully block the PI3K–PKCζ/PKCδ mediated increase in cath-B secretion and reduced CTRP8 mediated cell motility (Glogowska et al. 2013). These data strongly suggest that CTRP8 may play an importance role in promoting proliferation and invasion of GB cells.

1.5.3 Summary and prospective goals

The discovery of CTRP8 as a RXFP1 agonist in glioblastoma brain tumor is novel for a number of reasons: (i) RXFP1 is the first receptor to be identified for any of the CTRP members; (ii) CTRP8 is the first RXFP1 ligand discovered that is not structurally related to the relaxin like family; (iii) the CTRP8–RXFP1 ligand–receptor system is a novel factor in brain tumorigenicity; (iv) our discovery of a competitor peptide resembling a linear peptide sequence at the transition from the collagen- to the C1q globular domain of CTRP6, a close relative of CTRP8, provides the first intriguing evidence for a regulatory network of CTRP factors modulating RXFP1 functions in a tissue-specific context. These findings are the exciting start of an emerging field in CTRP and RXFP1 research with the potential to link the metabolic and immunological functions of CTRP members with molecular mechanisms in cancer (Schaffler and Buechler 2012). Future cancer research will elucidate the molecular signaling mechanisms and functional relevance of CTRP-derived RXFP1 regulation in a variety of tumors. The use of CTRP-based peptides capable of blocking CTRP8-mediated actions is currently being tested for potential clinical applications.

1.6 Brain tumors

Intracranial neoplasm or brain tumor is a growth of abnormal cells in the brain. Brain tumors can be benign or malignant. Primary brain tumors originate within the brain. Secondary or metastatic brain tumors originate from another part of the body and spread

to the brain (Schouten et al. 2002). Approximately 77,670 people have been diagnosed with primary brain tumors in the United States in 2016. Glioma, a common primary brain tumor, accounts for 27% of all primary brain tumors and for 80% of all malignant primary brain tumors (Ostrom et al. 2015). Glioma arises from glial cells that support and protect neurons. Glial cells include astrocytes, oligodendrocytes, and ependymal cells which can form astrocytomas, oligodendrogliomas and ependymomas, respectively. Astrocytomas are the most common glioma and are classified by their pathology (Gurney and Kadan-Lottick 2001, Jovcevska et al. 2013).

1.6.1 WHO classification of brain tumors 2016

The 2016 World Health Organization (WHO) grading system categorized glioma based on histological and molecular genetic features (Louis et al. 2016) **(Figure 1.6).** There are diffuse and non-diffuse glioma. **Grade I** pilocytic astrocytoma are benign tumors which can be treated by surgery only. The major diffuse gliomas groups can be divided into 3 subgroups, grade II, III and IV. **Grade II** diffuse astrocytoma and **grade III** anaplastic astrocytoma are divided into IDH-mutant, IDH-wildtype and IDH-NOS (not otherwise specified). IDH-mutants are characterized as R132H *IDH1* or R172G/K/M *IDH2* mutations (Yan et al. 2009). The IDH-mutant is the major characteristic in grade II glioma, which represents a low-grade malignancy. Grade III anaplastic astrocytoma, are IDH-mutant and malignant tumors that often lead to death within a few years. IDH-wildtype is uncommon in grade II and III astrocytomas. The IDH-NOS tumors that have not undergone molecular genetic testing (Louis et al. 2016). Finally, **grade IV** glioblastoma (GB) can be sub divided into **(i)** IDH-wildtype which accounts for 90% of cases **(ii)** IDH-mutants accounting for 10% of cases and **(iii)** NOS (Louis et al. 2016). GB are the most aggressive

brain tumors, being highly invasive and usually fatal within 9-17 months after diagnostic (Krex et al. 2007).

Figure 1.6 WHO classification of glioblastoma

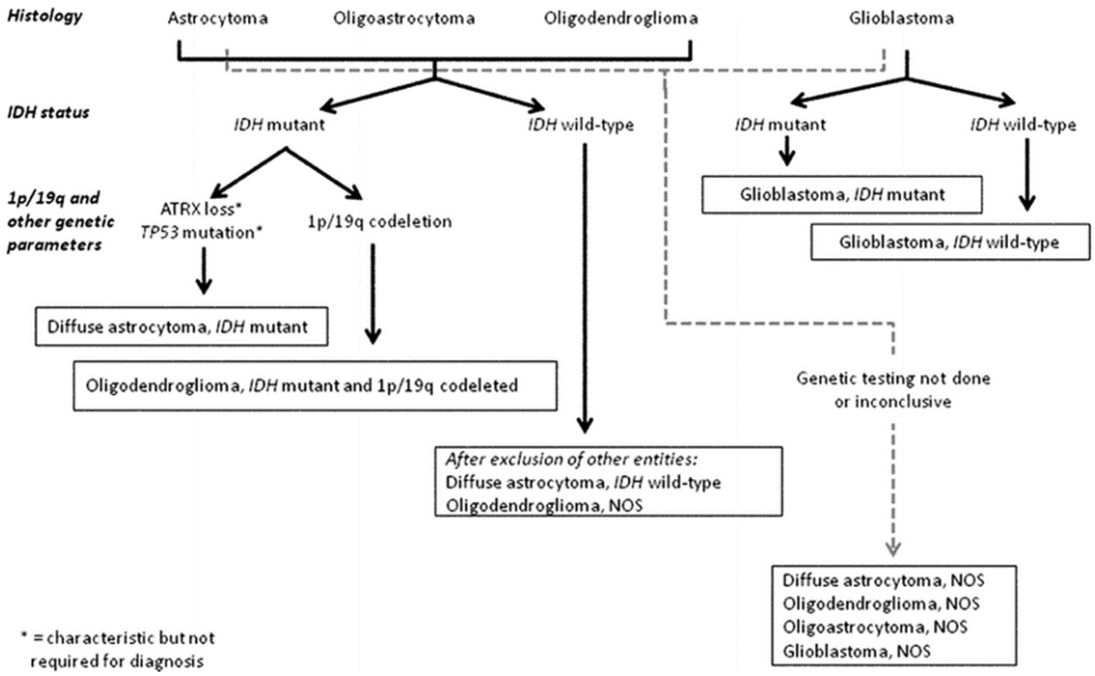

Figure 1.6 Schematic represents 2016 WHO classification of diffuse gliomas based on phenotype and genotype features. Reprinted from Louis, D. N., A. Perry, G. Reifenberger, A. von Deimling, D. Figarella-Branger, W. K. Cavenee, H. Ohgaki, O. D. Wiestler, P. Kleihues, and D. W. Ellison. 2016. The 2016 World Health Organization Classification of Tumors of the Central Nervous System: a summary. Acta Neuropathol 131: 803-820, with permission from Springer.

Oligodendroglioma accounts for 2.5% of all primary brain tumors and 8.9% of all gliomas (Ostrom et al. 2015). It is often associated with a loss of chromosome arms 1p or 19q. This type of tumor can be divided into grade II (low-grade oligodendroglioma) and grade III (high-grade, anaplastic oligodendroglioma). The molecular signatures of both grade II and III are the presence of IDH mutations together with chromosome 1p/19q co-deletion. (Louis et al. 2016). Oligodendrogliomas are not as aggressive as astrocytomas of the same grade (Huse et al. 2015). Oligodendroglioma patients respond to

chemotherapeutics and have a longer survival period (Ohgaki and Kleihues 2005). Oligodendrogliomas can be mixed with astrocytoma cells to generate mixed oligoastrocytomas.

1.6.2 Glioblastoma

Based on the 2015 report of the Central Brain Tumor Registry of the United States (CBTRUS), GB accounts for 15.1% of all primary brain and central nervous system (CNS) tumors and 55.1% of all gliomas. GB is more common in adults than in children. In young patients 0-19 years of age, these tumors accounts for 2.9% of all CNS tumors. The highest incidence rate occurs at 75-84 years of age. GB is 1.6 times more common in males and males have a higher mortality rate than females. GB has the highest number of cases of all malignant tumors, with 12,120 cases predicted in 2016. The survival rate of GB is 37.2% in the first year and declines to 5.1% and 2.6% at 5 and 10 years after diagnosis, respectively (Ostrom et al. 2015).

GB can be classified into primary and secondary GB. Primary GB develops *de novo* as an aggressive and highly invasive tumors and accounts for the majority (95%) of all GB cases. Secondary GB is less common and represents a malignant progression, during the course of several years from a pre-existing low-grade astrocytoma (grade II) or anaplastic (grade III) to the glioblastoma stage (grade IV) (Holland 2000, Wen and Kesari 2008, Gadji et al. 2009, Jovcevska et al. 2013). Primary GB is more common in older patients while secondary GB is more common in patients who are under 45 years of age (Ohgaki and Kleihues 2009). Primary and secondary GB have different molecular genetic alterations and genomic profiles **(Figure 1.7).**

Figure 1.7 Characteristics of primary and secondary glioblastoma.

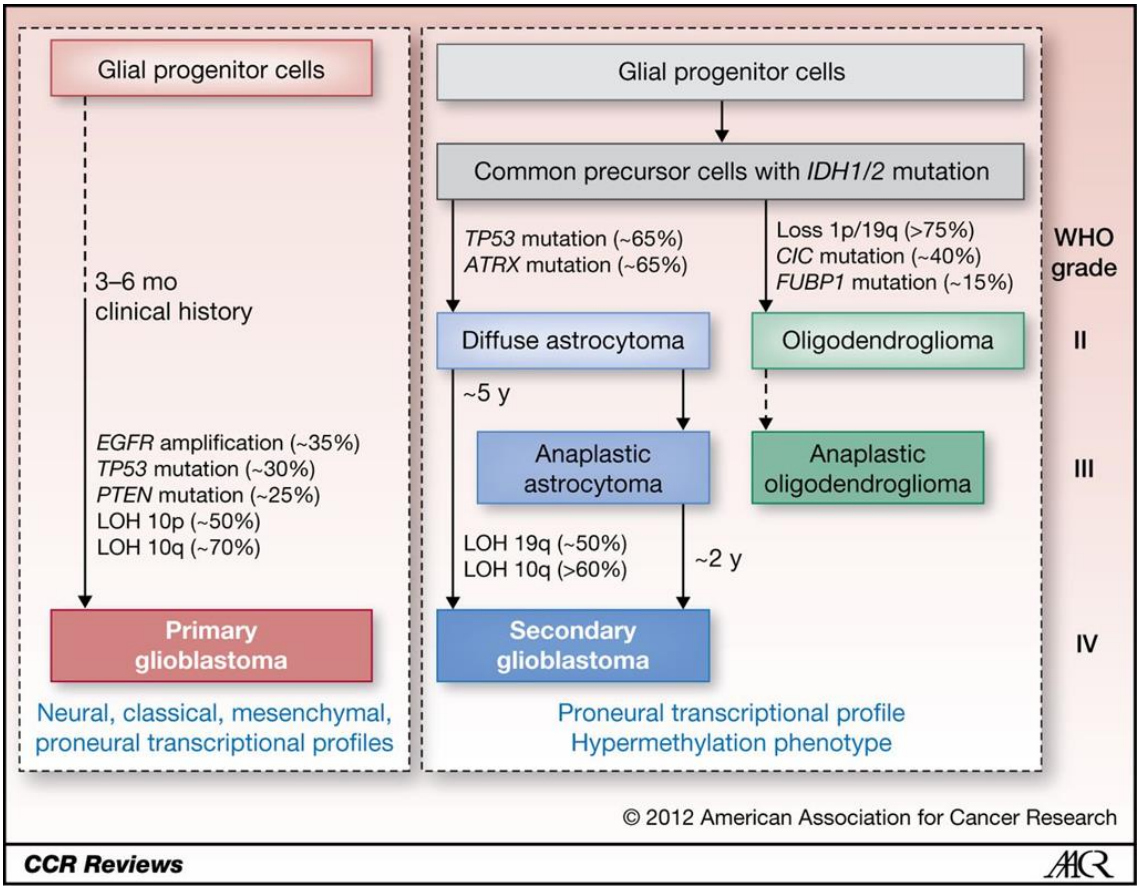

Figure 1.7 Schematic represents molecular genetic features of primary and secondary glioblastoma. Reprinted from Ohgaki, H., and P. Kleihues. 2013. The definition of primary and secondary glioblastoma. Clin Cancer Res 19: 764-772 with permission from AACR.

Primary GB frequently contain the amplification and/or mutation of epidermal growth factor receptor (EGFR) in chromosome 7p. The overexpression of mutant EGFR variant 3 (EGFCRvIII) is most common in primary GB. EGFCRvIII has an in-frame deletion of exon 2-7 in the EGFR gene, which leads to a loss of amino acids 6-271 of the extracellular domain. This leads to the expression of a truncated EGFR receptor that is constitutively active. The expression of a truncated and constitutively active EGFR protein results in increased proliferation and survival of mutated cells (Gan et al. 2013, Carrasco-

Garcia et al. 2014). Loss of heterozygosity (LOH) at locus 10p23.3, or mutation of the PTEN tumor suppressor gene, is found in 50-70% of primary GB (Ohgaki and Kleihues 2007) and TP53 mutations are observed in 30% of primary GB (Parsons et al. 2008, Ricard et al. 2012, Ohgaki and Kleihues 2013). (See GB subtypes below).

In contrast to primary GB, secondary GB more frequently show mutations of the TP53 gene located on chromosome 17p. Mutations of IDH1/2 have been identified in secondary GB, and are associated with LOH at loci 10q and 19q. These mutations have a better prognosis compared to IDH-wildtype. Amplifications of PDGFRα and PDGFRβ are also detected in secondary GB (Ohgaki and Kleihues 2007, Parsons et al. 2008, Dunn et al. 2012, Appin and Brat 2014).

1.6.3 GB subtypes

The Cancer Genome Atlas (TCGA) classifies GB into four subtypes based on gene expression patterns and copy number alteration. The four subtypes are classical, mesenchymal, proneural, and neural **(Figure 1.8).**

Figure 1.8 Genetic classification of glioblastoma subtypes

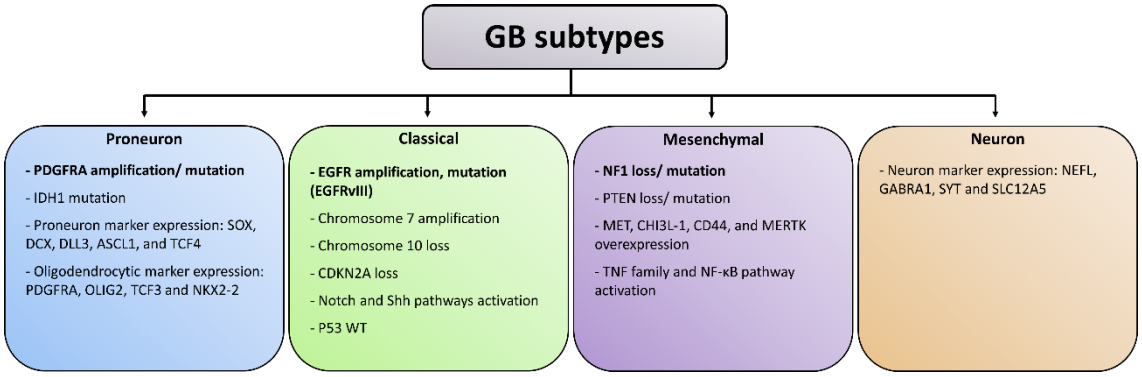

Figure 1.8 Schematic representation of glioblastoma subtypes. These classifications are defined based on the genetic alteration in different subtypes.

The **classical** subtype shows amplification of chromosome 7 in all cases. This is combined with chromosome 10 loss, high levels of EFGR amplification and point mutations, or EGFR-vIII mutation. Deletion of CDKN2A tumor suppressor gene and LOH 9p is also frequently observed in this subtype. Overexpression of the Notch and Sonic Hedgehog signaling pathways are also found in the classical GB subtype (Verhaak et al. 2010).

The **mesenchymal** subtype contains neurofibromatosis type 1 (NF1) and PTEN deletions and displays the expression of mesenchymal markers such as chitinase 3-like protein 1 (CHI3L-1) and MET proto-oncogene, receptor tyrosine kinase (MET). The mesenchymal and astrocytic markers, CD44 and c-mer proto-oncogene tyrosine kinase (MERTK), are also expressed in this subtype. Tumor necrosis factor (TNF) and NF-κB proteins are also highly expressed in this subtype (Verhaak et al. 2010). Mesenchymal features are controlled by multiple transcription factors including signal transducer and activator of transcription 3 (STAT3) and CCAAT enhancer-binding protein-β (C/EBP β) (Banerjee et al. 2010). Transcriptional co-activator with PDZ-binding motif (TAZ),

CTNND2 and rhophilin 2 (RHPN2) regulate mesenchymal transformation which associates with poor outcome (Bhat et al. 2011, Danussi et al. 2013, Frattini et al. 2013).

The **proneural** subtype displays high expression levels of platelet-derived growth factor receptor, alpha polypeptide (PDGFRA) and presents with point mutations in the isocitrate dehydrogenase 1 (IDH1) gene. Oligodendrocytic developmental genes such as PDGFRA, NKX2-2, TCF3 and OLIG2 are highly expressed in the proneural subtype, which also contains proneural development genes such as SOX, DLL3, DCX, TCF4 and ASCL1. Secondary GB which progresses from grade II and III astrocytoma belong to the proneural subtype (Phillips et al. 2006, Verhaak et al. 2010).

The **neural** subtype displays the expression of neuronal markers, including proteins associated with neuronal differentiation, such as NEFL, GABRA1, SYT1 and SLC12A5 (Verhaak et al. 2010). This subtype also shows features intermediate between proneural and mesenchymal subtypes.

The subventricular zone (SVZ) contains neural progenitor cells and is an important area associated with the pathogenesis of GB subtypes. Classical and mesenchymal subtypes are located further from the SVZ, whereas proneural and neural GB subtypes are closely associated with the SVZ (Steed et al. 2016). The proneural GB subtype has a better prognosis but the mesenchymal subtype is associated with poor survival (Phillips et al. 2006). Noushmehr et al. and Guanet al. indicated a glioma-CpG island methylator phenotype (G-CIMP) within the proneural subtype and low grade gliomas (Noushmehr et al. 2010, Guan et al. 2014). In younger patients proneural GB with G-CIMP is associated with a better outcome (median survival of 150 weeks) as compared to G-CIMP-negative proneural GB (median survival of 42 weeks) or all other non-proneural GB subtypes

(median survival of 54 weeks) (Guan et al. 2014). Moreover, mutant IDH1 always presents with a G-CIMP phenotype and these features correlate with a better prognosis (Baysan et al. 2012, Brennan et al. 2013).

1.6.4 Glioblastoma invasiveness

Aggressive invasiveness is a major feature of all malignant gliomas. GB cells can migrate along the extracellular matrix within the brain, resulting in extensive tumor infiltration of the brain (Hou et al. 2006). The constitutive GB migration pathways use the perivascular spaces in the brain parenchyma. The perivascular spaces are spaces filled with interstitial fluid that surround all blood vessels. Brain parenchyma contains functional tissues, including neurons and glial cells. Both perivascular spaces and parenchyma contain ECM and GB cells produce ECM binding molecules for their migration (Paw et al. 2015). GB invasiveness prevents a cure by surgical means only and presents a great challenge to radiation and chemotherapy.

GB cell invasion is facilitated by cell migration and degradation of ECM. Highly mobile GB cells at the leading edge of migration move and attach to ECM substrates through adhesion molecules, like integrins, and secrete proteases to degrade ECM locally to create a path for migration. Metalloproteases (MMPs) are the largest group of proteases involved in the ECM degradation process (Friedl and Wolf 2003, Rao 2003). MMP-2 and MMP-9 are common proteases that are upregulated in gliomas and are associated with an increased aggressiveness and a poor prognosis (Nakada et al. 1999, Fillmore et al. 2001, Pagenstecher et al. 2001, VanMeter et al. 2001, Rao 2003, Zhang et al. 2010).

Like other lysosomal cysteine proteases, cathepsin B (cath-B) degrades ECM components of the basement membrane and is implicated in GB invasiveness (Liotta et al.

1991, Buck et al. 1992, Lah and Kos 1998). The expression of cath-B was shown to be at the leading edge of GB cells infiltrating adjacent normal brain tissue (Mikkelsen et al. 1995). The increase in cath-B protein level and its activity are associated with progression from low to high grade glioma (Rempel et al. 1994, Demchik et al. 1999). MMPs activities might be regulated by cath-B (Eeckhout and Vaes 1977). Moreover, cath-B is upregulated in endothelial cells of high grade brain tumors and this may be relevant to the mechanism of angiogenesis. In conclusion, cath-B is part of a malignant glioma molecular signature (Demchik et al. 1999).

1.6.5 Glioblastoma chemoresistance

Standard treatments for malignant GB consist of surgical resection, as much as safely possible, or biopsy only, followed by radiation therapy, and chemotherapy. Chemotherapy of brain tumors is intended to prolong patient survival. However, chemotherapy only slows tumor growth temporarily in an attempt to sustain better quality of life for patients (Furnari et al. 2007, Krex et al. 2007, Ohgaki and Kleihues 2007).

There are many chemotherapeutic agents are used in clinical for the treatment of GB. Carmustine (BCNU) and lomustine (CCNU) are nitosoureas compounds which are used to treat GB patients. Adjuvant treatments with PCV (procarbazine, CCNU, and vincristine) improve survival rate in patients. These agents have a low capability to cross the blood brain barrier (BBB). These chemotherapies are given by intravenous, and causes side effects including nausea, vomiting, nephrotoxicity and myelosuppression (Graham and Cloughesy 2004). The most common chemotherapeutic agents widely used for GB treatment is temozolomide (TMZ) which has excellent oral bioavailability and good penetration cross the BBB. TMZ was approved by the United States Food and Drug

Administration (FDA) in March 2005 for the treatment of patients with newly diagnosed GB. TMZ administration with radiation is associated with improvement in overall and progression-free survival (Cohen et al. 2005). TMZ has a low incidence of manageable side-effects. However, tumor cell resistance can develop from fast growing GB cells, leading to low TMZ efficacy. This acquired TMZ resistance of GB cells results in relapse and the occurrence of more resistant and aggressive GB (Furnari et al. 2007, Ujifuku et al. 2010, Kohsaka et al. 2012).

TMZ is an imidazole derivative prodrug and a second generation alkylating chemotherapy agent which is stable at acidic condition but rapidly decomposes at basic and neutral conditions (Baker et al. 1999). In the systemic circulation, TMZ undergoes spontaneous hydrolysis to the active metabolite 3-methyl-(triazen-1-yl) imidazole-4-carboxamide (MTIC) which is rapidly converted to the inactive 5-aminoimidazole-4-carboxamide (AIC) and the highly reactive electrophilic alkylating methyladiazolium cation (half-life 0.4 sec). The methyladiazolium cation transfers a methyl group to DNA bases, which produces the cytotoxic effect of TMZ (Messaoudi et al. 2015) **(Figure 1.9)**. Purine bases of DNA are major sites for DNA methylation at the O^6 and N^7 positions of guanine and the N^3 position of adenine. N^7-methylguanine (N^7-MeG; 80-85%) and N^3-methyladenine (N^3-MeA; 8-18%) constitute the majority of the sites of DNA alkylation. About 5-10% of total DNA methylated lesions occur at the O^6 position of guanine which is a toxic lesion that induces apoptosis (Roos et al. 2007, Knizhnik et al. 2013). However, methylated DNA lesions produced by TMZ can be repaired by DNA repair mechanisms **(Figure 1.10)** which contributes to the development of TMZ resistance and tumor recurrence (Drablos et al. 2004, Zhang et al. 2012, Messaoudi et al. 2015).

Figure 1.9 Chemical structure and metabolism features of TMZ.

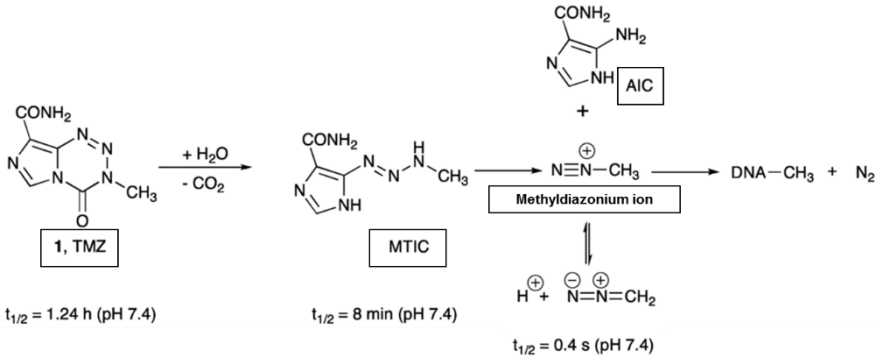

Figure 1.9 TMZ is a prodrug that hydrolyses to an active metabolite, MTIC. This active intermediate product degrades to AIC and methyldiazonium ion. The methyl group can adduct with nucleophilic sites on DNA. Adapted from Ramirez, Y. P., J. L. Weatherbee, R. T. Wheelhouse, and A. H. Ross. 2013. Glioblastoma multiforme therapy and mechanisms of resistance. Pharmaceuticals (Basel) 6: 1475-1506.

Figure 1.10 TMZ function on DNA repair pathways.

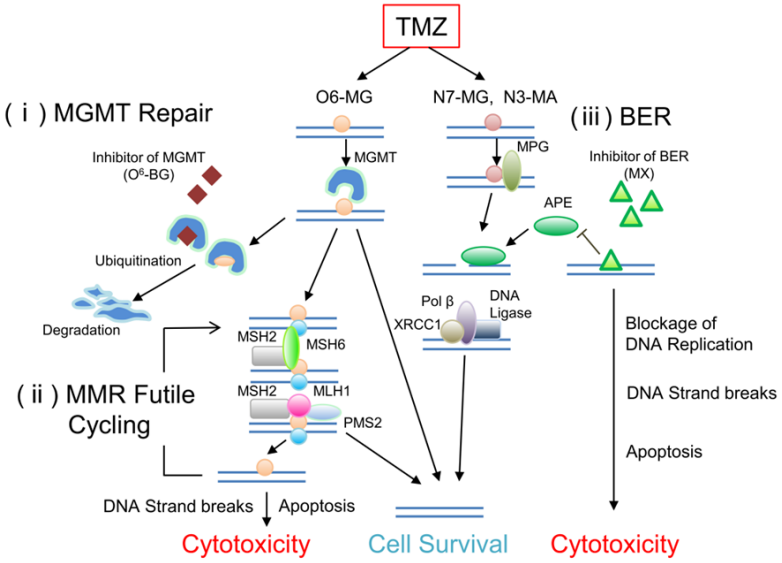

Figure 1.10 O^6-MeG, N^7-MeG, and N^3-MeA are cytotoxic lesions of TMZ which can repair by several pathways. MGMT can remove methyl group from O^6-MeG lesion. If MGMT cannot repair this lesion, unrepaired O^6-MeG is fixed by futile cycle of MMR resulting in cell death. N^7-MeG and N^3-MeA are repaired by BER. Reprinted from Shinji Kohsaka and Shinya Tanaka (2013). Chemotherapeutic Agent for Glioma, Clinical Management and Evolving Novel Therapeutic Strategies for Patients with Brain Tumors, Dr. Terry Lichtor (Ed.), InTech, DOI: 10.5772/54353. Available from: http://www.intechopen.com/books/clinical-management-and-evolving-novel-therapeutic-strategies-for-patients-with-brain-tumors/chemotherapeutic-agent-for-glioma.

1.7 DNA repair mechanisms

The O^6-methylaguanine (O^6-MeG) DNA lesion is repaired by **O^6-methylguanine-DNA methyltransferase (MGMT)** and high levels of MGMT are thought to contribute to TMZ resistance in gliomas. N^7-MeG and N^3-MeA make up over 80% of the TMZ-induced DNA lesions and are substrates for base excision repair **(BER)** (Jaiswal et al. 2009, Zhang et al. 2012). Failure to repair alkylated bases leads to cell death. Persistent O^6-MeG adducts can initiate DNA mismatch repair **(MMR)** resulting in DNA double strand breaks and apoptosis.

1.7.1 O^6-methylguanine-DNA methyltransferase (MGMT)

MGMT is an enzyme that binds to the minor groove of DNA and directly removes a methyl group from O^6-MeG without the need for co-factors. It acts as a suicide enzyme because the methyl group is transferred to a cysteine residue located within the active site of MGMT. The alkylated MGMT is degraded by the ubiquitin-proteasomal pathway. MGMT-mediated demethylation of O^6-MeG is a major mechanism of resistance in glioma where MGMT expression is regulated by epigenetic modifications (Sarkaria et al. 2008, Christmann et al. 2011, Silber et al. 2012, Fan et al. 2013). MGMT promoter methylation causes gene silencing and loss of MGMT activity is a predictor of an improved clinical outcome in GB patients receiving TMZ. Approximately 45-70% of high grade gliomas display a methylated (silenced) MGMT gene promoter and these GB patients show a better outcome (Hegi et al. 2005, Dunn et al. 2009, Uno et al. 2011, Yang et al. 2012). O^6-benzyl guanine (O^6-BG) and O^6-(4-bromothenyl) guanine are MGMT inhibitors which have been used in clinical trials preceded by TMZ treatment (Verbeek et al. 2008, Kaina et al. 2010). Both inhibitors transfer the benzyl or bromothenyl group to the active cysteine residue of

MGMT resulting in an irreversible inactivation of the enzyme (Hansen and Kelley 2000). Although a deficiency of MGMT increases the sensitivity of high grade gliomas to TMZ, brain tumors with low level MGMT can still show TMZ resistance, which suggests the possibility that additional factors contribute to chemoresistance (Fukushima et al. 2009).

1.7.2 DNA mismatch repair (MMR)

DNA mismatch repair (MMR) is a process to eliminate mismatched DNA bases during DNA replication. A TMZ induced O^6-MeG adduct may not be repaired by MGMT but mis-pairing of O^6-MeG with thymidine triggers either MMR or, in the case of futile MMR, it leads to double-strand DNA breaks, cell cycle arrest and apoptosis (Hickman and Samson 1999, Kaina et al. 2007, Sarkaria et al. 2008). Defects in the functional MMR system leads to an inadequate response to TMZ-induced mispairing and this contributes to TMZ resistance (Cahill et al. 2007, Yip et al. 2009). Normally, O^6-MeG pairing with thymidine is recognized by the heterodimeric MutS complex (MSH2 and MSH6 or MSH2 and MSH3) which recruits heterodimeric endonuclease MutL (PMS2 and MLH1). The exonuclease 1 (EXO1) removes the mismatched base and the abasic gap is filled and ligated by DNA polymerase δ/ε and DNA ligase, respectively (Iyama and Wilson 2013). In the case of mutations or defects in MMR proteins, TMZ resistance is enhanced. An inactivating mutation of MSH6 can result in unrecognized mismatch DNA bases. Upon TMZ treatment, MSH6 mutations or loss of expression can lead to TMZ resistance (Cahill et al. 2007, Yip et al. 2009). In addition, the presence of an endogenous MSH6 mutation before exposure to alkylating drugs must also be considered as a cause of TMZ resistance in gliomas (Nguyen et al. 2014).

1.7.3 Base excision repair (BER)

Base excision repair (BER) is the predominant DNA repair system in mammalian cells to repair small cytotoxic DNA base lesions resulting from oxidized, alkylated, or deaminated nucleotides. TMZ generates N^3-MeA and N^7-MeG which are recognized by the alkylpurine-DNA-N-glycosylase (APNG; also known as N-methylpurine DNA glycosylase [MPG] or 3-alkyladenine DNA glycosylase [AAG]) MPG removes the methylated base to generate an apurinic/ pyrimidinic (AP) abasic site with a cytotoxic 5'-deoxy-ribosyl phosphate (dRP) residue. This glycosylic backbone of the AP site is cleaved by the AP-lyase activity of AP endonuclease1 (APE1) and the removal of dRP site is achieved by the dRP lyase activity of DNA polymerase β. The latter adds the correct base and BER is completed by phosphodiester bond formation by the X-ray repair cross-complementing group 1 (XRCC1)/ DNA ligase III complex. Inhibition of BER improves TMZ sensitivity *in vitro* and *in vivo* (Tang et al. 2011, Kim and Wilson 2012, Wallace 2014).

The MPG expression level correlates directly with the IC_{50} of TMZ, thus, it suggests that MPG promotes TMZ resistance (Agnihotri et al. 2012). The MPG gene and protein expression increase from low to high grade gliomas and glioma patients with low MPG levels undergoing TMZ treatment have a better outcome compared to patients with high MPG expression. The presence of MPG has been described as an unfavorable independent prognostic factor for glioma patients (Liu et al. 2012). In glioma cell lines and GB tissues, MPG expression is regulated by promoter methylation and this may be linked to the methylation of the MGMT promoter. Expectedly, GB patients with methylated MGMT promoter and loss of MPG have a better outcome (Agnihotri et al. 2012).

Importantly, MPG is a direct substrate of ataxia telangiectasia mutated (ATM) kinase. MPG phosphorylation enhances enzyme function and leads to TMZ resistance in pediatric GB (Agnihotri et al. 2014). Recently, it has been reported that MPG expression is regulated by salinomycin, a drug that induces endoplasmic reticulum (ER)-stress (Xipell et al. 2016). DNA repair proteins, MGMT, MPG, and Rad51, are downregulated upon ER-stress, resulting in enhanced TMZ sensitivity and increased DNA damage. The combination treatment of salinomycin and TMZ increases apoptosis and results in longer survival of mice with brain tumors (Xipell et al. 2016).

APE1 is a key BER enzyme and high activity of APE1 is observed in several cancer cells, including GB, and correlates with resistance to alkylating drugs (Silber et al. 2002). APE1 may serve as a target for the therapeutic drug methoxyamine (MX). MX is a small molecule APE1 inhibitor that binds to AP-sites to block APE1 binding and subsequently inhibits further repair process, resulting in stalled DNA replication, DNA strand breaks and apoptosis. Hence, MX enhances the sensitivity of GB cells to TMZ (Goellner et al. 2011, Montaldi and Sakamoto-Hojo 2013).

1.8 The High Mobility Group (HMG) proteins

The high mobility group (HMG) proteins are the largest group of non-histone chromosome binding proteins. The HMG protein family can be classified into 3 sub-families: HMGA, HMGB, and HMGN. Each of sub-families has different functional binding domains. The HMGA family contains AT-hooks that allow them to bind to genomic DNA. The HMGB family has an HMG-box and the HMGN family contains a nucleosomal binding domain. All HMG proteins bind to specific structures on the DNA

resulting in conformation DNA changes to facilitate DNA transcription, DNA replication, DNA recombination and DNA repair (Cleynen and Van de Ven 2008).

1.9 High Mobility Group A (HMGA)

The sub-family of HMGA members HMGA1 and HMGA2 are architectural proteins that cause chromatin decompaction. The structure of HMGA proteins consist of 3 conserved DNA binding AT-hook motifs and an acidic C-terminal tail **(Figure 1.11)**. The AT-hook motifs are composed of K/RXRGRP (X is glycine or proline) motifs of positively charged arginine and lysine residues. These AT-hook motifs bind to AT-rich regions of the minor groove of DNA in its B-form conformation and this can facilitate gene transcription (Cleynen and Van de Ven 2008, Ozturk et al. 2014).

The level of HMGA2 expression is high in embryonic stem cells, during embryo/fetal development, and in the testis and ovary but is absent in mature differentiated adult cells (Cleynen and Van de Ven 2008, Ozturk et al. 2014). However, HMGA2 is re-expressed in many tumors, including tumors of the breast (Lin et al. 2015), colorectum (Esmailzadeh et al. 2016), prostate (Cai et al. 2016, Shi et al. 2016b), thyroid (Wu et al. 2015c), and brain (Liu et al. 2014).

Figure 1.11 Structure of HMG proteins superfamily.

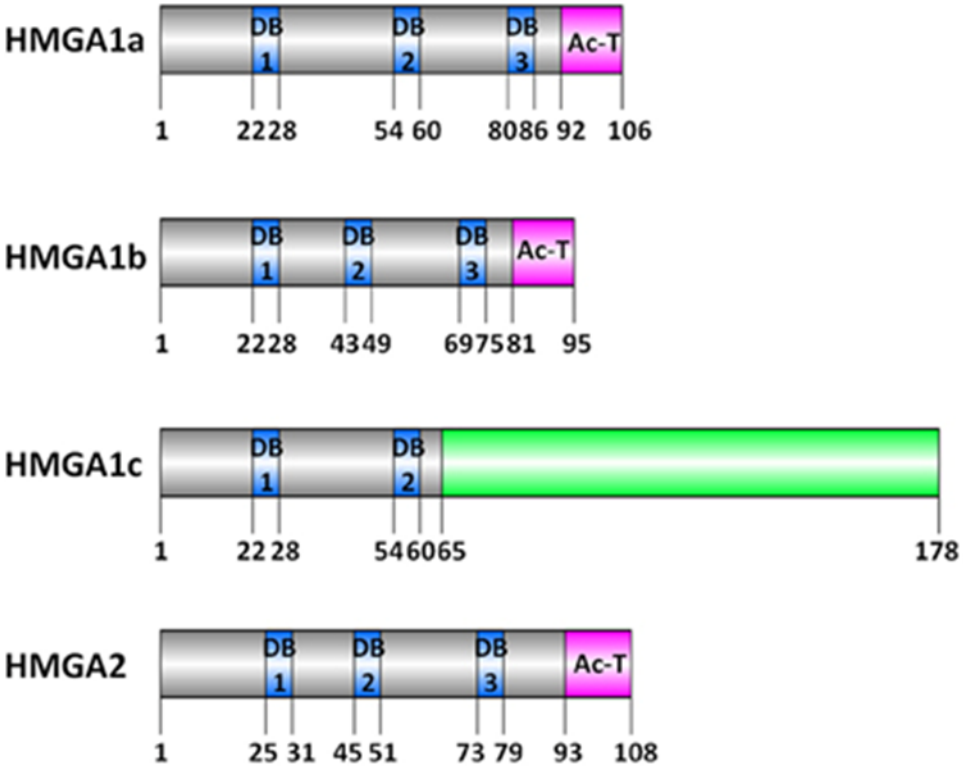

Figure 1.11 HMG proteins contain AT-hook DNA binding domains, indicate as blue boxes, and C-terminal acidic domain, indicates as pink boxes. HMGA1b lack of amino acids before the second DNA binding site compared to HMGA1a and ac. HMGA1c has different amino acids from HMGA1a and 1b, indicates as green box. Reprinted from Ozturk, N., I. Singh A. Mehta, T. Braun, and G. Barreto. 2014. HMGA proteins as modulators of chromatin structure during transcriptional activation. Front Cell Dev Biol 2: 5.

1.9.1 HMGA2 functions in embryo development

During embryogenesis HMGA2 is expressed in all tissues and is important in embryo development. Li et. al discovered the high level of HMGA2 expression during embryoid body formation in human embryonic stem cells (Li et al. 2006). Important functions of HMGA2 include mesenchymal cell lineage differentiation, human embryonic proliferation, and adipocyte cell differentiation (Li et al. 2007). The Hmga2 knockout mice

show a pygmy phenotype, including reduction in body size, and growth retardation due to decreased mesenchymal cell proliferation (Zhou et al. 1995). Moreover, Hmga2 null mice have impaired spermatogenesis which results in infertility (Chieffi et al. 2002, Di Agostino et al. 2004). Hmga2$^{-/-}$ mice have fewer adipocytes which demonstrates important roles of HMGA2 in fat cell proliferation and embryonic fibroblast proliferation (Anand and Chada 2000). Hmga2 has a role in self-renewal capacity of mouse hematopoietic and neural stem cells (Nishino et al. 2008, Copley et al. 2013). Transgenic mice carrying a gene modification resulting in a truncated HMGA2, has DNA binding domains but loss of the acidic C-terminal tail, produces a giant phenotype prone to obesity and lymphomas (Battista et al. 1999). It has also been reported that the HMGA2 chromosomal inversion in a 8-year-boy caused a truncated HMGA2 that resulted in the somatic overgrowth phenotype (Ligon et al. 2005).

1.9.2 HMGA2 in epithelial-mesenchymal transition (EMT) and stemness

The epithelial-mesenchymal transition (EMT) is a biological process, allowing cells to make the transition from an epithelial to mesenchymal phenotype. The epithelial cells lose their polarity and the interaction with the basement membrane resulting in multiple biochemical changes leading to a mesenchymal phenotype. This process enhances the production of ECM components, capacity of cell migration, cell invasion and resistance to apoptosis. Therefore, EMT is a crucial process during early embryonic development that can promote tumorigenesis, cell migration and invasion in several cancers (Kalluri and Weinberg 2009, Ye and Weinberg 2015). HMGA2 at the invasive front of the a tumor contributes to cell migration, invasion, and the recurrence after therapy (Morishita et al. 2013). The role of HMGA2 in controlling EMT involves several signaling pathways. The

transforming growth factor beta (TGF-β) signaling pathway is a key mechanism that is able to promote EMT in cancer and metastasis (Thuault et al. 2006). HMGA2 interacts with SMADs to induce the expression of SNAIL, SLUG and TWIST (transcriptional regulators of EMT), and inhibits E-cadherin expression, leading to mesenchymal transition (Thuault et al. 2008, Tan et al. 2012, Luo et al. 2013, Li et al. 2014). HMGA2 activates the Wnt/β-catenin signaling pathway to promote EMT in gastric cancer (Zha et al. 2013). Ras-MAP kinase signaling pathway is involved in the process of HMGA2 inducing EMT in human pancreatic cancers (Watanabe et al. 2009). Oncostatin M (OSM), a proinflammatory cytokine, is mediated by STAT3 signaling pathway that regulates HMGA2 to promote mesenchymal phenotype and increase the invasiveness of breast cancer cells (Guo et al. 2013).

Lee and Dutta identified the HMGA2 expression which is regulated by microRNA (miRNA), let-7 (Lee and Dutta 2007). miRNAs are small noncoding RNAs which are an important mechanism of post-transcriptional regulation. miRNAs bind to the 3' untranslated region (3'UTR) of specific mRNA targets and this leads to mRNA target degradation and translation repression (Jonas and Izaurralde 2015). Let-7 contains binding sites in the 3' UTR of the HMGA2 mRNA and the expression of let-7 is inversely correlated with HMGA2 expression (Lee and Dutta 2007). Let-7 expression is regulated by Lin28, a RNA-binding protein. Lin28 binds to the let-7 pre-miRNA to protect the production of mature let-7 miRNA. Hence, the downregulation of let-7 by Lin28 results in the increased expression of HMGA2 (Nguyen and Zhu 2015). Lin28 is highly expressed in undifferentiated embryonic stem cells and is downregulated in adult cells (Shyh-Chang and Daley 2013). However, the upregulation of Lin28 can be found in several cancer cells

(Viswanathan et al. 2009, King et al. 2011, Feng et al. 2012, Lv et al. 2012). Lin28 has roles in the regulation of self-renewal in stem cells, EMT and tumorigenesis (Liu et al. 2013). Let-7 functions as a regulator of EMT, infiltration and metastasis in cancers (Madison et al. 2013, Chen et al. 2014). Therefore, the balance between Lin28 and let-7 affects HMGA2 expression, all of which are crucial mechanisms for self-renewal in hematopoietic stem cells (Copley et al. 2013, Rowe et al. 2016), non-small cell lung cancer (NSCLC) (Alam et al. 2015) and ovarian cancer (Busch et al. 2016). The Lin-28-Let7-HMGA2 axis has effects on EMT and metastasis in NSCLC (Alam et al. 2015) and breast cancer (Guo et al. 2013).

The expression of HMGA2 promotes stem cell self-renewal capacity and proliferation in glioblastoma (Kaur et al. 2016, Zhong et al. 2016b). The expression of aldehyde dehydrogenase (ALDH) is correlated with the level of HMGA2 expression and contributes to self-renewal capacity, cell migration and chemoresistance (Moreb et al. 2008, Liu et al. 2013).ALDH is a marker for cancer stem cells and ALDH activity increased self-renewal capacity and formation of xenograft tumors and promoted resistance to chemotherapeutics (Ma et al. 2008, Ucar et al. 2009, Clay et al. 2010, Hellsten et al. 2011, Abdullah and Chow 2013). The suppression of ALDH expression causes the downregulation of HMGA2 expression in lung cancer (Moreb et al. 2008). The expression of Lin28 is positively correlated with ALDH activity to promote mammosphere formation and cell migration in breast cancer (Liu et al. 2013).

1.9.3 HMGA2 in cancer

HMGA1/2 act as proto-oncogenes that are highly expressed in several cancers and enhance oncogenic transformation. The overexpression of HMGA1 is directly associated

with phenotype transformation and xenograft tumorigenesis in immortalized cells. In malignant tumors, the level of HMGA1 increases from various embryonic tissues. Hence, it contributes to many types of cancers including breast, brain, lung, thyroid, pancreas, prostrate, colon, bladder, uterine corpus, head and neck, uterine cervix, liver, stomach, nervous system, and hematopoietic system. High expression of HMGA1 correlates with poor prognosis. (Fedele and Fusco 2010, Resar 2010, Huso and Resar 2014).

Chromosomal rearrangements of the HMGA2 gene at 12q15 results in deregulation of its tumor suppressor function and contributes to tumorigenesis of benign mesenchymal tumors, including lipomas, uterine leiomyomas, pulmonary chondroid hamartomas, fibroadenomas of the breast, endometrial polyps, pleomorphic adenomas of the salivary glands and vulvar aggressive angiomyxomas. Chromosomal aberrations of HMGA2 causes the deregulation of HMGA2, truncation of HMGA2 or fusion gene transcripts. The truncated HMGA2 lacks 3' UTR at the C-terminal as a result of the loss of the expression and function of fusion gene partners, including tumor suppressor genes, FHIT, RAD51L1, and HEI10.(Fusco and Fedele 2007, Cleynen and Van de Ven 2008, Fedele and Fusco 2010).

HMGA2 expression in cancers plays critical roles in epithelial-mesenchymal transition (EMT), migration, invasion and chemoresistance (Wang et al. 2011, Fan et al. 2016). The overexpression of HMGA2 promotes migration, invasion and correlates with tumor grade and poor prognosis in breast cancer (Wu et al. 2016b). HMGA2 can be regulated by protease activated receptor 1 (PAR1) to induce cell migration and invasion in MCF-7 cells (Yang et al. 2016). The Wnt/B-catenin signaling pathway activates upregulation of HMGA2 to induce cell proliferation in triple negative breast cancer

(TNBC). HMGA2 is used as a predictor for relapse-free-survival and metastasis in TNBC patients (Wend et al. 2013). HMGA2 is also used as a marker for the diagnosis of malignant thyroid tumors (Belge et al. 2008, Chiappetta et al. 2008).

There are several reports suggesting the expression of HMGA2 is higher in glioblastoma compared to normal brain (Kaur et al. 2016, Schwarm et al. 2016) and low grade glioma (Liu et al. 2014). Patients with HMGA2 overexpression have a shorter progression-free survival time. However, the single nucleotide polymorphisms (SNPs) of HMGA2 rs1563834 are correlated with long-term survival in glioblastoma patients (Liu et al. 2010). HMGA2 expression promotes self-renewal, invasion and tumorigenicity in GB. $CD133^{+}$ GB neurospheres have higher HMGA2 expression compared to $CD133^{-}$ cells (Kaur et al. 2016). The suppression of HMGA2 in GB neurospheres results in the loss of self-renewal and invasiveness, an increase in apoptosis and a lack of tumorigenic capacity in xenograft (Kaur et al. 2016, Zhong et al. 2016a). HMGA2 expression can be regulated by LIN28 in GB. LIN28A has a higher expression in GB compared to normal brain and low-grade glioma. The overexpression of LIN28A increases the tumor size and GB cell invasion (Mao et al. 2013). Lin28A inhibits let-7, then increases HMGA2 expression which activates a pro-invasion transcription factor, SNAI1, to promote GB cell invasion (Mao et al. 2013). Let-7a expression is lower in GB compared to normal brain. Li et. al revealed that downregulation of HMGA2 by let-7a causes a reduction of the TGF-β/Smad3 signaling pathway, leading to the inhibition of proliferation and invasion in U87 glioma cell lines (Li et al. 2016).

1.9.4 The protective roles of HMGA2

Several studies have shown that the loss of HMGA2 expression reduces cell growth, cell proliferation, colony formation and enhances apoptosis in several cancers (Kaur et al. 2015, Cai et al. 2016, Wu et al. 2016a, Zhong et al. 2016a). Knockdown of HMGA2 with paclitaxel treatment inhibits cell proliferation in breast adenocarcinoma (Mansoori et al. 2016). HMGA2 expression is regulated by let-7. Let-7 binds to the 3' UTR of HMGA2 mRNA and results in suppression of HMGA2 expression (Lee and Dutta 2007). The repression of let-7 induces HMGA2 expression and enhances chemoresistance in breast cancer (Wu et al. 2015a). The role of HMGA2 in chemoresistance remains poorly understood but includes DNA repair mechanisms.

HMGA2 has been identified as a new member of BER which can interact with APE1 to enhance chemoresistance in cancer cells. The DNA-binding domains of HMGA2 have AP-/dRP-lyase activities and promote the resistance to the alkylating agent methyl-methanesulfonate (MMS) (Summer et al. 2009). HMGA2 is a substrate of ataxia telangiectasia mutated (ATM). Upon DNA damage, ATM phosphorylates HMGA2 and this affects the regulation of ATM expression at the transcription level as HMGA2 binds to the promoter region of ATM and positively regulates ATM expression. This enhance cellular responses to DNA damage and resistance to chemotherapy in cancer cells (Palmieri et al. 2011). Also, HMGA2 interacts with ATM and Rad3-related protein (ATR) and activates checkpoint kinase 1 (CHK1) to coordinate the DNA damage response (DDR) and trigger G2/M arrest to promote chemoresistance in thyroid and fibrosarcoma cells (Natarajan et al. 2013).

1.9.5 HMGA2 as a novel therapeutic target

Overexpression of HMGA2 is associated with tumorigenesis, cell migration, invasion and chemoresistance in several cancers. Moreover, suppression of HMGA2 decreases cell proliferation, increases apoptosis, and inhibits xenograft tumors formation (Kaur et al. 2015, Cai et al. 2016, Shi et al. 2016a, Shi et al. 2016b). Therefore, HMGA2 is a potential therapeutic target. DNA minor groove binding agents, like netropsin, can compete with HMGA2 for the binding to the AT-rich DNA minor groove and impair the effects of HMGA2 (for further detail see below) (Cleynen and Van de Ven 2008). Other drugs and small molecules can reduce HMGA2 expression or interfere with Lin28-Let-7-HMGA2 regulatory pathways (Di Fazio et al. 2012, Koh et al. 2013, Wend et al. 2013, Zhang et al. 2015, Kao et al. 2016). These molecules may be used to target HMGA2 in cancer therapy.

1.9.6 DNA minor groove binding agents

Netropsin was reported as a competitor with HMGA2 to bind DNA at the specific regions of AT-hooks binding sites (Miao et al. 2008). Alonso et. al demonstrated that netropsin is a specific inhibitor of DNA binding of HMGA2, which inhibits the function of HMGA2 in the differentiation of adipocytes (Alonso et al. 2015). The inhibition of HMGA2 transcription activity by netropsin contributes to the inhibition of cell proliferation in leukemia cells (Wu et al. 2015b, Peter et al. 2016). The combination treatment of 5-azacytidine and netropsin shows a synergic effect on growth suppression in leukemia cells (Wu et al. 2015b). However, netropsin is highly toxic and its use is not clinically feasible.

Dovitinib (DOV) (TKI258/CHIR258) is an FDA-approved oral multi-tyrosine kinase inhibitor and has been used in clinical trial for several cancers. DOV is a piperazine-

linked benzimidazole-quinolinone compound and, like its structural relative Hoechst 33258 dye, DOV binds to the DNA minor groove (Hasinoff et al. 2012). DOV binding to DNA inhibits the activity of topoisomerase I and II which blocks cell growth (Hasinoff et al. 2012). DOV inhibits vascular endothelial growth factor receptor (VEGFR), fibroblast growth factor receptor (FGFR), platelet-derived growth factor receptor (PDGFR), RET proto-oncogene, and RET receptor tyrosine kinase (RET) in several cancers. DOV treatment improves the median progression-free survival (PFS). DOV inhibits the phosphorylation of STAT3 Tyr-705 residue which leads to the downregulation of downstream STAT3 targets MCL-1, survivin, and cyclin D1 and this increases apoptosis (Chen et al. 2012). Src homology region 2 domain-containing phosphatase-1 (SHP-1) is a negative regulator of STAT3 activation. DOV inhibits the growth of hepatocellular carcinoma (HCC) xenograft tumors by downregulation of phospho-STAT3 through the increased activity of SHP-1 activity (Tai et al. 2012). The DOV-SHP1-/STAT3 axis prevents EMT and metastasis and sensitizes cells to radiation and chemotherapy in hepatocellular carcinoma (Chen et al. 2012, Fan et al. 2015, Huang et al. 2016). It has been suggested that DOV is a potential therapeutic agent in cancer treatment.

Clinical trials of DOV treatment are being performed in several cancers. A phase I study is ongoing in pancreatic cancer and biliary cancers [NCT01497392]. Phase II trials are being performed in gastric cancer [NCT01719549], prostate cancer [NCT01994590], neuroendocrine tumors [NCT01635907], recurrent or metastatic salivary gland cancer of the head and neck [NCT02558387] and clear cell renal carcinoma [NCT01791387]. A phase III clinical trial with DOV was completed in metastatic renal cell carcinoma patients [NCT01223027]. The results from this study revealed that patients who received DOV did

not have a different outcome when compared to patients who received sorafenib (the third-line agent for metastatic renal cell carcinoma treatment) (Motzer et al. 2014).

DOV crosses the BBB and has been used in clinical trials on glioblastoma patients. A phase I study is ongoing in patients with recurrent glioblastoma [NCT01972750] to determine the safest dose for further testing in phase II. A phase II clinical trial is being performed in patients with recurrent or progressive glioblastoma [NCT01753713] to study how effective of the treatment.

1.10 Thesis Overview and hypotheses

Evidence suggests that the RLN2-RXFP1 system promotes cell growth and invasion in many cancers. RLN2 is a cognate ligand of RXFP1 but is not expressed in GB. This led us to attempt to identify the ligand for RXFP1 in human GB cells. P59 and P74 are small linear peptides which have sequences derived from the collagen and N-terminal region of the C1q domain of CTRP8. P59 and P74 stimulate cAMP responses via RXFP1. CTRP8 is highly expressed in GB cells.

First hypothesis: CTRP8 is an interaction partner of RXFP1 and contributes to cell migration and invasion in human GB cells.

Aim 1. To investigate whether RLN2/CTRP8-RXFP1-mediated cell migration involves PKCδ/ζ signaling which is a signaling pathway known to be activated by RLN2-RXFP1.

Aim 2. To explore whether STAT3 is a new signaling pathway for RLN2/CTRP8-RXFP1 to promote cell migration and invasion in GB cells.

Second hypothesis: RLN2/CTRP8-RXFP1 contributes to the development of TMZ chemoresistance in human GB cells.

Aim 1. To examine whether RXFP1 activation decreases DNA damage upon TMZ treatment.

Aim 2. To examine whether RXFP1 activation enhances cell survival to promote TMZ resistance.

Aim 3. To examine whether RXFP1-mediated TMZ chemoresistance involves apoptotic pathways.

Aim 4. To examine whether BER is regulated by RXFP1 and can lead to TMZ resistance.

I discovered that the RXFP1 activation by RLN2-CTRP8 upregulates the expression of HMGA2. This leads me to propose the following third hypothesis.

Third hypothesis: HMGA2 has a protective function in TMZ chemoresistance of GB cells.

Aim 1. To investigate whether HMGA2 promotes TMZ chemoresistance.

Aim 2. To investigate whether a DNA minor groove binder like HMGA2, DOV, can sensitize GB cells to TMZ in human GB cells.

Aim 3. To investigate whether the combination DOV and TMZ treatment decreases cell survival.

CHAPTER 2: MATERIALS AND METHODS

2.1 Cell culture and primary human brain isolation

Human GB tissues were obtained from GB patients treated at the Winnipeg Health Sciences Centre. This study was approved by the University of Manitoba and the Health Science Centre Department of Pathology ethics boards (ethics approval # H2010:116). Tumor tissues were washed with PBS before mincing. The small tissue pieces were digested with 0.5 mg/ml collagenase (Sigma, St Louis, MO, USA) and 10 μg/ml DNAse (Sigma) for 15-30 min at 37°C in Dulbecco's Minimal Essential and F-12 1:1 (DME/F12) medium (Hyclone, Thermo Scientific, Waltham, MA, USA) with frequent shaking. An equal volume of DME/F12 containing 10% fetal bovine serum (FBS) (Gibco, Thermo Scientific) was adding to inhibit the enzyme activities. Digested tissue pieces were filtered through a nylon mesh with 40 μm (BD Bioscience, San Diego, CA, USA) into a sterile conical tube and centrifuge at 800 rpm for 5 min. The supernatant was discarded and the pellet was resuspended in hypotonic buffer (154 mM NH_4Cl, 10 mM $KHCO_3$ and 0.1mM EDTA-Na_2) to lyse erythrocytes for 5 min at room temperature (RT) before adding sterile PBS and centrifuged at 800 rpm for 5 min. Patient GB cells were seeded into 6-well plates and grown in DME/F12 supplement with 10% FBS containing 1X penicillin/ streptomycin/ neomycin (Sigma). Cells were also cultured in stem cell medium composed of neurobasal A medium containing 1X B-27 supplement without vitamin A, 1X N2 supplement, 1X GlutaMax supplement (all Gibco, Thermo Scientific), 2 μg/ml heparin (StemCell Technologies, BC, Canada), 20 ng/ ml basic fibroblast growth factor (bFGF) and 20 ng/ml epidermal growth factor (EGF) (both Sigma). Cells were cultured passages at 37°C in a humidified 5% CO_2 atmosphere. When cells cultured at approximately 80% confluence,

cells were collected and froze in the freezing solution (DME/F12 medium containing 10% FBS with 10% DMSO) in liquid nitrogen. I have collected patient GB cells for 390 cases since December 2009.

Human GB cell lines U87MG, U251, A172, T98G, LN-18, LNT229, and U373 were cultured in DME/F12 medium containing 10% FBS at 37°C in a humidified 5% CO_2 atmosphere.

All experiments in the results part 1 and 2, cells were seeded in DME/F12 containing 10% FBS for 24 h and changed medium to DME/F12 with 1% FBS for 24 h prior the treatments. The treatments were performed in DME/F12 with 1% FBS. The experiments in the results part 3 were done in DME/F12 plus 10% FBS.

2.2 Human recombinant proteins

Human recombinant relaxin (hrRLN2) was derived from Corthera Inc. Human recombinant CTRP8 (hrCTRP8) was purchased from Creative Biomart (Shirley, NY, USA).

2.3 Recombinant CTRP8 production

The pET28a containing Flag tagged CTRP8 was manufactured by Life Technologies. The construct was transfected to *Escherichia coli* Rosetta strain. The construct pET28a-CTRP8 was cultured in LB medium with 50 μg/ml kanamycin (EMD, Millipore, Billerica, MA, USA) at 30°C in incubator shaker at 220 rpm for 16-18 h. Diluted pre-culture into 100 ml LB medium with 50 μg/ml kanamycin, incubated at 30°C until OD_{600} reached 0.6. The culture was induced with 2 mM IPTG (RPI Corp., Mount Prospect, IL, USA) for 1.30 h and samples were collected for purification. Samples were centrifuged at 6,000 rpm for 30 min at 4°C to pellet the cells. The pellets were recorded the weight and

store at -80°C or followed by the purification step. The recombinant Flag-tagged CTRP8 was purified by His-GraviTrap kit (GE healthcare, Mississauga, ON, Canada) according to the manufacturer's protocol. Flag-tagged CTRP8 was dialyzed against Tris buffer (50 mM Tris-HCl, 150 mM NaCl, pH 7.4) before determining the concentration by NanoVue spectrophotometer (GE Healthcare). The purity of the Flag-tagged CTRP8 preparation was assessed with 15% SDS-PAGE following Coomassie staining and immunoblot with the anti-Flag detection. The biological activities of CTRP8-Flag tagged were determined by the increasing of cAMP levels, the activation of PKC signaling pathway and motility assay.

2.4 Drugs and inhibitors

Temozolomide (TMZ), netropsin dihydrochloride (NET), pentamidine (PEN) and dovitinib (DOV) were purchased from Sigma.

Cells were pre-incubated with specific inhibitors in **Table 2.1** for 60 min prior to treatments with 100 ng/ml hrRLN2, 100 ng/ml hrCTRP8 or 3 μM synthetic peptides (p59 and p74; EZBiolab, Caemel, IN, USA), followed by TMZ treatment.

Table 2.1 List of inhibitors

Inhibitor name	Target	Working concentration	Company
Wortmanin	PI3-kinase	80 nM	Sigma
Tamoxifen	General PKC	1 μM	Sigma
Rottlerin	PKCδ	2.5 μM	Enzo Life Science, NY, USA
PKCζ (113-125) (myristoylated)	PKCζ	2.5 μM	Enzo Life Science
CA074	Cathepsin B	10 μM	EMD Millipore
STAT3 inhibitor VI, S3I-201	Stat3	30 μM	EMD Millipore

Table 2.2 Peptide sequences

Name	Sequences
Control peptide	GRKAFAAFAVGRKAFAAFAV
P59	GQKGQVGPPGAACRRAYAAFSVG
P74	GQKGQVGPPGAAVRRAYAAFSVGRRAYAAFSV
Competitor peptide	GSKMEGGSPGAPVQKRFFAFSVGRK

2.5 Motility assay

Cell motility was determined in 24-well Transwell chambers (BD Bioscience) with 8 μm pore size filters. The filters were coated with 40 μl of 10 μg/ml laminin (Sigma). 10,000 cells were seeded on the upper chamber of the filters and the treatments were added to the lower chamber. Cells were allowed to migrated for 24 h at 37 °C. Migrated cells at

the lower surface of filter were fixed in PBS/ methanol (1:1) for 5 min at RT followed by 10 min in methanol before staining cells with 0.1% toluidine blue in 2.5% sodium carbonate (both Sigma). The number of migrated cells was counted in five separate areas per filter under the light microscope (Olympus, Markham, ON, Canada) at 10-fold magnification. The experiments were performed with three filters per treatments. Experiments were done in triplicates.

2.6 RNA silencing

50,000 cells of primary patient GB cells per well in 6-well plates were transfected with 100 nM RXFP1 siRNA (Ambion, Thermo Scientific) using siLenFect lipid reagent (Bio-Rad, Mississauga, ON) following the treatments for 24 h. Total RNA and protein were collected for detecting RXFP1 expression level.

20,000 cells per well in 6-well plates or 2,000 cells per well in 96-well plates were transfected with 80 nM HMGA2 (Sigma), 20 nM MGMT and scrambled control siRNA (both Cell Signaling Technology) using siLenFect lipid reagent. Total protein lysates were collected at 72 h to check the protein expression levels.

2.7 RNA isolation, Reverse transcriptase polymerase chain reaction (RT-PCR) and Quantitative Real time PCR (qPCR)

Total RNA from primary human GB cells was extracted using the Trizol reagent (Ambion, Thermo Scientific) according to the manufacturers' protocol. RNA concentration was determined by measuring absorbance (A260) on the Nanovue spectrophotometer. cDNA was synthesized (**Table 2.3**) from 1 μg of total RNA and used to determine target genes expression (**Table 2.4**). PCR reaction and condition is shown in **Tables 2.5 – 2.8.** PCR products were determined by 1% agarose gel electrophoresis with

ethidium bromide staining. The images were documented by G:BOX Chemi XX6 (Syngene, Frederik, MD, USA).

Table 2.3 cDNA synthesis

component	Stock concentration	Final concentration	20 µl reaction
RNase-free water	N/A	N/A	to 11 µl
RNA samples	N/A	N/A	1 µg
dNTPs (Invitrogen, Thermo Scientific)	10 mM	0.5 mM	1
Random hexamers (Promega, Madison, WI, USA)			1
Incubation at 65 °C for 5 min and subsequently chilling on iced water for 2 min Then adding the reagents below			
First-strand buffer	5X	1X	4
DTT	100 mM	10 mM	2
SuperScript II Reverse Transcriptase (Invitrogen, Thermo Scientific)	200 U/µl	200 U	1
Incubation the reaction in the thermal cycler under the following condition			
Temperature °C		**Time (min)**	
25		10	
42		50	
72		15	

Table 2.4 Primer sequences used for RT-PCR and qPCR

Target gene	Primer's name	Primer's sequence (5' to 3')	Annealing temperature (°C)	Product size (bp)
GAPDH	F_GAPDH	CATCACCATCTTCCAGGAGCG	60	443
	R_GAPDH	TGACCTTGCCCACAGCCTTG		
RXFP1	F_RXFP1.1	AAAAGAGATGATCCTTGCCAAACG	60	297
	R_RXFP1.1	CCACCCAGATGAATGATGGAGC		
RLN2	F_Rel1/2	TCTGTTTACTACTGAACCAATTT	55	485
	R_Rel2	CATGGCAACATTTATTAGCCAA		
HMGA2	F_HMGA2.1	CACTTCAGCCCAGGGACAACC	63	290
	R_HMGA2.1	CCTCTTCGGCAGACTCTTGTGA		
CTRP1	F_CTRP1.2	ACCGCCGTGCCCCAGATCAAC	65	399
	R_CTRP1.1	CACCACCTCCTCCTCGTTCTTC		
CTRP6	F_CTRP6	ATGGTGGAGCTCACCTTTGACA	62	400
	R_CTRP6	AGCACCCATCAAGGTTCACA		
CTRP8	F_CTRP8.1	ACGGCCCACTATAGACATCGAA	58	350
	R_CTRP8.1	TGTAGTTCCAGGTGTGCACGTT		

Table 2.5 PCR master mix

Component	Stock concentration	Final concentration	25 µl Reaction (µl)
Double distilled water (ddH_2O)	N/A	N/A	18.8
PCR buffer, minus $MgCl_2$	10X	1X	2.5
$MgCl_2$	50 mM	2 mM	1.0
dNTPs	10 mM	200 µM	0.5
Forward primer	10 µM	0.2 µM	0.5
Reverse primer	10 µM	0.2 µM	0.5
Taq DNA polymerase (Invitrogen, Thermo Scientific)	5 U/µl	1 U	0.2
cDNA	N/A	N/A	1.0

Table 2.6 Thermocycling conditions for amplification of primers

Step		Annealing temperature (°C)	Time (min)
Initial denaturation		95°C	3
20-40 cycles of	Denaturation	95°C	1
	Annealing	55°C - 62°C	1
	Extension	72°C	2
Final extension		72°C	5
Hold		4°C	-

Table 2.7 PCR master mix for CTRP8

Component	Stock concentration	Final concentration	20 µl Reaction (µl)
Double distilled water (ddH_2O)	N/A	N/A	11.8
Phusion GC buffer	5X	1X	4.0
dNTPs	10 mM	200 µM	0.4
Forward primer	10 µM	0.5 µM	1.0
Reverse primer	10 µM	0.5 µM	1.0
DMSO	100%	3%	0.6
Phusion DNA polymerase (New England Biolabs, USA)		1U	0.2
cDNA	N/A	N/A	1.0

Table 2.8 Thermocycling conditions for CTRP8 amplification

Step		Annealing temperature (°C)	Time (sec)
Initial denaturation		98°C	30
40 cycles of	Denaturation	98°C	10
	Annealing	62°C	30
	Extension	72°C	30
Final extension		72°C	10
Hold		4°C	

Quantitative real-time PCR (qPCR) was performed as shown in **Table 2.9** using QuantStudio® 3 system (Applied Biosystems, Thermo Scientific). Each sample was done in triplicate. Data analysis was performed by the comparative C_T ($\Delta\Delta C_T$) method using

QuantStudio® Design & Analysis software. Samples were normalized to the expression of GAPDH.

Table 2.9 qPCR master mix

Component	Stock concentration	Final concentration	20 µl Reaction (µl)
Double distilled water (ddH_2O)	N/A	N/A	8.2
PowerUp ™ SYBR ® green Master Mix (Applied Biosystems, Thermo Scientific)	2X	1X	10
Forward primer	10 µM	0.2 µM	0.4
Reverse primer	10 µM	0.2 µM	0.4
cDNA	N/A	N/A	1.0

2.8 Cell viability assay (WST assay)

5,000 cells of primary patient GB cells were cultured in 96-well plates and treated with 100 ng/ml hrRLN2, hrCTRP8 for 24 h followed by 1.5 mM TMZ 24 h. Cell cytotoxicity was measured using WST-1 reagent (10 µl/ well; Roche, Indianapolis, IN, USA). The plates were incubated for 4 h at 37 °C and the absorbance was measured at 450 nm using a 96-well plate reader (Wallac, PerkinElmer, Boston, MA, USA).

The xCelligence system (ACEA Biosciences, Inc., San Diego, CA, USA) is a new technology for monitoring real-time cell analysis. This technology relies on the 96-well culture plates with gold micro electrode at the bottom of the plate (E-plate). The system detects the changing of cellular impedance across the electrodes and represented the data

as cell index (CI) which is automatically calculated by the system. CI value is influenced by cell number, cell size, and cell attachment. This system can also determine real-time cell cytotoxicity, cell growth and cell death. The cellular impedance is recorded every 15 min using the RTCA software. Patient GB cells were cultured in E-plate and treated with siRXFP1 followed by 100 ng/ml hrCTRP8/hrRLN2 and 1.5 mM TMZ. Cell cytotoxicity was monitored and recorded. CI values were calculated accordingly based on changes in cell growth during an experiment.

2.9 Caspase 3/7 activity assay

Caspase 3/7 activity assay was determined by using commercial Caspase-Glo 3/7 reagent (Promega). The assay was performed according to the manufacturer's instructions. To determine caspase 3/7 activity after the treatments as indicated, an equal volume of Caspase-Glo 3/7 reagent was added to the samples in a 96-well plate and incubated with a shaking at 350 rpm for 4 h at RT prior to detecting luminescence signal on a plate-reading luminometer (Wallac, PerkinElmer).

2.10 Comet assay

Cells were plated at 50,000 cells per well into 6-well plates. After treatment with 100 ng/ml hrRLN2/hrCTRP8 and 1.5 mM TMZ, cells were harvested and DNA damage was assessed using a comet assay kit (Trivigen, Gaithersburg, MD, USA) according to manufacturer's instructions. Briefly, cells were embedded in low melting point agarose on glass slides. Once the agarose on the slides was solidified, the slides were maintained in a pre-chilled lysis solution at 4°C for 45 min. Slides were then incubated in an alkaline solution for 20 min at RT followed by electrophoresis with the fresh electrophoresis buffer for 15 min at 25 volts and 0.8 amps. Next, slides were successively dehydrated with 70%

and 100% ethanol for 20 min. Dried slides were stained with SYBR green. Comet images were observed using a Z2 microscope (Zeiss, Jena, Germany). The comet tail length was quantified using the Comet Assay IV software (Perceptive, Bury St Edmunds, UK).

2.11 Immunofluorescence

Patient GB cells were seeded on a cover slip for 24 h. Cells were treated with 100 ng/ml hrRLN2/hrCTRP8, and 1.5 mM TMZ for 24 h, then fixed in 3.7% formaldehyde for 20 min at RT. The nonspecific antibody binding sites were blocked for 2 h at RT with 1% BSA (EMD, Millipore) in 0.1% Triton X-100 plus 5% rabbit normal serum (blocking buffer; Sigma). GB cells were immunostained overnight with γH2AX (EMD, Millipore) in blocking buffer at 4°C prior to incubation with AlexaFlour-594-conjugated rabbit anti-mouse (Invitrogen, Thermo Scientific) for 1 h at RT. For nuclear staining, cells were counterstained with 0.1 μg/ml DAPI (Sigma) and mounted with Fluoromount aqueous mounting medium (Sigma). Cells were imaged using a Z2 microscope (Zeiss).

To detect HMGA2 expression, U251 cells were transfected with 80 nM HMGA2 siRNA for 72 h and then fixed with 3.7% formaldehyde, blocked with 1% BSA in 0.1% Triton X-100 plus goat normal serum for 2h at RT and incubated with HMGA2 (Cell Signaling Technology) overnight at 4 °C. AlexaFluor-594 conjugated goat anti rabbit (Invitrogen, Thermo Scientific) was used as a secondary antibody for 1 h at RT. Cells were counterstained with DAPI and mounted with Fluoromount aqueous mounting medium.

2.12 Immunohistochemistry

Deparaffinated human GB tissue sections (5 μm) were incubated with 3% H_2O_2 in methanol for 20 min at RT in the dark to quench endogenous peroxidase. Antigen retrieval was performed by boiling the tissue sections in citrate buffer for 4 min prior to incubate at

90°C for 30 min. The tissue sections were incubated with blocking buffer (10% goat normal serum in Tris buffered saline (TBS) with 0.1% Tween-20 (TBS/T)) for 1 h at RT and incubated with goat anti-CTRP8 (1:100) (Santa Cruz Biotechnology, Dallas, Texas, USA) and rabbit anti-RXFP1 (1:200) (Phoenix Pharmaceuticals, CA, USA) at 4°C overnight. Goat and rabbit isotype IgG (Vector Laboratories, Burlington, ON, Canada) were used as negative controls. The sections were incubated with biotinylated IgG (1:200) (Vector Laboratories) for 1 h at RT, followed by incubation with avidin complexed to biotin-conjugated horseradish peroxidase (Vectastain Elite ABC kit; Vector Laboratories) for 30 min. The immunostaining was developed with DAB substrate (Thermo Scientific) prior counterstained with hematoxylin, coverslipped and imaged by bright field A2 microscope (Zeiss)

Tissue microarrays from US Biomax, Inc were blocked endogenous peroxidase by 3% H_2O_2 followed by antigen retrieval as previously described. Non-specific binding sites in the tissue arrays were blocked with 5% goat normal serum in TBS/T for 1 h at RT. The arrays were incubated with rabbit anti-HMGA2 (1:200) (Cell signaling Technology) at 4 °C overnight prior incubated with biotinylated anti-rabbit IgG (1:200) for 1h at RT. The avidin complexed to biotin-conjugated horseradish peroxidase was incubated with the arrays for 30 min followed by DAB stain development. Tissue array sections were counterstained with hematoxylin, coverslipped and imaged by bright field A2 microscope (Zeiss).

2.13 Western blot analysis

Protein lysates were subjected to 10-15% SDS-PAGE and the proteins were transferred to a nitrocellulose membrane. For immunodetection, the blocking of non-

specific protein binding sites was done by incubating in 5% non-fat milk in TBS/T for 1 h at RT. Membranes were washed with TBS/T 3 times for 5 min each before being incubated with primary antibody in blocking buffer or 5% BSA in TBS/T at 4°C overnight, depending on the manufacturer's recommendation. Membranes were then washed with TBS/T 3 times 5 min each at RT before adding the secondary antibody in blocking buffer for 1 h at RT. The antigen-antibody complexes were detected with ECL (Thermo Scientific) or ECL prime (GE Healthcare) and by exposing membranes to Amersham Hyperfilm (GE Healthcare). If necessary, membranes were stripped with stripping solution (20% SDS in Tris pH 6.8) for 20 min at 72°C and reprobed with primary antibody. The antibodies that were used are listed in the **Table 2.10**

Table 2.10 List of antibodies

Target protein	Company and catalog number	Specie	Dilution	Expected size (kDa)
β-actin	Sigma #A5441	Mouse monoclonal	1:10000	47
Flag® M2	Sigma #F1804	Mouse monoclonal	1:1000	N/A
Phospho-PKCδ (Thr505)	Cell Signaling Technology #9374	Rabbit polyclonal	1:1000	76
PKCδ	Cell Signaling Technology #2058	Rabbit polyclonal	1:1000	76
Phospho-PKCζ/λ (Thr410/403)	Cell Signaling Technology #9378	Rabbit polyclonal	1:1000	78
PKCζ (C24E6)	Cell Signaling Technology #9368	Rabbit monoclonal	1:1000	78

Phospho-Stat3 (Tyr705) (D3A7) XP®	Cell Signaling Technology #9145	Rabbit monoclonal	1:1000	86
Stat3 (79D7)	Cell Signaling Technology #4904	Rabbit monoclonal	1:2000	86
Cathepsin B	Dr. E. Weber-Martin Luther University, Halle, Germany	Mouse monoclonal	1:500	25, 30
MPG [EPR10959(B)]	Abcam (Toronto, ON, Canada) #AB155092	Rabbit monoclonal	1:3000	33
Bcl-2 (50E3)	Cell Signaling Technology #2870	Rabbit monoclonal	1:1000	26
Bcl-XL (54H6)	Cell Signaling Technology #2764	Rabbit monoclonal	1:1000	30
Phospho-Histone H2A.X (ser139), (γH2AX)	Cell Signaling Technology #2577	Rabbit	1:1000	15
HMGA2	Cell Signaling Technology #5269	Rabbit polyclonal	1:1000	18
HMGA1 (D6A4) XP®	Cell Signaling Technology #7777	Rabbit monoclonal	1:1000	18
APE1 [13B8E5C2]	Abcam #AB194	Mouse monoclonal	1:2000	36
XRCC1	Cell Signaling Technology #2735	Rabbit monoclonal	1:1000	82
DNA pol β [61]	Abcam #AB1831	Mouse monoclonal	1:500	38
PARP-1 (46D11)	Cell Signaling Technology #9532	Rabbit monoclonal	1:1000	89, 116

Fen 1	Bethyl Laboratories (Montgomery, Texas, USA) #A300-256A	Rabbit polyclonal	1:1000	45
MGMT	Cell Signaling Technology #2739	Rabbit monoclonal	1:1000	21
Lin28A	Abcam #AB124765	Rabbit monoclonal	1:1000	28
Lamin A/C (N-18)	Santa Cruz Biotechnology #sc-6215	Goat polyclonal	1:500	62, 69
α-tubulin	Cell Signaling Technologies #2144	Rabbit polyclonal	1:1000	56
Mouse HRP	Sigma #A5278	Goat	1:10000	
Rabbit HRP	Cell Signaling Technologies #7074	Goat	1:2000	
Goat HRP	Santa Cruz Biotechnology #sc-2768	Rabbit	1:10000	

2.14 MPG molecular beacon activity assay

I applied real-time molecular beacon assay to measure the activity of DNA glycosylase MPG in nuclear lysates (Svilar et al. 2012). The molecular beacon substrate is a stem-loop hairpin oligodeoxynucleotides structure which contains deoxyinosine (dI) as a substrate for MPG to remove. There is a 5' 6-FAM (fluorescein) and a 3' Dabcyl (quencher) at the ends of the hairpin loop beacons. Once the removal of dI, a 6-base pair single strand DNA which contains 6-FAM at 5' end, is separated from the quencher at 3' end of beacon substrate there is an increase in the fluorescence signal. Oligodeoxyribonucleotides (**Table 2.11)** were purchased from Integrated DNA

Technologies (Coralville, IA, USA). The activity assay was performed as previously described (Svilar et al. 2012). Briefly, to confirm that the beacons formed a stem loop structure, the beacons were incubated at 95 °C for 3 min and slowly cooled to RT on the benchtop. There was no fluorescence signal when the beacons formed a stable hairpin loop at 37°C. Once, the hairpin loop beacons were heated to 95°C, the structures were unfolded resulting in the maximum fluorescence signal. Nuclear protein lysates were extracted using NE-PER nuclear and cytoplasmic extraction reagents (Thermo Scientific) according to manufacturer's instruction. Nuclear protein lysates (10 μg) were incubated with 40 nM beacon probes. The fluorescence signal was detected at 37°C every 20 secs and monitored for 120 min using a QuantStudio® 3 system.

Table 2.11 Molecular beacon probe sequences

Name	Sequences	X
control	5'-/6-FAM/ GCACTATTGAATTGACACGCCATGTCGATCA ATTCAATAGTGC/3Dab/-3'	
MPG	5'-/6FAM/ GCACT/**X**/TTGAATTGACACGCCATGTCGATC AATTCAATAGTGC/3Dab/-3'	Deoxyinosine (dI)

2.15 Measurement of apoptosis by flow cytometry

I used the Nicoletti method to measure apoptosis. Briefly, 20,000 cells of U251 and 50,000 of primary patient GB cells were seeded into 6-well plates and treated with either 100 μM TMZ, 2 or 5 μM DOV, or combination of DOV and TMZ for 24-48h. Cells were detached using an EDTA solution and then harvested by centrifugation at 1,500 g, 4°C for

5 min. Cells were wash once with ice-cold PBS and then resuspended in hypotonic propidium iodine (PI, Sigma) lysis buffer (1% sodium citrate, 0.1% Triton X-100, 0.5 mg/ml RNase A, 40 μg/ml PI), and incubated at RT for 20 min under dark conditions. Cell nuclei were then analyzed by flow cytometry (two laser FacsCalibur from BD). Nuclei to the left of the M1 peak containing hypodiploid DNA were considered to be apoptotic.

2.16 Colony formation assay

20,000 cells of U251 and 30,000 cells of PBS-10 were seeded in triplicates into 6-well plates and 5 cycles of alternating treatments of 5 μM DOV and 100 μM TMZ were performed every 3 days followed by recovery in normal medium for 9 days. At the end of the treatment cycles, live cells were counted by trypan blue exclusion staining and 100 trypan blue negative and presumed living cells were seeded in a 6 well plate for the recovery experiment. Control experiments were conducted in triplicate wells in 6-well plates where 5 cycles of alternating treatment were performed in normal growth medium and 100 μM TMZ every 3 days, followed by recovery in normal growth medium for 9 days. At the end of the recovery period, the number of colonies formed were counted with a 20x objective under phase contrast with an inverted microscope (Zeiss).

2.17 Statistical analysis

All experiments were done in triplicate. The results are showed as mean ± standard deviation (SD). Data were analyzed with GraphPad Prism 6 statistical software using One-way and Two-way ANOVA. Bonferroni and Tukey's post-hoc statistical tests were performed to confirm the differences between groups. P values less than 0.05 were considered as significant. The level of significance was defined as *$p<0.05$, **$p<0.01$, and ***$p<0.001$.

CHAPTER 3: RESULTS

Part I. Human CTRP8 is a new ligand of RXFP1 and induces migration of brain cancer cells

In patient GB cells, I detected high gene expression of RXFP1 but not of the cognate ligand RLN2. This leads me to search for a new ligand which can bind and activate the signal through RXFP1. Two snall peptides, P59 and P74 were shown to bind to and activate RXFP1 as determined by an increase in cellular cAMP in CHO-1 cells (Shemesh et al. 2008). Moreover, part of the sequence of P59 and P74 was identical to an amino acid region located within C1Q globular domain of CTRP8 protein. RXFP1 activation has been shown to enhance cell migration and cell invasion in thyroid, breast, and prostate cancer cells (Hombach-Klonisch et al. 2006, Radestock et al. 2008, Feng et al. 2009) . Therefore, I hypothesized that CTRP8 is a new agonist of RXFP1 and can promote cell migration and invasion in human GB cells. The data from this part of my studies were published in Glogowska, A., et al., *C1q-tumor necrosis factor-related protein 8 (CTRP8) is a novel interaction partner of relaxin receptor RXFP1 in human brain cancer cells*. J Pathol, 2013. Dec; 231 (4):466-79. The data from the experiments I had performed are presented in my thesis below.

3.1 Expression of RXFP1 and CTRP8 in GB cell lines and human primary brain tumor cells

A tumor cell bank of patient GB cells derived from brain tumor patients was established in collaboration with the Section of Neurosurgery and the Department of Human Anatomy & Cell Science, University of Manitoba. I investigated the expression of RXFP1, human relaxin 2 (RLN2) and CTRP8 by RT-PCR in normal human astrocytes

(HA), patient GB cells and GB cell lines. RXFP1 expression was detected in HA, and GB cell lines including, U87MG, T98G, LN18, and LNT229 **(Figure 3.1A)** and in all patient GB cells **(Figure 3.1B)**. None of the patient GB cells expressed RLN1 or RLN2 but RLN2 transcripts were weakly expressed in some GB cell lines, U373, U251, LNT229 **(Figure 3.1C and D)**. CTRP8 was strongly expressed in HA, all patient GB cells, GB cell lines **(Figure 3.1A and B)**. I also investigated the expression of CTRP1 and CTRP6, which are structurally closely related to CTRP8. CTRP1 and CTRP6 mRNA were detected in HA and GB cells **(Figure 3.1A and B)**. Using immunohistochemistry, I detected the presence of cells weakly positive for RXFP1 and CTRP8 in human GB tissues **(Figure 3.2A and C)**. When the specific immune serum was replaced by an isotype IgG non-immune serum no specific immunostaining was observed **(Figure 3.2B and D)**.

Figure 3.1 Expression of RXFP1 and RXFP1 agonists.

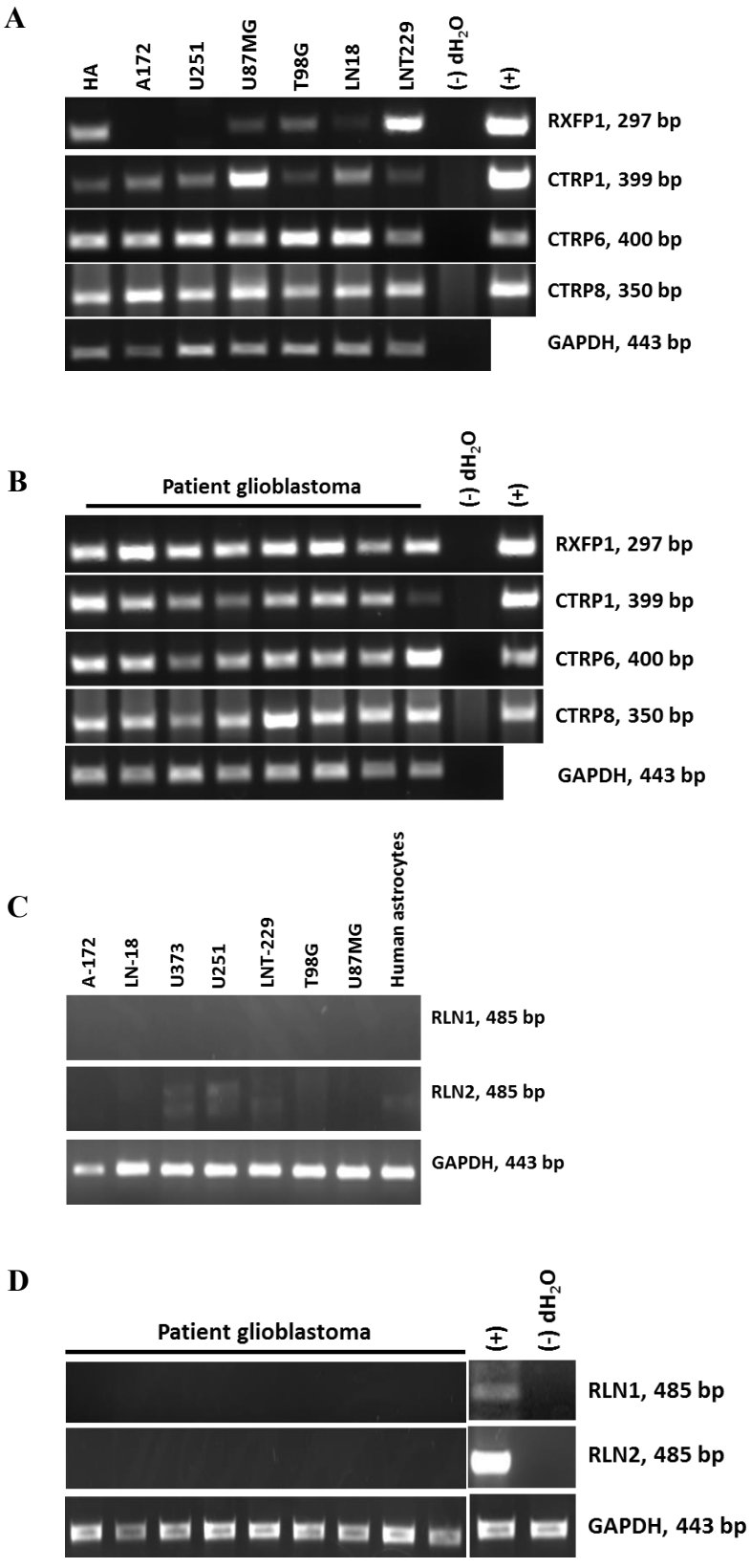

Figure 3.1 Gene expression of RXFP1 and RXFP1 agonists in human patient GB cells and established GB cell lines. mRNA levels of RXFP1, CTRP1/6/8, RLN1/2 were determined by semiquantitative RT-PCR. The expression of RXFP1, CTRP1/6/8 are shown in **A** and **B**. RLN1 and RLN2 were expressed in **(C)** GB cell lines and **(D)** patient GB cells. Some data were published in Glogowska, A., et al., C1q-tumor necrosis factor-related protein 8 (CTRP8) is a novel interaction partner of relaxin receptor RXFP1 in human brain cancer cells. J Pathol, 2013.

Figure 3.2 Representative images of immunohistochemical detection of human patient.

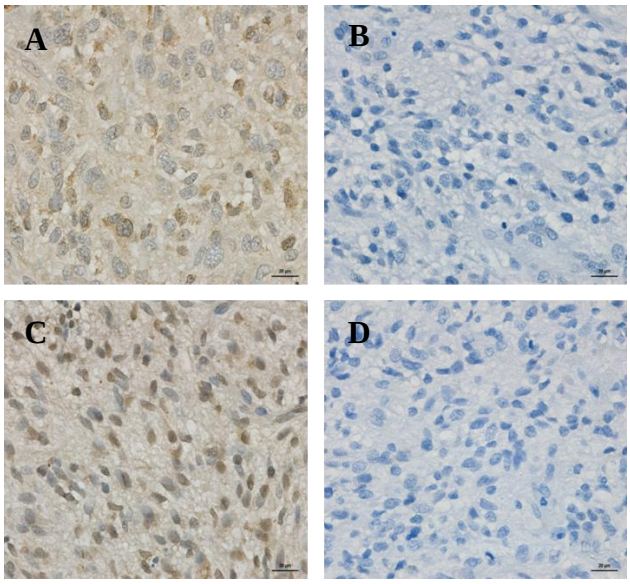

Figure 3.2 (A) RXFP1^{+} and **(C)** CTRP8^{+} GB tissue sections. For negative control, the **(B)** rabbit and **(D)** goat IgG isotype control shoed no immunostaining. Magnification: A-D, x400. Data were published in Glogowska, A., et al., C1q-tumor necrosis factor-related protein 8 (CTRP8) is a novel interaction partner of relaxin receptor RXFP1 in human brain cancer cells. J Pathol, 2013.

3.2 RXFP1 activation induced cell migration by PKC-dependent pathways

To explore the function of CTRP8 and the short linear peptides P59 and P74 on cell migration, transwell migration assays were performed with patient RXFP1^{+} GB cells treated with human recombinant (hr)RLN2 and hrCTRP8. It has been previously reported that P59 and P74 increase intracellular cAMP levels via activation of RXFP1. GB cell migration was significantly increased upon 24h treatment with hrRLN2, hrCTRP8, and P59 but not P74 **(Figure 3.3A)**. Treatment with hrRLN2, hrCTRP8 or peptides failed to increase GB cell migration upon knockdown of RXFP1 with a specific siRNA to RXFP1. RT-PCR showed the successful downregulation of RXFP1 expression upon siRXFP1 treatment **(Figure 3.3B)**. A control peptide with scrambled amino acid (aa) sequence was used as a negative control in the migration assay with the peptides P59 and P74. The scrambled peptide had no effect on GB cell migration. The results suggested that hrRLN2, hrCTRP8, P59, and P74 required RXFP1 to induce cell migration.

Figure 3.3 hrRLN2, hrCTRP8, P59, and P74 induced cell migration.

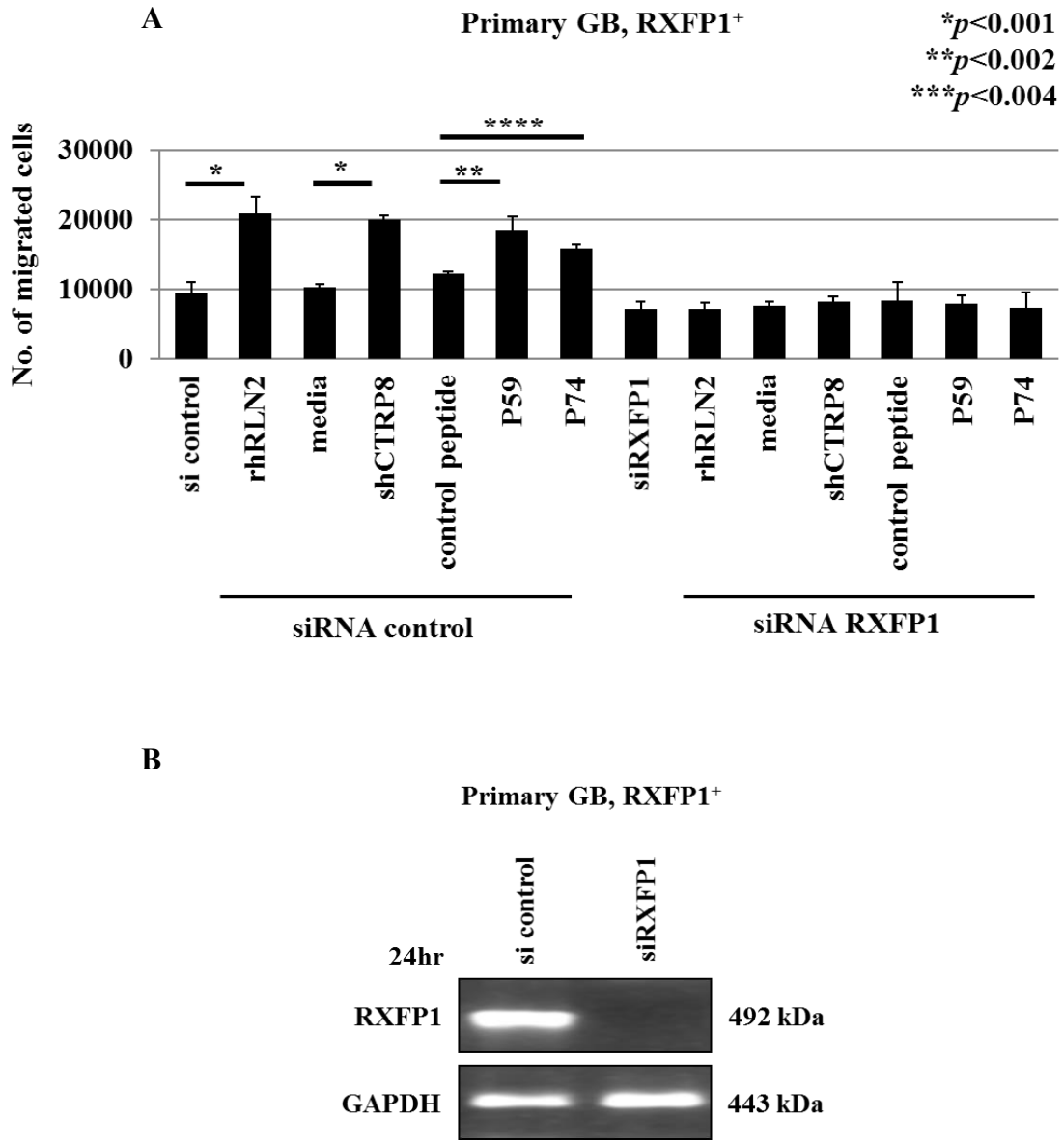

Figure 3.3 Effect of 100 ng/ml of hrRLN2, hrCTRP8, 3μM of P59 and P74 on cell migration. **(A)** Cell migration was performed by transwell chamber migration assay in patient RXFP1+/- GB cells. **(B)** RT-PCR was showed a knockdown of RXFP1 expression by a specific siRNA to RXFP1. Data were published in Glogowska, A., et al., C1q-tumor necrosis factor-related protein 8 (CTRP8) is a novel interaction partner of relaxin receptor RXFP1 in human brain cancer cells. J Pathol, 2013.

It has been reported that hrRLN2 binding to RXFP1 activates the PKC pathway (Bathgate et al. 2013). I investigated whether hrCTRP8, P59 and P74 peptides, in addition to hrRLN2, activates the PKC signaling pathway. Exposure of patient RXFP1^{+} GB cells to hrRLN2, hrCTRP8, P59, and P74 increased the phosphorylation of PKCδ and PKCζ **(Figure 3.4A, left panel)**, whereas the control peptide did not induce phosphorylation of these or other PKC isoforms. The phosphorylation of PKCδ and PKCζ was inhibited by wortmanin, a PI3 kinase inhibitor. Rottletin and PKCζ myristoylated peptide$^{113\text{-}125}$, specific inhibitors for PKCδ and PKCζ, respectively, blocked the phosphorylation of both PKCδ and PKCζ in the presence of the RXFP1 ligands hrRLN2, hrCTRP8 and peptides. Total PKCδ and PKCζ protein levels were not changed under the specific inhibitor treatments **(Figure 3.4A, right panel)**. I performed cell migration assays to investigate whether this PKC signaling response triggered by RXFP1 agonists contributed to cell migration. When cells were exposed to rottletin **(Figure 3.4B)** or PKCζ myristoylated peptide$^{113\text{-}125}$ **(Figure 3.4C)**, hrRLN2, hrCTRP8 and peptides failed to induce cell migration in patient RXFP1^{+} GB cells, suggesting that the activation of RXFP1 promotes PKCδ/ζ signaling and the increase in cell migration.

Figure 3.4 hrRLN2, hrCTRP8, P59, and P74 induced cell migration through PKC-dependent pathway.

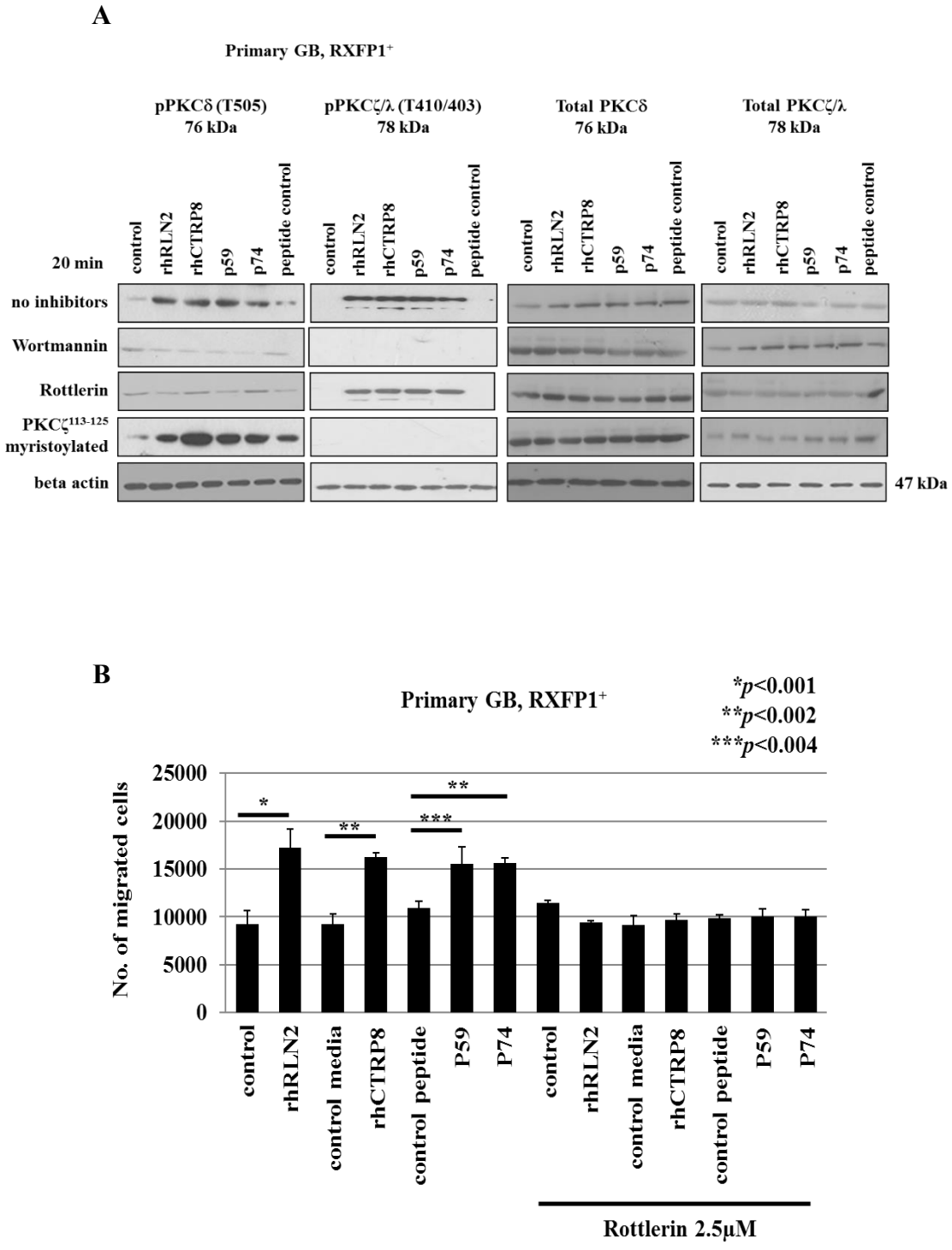

C

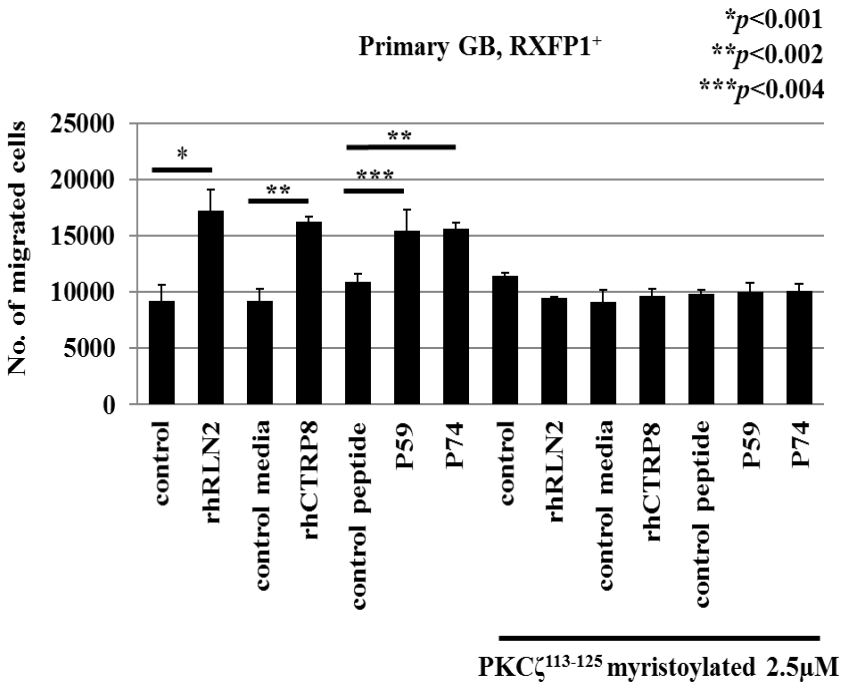

Figure 3.4 (A) Western blot analysis of total and phosphorylated (p)PKCδ and PKCζ in patient RXFP1^{+} GB cells following exposure to RXFP1 agonists in the presence 80 nM of wortmanin, 2.5 μM of rottlerin, or PKCζ myristoylated peptide$^{113-125}$. Transwell cell migration was performed with patient GB cells exposed to RXFP1 agonists in the presence of **(B)** rolttlerin or **(C)** PKCζ myristoylated peptide$^{113-125}$. Data were published in Glogowska, A., et al., C1q-tumor necrosis factor-related protein 8 (CTRP8) is a novel interaction partner of relaxin receptor RXFP1 in human brain cancer cells. J Pathol, 2013.

It was previously shown that RLN2 can increase the expression of cathepsin proteins (Hombach-Klonisch et al. 2006). Here, I studied whether hrRLN2, hrCTRP8, P59, and P74 can induce the expression and secretion of cathepsin B, a lysosomal protease, which is a marker for cell invasiveness in malignant brain tumors (Glogowska et al. 2013). Cathepsin B expression and secretion increased in patient GB cells upon RXFP1 activation **(Figure 3.5A)**. The increase in both the expression and secretion of cathepsin B was blocked by wortmanin, rottletin and PKCζ myristoylated peptide$^{113\text{-}125}$. I performed a laminin migration assay to demonstrate the ability of GB cells in the presence of enhanced secretion of cathepsin B to penetrate the laminin ECM. Laminin is a major component of basement membrane in the brain and a substrate for cathepsin B. Treatment with hrRLN2, hrCTRP8, P59 or P74 markedly increased invasion of RXFP1^{+} GB cells into the laminin matrix **(Figure 3.5B)**. The specific cathepsin B inhibitor CA074 was able to inhibit the ability of the RXFP1 agonists to enhance invasion of GB cells into the matrix. The results indicated that hrRLN2, hrCTRP8, P59, and P74 can activate RXFP1 which results in the activation of PI3 kinase and subsequent phosphorylation of PKCδ and PKCζ. This contributes to an increase in the production and secretion of cathepsin B and leads to enhanced cell migration.

Figure 3.5 RFXP1 activation induced the production and secretion of cathepsin B.

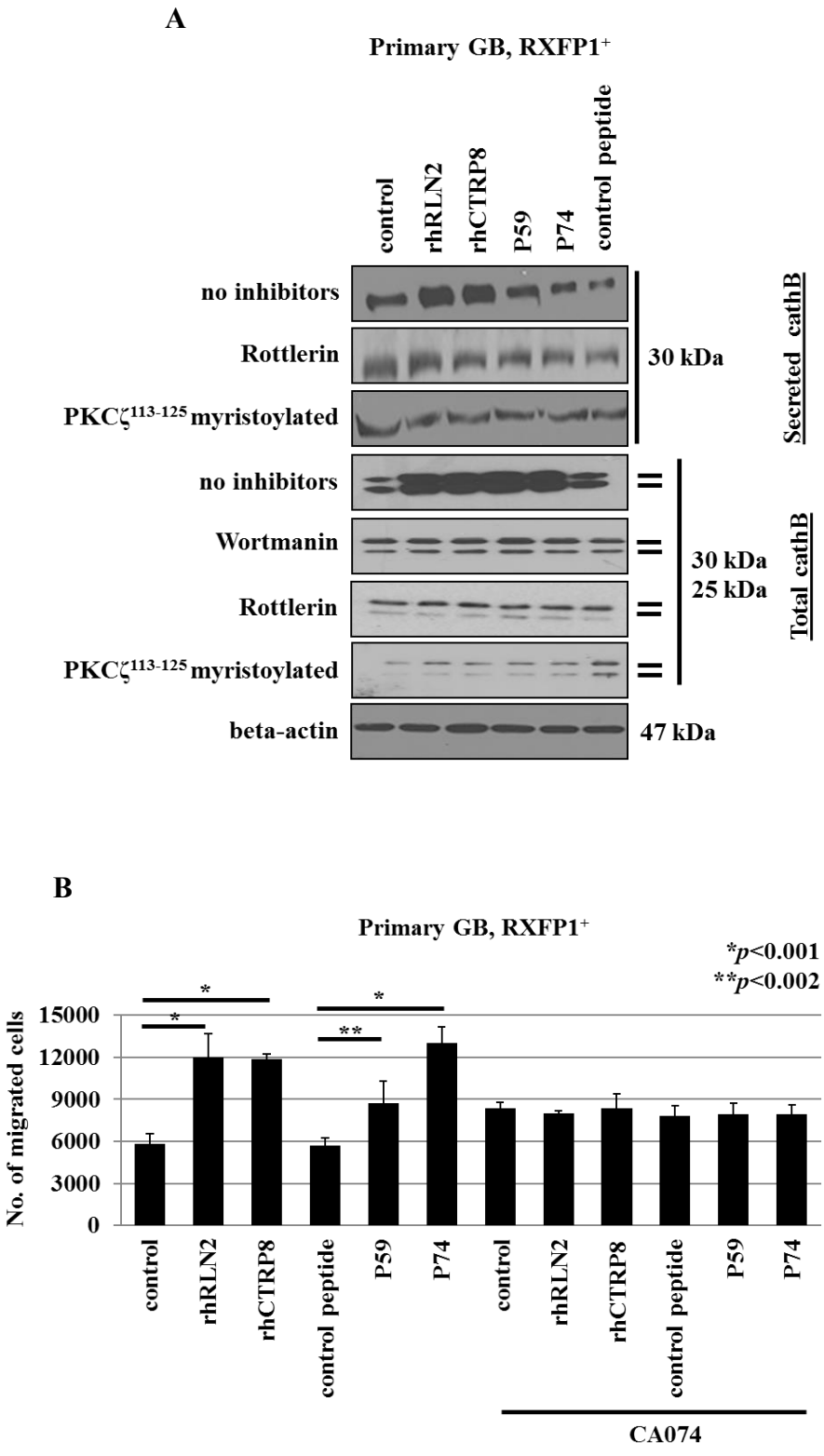

Figure 3.5 (A) Western blot detection of intracellular and secreted cathepsin B. The increase in cathepsin B secretion induced by RXFP1 activation was abrogated by rolttlerin or PKCζ myristoylated peptide$^{113-125}$. Beta actin was used as loading control. **(B)** Laminin coated transwell cell migration assay was determined following hrRLN2, hrCTRP8 and short peptided exposure in the presence and absence of a specific cathepsin B inhibitor, CA074 (10 μM). Data were published in Glogowska, A., et al., C1q-tumor necrosis factor-related protein 8 (CTRP8) is a novel interaction partner of relaxin receptor RXFP1 in human brain cancer cells. J Pathol, 2013.

The interaction between RXFP1 and hrCTRP8 was confirmed by co-immmunoprecipitation (IP) in HA-tagged HEK293-RXFP1 stable transfectants (generously provided by Dr. A.I. Agoulnik, International University of Florida, Miami, USA). The IP experiemts were done by Dr. Aleksandra Glogowska (data were published in (Glogowska et al. 2013)). Dr. Joerg Stetefeld, Department of Chemistry, Univeristy of Manitoba, performed structural protein interaction algorithms which predicted that the leucine-rich extracellurt region (LRR) 7 and LRR8 of RXFP1 can interact with the aa sequence "YAAFSVG" of the C1Q globular domain of CTRP8 (data were published in (Glogowska et al. 2013)). CTRP8 induced intracelluar cAMP level in HEK293-RXFP1 but failed to increase cAMP induction in HEK293-RXFP2 (Glogowska et al. 2013). The results suggested that CTRP8 selective activated RXFP1 not RXFP2.

3.3 Human recombinant Flag-tagged CTRP8 protein production

Human recombinant Flag-tagged CTRP8 (hrCTRP8) was expressed and purified from *E. coli (Rosetta)* containing the pET-28a-His-CTRP8-Flag expression vector. SDS-PAGE and Coomassie staining showed increased expression of hrCTRP8 protein following exposure to IPTG for 90 min **(Figure 3.6A)**. **Figure 3.6B** displays hrCTRP8 in a Coomassie stained gel after the completed purification process. To confirm the identity of the recombinant protein as hrCTRP8, Western blot analysis was performed with a Flag

antibody to detect the Flag-tag. There was only one specific band at the expected size of 29 kDa corresponding to the molecular size of hrCTRP8 with C'-terminal Flag-tag **(Figure 3.6C)**. The isolation of a single full size hrCTRP8-Flag protein excluded the possibility of proteolytically cleaved side-products that could potentially interfere with the assays. A concern associated with the production of hrCTRP8 in *E. coli* is endotoxin contamination. Endotoxin is a complex of lipopolysaccharides (LPS) released from the outer membrane of these Gram-negative bacteria. High levels of endotoxin negatively affect cell growth and cell function in cell culture experiments (Cohly et al. 2001). To confirm that rhCTRP8 was free of endotoxin contamination, the endotoxin level was assayed using a commercial chromogenic Limulus Amebocyte Lysate (LAL) endotoxin detection assay kit from GenScript (Piscataway, NJ, USA). The endotoxin level of 0.1482 EU was well below < 1 EU, which is considered acceptable for cell culture work.

Figure 3.6 Human recombinant CTRP8 protein production.

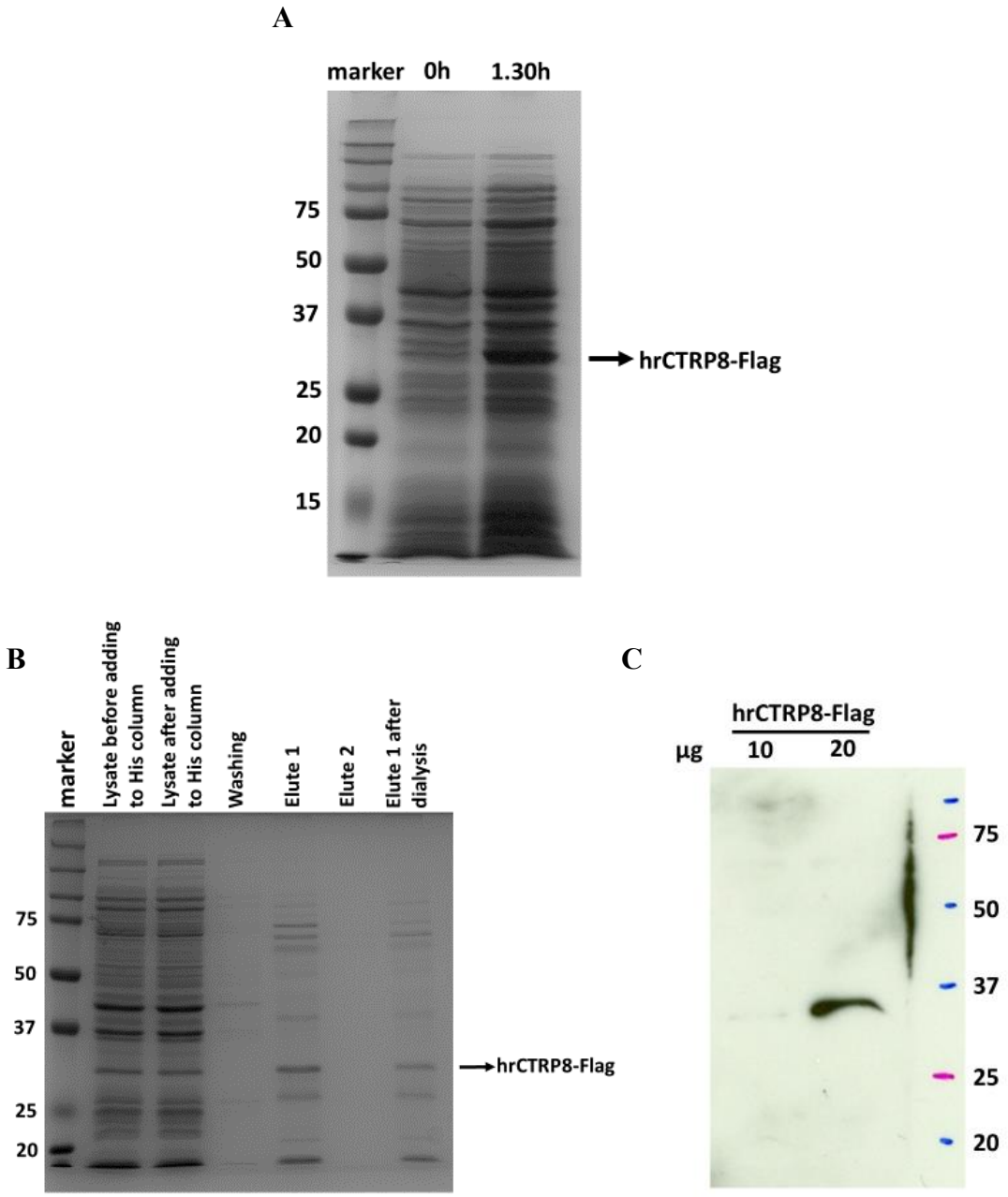

Figure 3.6 SDS-PAGE analysis of hrCTRP8 **(A)** expression and after **(B)** purification using His GraviTrap column by coomassie staining. **(C)** Western blot detection of hrCTRP8 after purification process.

The bioactivity of hrCTRP8 was tested by demonstrating the ability of this recombinant RXFP1 agonist to activate the PKC signaling pathway. HrCTRP8 was able to increase PKCδ phosphorylation in patient GB cells **(Figure 3.7A)**, with hrRLN2 being a positive control. In addition, hrCTRP8 increased the expression and secretion of cathepsin B **(Figure 3.7B)**. Also, hrCTRP8 significantly increased the ability of patient RXFP1^{+} GB cells to invade laminin matrices (**Figure 3.7C**). These results suggested that the produced hrCTRP8 was bioactive.

Figure 3.7 Validation of hrCTRP8 protein production.

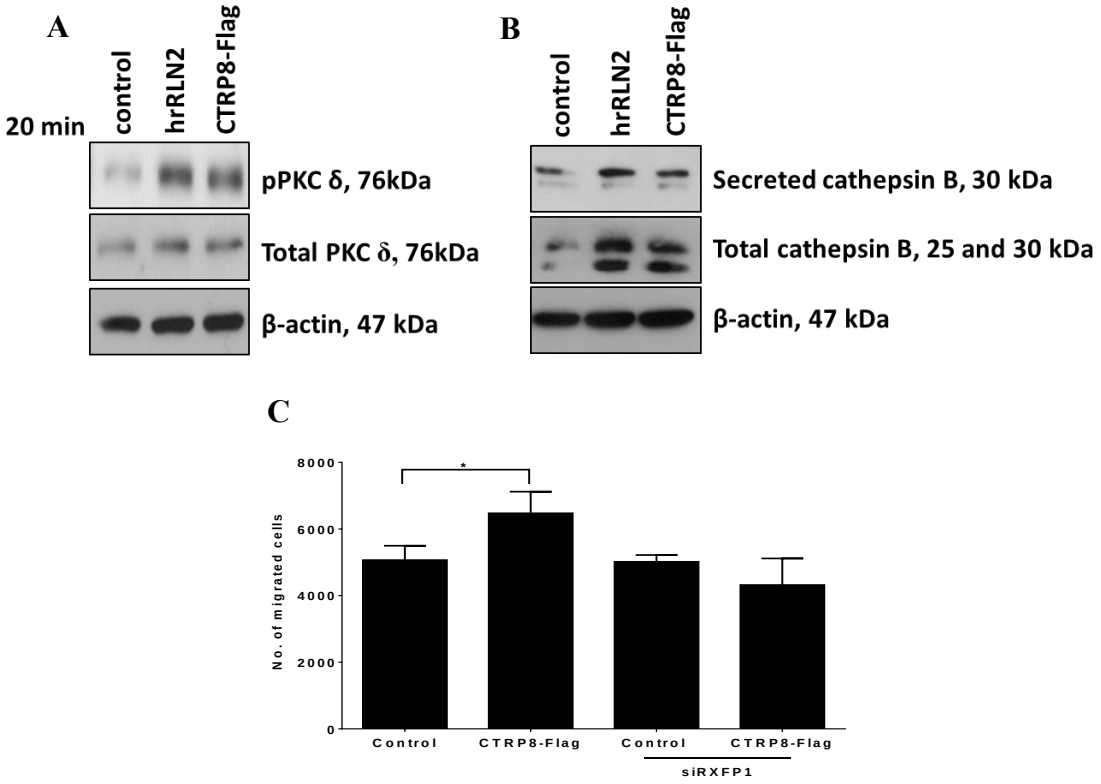

Figure 3.7 Western blot analysis detection of **(A)** phosphorylated PKCδ and **(B)** intracellular and secreted cathespin B upon 100 ng/ml hrCTRP8 treatment in patient RXFP1^{+} GB cells. **(C)** Cell migration assay was performed in patient GB cells when exposed to hrCTRP8.

3.4 RXFP1 activation induces cell migration by a STAT3-dependent pathway

The STAT3 signaling pathway is frequently activated in tumors. To investigate whether RXFP1 activation subsequently activates the STAT3 signaling pathway, the STAT3 phosphorylation status was determined. Phosphorylation of STAT3 at residues tyrosine 705 ($pSTAT3^{Tyr705}$) and serine 727 ($pSTAT3^{Ser727}$) was detected following treatment of patient GB cells with hrRLN2- or hrCTRP8 **(Figure 3.8A-D)**. This effect was inhibited by the specific STAT3 inhibitor S3I-201 **(Figure 3.8A and B)**. S3I-201 treatment did not change total STAT3 expression levels. When RXFP1 was silenced by specific siRNA treatment **(Figure 3.8C and D)**, RLN2 and CTRP8 did not induce STAT3 phosphorylation. SiRXFP1 treatment had no effect on total STAT3 levels in patient GB cells. These results identified the STAT3 signaling pathway as a novel RXFP1-mediated signaling route in patient GB cells. Corresponding control experiments showed that upon siRXFP1 treatment the RXFP1 expression levels were significantly downregulated as determined by RT-PCR in patient GB cells **(Figure 3.8E)**. Moreover, S3I-201 was not cytotoxic in patient GB cells **(Figure 3.8F)**.

The established human $RXFP1^{+}$ GB cell line U87MG was also used to investigate this signaling pathway. U87MG cells expressed high level of $pSTAT3^{Tyr705}$ and both hrRLN2 and hrCTRP8 further increased $pSTAT3^{Tyr705}$ levels **(Figure 3.8G-I)**. Similar to patient GB cells, this increase of $pSTAT3^{Tyr705}$ was inhibited by S3I-201 **(Figure 3.8G and H)** and siRXFP1 **(Figure 3.8I)**. Analysis by qPCR demonstrated a decrease in RXFP1 expression upon siRXFP1 treatment of U87MG cell line **(Figure 3.8J)**.

Figure 3.8 RXFP1 activated the STAT3 signaling pathway.

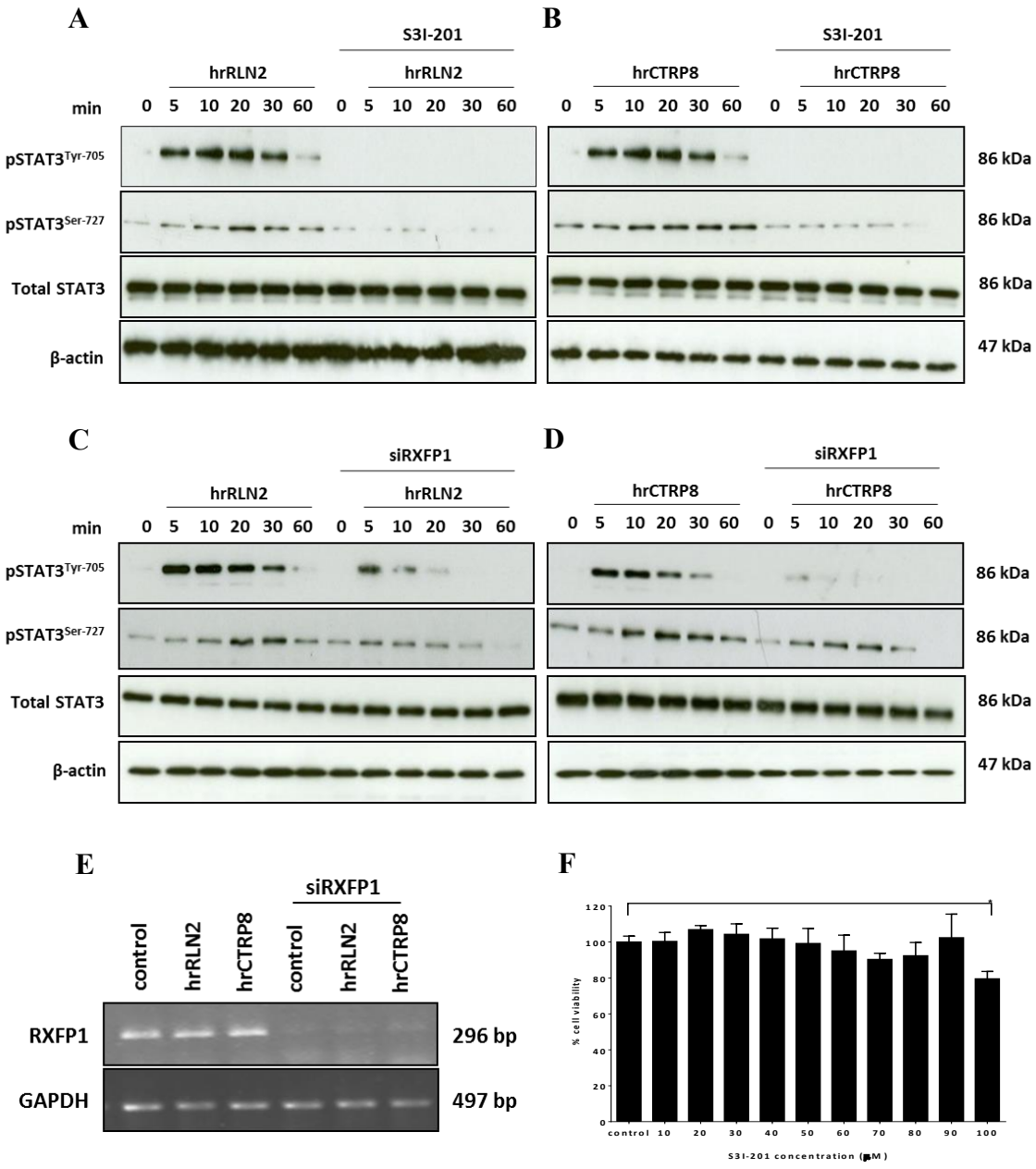

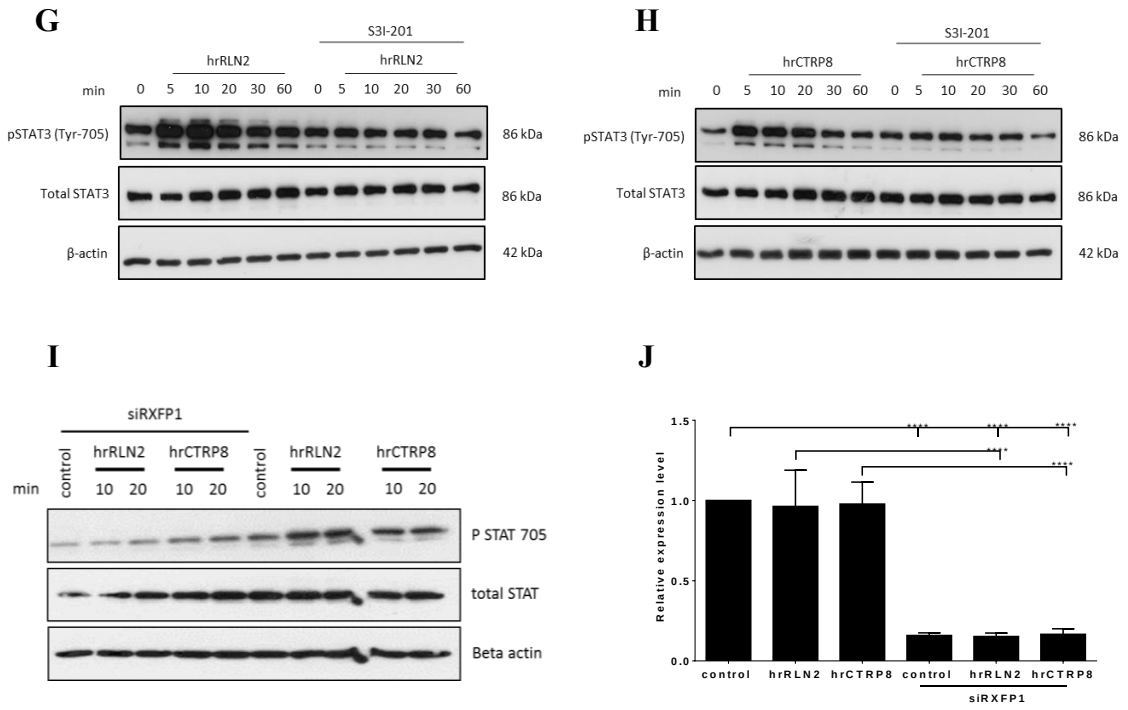

Figure 3.8 Western blot detection of phosphorylated total and pSTAT3$^{Tyr\ 705}$ and pSTAT3$^{Ser\ 727}$ in **(A-F)** RXFP1^{+} GB cells and **(G-J)** U87 GB cell lines. Treatment with hrRLN2 and hrCTRP8 increased patient pSTAT3$^{Tyr\ 705}$ and pSTAT3$^{Ser\ 727}$. This was abolished upon **(A, B, G, and H)** a specific STAT3 inhibitor (S3I-201, 25 μM) and **(C, D, and I)** specific RXFP1 knockdown. β-actin used as loading control. **(E)** RT-PCR or **(J)** qPCR was used to confirm the siRNA knockdown of RXFP1 in RXFP1^{+} patient GB cells or U87, respectively. **(F)** WST assay showed no cytotoxicity of S3I-201 in patient GB cells.

Cell migration and transwell laminin invasion assays were performed to investigate whether RXFP1-mediated activation of the STAT3 signaling pathway can enhance GB cell motility and invasion. HrRLN2 and hrCTRP8 markedly induced both motility and matrix invasion and this was inhibited by S3I-201 **(Figure 3.9A)**. To study whether STAT3 signaling pathway also increased cathepsin B production and secretion, the inhibition of STAT3 signaling by a STAT3 inhibitor and specific siRXFP1mediated knockdown of RXFP1 were performed **(Figure 3.9B)**. The expression and secretion of cathepsin B were both inhibited following S3I-201 or siRXFP1 treatment **(Figure 3.9B)**. I concluded that the activation of RXFP1 by hrRLN2 and hrCTRP8 induced a pSTAT3-mediated increase

in invasive behavior and cathepsin B secretion leading to enhanced matrix invasion by GB cells.

Figure 3.9 RXFP1 regulates cathepsin B and induces cell invasion through STAT3 signaling.

A

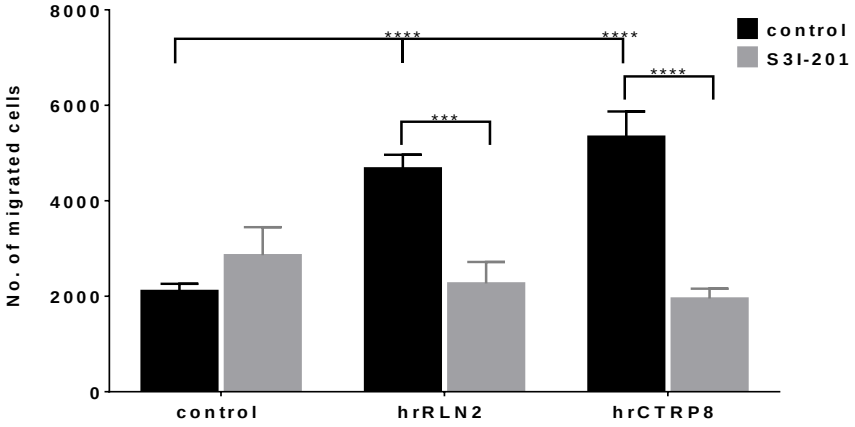

B

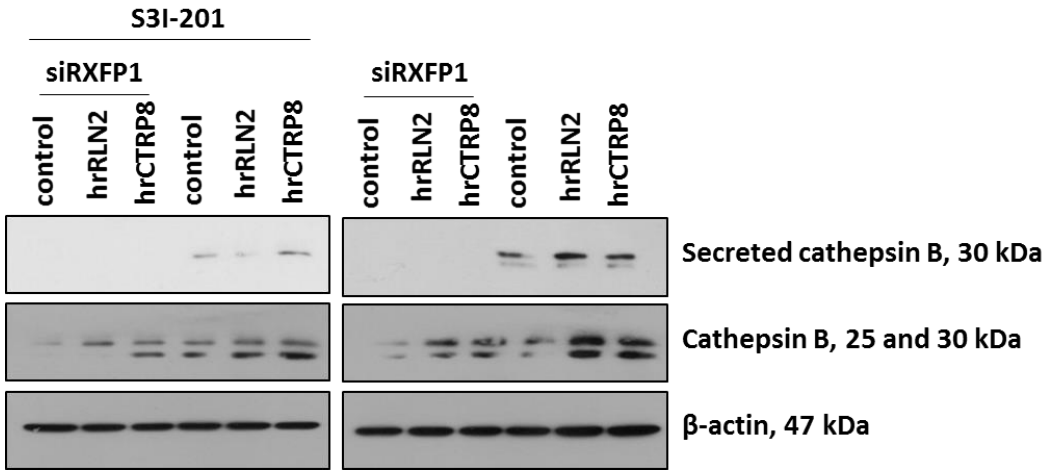

Figure 3.9 (A) Laminin transwell invasion assay was used to study patient GB cell invasion upon 100ng/ml hrRLN2/hrCTRP8 in the presence and absence of S3I-201. **(B)** Western blot detection of intracellular and secreted cathepsin B when patient GB cells exposed to RXFP1 agonists in the presence of S3I-201 or siRXFP1.

Part II: The CTRP8-RXFP1 system protects GB against DNA damage and apoptosis

The results of part I suggested that RLN2/CTRP8 activate RXFP1 to increase pPKCδ/ζ and pSTAT3 signaling which caused the secretion of cathepsin B. This resulted in enhance cell migration and matrix invasion which are fundamental features of GB cells. STAT3 signaling is an oncogenic pathway to enhance cell proliferation, survival, migration, invasion, suppresses apoptosis and promotes chemoresistance in GB cells (Lee et al. 2011, Kim et al. 2014). TMZ is the first line chemotherapy for treatment of GB patients. TMZ chemoresistance is a common feature in GB. For these reason, Part II of my studies will address whether the newly discovered CTRP8-RXFP1-pSTAT3 signaling axis can promote TMZ chemoresistance in GB cells.

3.5 RXFP1 activation protects GB cells from Temozolomide (TMZ) induced DNA damage

TMZ is the DNA alkylating chemotherapeutic drug of choice for the treatment of patients with GB. TMZ induced methylation of DNA bases is repaired by two mechanisms involving methylguanine- methyltransferase (MGMT) and base excision repair (BER) (Zhang et al. 2012). Incomplete repair results in unresolved single strand DNA breaks that can progress to double strand DNA breaks (DSB). I examined whether RXFP1 activation can protect against TMZ-mediated DNA damage in GB cells. Immunofluorescence staining was used to detect and quantify γ-H2AX foci, a marker of double stranded DNA breaks. Frequent and strongly positive γ-H2AX foci were observed in TMZ treated patient GB cells **(Figure 3.10A)**. In the presence of hrCTRP8 or hrRLN2, the number of γ-H_2AX foci was significantly diminished upon TMZ treatment of GB cells. This suggested a protective role of RXFP1 agonists on TMZ induced DNA damage in patient GB cells.

To examine whether the protective role of RXFP1 agonists was RXFP1 dependent, knockdown (KD) of RXFP1 was performed using a specific siRNA. The KD of RXFP1 completely abolished the DNA protective role of hrCTRP8 and hrRLN2 in TMZ-treated GB cells **(Figure 3.10A)**. These immunofluorescence results were confirmed by Western blot detection of phosphorylated γ-H_2AX. Patient GB cell were treated with TMZ in the presence of hrCTRP8, hrRLN2 or TMZ alone **(Figure 3.10B and C)**. Specific silencing of RXFP1 expression followed by hrCTRP8 or hrRLN2 plus TMZ treatment failed to diminish γ-H_2AX levels when compared to TMZ alone. The expression level of RXFP1 in patient GB cells upon a siRNA specific for RXFP1 was confirmed by real-time PCR **(Figure 3.10D)** and RXFP1 expression was dramatically decreased upon RXFP1 KD. I concluded that RXFP1 was essential for hrCTRP8 and hrRLN2 to elicit their DNA protective functions in human GB cells.

To determine the involvement of STAT3 in RXFP1-mediated protection from TMZ induced DNA damage, GB cells were exposed to the specific STAT3 inhibitor S3I-201. No significant difference in γ-H_2AX levels were observed in GB cells treated with either TMZ plus S3I-201 or TMZ alone suggesting that this STAT3 inhibitor did not affect TMZ induced DNA damage. However, STAT3 inhibition blocked the decrease in γ-H_2AX levels observed in the presence of hrCTRP8 and hrRLN2 **(Figure 3.10C)**. These results demonstrated that the DNA protective effect of activated RXFP1 was mediated by a STAT3 dependent signaling pathway.

Figure 3.10 RXFP1 activation protected cells from DNA damage induced by TMZ.

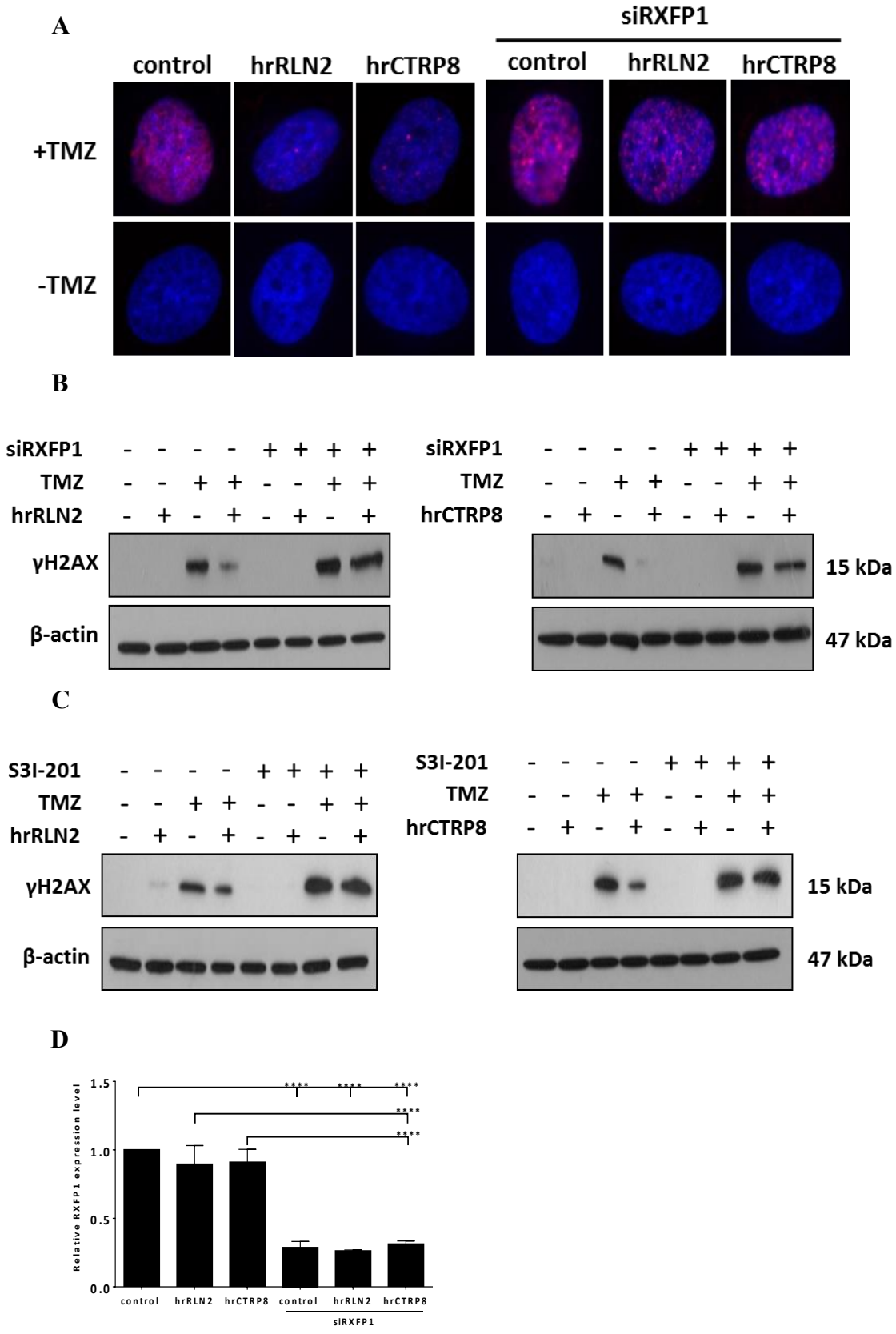

Figure 3.10 (A) Representative images of cell nuclei from the treatments. Immunofluorescence detection of γH2AX, a marker of DSBs. Strong γH2AX foci were detected in TMZ treated patient GB cells alone but were reduced when cells exposed to 100ng/ml of hrRLN2 or hrCTRP8 upon 1.5 mM TMZ treatment for 24h. The protective role of hrRLN2 and hrCTRP8 was dependent on RXFP1. **(B and C)** Western blot detection showed the significant increasing of γH2AX protein level in TMZ treatment. The combination of TMZ and hrRLN2/hrCTRP8 markedly reduced γH2AX in patient GB cells. The effect of hrRLN2 and hrCTRP8 was RXFP1- and STAT3- dependent and abolished upon siRXFP1 or 25 μM of STAT3 inhibitor (S3I-201) treatment. β-actin used as loading control. **(D)** qPCR showed the specific knockdown of RXFP1 in $RXFP1^{+}$ patient GB cells.

To confirm the protective effects of hrCTRP8 and hrRLN2 on TMZ-induced DNA damage, single-cell gel electrophoresis studies, also known as Comet assays, were performed to determine double strand DNA breaks. In this assay, single cell nuclei are exposed to an electrical field to separate fragmented DNA of DSBs from the nucleus which presents a comet tail of fragmented DNA trailing behind the nucleus (head of comet). The intensity and shape of the comet tail is directly related to the severity of DSBs and amount of fragmented DNA released from the nucleus. The olive tail moment was determined as an index of both comet tail length and the amount of DNA in the tail as quantified by SYBR green fluorescence dye. Thus, a high level of olive tail moment indicates increased double strand DNA damage. Untreated GB cells showed a large head without any tail suggestive of few, if any, DSBs **(Figure 3.11A and B)**. In contrast, I observed an olive tail moment and corresponding smaller head length in the TMZ treated GB cells **(Figure 3.11A-F)**. Both, hrCTRP8 or hrRLN2 antagonized this TMZ effect and caused a diminished olive tail moment and decreased head length **(Figure 3.11A-F)**. Next, I determined the role of STAT3 signaling in the DNA protective functions of hrCTRP8 and hrRLN2. S3I-201 abolished the protective effect of hrCTRP8 and hrRLN2 in TMZ treated GB cells as seen by an increased olive tail moment and smaller head length **(Figure 3.11A-F)**. Comet assays

confirmed the results from the γ-H_2AX experiments in that neither hrCTRP8, hrRLN2, nor S3I-201 alone caused any DNA damage. However, hrCTRP8 or hrRLN2 significantly reduced DSBs upon TMZ treatment, causing shorter and less intense comet tails than TMZ alone.

Figure 3.11 RXFP1 activation reduced DNA damage induced by TMZ as detection by comet assay.

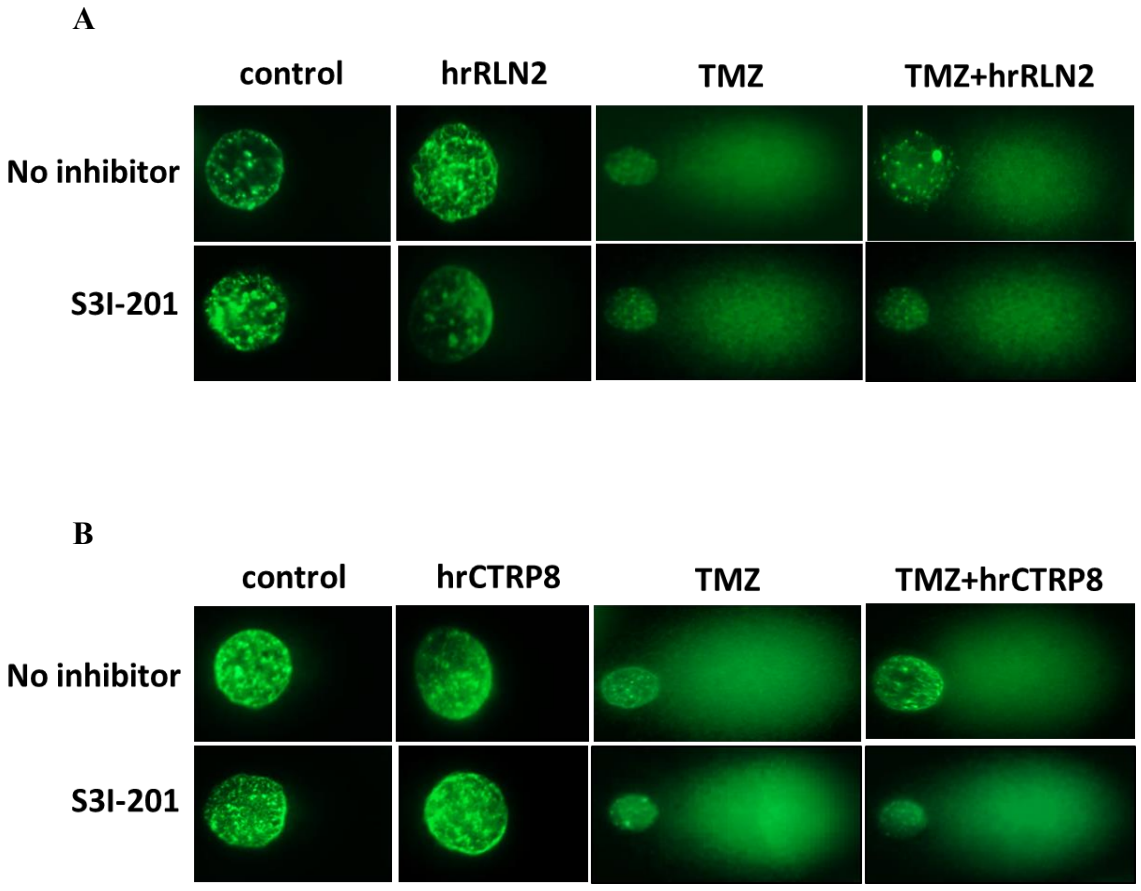

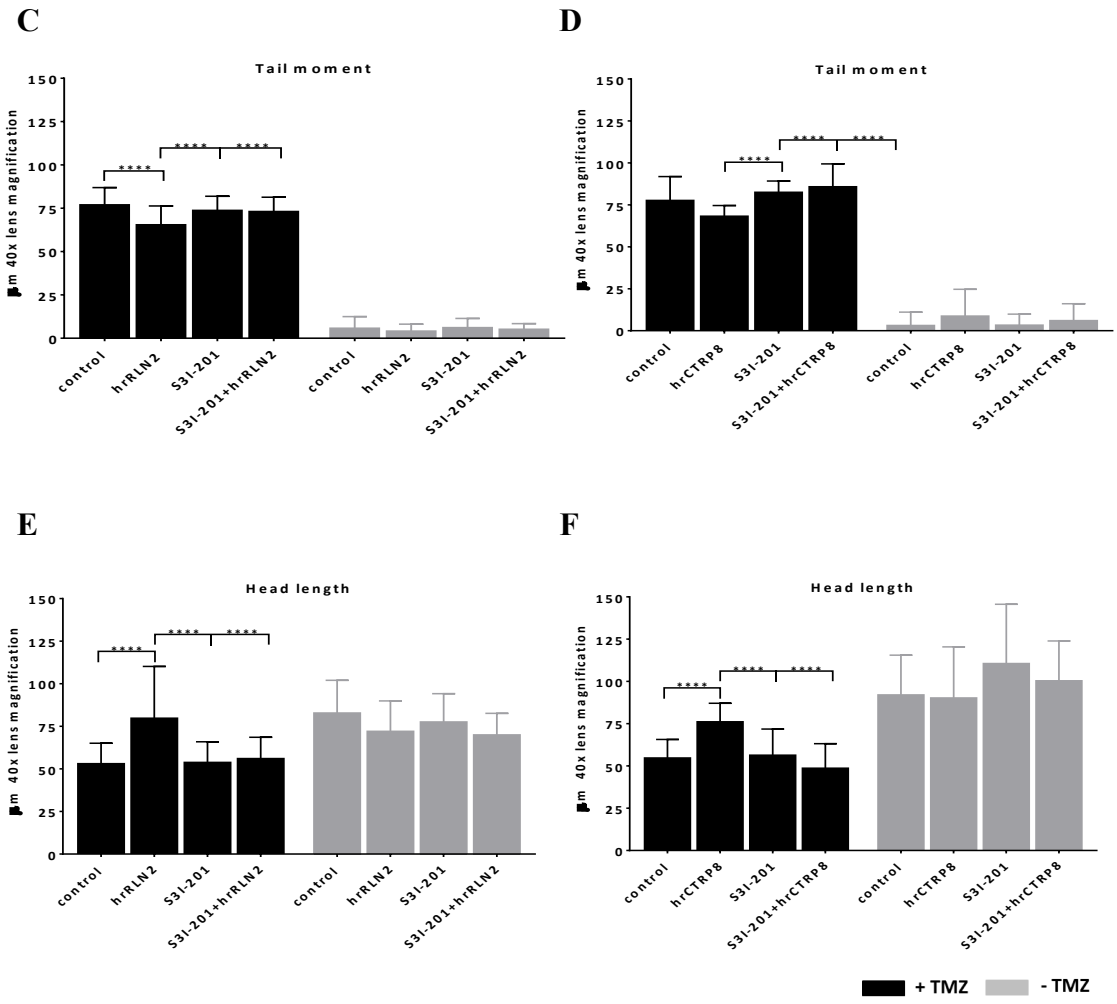

Figure 3.11 The analysis was done under 1.5 mM TMZ treatment +/- 100 ng/ml hrRLN2 or hrCTRP8 at 100 ng/ml for 24h. **(A and B)** Representative images of cell nuclei from the treatments. **(C and D)** Quantification of the olive tail moment and **(E and F)** quantification of nuclei head length was displayed. 50 cells were scored for tail moments and the data represents mean ± SD.

3.6 RXFP1 activation enhances cell survival

HrCTRP8 and hrRLN2 significantly increased viability of GB cells in the presence of TMZ as determined by WST studies **(Figure 3.12A and B)**. Silencing of RXFP1 expression, or inhibition of STAT3 activation prevented this cytoprotective effect of hrCTRP8 or hrRLN2. Specific knockdown of RXFP1 and SI3-201 treatment were not cytotoxic. TMZ caused a significant increase in caspase 3/7 activity, indicating the activation of the intrinsic apoptosis pathway in GB cells. HrCTRP8 and hrRLN2 significantly diminished TMZ induced cell death in GB cells from patients **(Figure 3.12C and D)**. Irrespective of the presence of RXFP1 agonists, RXFP1 knockdown **(Figure 3.12C)** and S3I-201 mediated STAT3 inhibition **(Figure 3.12D)** increased the pro-apoptotic caspase 3/ 7 activity in TMZ treated U87MG cells **(Figure 3.12E and F)**. Real-time monitoring of the cellular responses to TMZ treatment (24h) in patient GB cells by xCelligence E-plate assays (Acea BioSciences, Inc., San Diego, CA, USA) revealed a significant decrease in Cell index (CI) values over time (**Figure 3.12G and H)**. CI values reflect cell number, cell size, and/or the level of cell attachment. The CI time curves decreased with exposure to TMZ when compared to untreated GB cell controls. In the presence of either hrCTRP8 or hrRLN2 in combination with TMZ, CI values remained unchanged compared to controls, suggesting that hrCTRP8 and hrRLN2 effectively reduced TMZ toxicity in GB cells **(Figure 3.12G-J)**. This protective effect was completely abolished upon RXFP1 knockdown. The specific knockdown of RXFP1 alone without TMZ treatment had no effects on the xCelligence readout. In conclusion, the results obtained from the real-time cell assay (RTCA; xCelligence) monitoring system and the caspase 3/7 and WST cell cytotoxicity assays uniformly showed a cytoprotective effect of

activated RXFP1 in cells exposed to TMZ. These results indicate that the consecutive activation of RXFP1 and STAT3 signaling pathway by both hrCTRP8 and hrRLN2 diminished the intrinsic caspase-induced apoptotic pathway and enhanced cell survival.

Figure 3.12 RXFP1 activation enhanced cell survival of patient GB cells treated with TMZ.

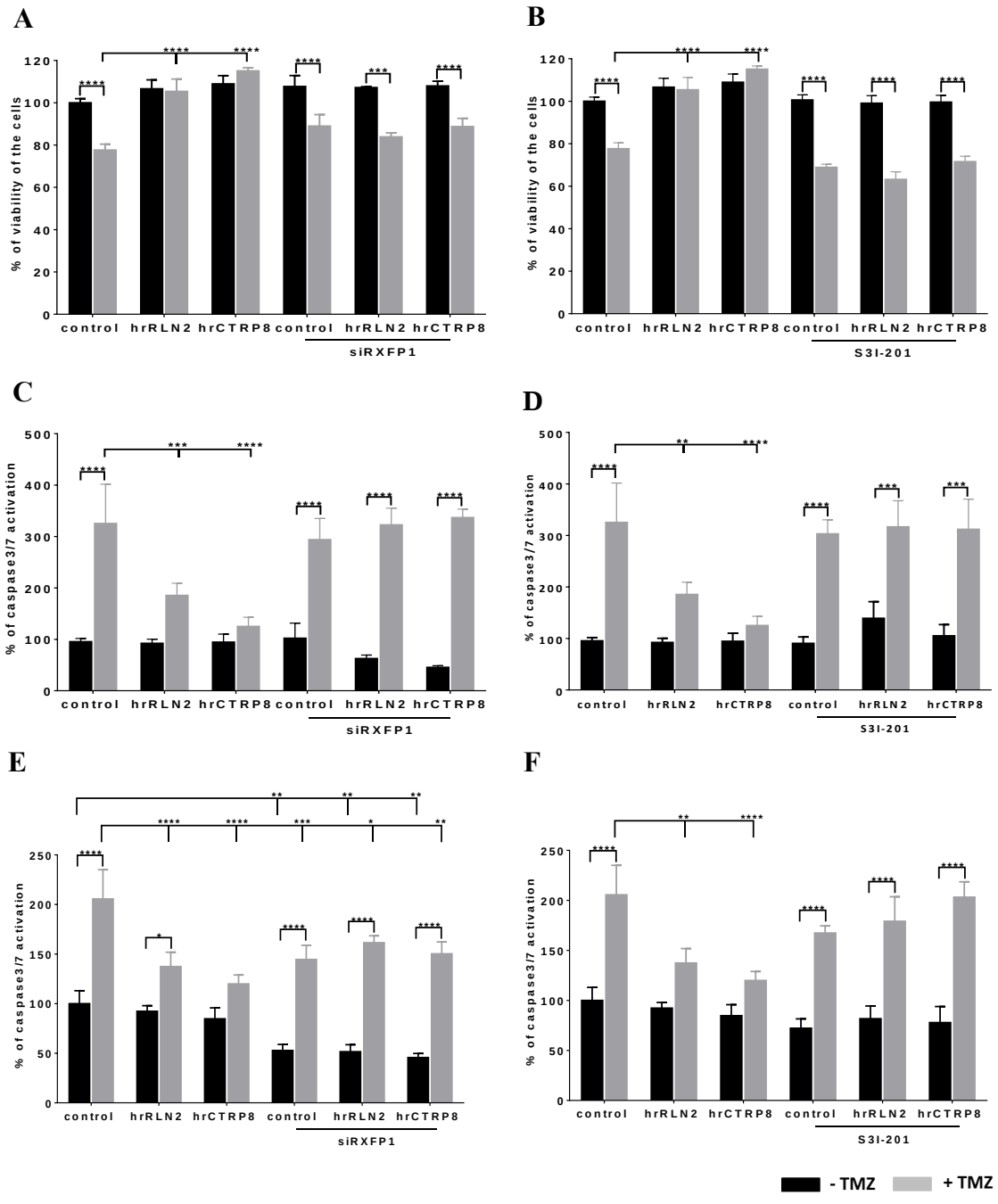

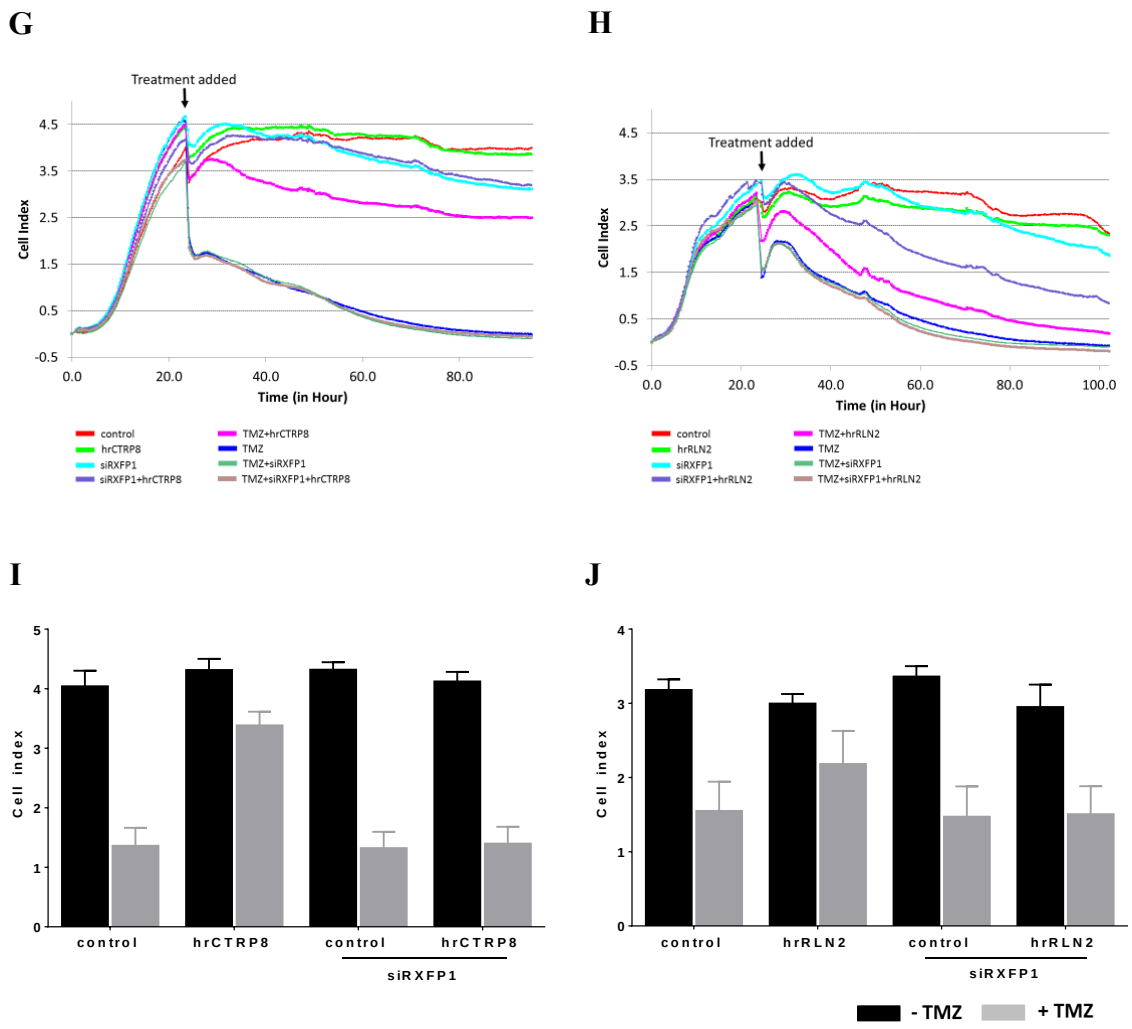

Figure 3.12 WST cytotoxicity assay **(A and B)** and Caspase3/7 activity assay **(C and D)** of patient GB cells exposed to RXFP1 agonists +/- TMZ. Cells were treated with 100 ng/ml of hrRLN2 or hrCTRP8 with or without 1.5 mM TMZ for 24h. The experiments in C and D were replicated in U87MG cells **(E and F).** The xCelligence system was used to determine real-time cellular response of patient GB cells upon hrRLN2 or hrCTRP8 incubation with TMZ. **(G and H)** The kinetic curves represented the real-time data which was recorded every 15 min. Data analysis were performed using RTCA software 2.0 for calculating the cell index. **(I and J)** The column graphs showed the cell index at time 24 h after incubation.

3.7 RXFP1 activation increases expression of anti-apoptotic proteins Bcl-2 and Bcl-XL

STAT3 was shown to increase the expression of the anti-apoptotic molecules Bcl-2 and Bcl-XL (Zhuang et al. 2007). I used western blot analysis to investigate whether RXFP1 activation can increase the expression of Bcl-2 and Bcl-XL. RXFP1 activation caused a significant increase in the expression of Bcl-2 and Bcl-XL in patient GB cells. This effect was abolished in the presence of the STAT3 inhibitor S3I-201 **(Figure 3.13A)** and upon specific knockdown of RXFP1 **(Figure 3.13B)**. These results suggest that the increased expression of Bcl-2 and Bcl-XL due to the activation of the hrCTRP8/hrRLN2-RXFP1-STAT3 pathway contributes to their anti-apoptotic effect in GB cells.

Figure 3.13 RXFP1 activation increased expression of anti-apoptotic proteins.

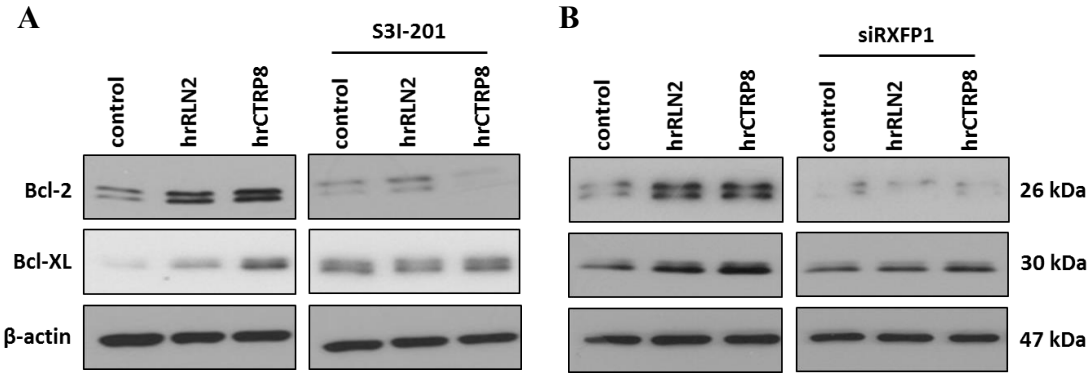

Figure 3.13 Western blot detection of anti-apoptotic protein, Bcl-2 and Bcl-XL in patient GB cells upon treatment with RXFP1 agonists hrRLN2 or hrCTRP8. The exposure of 100ng/ml of hrRLN2 or hrCTRP8 for 24h resulted in upregulation of Bcl-2 and Bcl-xL which was blocked by **(A)** S3I-201 or **(B)** siRXFP1. β-actin was used as loading control.

3.8 The DNA protective function of RXFP1 involves members of the base excision repair (BER) pathway

RXFP1 activation is associated with enhanced cell survival and resistance to TMZ-induced DNA damage. The majority of TMZ-induced DNA lesions (N^7-MeG and N^3-MeA) are substrates for the BER pathway. Thus, the BER pathway qualified as a potential target for the hrRLN2/hrCTRP8-RXFP1 pathway of TMZ resistance. As a first step, I investigated whether the activation of RXFP1 could regulate the expression of BER protein members, including MPG1, APE1, XRCC1, and DNA polymerase β. Upon hrCTRP8 and hrRLN2 treatment of RXFP1 positive GB cells, I detected enhanced cellular protein levels of the monospecific DNA glycosylase MPG protein **(Figure 3.14A and B)** whereas the expression of APE1, XRCC1, DNA polymerase β remained unchanged. The knockdown of RXFP1 **(Figure 3.14A)** and the inhibition of STAT3 signaling **(Figure 3.14B)** abolished the ability of hrCTRP8 or hrRLN2 to increase DNA glycosylase MPG protein levels. This identified the hrCTRP8/hrRLN2-RXFP1-STAT3 pathway as a novel positive regulator of MPG in patient GB cells.

Next, I used a real-time molecular beacon assay (Svilar et al. 2012) to quantify the MPG enzymatic activity in human U87MG GB cells that had been treated with hrCTRP8 or hrRLN2 and compare this to the MPG activity in untreated cells. MPG glycosylase activity was detected by an increase in fluorescence signal detection with a specific MPG molecular beacon probe described previously (Svilar et al. 2012) **(Figure 3.14C)**. The MPG molecular probe contains a deoxyinosine (dI) which serves as a substrate for and is removed by MPG. The same molecular beacon structure with a normal adenosine was used as control probe. Upon the removal of dI, a 6-base pair single strand DNA attached to a

fluorophore is separated from the quencher on the opposing DNA strand and this results in the detection of a fluorescence signal **(Figure. 3.14C)**. When nuclear extracts of GB cell lysates were incubated with control probe, no change in fluorescence signal was detected, indicating that nuclear MPG failed to process the control probe **(Figure 3.14D and E)**. However, increased fluorescence signal was detected in nuclear lysates incubated with the MPG probe, indicative of increased MPG glycosylase activity **(Figure 3.14D and E)**. Treatment with hrCTRP8 and hrRLN2 resulted in a significantly increased fluorescence signal measured every 20 second for 180 minutes, reflecting increased MPG glycosylase activity when compared to untreated U87MG cells. This MPG activity was abolished in the presence of STAT3 inhibitor S3I-201 **(Figure 3.14D and E)**. I quantified the MPG activity by calculating the fluorescence intensity at 60, 120, and 180 min **(Figure 3.14F and G)** and Western blot analysis was used to validate the upregulation of MPG protein upon hrRLN2 and hrCTRP8 treatments **(Figure 3.14H)**. The results identified the hrRLN2/hrCTRP8-RXFP1-STAT3 pathway as a new mechanism for the increased production and activity of MPG DNA glycosylase in human GB cells.

Figure 3.14 RXFP1 activation increased protein and activity of N-methylpurine DNA glycosylase (MPG).

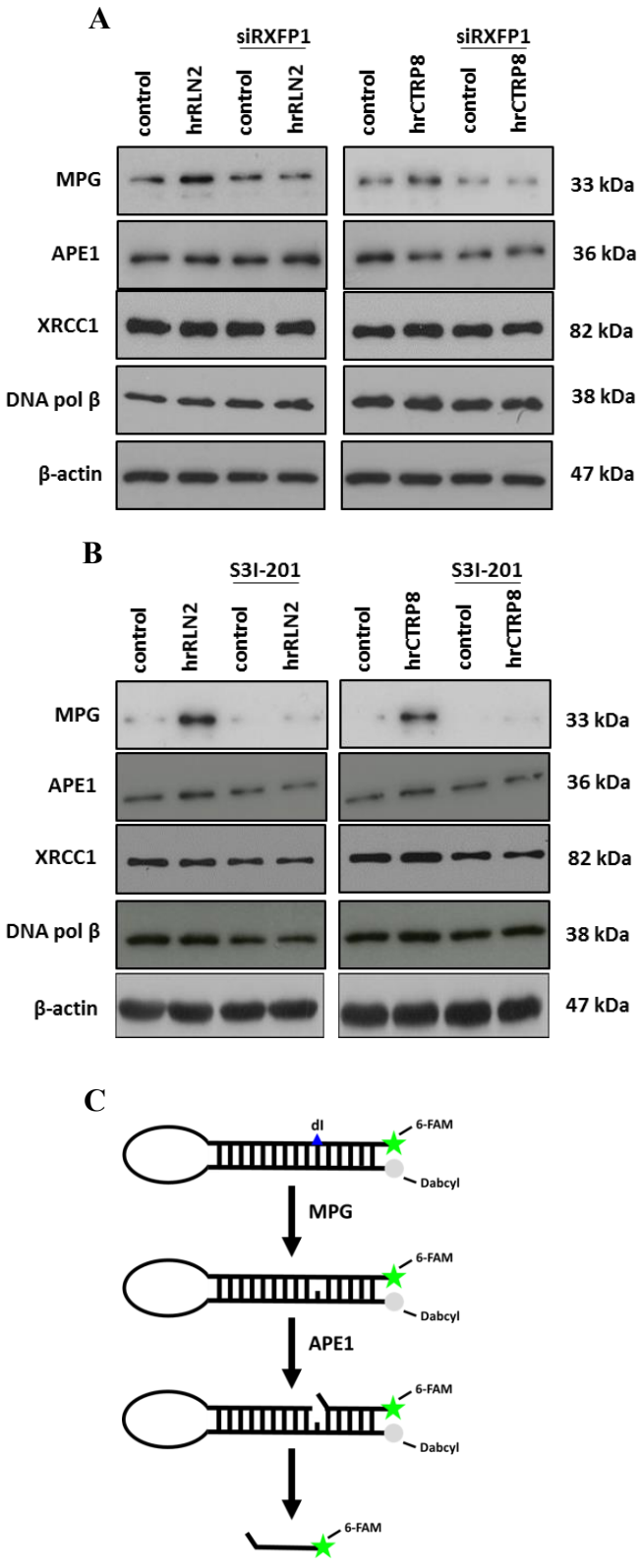

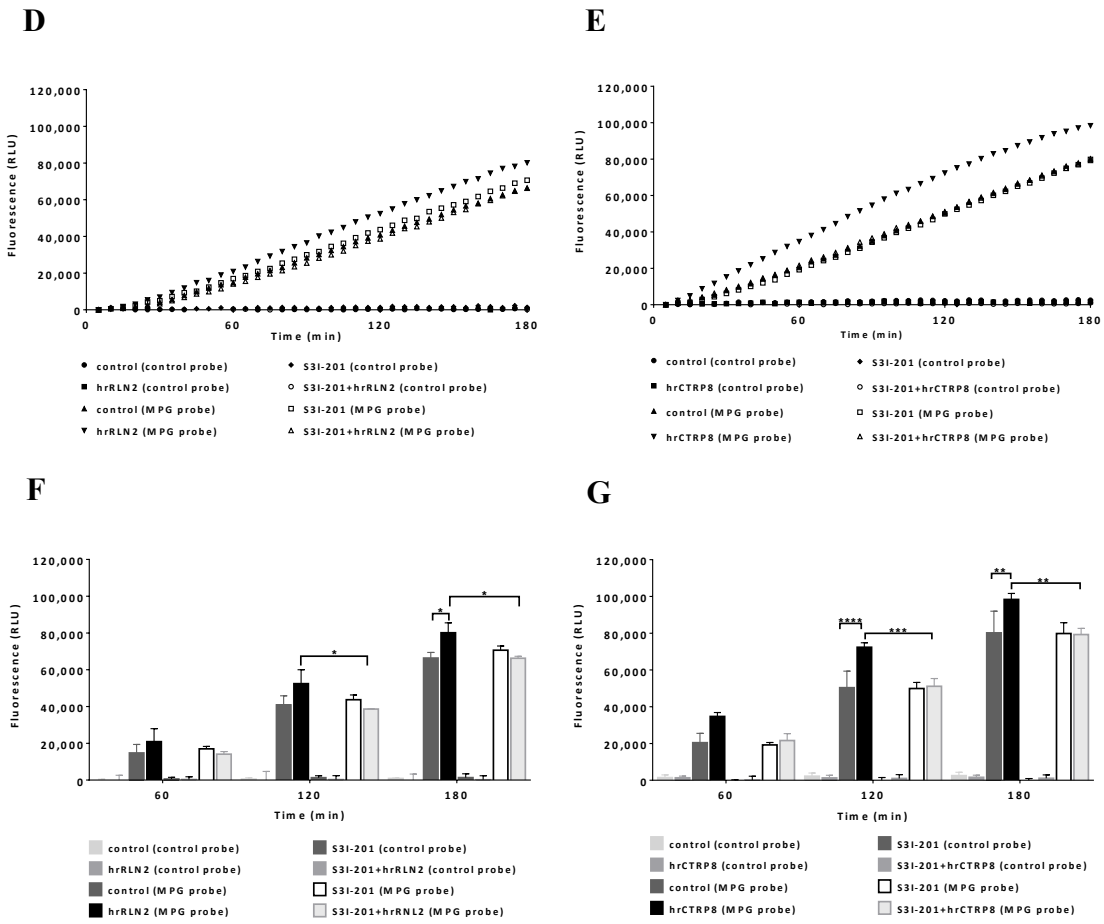
D
E
F
G
Fluorescence (RLU)
Time (min)
control (control probe)
hrRLN2 (control probe)
control (MPG probe)
hrRLN2 (MPG probe)
S3I-201 (control probe)
S3I-201+hrRLN2 (control probe)
S3I-201 (MPG probe)
S3I-201+hrRLN2 (MPG probe)
hrCTRP8 (control probe)
hrCTRP8 (MPG probe)
S3I-201+hrCTRP8 (control probe)
S3I-201+hrCTRP8 (MPG probe)
S3I-201+hrRNL2 (MPG probe)

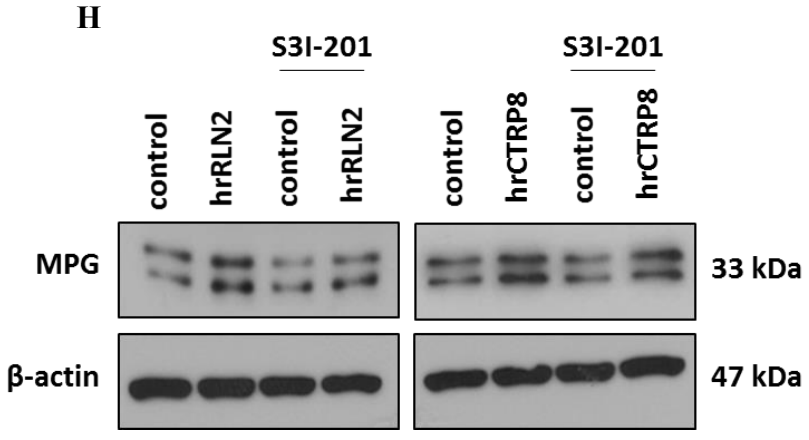
H
S3I-201
S3I-201
control
hrRLN2
control
hrRLN2
control
hrCTRP8
control
hrCTRP8
MPG
β-actin
33 kDa
47 kDa

Figure 3.14 Western blot detection of BER protein members upon 100 ng/ml of hrRLN2 or hrCTRP8 treatment for 24h in patient GB cells. The protein level of DNA glycosylase MPG was increased upon exposing to RXFP1 agonists. **(A)** The RXFP1 knockdown and **(B)** STAT3 inhibitor (S3I-201) treatment abolished the enhancing of MPG protein level. Molecular beacon activity assay was used to detect MPG activity upon hrRLN2/ hrCTRP8 incubation in U87MG. **(C)** The schematic diagram displayed the structure and mechanism of molecular beacon assay for detecting MPG glycosylase activity. The MPG activity was measured by the removal of the MPG substrate, dyoxyinosine, at the MPG probe. The control probe was the sequence without a substrate for MPG. The results were shown as fluorescence unit. **(D and E)** The scatterplot showed hrRLN2/ hrCTRP8 recruited MPG to remove the substrate quicker than control. **(F and G)** Quantification of fluorescence intensity after incubating cell lysates with molecular beacon probes for 60, 120, and 180 min. **(H)** Western blot detection of MPG expression upon hrRLN2 or hrCTRP8 exposure with S3I-201 in U87MG GB cell lines. Beta actin was used as loading control.

Summer et al. identified HMGA2 as a new member of BER and reported that HMGA2 has AP-/dRP-lyase activities and promotes the resistance to the alkylating agent MMS (Summer et al. 2009). HMGA2 expression is regulated by the STAT3-lin28-let7 pathway (Lee and Dutta 2007, Guo et al. 2013). Hence, to investigate whether the expression of HMGA2 is regulated by RXFP1-mediated STAT3 activation in patient GB cells. GB cells were also treated with a STAT3 inhibitor before incubating with hrCTRP8 or hrRLN2. I found that HMGA2 expression was up-regulated by hrCTRP8 and hrRLN2 but the increase in HMGA2 was blocked by inhibition of STAT3 signaling by S3I-201 **(Figure 3.15A and B)** and knocking down RXFP1 with a specific siRNA **(Figure 3.15 C and D)**. This indicated that increased HMGA2 expression induced by activation of RXFP1 was mediated by STAT3 signaling. The increase in caspase 3/7 activity produced by exposure of patient GB cells to TMZ was further enhanced with exposure of the cells to a siRNA against HMGA2 **(Figure 3.15E)**. Upon HMGA2 knockdown, hrRLN2 or hrCTRP8 treatment were able to significantly reduce caspase 3/7 activity in patient GB cells treated with TMZ. Specific siRNA knockdown of HMGA2 is showed in **Figure 3.15F**. The results

indicated that under TMZ stress HMGA2 contributed to the protective effect against apoptosis. However, HMGA2 knockdown did not abolish the protective effect of the RXFP1 ligands on GB cells exposed to TMZ, suggesting additional currently unknown mechanisms are involved in ensuring survival upon activation of RXFP1 in these GB cells.

Figure 3.15 RXFP1 activation regulated HMGA2 expression.

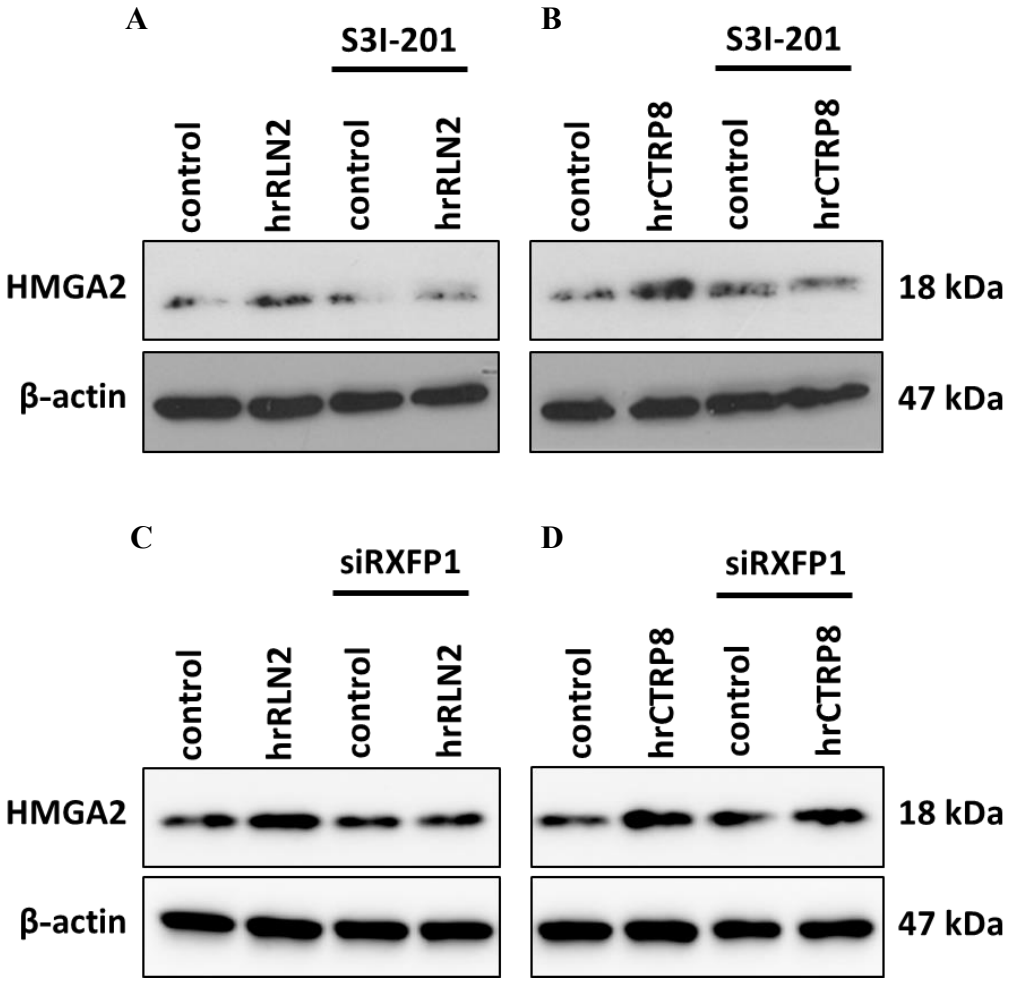

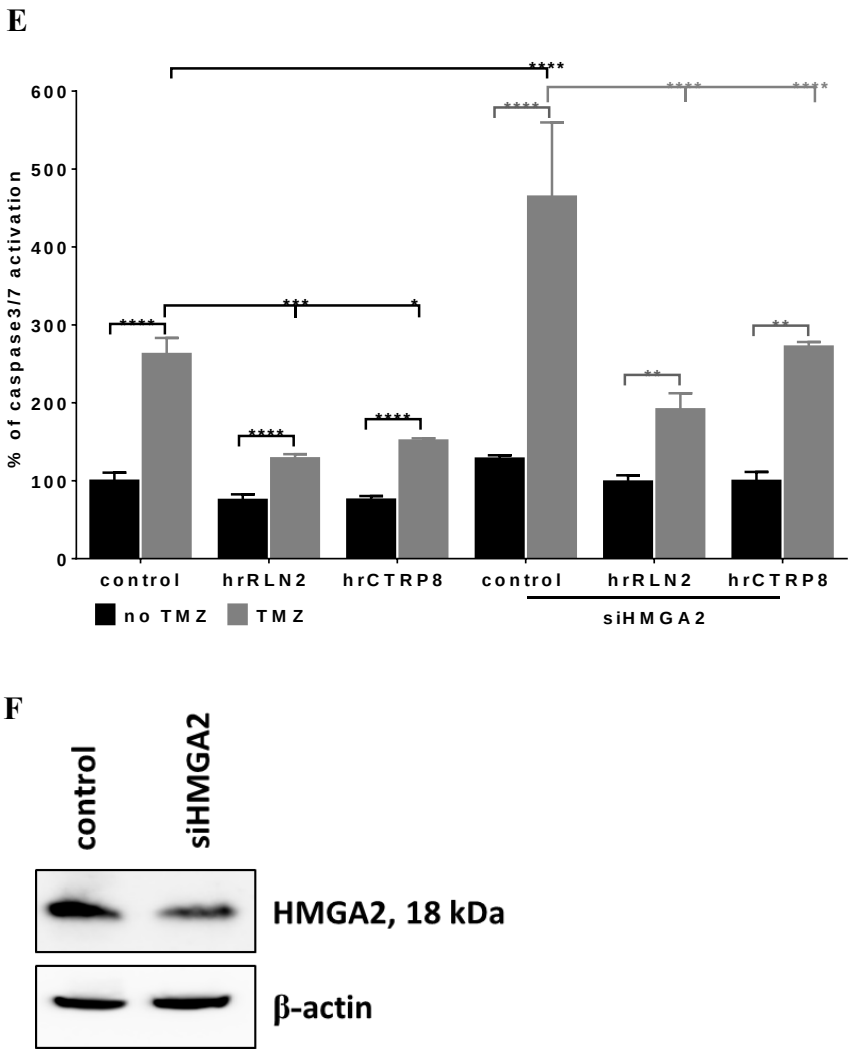

Figure 3.15 Western blot detection of HMGA2 in patient GB cells upon treatment with RXFP1 agonists hrRLN2 or hrCTRP8. The exposure of 100ng/ml of hrRLN2 or hrCTRP8 for 24h showed the upregulation HMGA2 which was inhibited by **(A and B)** S3I-201 or **(C and D)** siRXFP1. β-actin was used as loading control. **(E)** Caspase 3/7 activity assay of patient GB cells upon siHMGA2 treatment followed by 100 ng/ml hrRLN2 or hrCTRP8 with 1.5 mM TMZ for 24h. **(F)** Western blot detection of HMGA2 upon siHMGA2 treatment in patient GB cells.

Part III. High Mobility Group AT Hook 2 protein (HMGA2) increases temozolomide resistance in glioblastoma

The results from Part II suggested that the activation of RXFP1 increases pSTAT3 levels. This resulted in enhanced MPG expression and activity and contributed to chemoresistance against TMZ. RXFP1 activation also increased cellular levels of the new BER member HMGA2 and this was dependent on STAT3 activation. HMGA2 promotes chemoresiatance in cancers (Summer et al. 2009, Palmieri et al. 2011, Natarajan et al. 2013, Wu et al. 2015a). In this part III, I will examine whether HMGA2 can promote TMZ resistance in GB cells. Moreover, I will investigate whether the multi-tyrosine kinase inhibitor Dovitinib (DOV) can cooperate with TMZ to increase the efficacy of TMZ in killing GB cells. The results in this part III were recently published: Thanasupawat, T., et al., *Dovitinib enhances temozolomide efficacy in glioblastoma cells*. Mol Oncol, 2017.

3.9 HMGA2 is expressed in the nucleus of GB cells

I explored the expression of HMGA2 mRNA transcripts in patient GB cells derived from glioblastoma patients by RT-PCR. HMGA2 transcripts were expressed in all isolated patient GB cells and HMGA2 was also highly expressed in established U87MG and U251 GB cell lines **(Figure 3.16A)**. Western blot analysis revealed HMGA2 protein to be exclusively present in the nuclear fraction of patient GB cells, U87MG and U251 **(Figure 3.16B)**. Immunohistochemistry confirmed the nuclear localization of HMGA2 in GB xenografts derived from U87MG cells **(Figure 3.16C),** primary patient GB tissue sections **(Figure 3.16D)** and GB tissue microarray cores **(Figure 3.16E)**. There was no positive staining with non-immune rabbit serum used as negative control **(Figure 3.16F)**.

Figure 3.16 Expression of HMGA2 in GB cells.

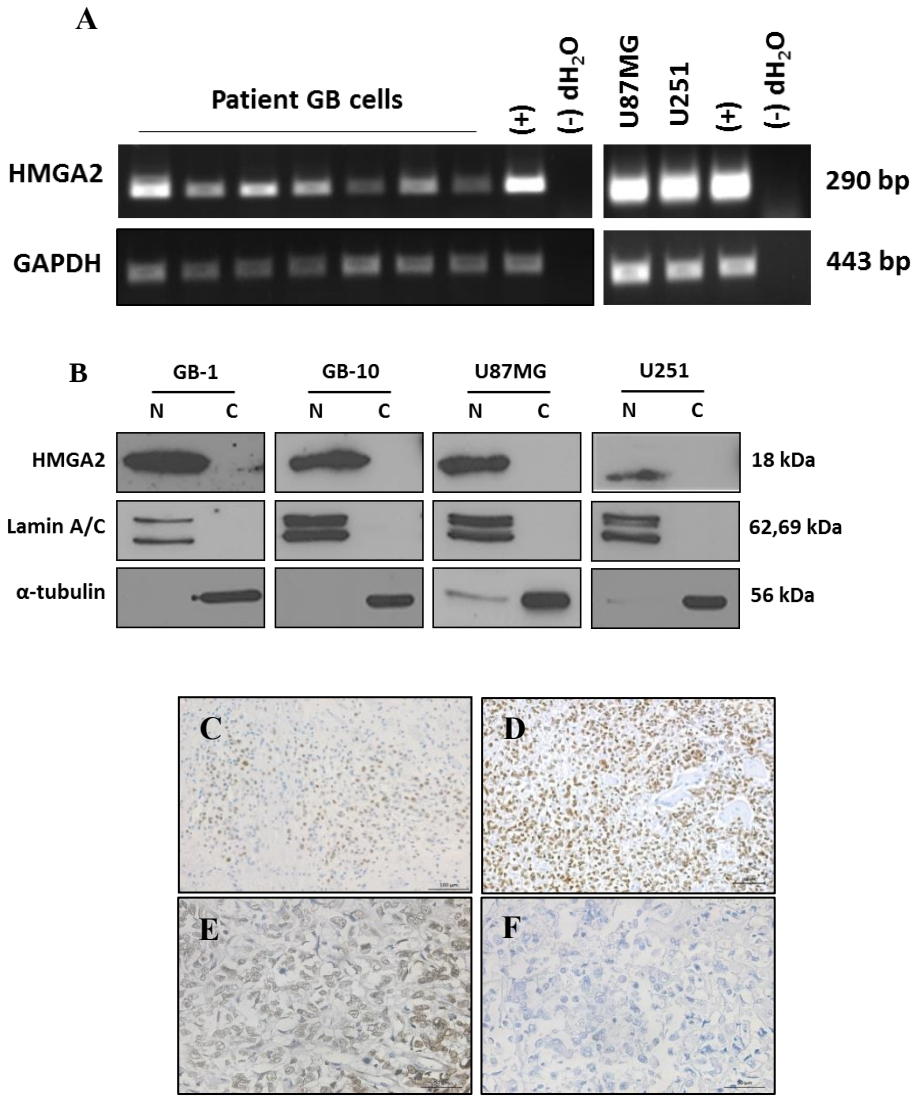

Figure 3.16 (A) mRNA levels of HMGA2 were performed by semiquantitative RT-PCR in patient GB cells, U87MG and U251 GB cell lines. GAPDH was used as internal control. **(B)** Nuclear and cytoplasmic western blot detection was used to detect HMGA2 expression. Lamin A/C and α-tubulin were used as loading control for nuclear (N) and cytoplasmic (C) protein fraction, respectively. Immunohistochemical detection of HMGA2 in **(C)** human U87MG xenografts, **(D)** patient human GB tissue, and **(E)** GB tissue microarray cores of brain tumor tissues. **(F)** Rabbit IgG isotype was used as negative control. Magnification: C and D, x100; E and F, x400. The data were the same in Suchitra Natarajan's thesis "Roles of high mobility group AT-hook protein 2 (HMGA2) in human cancer". Data were published in Thanasupawat, T., et al., Dovitinib enhances temozolomide efficacy in glioblastoma cells. Mol Oncol, 2017.

3.10 HMGA2 promoted TMZ chemoresistance

HMGA2 has been shown to contribute to BER which provided the rationale to determine whether HMGA2 may represent a second new mechanism that, in addition to MPG, may contribute to TMZ chemoresistance in GB cells. I successfully performed specific siRNA mediated knockdown of HMGA2 expression in U251 which was confirmed by Western blot **(Figure 3.17A)**. The effect of HMGA2 on GB cell viability and caspase 3/7 activation was investigated in the presence and absence of TMZ, using an IC_{50} TMZ concentration determined at 1.5 mM by WST assays in U251 parental cells after 24h of TMZ incubation **(Figure 3.17B)**. In U251 cells treated with TMZ treatment, knockdown of HMGA2 significantly reduced cell viability compared to cells treated with scrambled siRNA control **(Figure 3.17B)**. Similarly, TMZ increased caspase 3/7 activity in U251 cells and knockdown of HMGA2 caused a further significant increase in caspase 3/7 activity **(Figure 3.17C)**.

I investigated the effect of HMGA2 on TMZ-induced induction of DNA damage by detecting γH_2AX, a marker of double strand DNA breaks. TMZ caused the appearance of multiple γH_2AX foci **(Figure 3.17D)** and HMGA2 silencing caused another increase in the number and fluorescence intensity of γH_2AX foci compared to scrambled si control cells and was quantified as average number of γH_2AX foci per cell shown in **Figure 3.17E**. These results clearly indicated that HMGA2 has a critical role in protecting GB cells from the DNA damaging effects of TMZ and decreased HMGA2 levels are associated with increased caspase activity.

Figure 3.17 HMGA2 promoted TMZ chemoresistance.

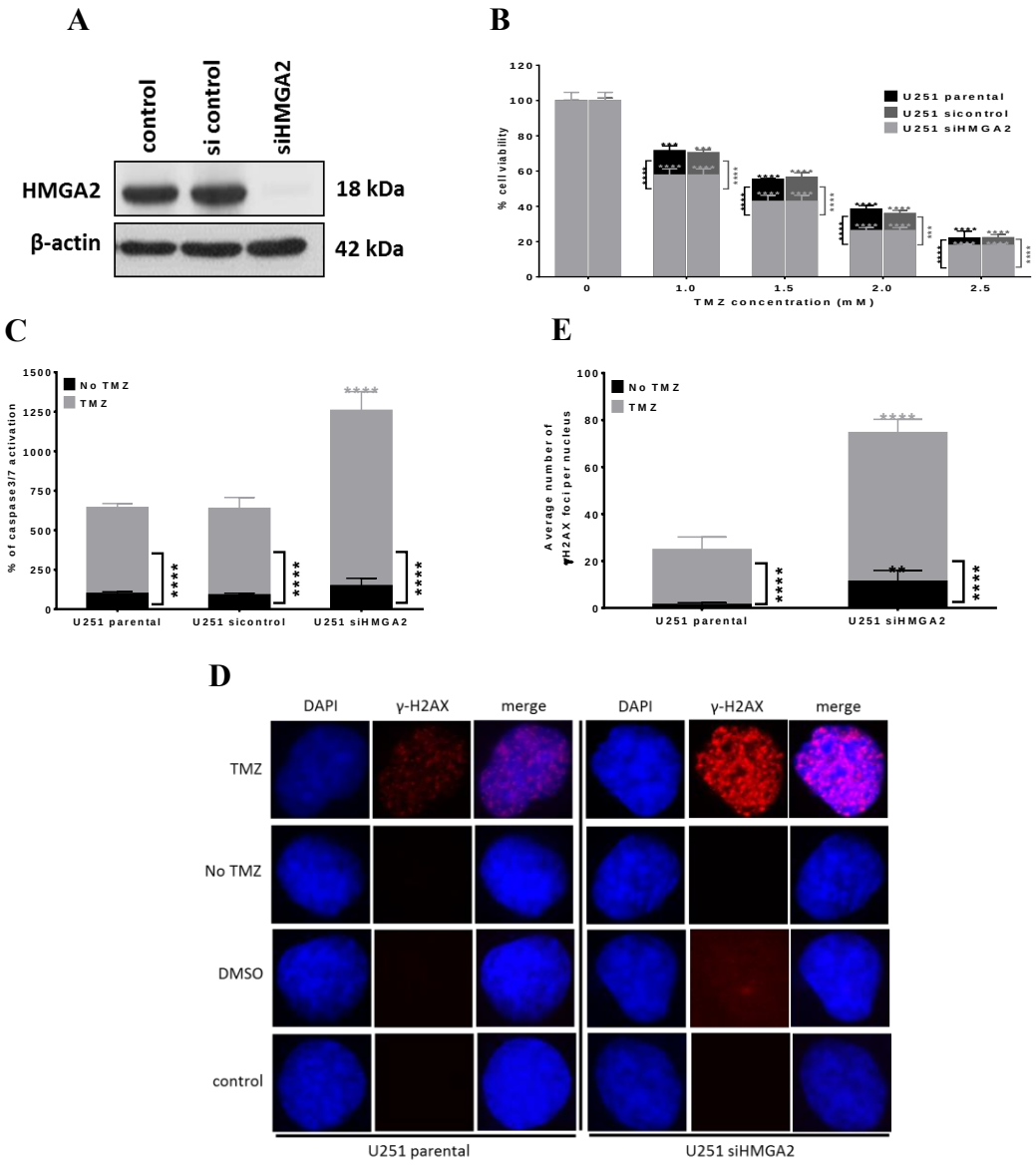

Figure 3.17 (A) Western blot detection of knockdown HMGA2 by a specific siHMGA2 at 72h in U251. Scramble sequences was used as negative control. β-actin was used as loading control. **(B)** WST assay was performed to determine the reduction cell viability after HMGA2 knockdown followed by TMZ treatment for 24h. **(C)** Caspase3/7 activity assay was used to examine the induction of apoptosis after 1.5 mM TMZ incubation for 24h. **(D)** Representative nuclear images of imunofluorescence detection of γH2AX in U251 under TMZ treatment. **(E)** 30 nuclear cells were used to examined the number of γH2AX foci which was presented as an average number of foci per cell. The data were the same in Suchitra Natarajan's thesis "Roles of high mobility group AT-hook protein 2 (HMGA2) in human cancer". Data were published in Thanasupawat, T., et al., Dovitinib enhances temozolomide efficacy in glioblastoma cells. Mol Oncol, 2017.

TMZ-induced O^6-MeG is repaired by O^6-methylguanine-DNA methyltransferase (MGMT). MGMT is a key factor to promote TMZ chemoresistance in GB patients. Patients who have MGMT promoter methylation will have the better outcome under TMZ treatment (Hegi et al. 2005, Dunn et al. 2009, Uno et al. 2011, Yang et al. 2012). In this study, MGMT expression was demonstrated in patient GB cells but found to be absent in U251 **(Figure 3.18A)**. I wanted to investigate whether HMGA2 and MGMT cooperated in chemoresistance to TMZ in GB cells. I performed single and double knockdown of HMGA2 and MGMT and confirmed by Western blots the successful single and double knockdown of HMGA2 and MGMT in patient GB cells **(Figure 3.18B)**. In GB cells treated with TMZ, silencing of HMGA2 caused a marked increase in caspase3/7 activation but this did not occur with MGMT knockdown **(Figure 3.18C)**. Dual KD of HMGA2 and MGMT showed an increased caspase3/7 activity similar to HMGA2 KD alone, excluding the possibility of MGMT and HMGA2 exerting additive or synergistic effects on caspase activity. This suggested that reduction in MGMT does not cause apoptosis, and previous research work has shown that in the absence of MGMT TMZ-induced O^6-MeG-DNA lesions are repaired by the mismatch repair pathway and do not induce apoptosis immediately (Quiros et al. 2010).

Figure 3.18 Effect of double knockdown HMGA2 and MGMT under TMZ treatment.

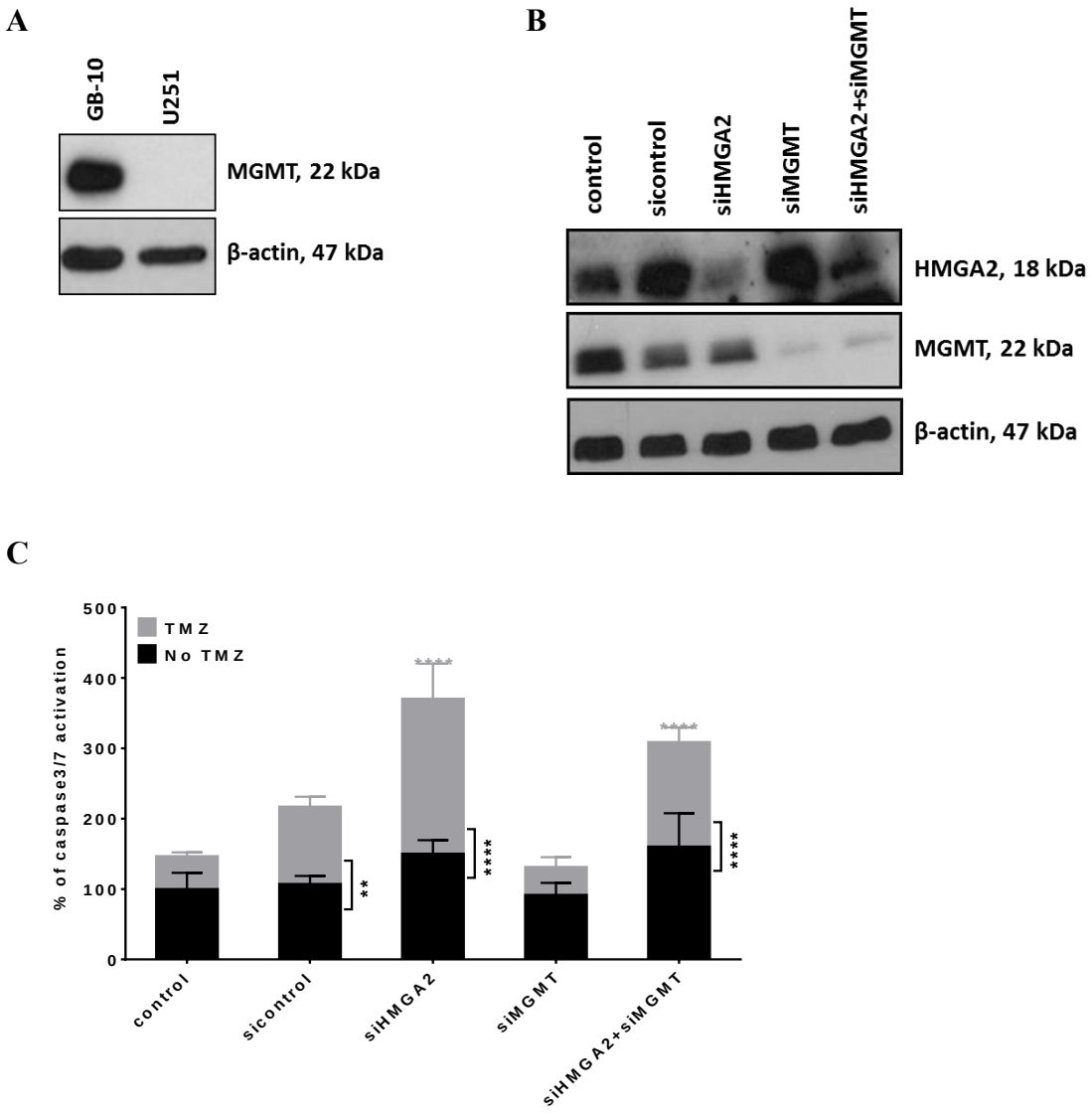

Figure 3.18 (A) Western blot detection of MGMT expression in U251 and patient GB cells (GB-10). **(B)** Either individual knockdown of HMGA2/ MGMT or double knockdown for 72h was showed and then performed **(C)** caspase3/7 activity assay to determined apoptosis phenomenon under 2 mM TMZ (IC_{50} for GB-10) incubation for 24h in GB-10. Scramble sequences was used as negative control. β-actin was used as loading control. Data were published in Thanasupawat, T., et al., Dovitinib enhances temozolomide efficacy in glioblastoma cells. Mol Oncol, 2017.

3.11 DNA minor groove binder agents show additive reduction in cell viability upon TMZ treatment

The antimicrobial drugs pentamidine (PEN) and netropsin (NET) share with HMGA2 the ability to bind to AT-rich regions within the minor groove of double stranded DNA (Nguyen et al. 2004, Hasinoff et al. 2012). I tested the hypothesis that both drugs can compete with HMGA2 for binding to these DNA sites and diminish the chemoprotective role of HMGA2 in GB cells treated with TMZ. I used WST cell viability assays to determine IC_{50} doses for PEN in patient GB cells which were 75 μM and 100 μM in U251 and patient GB cells, respectively **(Figure 3.19A and B)**. Dual treatment with PEN and TMZ (both at IC_{50} concentrations) resulted in reduction in cell viability compared either drug alone. A similar additive reduction in cell viability was observed for the dual NET plus TMZ treatment in U251 and patient GB cells **(Figure 3.19C and D)**. These data indicated that minor groove binders may compete with HMGA2 for DNA binding and, thus, reduce the ability of this stem cell factor to protect GB cells from TMZ induced DNA damage.

3.12 DOV increased the sensitivity to TMZ and reduced BER proteins expression

Both PEN and NET are relatively toxic and do not cross the blood brain barrier (BBB) excluding their use in GB patients. The multi-tyrosine kinase inhibitor Dovitinib (DOV) binds to the minor groove of DNA at AT-rich regions and can penetrate the BBB. DOV is currently used in clinical trials on recurrent GB patients (Schafer et al. 2016). U251 and patient GB cells responded to DOV with a dose-dependent reduction in cell viability after 24h, with an IC_{50} of 15 μM in U251 and 14.5 μM in patient GB cells **(Figure 3.19E and F)**. Dual treatment with DOV and TMZ resulted in a further reduction in cell viability

compared to TMZ alone. Next, I investigated the additive effect of DOV and TMZ in human GB cells. Western blot analysis of selected proteins known to be associated with BER revealed that DOV at concentrations 14.5 μM was able to diminish the protein content of a number of BER factors after 24h of exposure in patient GB cells **(Figure 3.19G)**. Those factors downregulated by DOV included HMGA2, MPG, APE1, and MGMT; all key factors in single strand DNA repair.

Figure 3.19 DNA minor groove binder agents increase sensitivity of TMZ in GB cells.

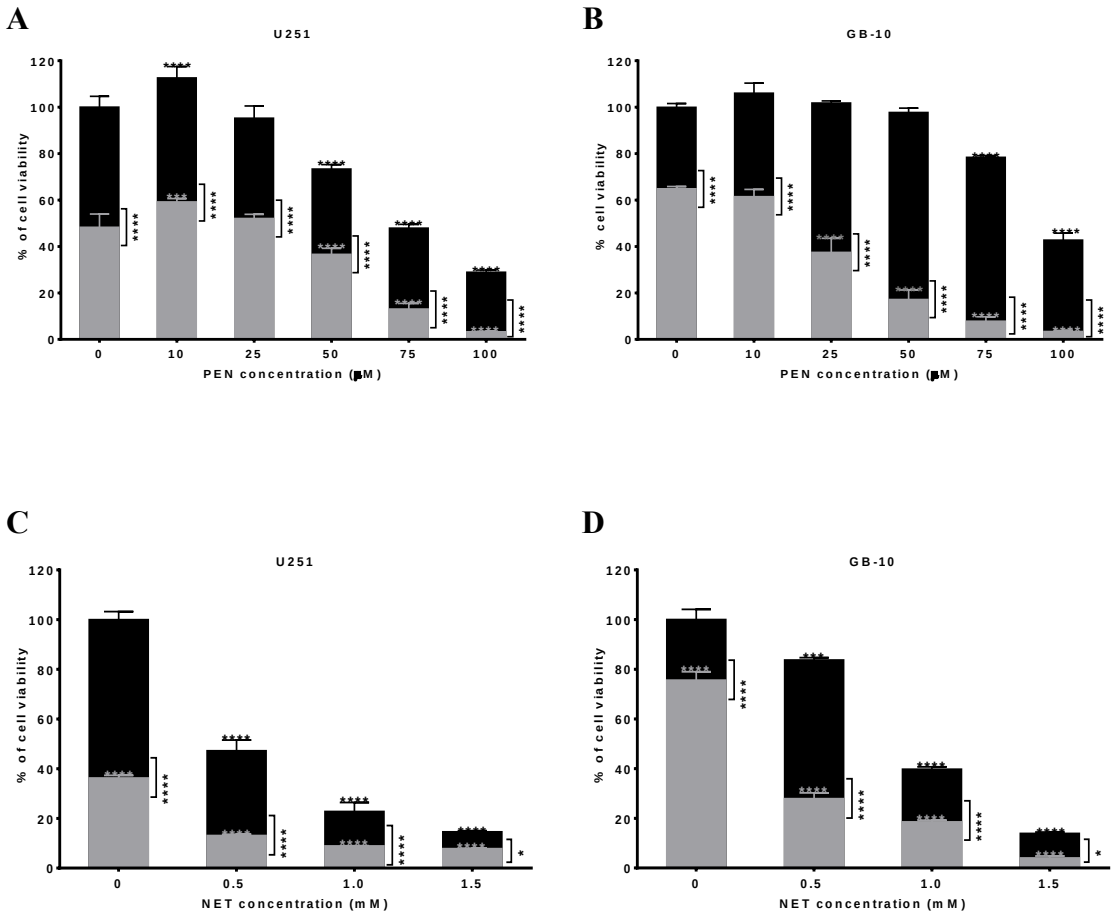

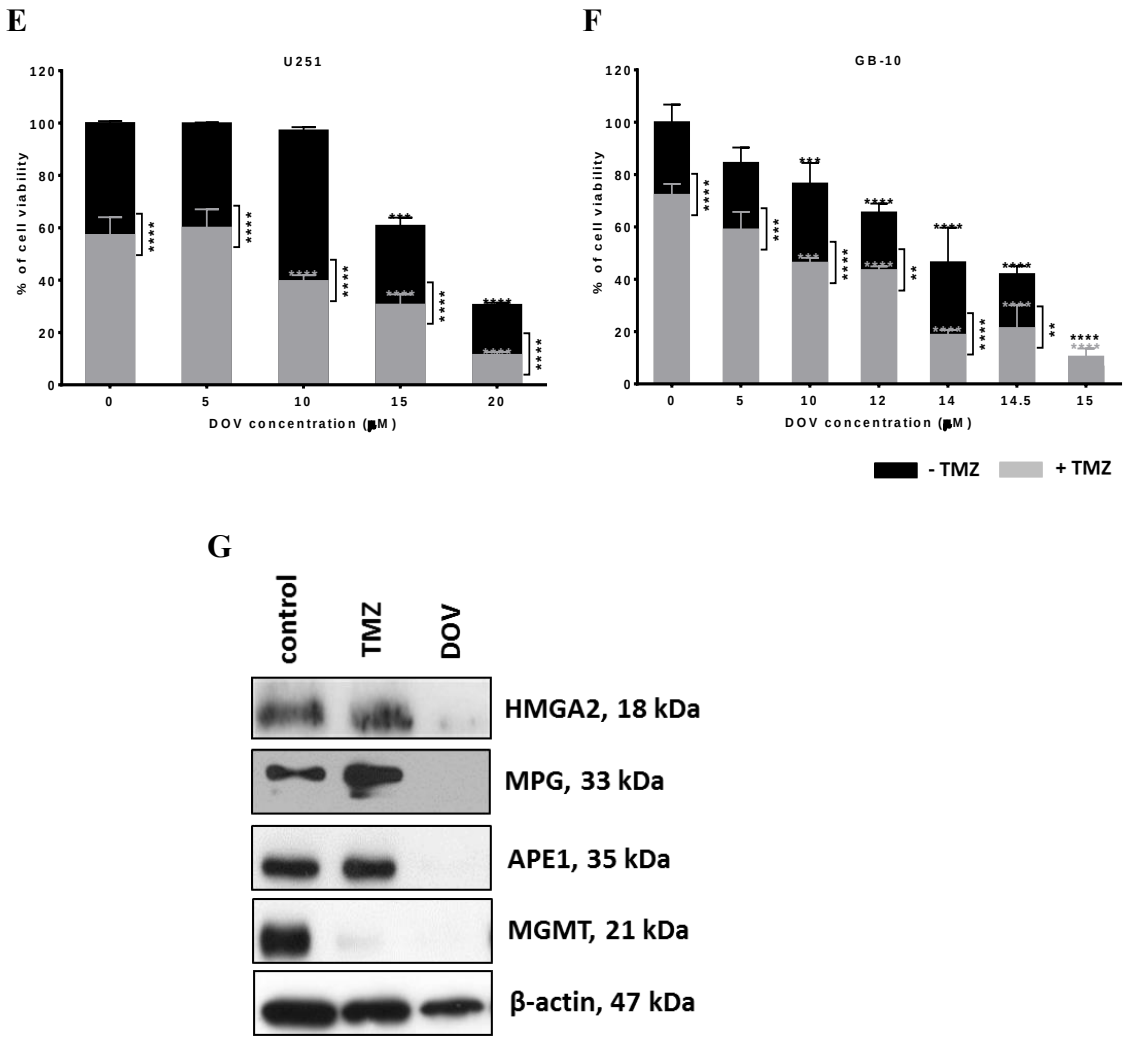

Figure 3.19 (A-F) WST assay was performed to determine cytotoxicity under PEN, NET, DOV treatment alone and in combination with TMZ for 24h. The results were presented as percentage of cell viability in U251 and GB-10. **(G)** Western blot detection of HMGA2, BER protein members, and MGMT upon single treatment of TMZ or DOV at IC_{50} for 24h in GB-10. β-actin was used as loading control. Data A-F were the same in Suchitra Natarajan's thesis "Roles of high mobility group AT-hook protein 2 (HMGA2) in human cancer". Data were published in Thanasupawat, T., et al., Dovitinib enhances temozolomide efficacy in glioblastoma cells. Mol Oncol, 2017.

Low dose DOV (1, 2, and 5 μM) treatment significantly increased the sensitivity towards TMZ (100 μM) as determined by cell viability assays in U251 cells, whereas each drug alone failed to cause a marked reduction in cell viability over a 72h incubation period **(Figure 3.20A)**. Contrary to U251, patient GB cells displayed a significant reduction in cell viability with either DOV or 100 μM TMZ treatment and there was no further reduction in cell survival when the drug combination was applied **(Figure 3.20B)**.

Low concentration of DOV (1, 2 and 5 μM) down-regulated HMGA2 as early as 24h of DOV treatment and this effect lasted for up to 72h in U251 and patient GB cells **(Figure 3.20C)**. MGMT protein content was diminished at 72h in patient GB cells **(Figure 3.20E)**. At these concentrations, DOV also suppressed the cellular level of other BER protein members investigated which included MPG, APE1, FEN1, PARP1, XRCC1, and HMGA2 **(Figure 3.20C)**. These changes on BER protein levels coincided with a strong induction of γH_2AX foci as determined at 5 μM DOV treatment **(Figure 3.20D)**.

Figure 3.20 Dovitinib increased TMZ sensitivity and reduced BER proteins expression.

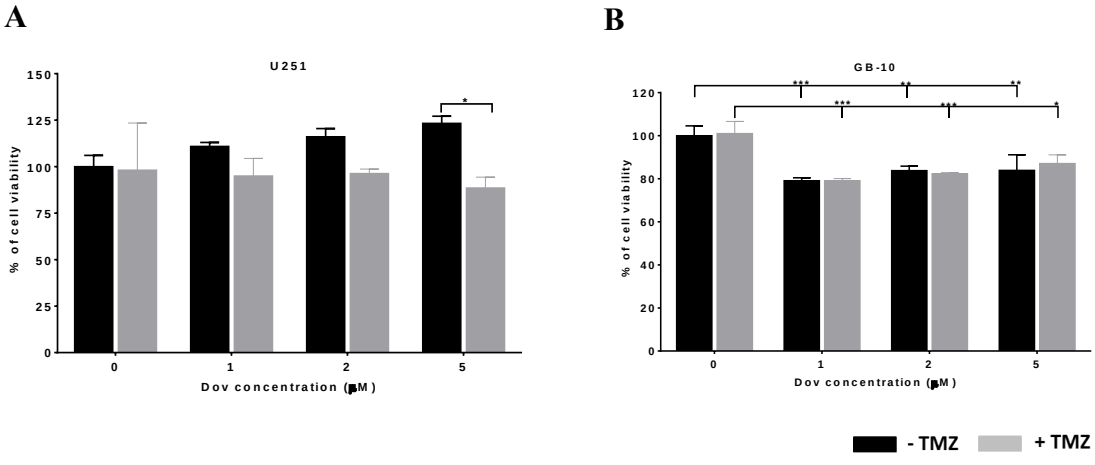

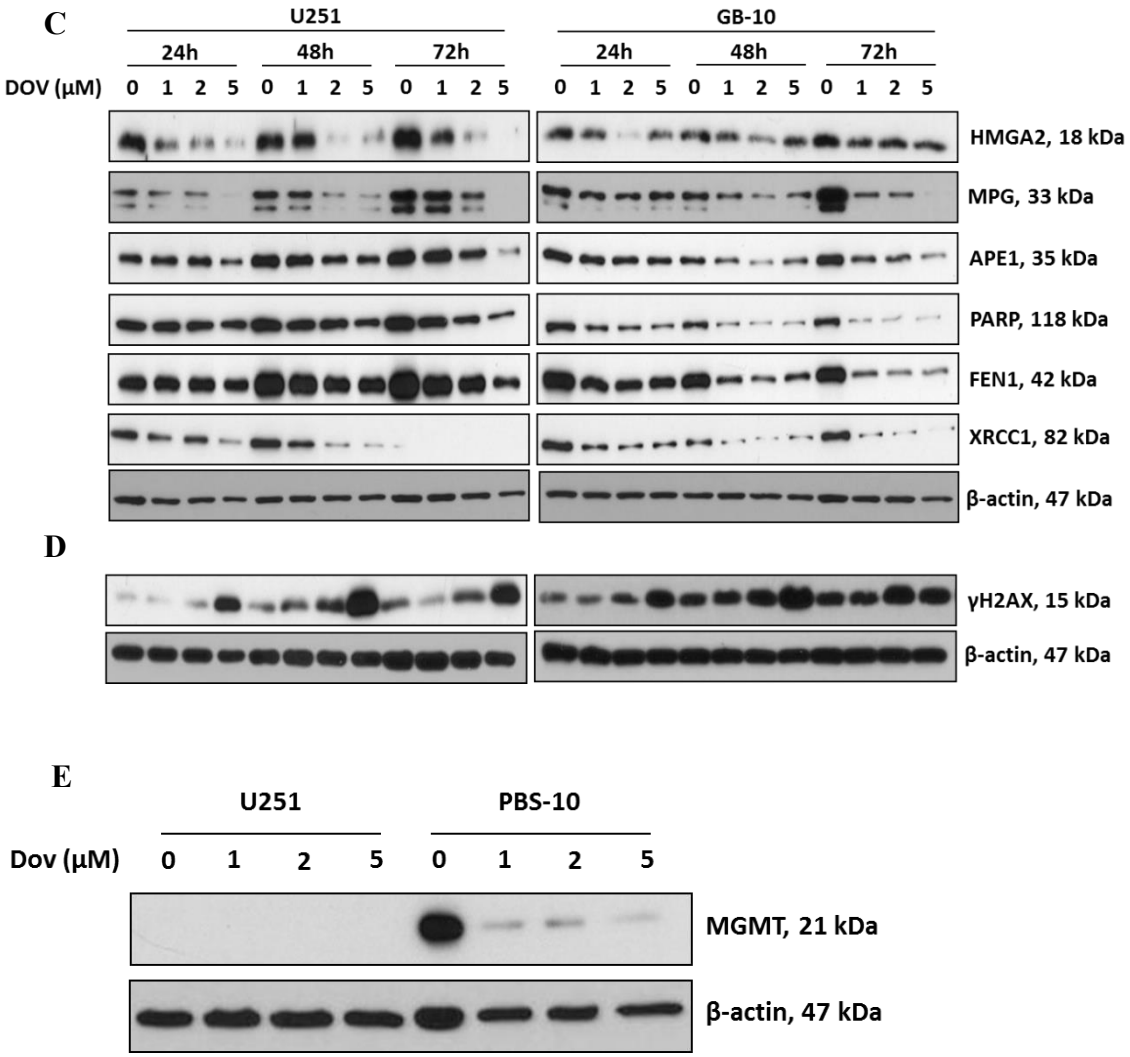

Figure 3.20 (A and B) WST assay was performed to determine the effect of DOV at low concentrations (1, 2, and 5 μM) and 100 μM TMZ on cell viability upon 72h incubation in U251 and patient GB cells. **(C)** Western blots detected downregulation of HMGA2 and BER protein members expression upon 1, 2, and 5 μM DOV at 24, 48, and 72 incubation times. **(D)** Upregulation of γH2AX expression was showed under these treatments. **(E)** MGMT detection was performed under 1, 2, and 5 μM DOV treatment for 72h in U251 and GB-10. β-actin was used as loading control. Data C and D were the same in Suchitra Natarajan's thesis "Roles of high mobility group AT-hook protein 2 (HMGA2) in human cancer". Data were published in Thanasupawat, T., et al., Dovitinib enhances temozolomide efficacy in glioblastoma cells. Mol Oncol, 2017.

HMGA2 expression has been shown to be regulated by a STAT3-Lin28-Let7 pathway. STAT3 stimulates lin28A which suppresses let-7, a microRNA known to bind to the 3'UTR of HMGA2 transcripts and inhibit HMGA2 translation (Guo et al. 2013)**.** My discovery that hrCTRP8/hrRLN2-RXFP1-STAT3 pathway was able to increase HMGA2 protein expression, I asked whether DOV could interfere with this process by reducing STAT3 activation. Indeed, the phosphorylation of STAT3 at Tyr705 ($pSTAT3^{Tyr705}$) was inhibited by DOV in U251 **(Figure 3.21A)** and this coincided with the ability of DOV to suppress Lin28A and HMGA2 expression at 48 and 72h **(Figure 3.21B)**.

Figure 3.21 Dovitinib suppressed phospho-STAT3 in GB cells.

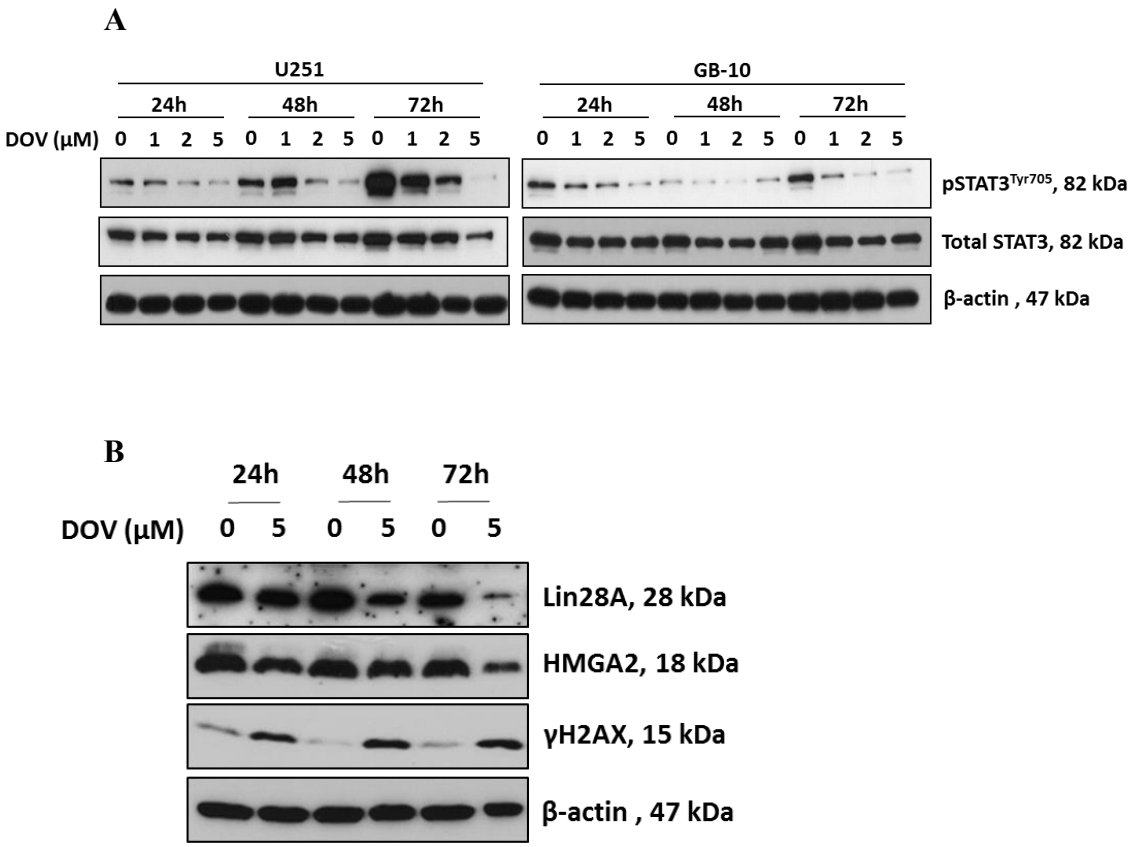

Figure 3.21 (A) Western blot detection of the reduction of phosphorylation STAT3 at tyr705 (pSTAT3^{tyr705}) upon 1, 2, and 5 μM DOV for 24-72h treatments in U251 and GB-10. **(B)** Upon 5 μM DOV, blots showed the suppression of lin28A and HMGA2 but induction of γH2AX in U251. β-actin was used as loading control. Data A were the same in Suchitra Natarajan's thesis "Roles of high mobility group AT-hook protein 2 (HMGA2) in human cancer". Data were published in Thanasupawat, T., et al., Dovitinib enhances temozolomide efficacy in glioblastoma cells. Mol Oncol, 2017.

The downregulation in protein content of HMGA2 and specific BER members by low dose DOV treatment coincided with enhanced cell apoptosis upon TMZ treatment. Caspase3/7 activity significantly increased upon treatment with either TMZ, DOV, or dual DOV/TMZ treatment at 48h in U251 but did not differ between these treatments **(Figure 3.22A)**. However, in patient GB cells only the dual DOV/TMZ treatment was able to increase caspase 3/7 activity as determined at 48h **(Figure 3.22B)**. I applied the Nicoletti technique of flow cytometry analysis upon PI staining of GB cells (Riccardi and Nicoletti 2006). To evaluate the DNA contents in U251 exposed to the different treatments **(Figure 3.22C)**. The percentage of apoptotic cells was increased in all treatments at 24h to 48h, with the highest number of apoptotic cells observed at 48h with dual DOV (2 μM)/TMZ (100 μM) treatment **(Figure 3.22D)**. I confirmed by Western blot that HMGA2 protein levels were reduced upon treatment with DOV alone and in combination with TMZ, whereas TMZ alone had no such effect **(Figure 3.22E)**. These results suggest that the combination DOV/ TMZ treatment may be advantageous in reducing GB cell survival.

Figure 3.22 Combination treatment dovitinib and TMZ induced apoptosis in GB cells.

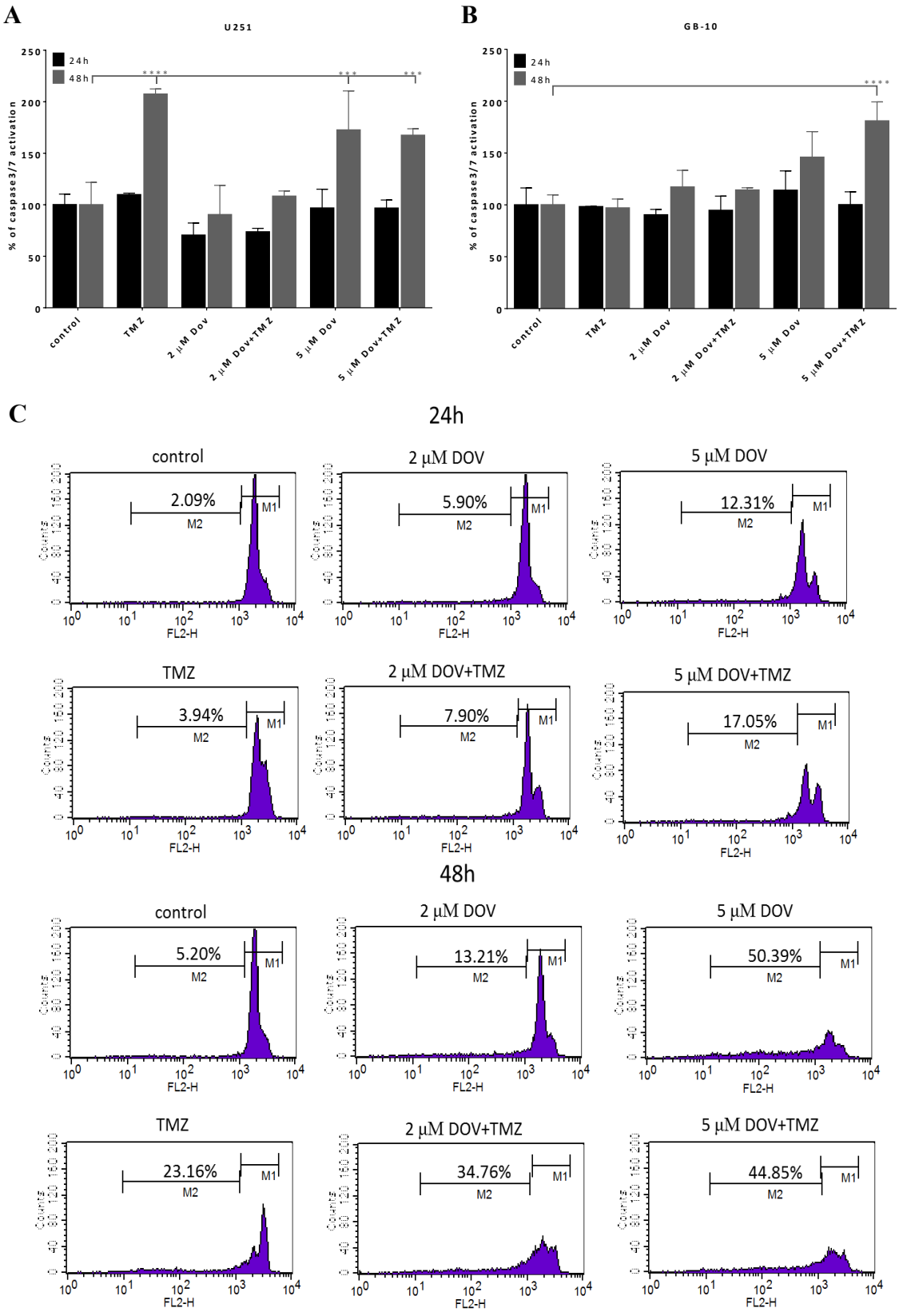

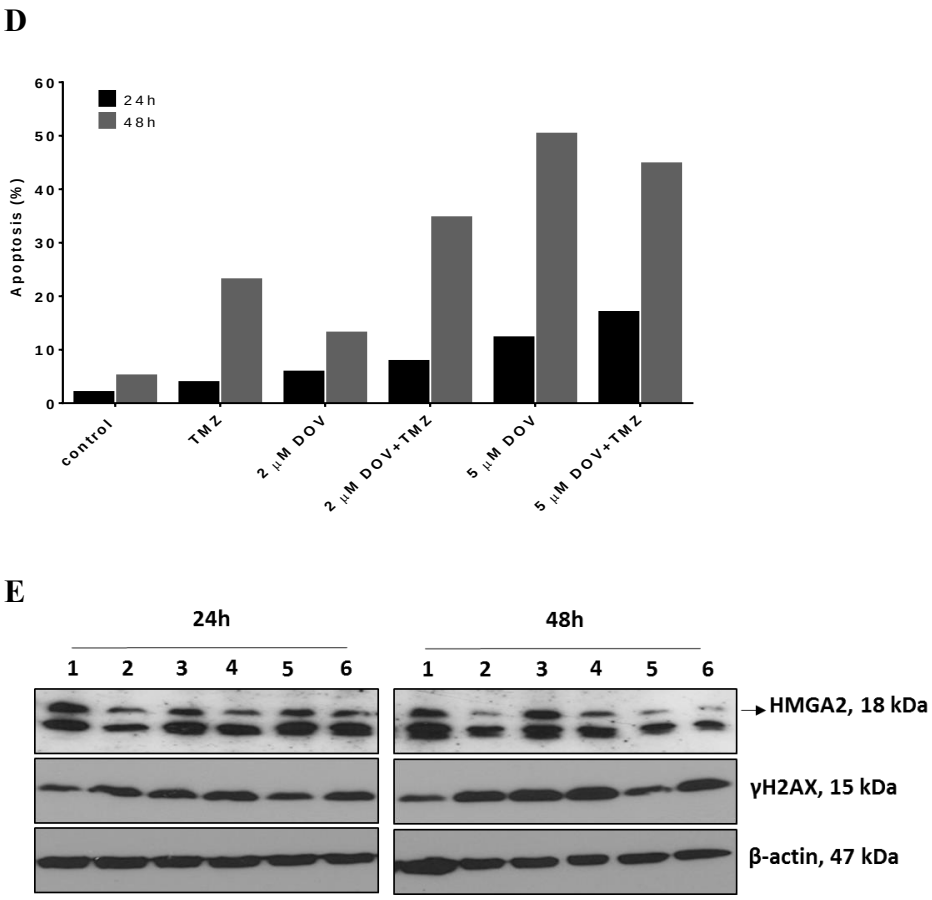

Figure 3.22 Capase3/7 activity assay was performed to study the induction of apoptosis upon 2 and 5 μM DOV treatment alone or combination with 100 μM TMZ at 24 and 48h in **(A)** U251 and **(B)** GB-10. **(C)** Flow cytometry with PI staining was performed in U251. Flow cytometry was used to study apoptotic cells under cell cycle distribution by Nicoletti method. M1 peak represented the percentage of cells in the S/G2/M phase of cell cycle. M2 peak indicated apoptotic cells in the sub-G1 (subdiploid) peak. Percentage of apoptotic cells in M2 peak was presented in **D**. **(E)** Western blot analysis of HMGA2 and γH2AX in U251 under the treatments as indicated: **1**: medium control, **2**: 5 μM DOV, **3**: 100 μM TMZ, **4**: 5 μM DOV plus 100 μM TMZ, **5**: 2 μM DOV, and **6**: 2 μM DOV plus 100 μM TMZ. Data were published in Thanasupawat, T., et al., Dovitinib enhances temozolomide efficacy in glioblastoma cells. Mol Oncol, 2017.

3.13 Combined treatment with DOV and TMZ reduces GB cell survival

I showed that at concentrations measured in the blood of patients (Kang et al. 2013), DOV was able to suppress the protein expression of HMGA2 and BER factors in a GB cells. Based on these findings, I reasoned that pre-treatment with DOV alone may sensitize GB cells to TMZ. To test this, U251 and patient GB cells were treated with DOV (5 μM) for 3 days followed by TMZ exposure alone for another 3 days. This successive treatment significantly decreased cell viability and exhibited even greater cell death with an additional 24h of DOV treatment **(Figure 3.23A-C)**. I examined long term GB cell survival following a recovery period after these sequential treatments. The experiment was performed for 24 days. Treatment comprised of 3 days DOV followed by 3 days TMZ and this cycle was repeated until day 15 days, alternating between DOV and TMZ. The remaining 9 days, cells were grown in normal growth medium for recovery. For the control experiment, the same method was used but normal culture medium was used to replace DOV **(Figure 3.24A)**. Colony formation was determined after 9 days of recovery time in normal growth medium. The number of colonies after recovery time was significantly decreased in DOV and TMZ treatment compared to the TMZ only treatment in U251 **(Figure 3.24B and C).** Importantly, patient GB cells failed to form any colonies upon sequential treatment **(Figure 3.24B)**. These results were likely not dependent on the MGMT status. U251 is negative for MGMT, whereas the patient GB cells expressed MGMT and, thus, would be expected to exhibit higher repair capacity and be more resistant to TMZ. However, the fact that no colonies were observed with patient GB cells suggested that the sequential DOV-TMZ treatment may have successfully diminished cellular

MGMT protein content which contributed to a more effective TMZ sensitization **(Figure 3.24D-E)**.

Figure 3.23 Sequential treatment with DOV and TMZ sensitized GB cells to TMZ.

A

Treatments	Day 1	Day 2	Day 3	Day 4	Day 5	Day 6	Day 7
1	Normal growth medium						
2	Normal growth medium				DOV		
3	Normal growth medium				TMZ		
4	Normal growth medium						DOV
5	Normal growth medium	DOV			TMZ		
6	Normal growth medium			TMZ			DOV
7	DOV			TMZ			DOV

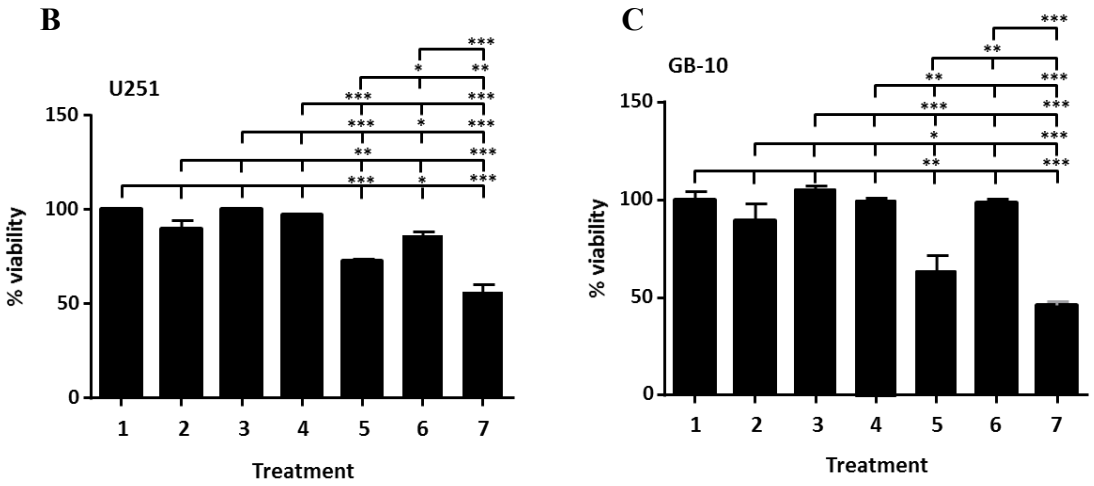

Figure 3.23 (A) Schematic represented sequential treatment of 5 μM DOV and 100 μM TMZ. WST assay was performed to determine cell viability in **(B)** U251 and **(C)** GB-10. Data were published in Thanasupawat, T., et al., Dovitinib enhances temozolomide efficacy in glioblastoma cells. Mol Oncol, 2017.

Figure 3.24 Alternating DOV and TMZ treatments reduce cell survival upon recovery.

A

Day	1	2	3	4	5	6	7	8	9	10	11	12	13	14	15	16	17	18	19	20	21	22	23	24
I		DOV			TMZ			DOV			TMZ			DOV			Recovery in normal growth medium for 9 days							
II		Normal growth medium			TMZ			Normal growth medium			TMZ			Normal growth medium			Recovery in normal growth medium for 9 days							

B

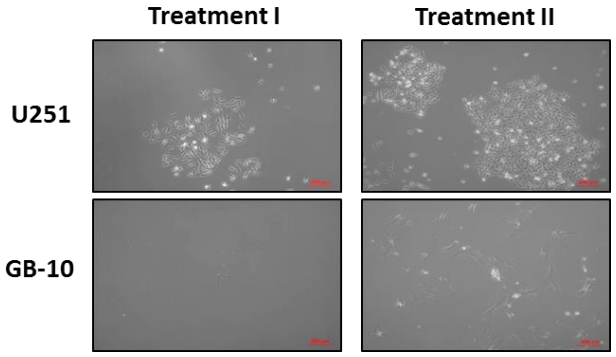

C

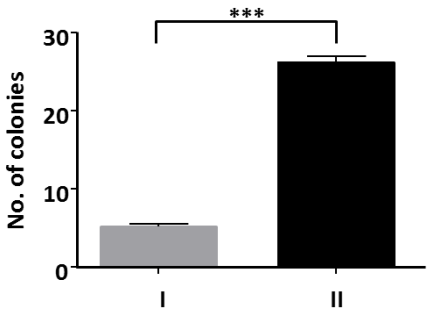

D

Treatment	Day1	Day2	Day3	Day4	Day5	Day6	Day7
1					DOV		
2		DOV			TMZ		
3	DOV			TMZ			DOV

E

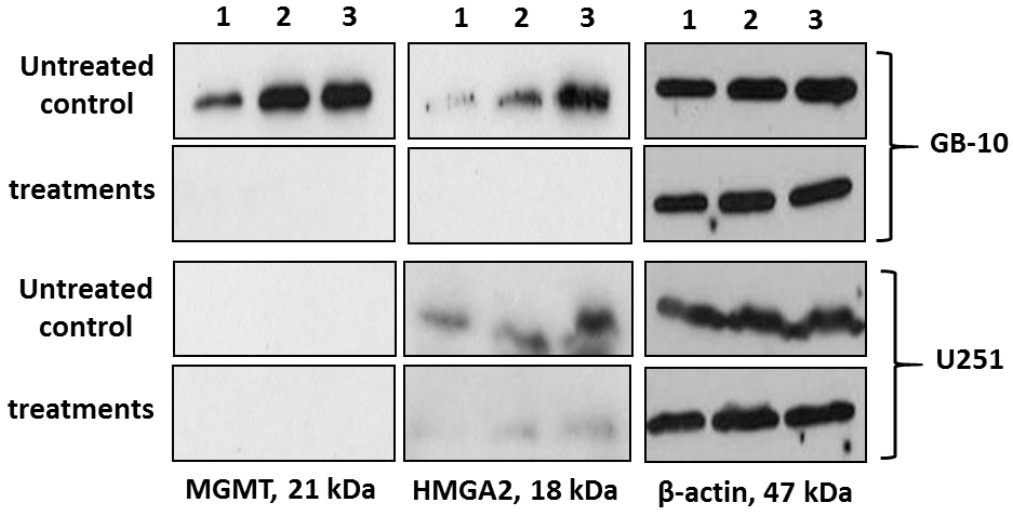

Figure 3.24 (A) Schematic represented the alternating treatment between 5 μM DOV and 100 μM TMZ followed by recovery in normal growth medium for 9 days in U251 and GB-10. Colony formation was observed after recovery period. **(B)** Phase contrast microscope was used to determine the number of colonies. Colonies number of U251 were counted and presented in **C**. **(D)** Schematic represented the treatment of 5 μM DOV and 100 μM TMZ before performing **(E)** western blot to detect HMGA2 and MGMT expression in U251 and GB-10. β-actin was used as loading control. Data were published in Thanasupawat, T., et al., Dovitinib enhances temozolomide efficacy in glioblastoma cells. Mol Oncol, 2017.

CHAPTER 4: DISCUSSION

4.1 Part I. Human CTRP8 is a new ligand of RXFP1 and induces migration of brain cancer cells

Cancer cell models of the breast, thyroid and prostate have mainly been used to establish novel autocrine/paracrine molecular mechanisms by which the relaxin-RXFP1 ligand-receptor system contributes to tumor propagation, tissue invasion, and metastasis (Tashima et al. 1994, Hombach-Klonisch et al. 2000, Silvertown et al. 2003, Hombach-Klonisch et al. 2006, Klonisch et al. 2007, Feng et al. 2009, Halls and Cooper 2010, Summers 2012, Halls et al. 2015). With the exception of one report on relaxin-3 expression and function in the mouse neuroblastoma cell line Neuro2a (Tanaka et al. 2009), I was the first to investigate the expression of RXFP1 and RLN1/2 in human brain tumors. I focused on glioblastoma (GB), the most frequent and most malignant forms of brain tumors in humans. While RXFP1 transcripts were present in all GB cells tested, RXFP2 or the classical RXFP1 ligands RLN1-3 and INSL3 were undetectable. This suggested the presence of another as yet unidentified novel ligand of RXFP1 in GB (Bathgate et al. 2013). Further evidence in support of this notion came from a peptide library screen using a Chinese hamster ovary (CHO) reporter cell line stably transfected with RXFP1 (Shemesh et al. 2008, Shemesh et al. 2009). This screen identified two small linear peptides, P59 and P74, which, at a final concentration of 1μM, bound to RXFP1 and elicited a weak cAMP response (Shemesh et al. 2008). Both peptide sequences were identical to a peptide region located at the transition from the collagen-like to the C1Q-like domain of C1Q-tumor necrosis factor related peptide 8 (CTRP8), a recently discovered member of the CTRP peptide family (Peterson et al. 2009). Expression of CTRP8 was observed in both GB cell

lines and patient GB cells and coincided with RXFP1 expression suggesting that, like RLN2 in other normal and neoplastic tissues, CTRP8 may exert autocrine/paracrine functions in GB tissues. P59, P74, and recombinant human full size CTRP8 were bioactive and increased cAMP production in $RXFP1^{+}$ patient GB cells (Glogowska et al. 2013). Similar responses were obtained with recombinant RLN2 and specific RXFP1 knockdown completely blocked cellular functions of these ligands in GB cells. This indicated that the presence of native functional RXFP1 was essential for activating cell signaling pathways by cognate RLN2 and the new RXFP1 ligand, CTRP8 or derived peptides. RLN2-RXFP1 is known to promote a pro-migratory phenotype and remodel the ECM by increasing the expression and secretion of a range of proteolytic enzymes. This includes the altered expression and secretion of matrix-metalloproteinases, their tissue inhibitors (TIMPs) and the secretion of powerful lysosomal hydrolases of the cathepsin family (Hombach-Klonisch et al. 2006, Samuel et al. 2007, Bialek et al. 2011, Samuel et al. 2016). I identified cathepsin B (cath-B) as a novel CTRP8-RXFP1 target gene in GB. Cath-B has a dual function by promoting the degradation of basal lamina to facilitate tissue invasion of GB cells and inhibiting apoptosis in brain tumors (Levicar et al. 2003b, Levicar et al. 2003a). Importantly, high serum levels of cath-B are associated with poor prognosis of GB patients (Strojnik et al. 2014). This is the first indication of a clinically relevant involvement of the CTRP8-RXFP1 system in brain tumors and identifies CTRP8 and RXFP1 as potential new therapeutic targets.

Next, I determined the cellular signaling pathways responsible for the enhanced cell migration, matrix invasion, and cath-B expression/secretion in human GB cells. Intriguingly, RXFP1 activation identified PI3 kinase, PKCδ and PKCζ as important

RXFP1 signaling pathways. In fibrocartilaginous cells, an important role of PI3 kinase as a key regulator of RXFP1 activation of AKT and PKCζ for induced MMP9/MMP13 mediated ECM turnover has been shown (Ahmad et al. 2012). In patient GB cells, RXFP1 activation by CTRP8/RLN2/P74 resulted in the activation of PI3 kinase and downstream novel isoform (nPKC) PKCδ and the atypical isoform (aPKC) PKCζ. PKC isoforms are categorized based on the secondary messenger requirements for the activation. Conventional PKCs (cPKCs) are Ca^{2+}-dependent and are activated by Ca^{2+} and diacylglycerol (DAG). The nPKCs are Ca^{2+}-independent which need only DAG for the activation. The aPKCs do not require both Ca2+ and DAG but are activated by the interaction between Phox/Bem (PB1) domain with partitioning defective-6 (PAR-6) (Steinberg 2008, Rosse et al. 2010). Relaxin binding was shown to link RXFP1 to $G\alpha_{s,}$ $G\alpha_{oB}$ and to $G\alpha_{i3}$ G-proteins and cause the activation of the $G\alpha_{i3}$-Gβγ-PI3K-PKCζ signalling pathway in several human cell types (Nguyen and Dessauer 2005). My results in patient GB cells treated with CTRP8 or the small CTRP8-derived peptides P59 and P74 suggest activation of an RXFP1-PI3K-PKCζ/PKCδ signaling cascade. The specific pharmacological blockade of either of the three cell signaling molecules or specific RXFP1 knockdown terminated the enhanced cell migration, matrix invasion and cath-B production observed in patient GB cells exposed to RXFP1 ligands. Moreover, my discovery of STAT3 signaling pathway suggested that the autocrine/paracrine RXFP1 activation with enhanced stimulation of oncogenic signaling pathways may support GB growth and survival. In many tumors, STAT3 and PKC signaling pathways are known to promote tumor cell survival, angiogenesis, cell migration and invasion (Chen et al. 2008, Aziz et al. 2010, Urtreger et al. 2012, Butler et al. 2013, Ouedraogo et al. 2016, Miyata et al. 2017).

The different members of the serine-threonine kinase family of PKCs have important roles in cell invasion and survival and several studies demonstrated the phosphorylation/ activation of STAT3 by PKCδ or PKCζ (Gartsbein et al. 2006, Litherland et al. 2010). Gartsbein et al. revealed insulin-mediated PKCδ activation to activate $STAT3^{Ser727}$ phosphorylation which triggered keratinocyte proliferation (Gartsbein et al. 2006). Insulin/IL-6-induced $STAT3^{Tyr705}$ and $STAT3^{ser727}$ phosphorylation was inhibited by a PKCδ inhibitor (rottlerin) in mouse 3T3-L1 adipocytes and mouse embryonic fibroblasts (MEFs). The downregulation of phospho-$STAT3^{Tyr705}$ was associated with decreased STAT3 nuclear translocation in MEFs (Wallerstedt et al. 2010). The knockdown of PKCδ inhibited the activation of $STAT3^{Tyr705}$ and $STAT3^{Ser727}$ phosphorylation which resulted in the reduction of collagen synthesis cardiac fibroblast (Naskar et al. 2014). PKCζ regulated pancreatic cancer cell growth and invasion and this required STAT3 activation (Butler et al. 2013, Butler et al. 2015). Although several studies have reported the activation of STAT3 by G protein-coupled receptors (GPCRs) in tumor progression (Lee et al. 2010), my discovery of the CTRP8-RXFP1 mediated phosphorylation of a cascade composed of PI3K-PKCδ/ PKCζ and STAT3 and its involvement in GB cell migration represents a novel signaling pathway and underscores the oncogenic signature of the relaxin receptor RXFP1 in GB.

The interaction of RLN2 with different extracellular domains of RXFP1 is a complex sequence of events that result in conformational changes to the receptor which trigger signaling. RLN2 binds with high affinity to the leucine-rich repeats (LRR) 4-8 of RXFP1 and the N-terminal linker between the LRRs and the low-density lipoprotein class A (LDA-A) module. This leads to the conformational change and allows RLN2 and the

LDL-A module to interact with the extracellular loop 2 (ECL2) which activates cell signaling (Sethi et al. 2016).

We confirmed by immunoprecipitation (IP) that CTRP8 interacts directly with RXFP1. Our preliminary protein binding algorithms studies (Glogowska et al. 2013) suggested that the CTRP8 peptide motif "YAAFSVG" present in both P59 and P74 and identified as being important for the RXFP1 interaction likely had contact with LRR domains 7 and 8 of the RXFP1 extracellular domain. The YAAFSVG motif is located at the very N-terminus of the barrel-shaped C1Q-like globular domain of CTRP8. Additional structural simulation analysis combined with in vitro RXFP1 mutational work are ongoing in the lab to provide a more detailed understanding of the structural requirements for the CTRP8-RXFP1 interaction. Binding studies with a small RXFP1 agonist suggest that the ability of this GPCR to activate certain signaling pathways depends on the structural requirements for a specific ligand to bind to RXFP1. Contrary to RLN2 and CTRP8, the allosteric agonist ML290 closely interacts with the helix 7 of the 7TM domain and ECL3 of RXFP1 (Takematsu et al. 2016) and RXFP1 activation by ML290 does not require the LDL-A module of RXFP1 (Xiao et al. 2013). Thus, it seems plausible that by utilizing partially distinct RXFP1 binding sites, RLN2 and CTRP8 may be able to trigger common as well as distinct downstream signaling events.

The archetypical adiponectin and all 16 CTRP members (CTRP1-9, 9B, 10-15) share a similar domain architecture with the highest homology in their globular C-terminal domains (54%) (Peterson et al. 2009). Reflecting their close structural relationship, CTRP1, CTRP6 and CTRP8 form a separate phylogenetic branch among CTRPs. I recently reported that of the 138 residues of human CTRP1 and CTRP8 and the 137 residues of

human CTRP6 that constitute their C1q/TNF globular domains there are 64 identical amino acid residues (46%) and additional conservative amino acid changes within their C1q/TNF domains (Ressl et al. 2015, Thanasupawat et al. 2015, Klonisch et al. 2016). This high sequence conservation between CTRP1/6/8 is further emphasized by a high number of identical residues shared among the β-sheets A (4/5), C (7/9), D (8/10), F (7/10), and H (5/7) (Klonisch et al. 2016). While the conserved amino acid sequences of the β-sheets likely supports a similar jelly roll conformation of CTRP1/6/8, far less constraints apply to the linker regions that connect the β-sheets, suggesting less evolutionary pressure and the potential of interactions with distinct protein partners. Importantly, CTRP8 and CTRP1 share the identical putative RXFP1 interacting motif "YAAFSVG" located at the N-terminus of the C1q/TNF globular domain of CTRP8 (Shemesh et al. 2008), suggesting that, in addition to CTRP8, CTRP1 may be a potential new agonist for RXFP1. This option is a topic of another investigation. Intriguingly, a small linear peptide ("FFAFSVG") derived from the N-terminal part of the C1q/TNF globular domain of CTRP6 and distantly related to the CTRP1/8 RXFP1 binding motif was able to partially block recombinant human CTRP8 from inducing increased GB migration. On its own, this synthetic peptide was unable to induce cell migration (Glogowska et al. 2013). This suggests the intriguing possibility that CTRP1/6/8 form a novel network of agonists displaying different affinities for RXFP1 capable of modulating RXFP1 activity depending on their local concentration in the GB microenvironment.

While my findings are the first that outline a role for CTRP8 in cancer, CTRP8 likely has additional roles that extend beyond GB motility and tissue invasion. CTRP peptides have been shown to have multiple functions in metabolism and immunity

(Schaffler and Buechler 2012). Of CTRP1/6/8, only CTRP6 had previously been linked to cancer. CTRP6 is highly expressed in human hepatocellular carcinoma tissues and CTRP6 overexpression reduces necrotic cell death in HepG2 cells, thus, protecting these human hepatocellular cancer cells from toxic stress (Takeuchi et al. 2011). Also, the C-terminal C1q domain of recombinant CTRP6 was shown to activate AKT phosphorylation and promote tumor angiogenesis in hepatocellular carcinomas. As indicated by the role of CTRP6 peptide in diminishing CTRP8-induced GB migration, CTRP6 appears to attenuate tumor cell proliferation and migration. Inhibition of CTRP6 expression by the microRNA miR-29b results in increased cell invasion in human MCF7 breast cancer cells (Wang et al. 2012). In ovarian cancer, CTRP6 inhibits cell proliferation and invasion by blocking IL-8/VEGF pathway (Wang et al. 2015). These attenuating functions of CTRP6 bear similarities with the RXFP1 antagonist ΔH2 relaxin which has the two key arginine residues (B13, B17) converted to lysines (ΔH2) within the receptor binding domain of the B-chain of human RLN2 ("GRELVR") (Chen et al. 2013, Xiao et al. 2013). ΔH2 diminished the bioactivity and cAMP production in $RXFP1^+$ myelo-monocytic THP1 cells and RXFP1 expressing HEK293 cells and, upon binding to RXFP1, functioned as a partial antagonist to functional RLN2 in an *in-vivo* xenograft model of prostate cancer (Silvertown et al. 2007). Chemically synthesized ΔH2 antagonist, known as AT-001, was able to block RXFP1 activation and significantly inhibit RLN2-induced migration of renal myofibroblasts and MCF-7 breast cancer cells (Hossain et al. 2010).

In conclusion, my discovery of CTRP8 as an RXFP1 agonist has identified novel RXFP1 dependent PI3K-PKCδ/PKCζ and STAT3 signaling pathways that contribute to cath-B mediated cell migration and matrix invasion in $RXFP1^+$ patient GB cells. My studies

provide first evidence suggesting a regulatory CTRP1/6/8 network with intriguing new and complex mechanisms that produce upregulation of GB growth and invasion.

4.2 Part II: The CTRP8-RXFP1 system protects GB against DNA damage and apoptosis

The DNA alkylating chemotherapeutic drug temozolomide (TMZ) is the standard therapy for glioblastoma (GB) patients but this treatment generally results in TMZ chemoresistance which leads to treatment failure, GB recurrences, and fatal outcome (Furnari et al. 2007, Sarkaria et al. 2008, Gadji et al. 2009, Kohsaka et al. 2012). I proposed a role for CTRP8-RXFP1 in promoting GB survival through a protective effect against TMZ induced DNA damage. Relaxin mediated activation of RXFP1 was shown to promote tumor cell growth, inhibit apoptosis (Feng et al. 2009, Radestock et al. 2010) and induce increased cisplatin chemoresistance through modulation of the AKT/NF-kB signaling pathway in osteosarcoma cells (Ma et al. 2015). These studies and my finding that CTRP8-RXFP1 caused the activation of the oncogenic and anti-apoptotic STAT3 signaling pathway prompted us to investigate the role of the RXFP1 system in TMZ-induced DNA damage apoptosis in patient GB cells.

The TMZ active metabolite 5-(3-methyl-1-triazeno)imidazole-4-carboxamide (MTIC) causes the formation of N^7-methylguanine (N^7-MeG; 60-80%), N^3-methyladenine (N^3-MeA; 10-20%) and O^6-methylguanine (O^6-MeG; 5-10%) base alkylations (Bobola et al. 2012). O^6-MeG methylations are repaired by O^6-MeG DNA methyltransferase (Spiegl-Kreinecker et al. 2010) and low MGMT expression due to MGMT promoter hyper-methylation in GB patients is a predictor of poor outcome (Hegi et al. 2008). Remarkably, >90% of TMZ lesions activate the DNA base excision repair (BER) pathway (Yoshimoto et al. 2012). The BER pathway promotes the resistance to alkylating agents (Fishel et al. 2007, Tang et al. 2011, Agnihotri et al. 2012) and the level of expression of BER factors

affect the sensitivity of GB to TMZ (Trivedi et al. 2008, Goellner et al. 2011, Agnihotri et al. 2014). Upon TMZ treatment, RXFP1 activation by either RLN2 or CTRP8 significantly decreased the occurrence of γH2AX foci, a marker of double strand (ds) DNA damage (Sharma et al. 2012). RXFP1 agonists markedly reduced tail moments in single cell gel electrophoresis (Comet) assays, which indicate reduced dsDNA breaks. While RLN2 and CTRP8 had no effect on MGMT expression in GB, RXFP1 activation resulted in the upregulation of N-methylpurine DNA glycosylase (MPG), a monofunctional enzyme that catalyzes the initial step of BER which involves the removal of the methylated base (Kim and Wilson 2012). The activation of RXFP1 coincided with enhanced MPG activity as determined by a PCR-beacon based MPG activity assay. Importantly, GB treatment with RLN2 or CTRP8 did not result in changes in the expression of other BER protein members, including APE1, DNA polymerase β and XRCC1. A balanced MPG activity is a key requirement for cell survival and DNA damage-induced ataxia telangiectasia mutated (ATM)-dependent phosphorylation/activation of MPG contributes to TMZ resistance in GB (Agnihotri et al. 2014).

Overexpression of MPG is also linked to carcinogenesis in cervical and breast cancer (Cerda et al. 1998, Sohn et al. 2001). However, dysfunctional MPG enzyme activity can result in the accumulation of highly cytotoxic 5'deoxyribose phosphate (5'dRP) residues upon removal of the methylated base by MPG to create an apurinic/apyrimidinic (AP) site (Trivedi et al. 2008). If not removed instantly, the sensitivity of tumors to alkylating drugs increases as shown for osteosarcoma, ovarian and breast cancer (Rinne et al. 2004, Wang et al. 2006, Fishel et al. 2007).

The DNA polymerase β-mediated hydrolysis of cytotoxic 5'deoxyribose phosphate (5'dRP) groups is the rate-limiting step in BER repair but normal and tumor cells have varying cellular levels of DNA polymerase β which limits their ability to respond efficiently to alkylating DNA damage and puts them at risk of apoptosis (Fishel et al. 2007, Trivedi et al. 2008, Tang et al. 2011). I, therefore, wanted to determine mechanisms that, in addition to increased MPG expression/activity, could assist in the rescue of GB cells from TMZ and dysregulated MPG activity. Ideally, this factor should be associated with BER, have powerful AP-lyase and dRP-lyase activities for efficient cleavage of AP sites and removal of dRP sites for expedient downstream BER repair (Summer et al. 2009), and block apoptosis. I identified the non-histone DNA binding factor High Mobility Group A2 (HMGA2) as a factor that was up-regulated upon RXFP1 activation. Previously research showed that HMGA2 has AP- and dRP-lyase activities, interacts with the key BER factor APE-1 and promotes more efficient BER following alkylating DNA damage (Summer et al. 2009). HMGA2 also demonstrates an important role in preventing apoptosis in human tumor cells (Natarajan et al. 2013). HMGA2 is highly expressed in embryonic tissues and stem cells, but absent in most adult tissues (Li et al. 2007, Pfannkuche et al. 2009). During cell differentiation, loss of the stem cell protein LIN28A in differentiated cells increases levels of the microRNA Let7, which down-regulates HMGA2 transcript levels by targeting the 3'UTR of the HMGA2 mRNA for degradation (Hammond and Sharpless 2008). The three AT-hook DNA-binding domains of HMGA2 bind to AT-rich regions in the minor groove of DNA (Pfannkuche et al. 2009) and the resulting DNA conformational changes modulate transcription of genes involved in cell proliferation, differentiation and migration (Cleynen and Van de Ven 2008). HMGA2 is re-expressed in many tumors, including GB

(see below), and is associated with increased metastasis and poor prognosis (Chiappetta et al. 2008, Califano et al. 2014, Liu et al. 2014). HMGA2 is important for neural stem cell renewal (Nishino et al. 2008) and was recently shown to promote self-renewal and invasiveness of GB-initiating cells (Zhong et al. 2016b). Human glioma-initiating cells expressing the stem cell protein Lin28A, an upstream positive regulator of HMGA2, showed increased proliferation, tumor sphere formation and xenograft tumor growth (Mao et al. 2013). I found that the upregulation of both MPG and HMGA2 was mediated by a novel CTRP8-RXFP1-STAT3 pathway. Pharmacological inhibition of STAT3 blocked the upregulation of HMGA2 and MPG, which increased sensitivity of GB to TMZ.

In addition to its key role in promoting single strand DNA repair to mitigate TMZ induced DNA damage in human GB, the CTRP8-RXFP1-STAT3 pathway protected against apoptosis, as seen with my caspase 3/7 data. Chemotherapeutic drugs frequently trigger apoptosis in numerous different tumor types (Ghavami et al. 2009b, Elkholi et al. 2014, Kontos et al. 2014, Wurstle et al. 2014). Intracellular caspases are the executing enzymes (Fulda and Debatin 2006, Ghavami et al. 2009a, Fiandalo and Kyprianou 2012) of both extrinsic and intrinsic apoptotic cascades activated by extracellular or intracellular stimuli, respectively (Rashedi et al. 2007, Call et al. 2008, Yeganeh et al. 2013, Iranpour et al. 2016). Mitochondria are the key organelle for the intrinsic apoptotic pathway. Pro- and anti-apoptotic molecules regulate the outer mitochondrial membrane permeability for cytochrome C release into the cytosol which initializes the intrinsic apoptotic pathway (Tait and Green 2010). RXFP1 activation resulted in the upregulation of Bcl-2 and Bcl-XL, two anti-apoptotic molecules. Bcl-2 and Bcl-XL interact with the pro-apoptotic molecules Bak or Bax at the outer mitochondrial membrane and this prevents cytochrome

C release and caspase activation (Das et al. 2004, Shi et al. 2010). Bcl-2 and Bcl-XL overexpression blocks apoptosis in GB cells exposed to TMZ and other chemotherapeutic drugs (Guensberg et al. 2002, Gielen et al. 2013, Han and Chen 2015). Importantly, the promoters of the Bcl-2 and Bcl-XL gene contain STAT3 binding sites and both factors are known STAT3 target genes (Zhuang et al. 2007). In the context of glioma, the anti-apoptotic function is an important contributor to the oncogenic STAT3 transcriptional function in cell proliferation, angiogenesis, and GB tumor invasion (Kim et al. 2014) and STAT3 mediated upregulation of Bcl-2 and Bcl-XL proteins was shown to promote TMZ chemoresistance in glioblastoma (Lee et al. 2011).

In conclusion, I have discovered CTRP8-RXFP1 as a new signaling pathway that utilizes STAT3 to enhance the expression of BER members MPG and HMGA2 and anti-apoptotic members Bcl-2 and Bcl-XL and orchestrate a powerful defense against genomic damage induced apoptosis in patient GB cells.

4.3 Part III. High Mobility Group AT Hook 2 protein (HMGA2) increases temozolomide resistance in glioblastoma

Fatalities due to TMZ chemoresistance often coincide with the emergence of a more aggressive phenotype in patients with primary and recurrent GB. My studies demonstrated that the presence of the stem cell factor and chromatin binding protein HGMA2 protects GB cells from TMZ induced DNA damage. With the exception of one earlier report (Akai et al. 2004), my data confirm recent reports that identified HMGA2 expression in patient GB tissues and GB cell lines (Liu et al. 2014, Kaur et al. 2016). HMGA2 was shown to promote stemness, proliferation, invasion, and survival (Morishita et al. 2013, Cai et al. 2016, Zhong et al. 2016b). My mouse models demonstrated the specific and exclusive presence of HMGA2 in GB tumor cells and nestin positive progenitor-like GB cells, whereas neighboring normal brain tissue was devoid of HMGA2 (data not shown). I showed that the knockdown of HMGA2 coincides with increased sensitivity to TMZ in human and mouse GB cells. In embryonic stem (ES) cells and cancer (stem) cells, the upregulation of HMGA2 likely protects against DNA damage which the resulting accumulation of mutations, genomic instability and apoptosis (Summer et al. 2009). In the absence of TMZ, HMGA2 silencing increased γH_2AX levels which signaled enhanced dsDNA breaks. Combined TMZ treatment and knockdown of HMGA2 dramatically increased cytotoxicity and apoptosis. My data suggested a genome protective function of HMGA2 in mouse and human GB cells. The MGMT status of human GB cells affected the ability of HMGA2 to protect against DNA damage. O^6-methylguanine-DNA methyltransferase (MGMT) specifically repairs O^6-MeG sites and is known to promote TMZ resistance in GB (Hegi et al. 2008, Fukushima et al. 2009, Stupp et al. 2009), whereas

the TMZ induced adducts, N^7-MeG and N^3-MeA, are removed by the DNA glycosylase MPG to generate an apurinic/ apyrimidinic (AP) sites which are intermediates of base-excision-repair (BER) pathway (Tang et al. 2011). Low dose TMZ (100 µM) alone failed to induce DNA damage in patient GB cells with MGMT expression but did increase γH_2AX foci in U251 cells that lack MGMT and are expected to undergo mismatch repair (MMR) cycles with resulting double strand breaks and caspase 3/7-depedent apoptosis in subsequent cell cycles (Quiros et al. 2010). TMZ-induced apoptosis was not induced by MGMT silencing in $HMGA2^+$ patient GB cells but was triggered by HMGA2 silencing. Thus, HMGA2 had an anti-apoptotic role in $MGMT^+$ patient GB cells.

Targeting HMGA2 in tumor and ES cells (Fusco and Fedele 2007) may provide a strategy to block its DNA protective actions and significantly enhance chemosensitivity to alkylating agents, like TMZ, in GB, especially since intratumoral TMZ concentrations were reported to be low (Portnow et al. 2009). I tested the minor groove binder Dovitinib (DOV) which is an FDA-approved multi-kinase inhibitor able to cross the BBB (Hasinoff et al. 2012, Schafer et al. 2016) and currently tested as a single treatment use in ongoing clinical trials for patients with advanced and recurrent GB in Germany [NCT01972750] and the US [NCT01753713]. Low concentrations of DOV were effective in enhancing TMZ sensitivity in GB cells and, like HMGA2 silencing, low-dose DOV treatment increased basal levels of γH_2AX indicating increased dsDNA breaks. I found that DOV specifically down-regulated HMGA2 in GB with negligible effects on HMGA1 expression in GB cells. Importantly, DOV also decreased other key BER factors and MGMT. Thus, I anticipate DOV to attenuate single strand DNA repair functions and compromise MGMT mediated DNA repair mechanism involved in TMZ resistance in GB.

DOV mediated down-regulation of MGMT in GB cells with unmethylated MGMT promoter may translate into an immediate treatment benefit for GB patients for whom there is currently no established standard of care. The presence of MGMT blocks TMZ-induced apoptosis in GB cells (Roos et al. 2007). Low MGMT levels due to MGMT promoter methylation was shown to increase the median survival time and the progression-free survival of GB patients under TMZ treatment (Hegi et al. 2005, Hegi et al. 2008, Stupp et al. 2009) and MGMT protein expression in the tumor predicts TMZ response in GB patients (Spiegl-Kreinecker et al. 2010). Based on these results, I devised a sequential treatment starting with DOV "priming" followed by TMZ exposure to attenuate cellular HMGA2, BER, and MGMT activities and improve the efficacy of both drugs in GB cells. Following a recovery period after treatments, long-term GB cell survival in colony-formation assays was significantly reduced in MGMT-negative U251 cells and $MGMT^+$ patient GB cells. I concluded that this novel sequential dual-hit DOV-TMZ treatment is effective with $MGMT^+$ GB cells and may reduce the survival of GB cells.

The STAT3-LIN28-Let-7-HMGA2 axis is an emerging oncogenic pathway for HMGA2 promoting self-renewal of stem cells in a subset of GB and breast cancer cells (Guo et al. 2013, Mao et al. 2013, Han et al. 2016, Kaur et al. 2016). HMGA2 expression is decreased by specific let-7 microRNA members that bind to the 3'UTR of HMGA2 to cause reduced mRNA stability and translation (Hammond and Sharpless 2008). Inactivation of let-7 family members by the Let-7 binding protein LIN28 up-regulates HMGA2 (Droge and Davey 2008, Hammond and Sharpless 2008, Weingart et al. 2015). Lin28 is expressed in GB patients with poor prognosis (Qin et al. 2014) and HMGA2 is present in a LIN28A expressing subset of GB (Mao et al. 2013). I confirmed the expression

of HMGA2 in nestin^{+} GB progenitors in my mouse allografts. DOV reduced the cellular levels of pSTAT^{Tyr705} in GB cells and this STAT3 de-activation step was shown to involve SHP-1 protein tyrosine phosphatase in colorectal (Fan et al., 2015) and hepatocellular carcinoma (Huang et al. 2016). STAT3 activation upregulates the LIN28-Let-7-HMGA2 axis in breast cancer cells (Guo et al. 2013). Like HMGA2 silencing, DOV-mediated down-regulation of HMGA2 in GB cells resulted in reduced tumor sphere formation and decreased cell viability of sphere-forming GB cells. This coincided with attenuated LIN28A levels and identified a hitherto unknown role of DOV as an inhibitor of the LIN28-Let-7-HMGA2 axis in human GB (Droge and Davey 2008, Hammond and Sharpless 2008). DOV may elicit its suppressive action on LIN28A by SHP-1-mediated inhibition of pSTAT3^{Tyr705} phosphorylation in GB cells. STAT3 activation is promoted by cytokines such as IL-6 (Zhong et al. 1994). The poor survival of GB patients with up-regulated IL-6 and HMGA2 (Chiou et al. 2013) demonstrates the urgent need for therapeutic targeting of regulatory pathways upstream of HMGA2 in GB patients.

In summary, DOV treatment compromised the BER, MGMT and the STAT3-LIN28-Let-7-HMGA2 axis. This was most evident with combined DOV-TMZ drug regimens and coincided with increased TMZ induced apoptosis and reduced GB stem cell self-renewal capacity in GB. My findings have revealed the rationale for novel treatment options for a more efficacious use of TMZ in GB patients independent of their MGMT status.

4.4 Limitation and future directions

The present study is based on in-vitro experiments done on cultured primary GB cells. Primary cells are considered a heterogeneous population of cells and often can only be maintained in culture for a limited period of time. The characteristics of primary cells may change during subsequent passages, resulting in different responses to treatment over time. I addressed these issues by working with similar low passage numbers of primary GB cells to ensure consistent and comparable results. Another aspect to be considered is the fact that primary GB cells were isolated from different patients. Therefore, the characteristics and genetic profiles may differ between different isolates and result in distinct responses which will affect the experimental outcome. Future studies are needed to identify molecular characteristics of individual primary GB cells as I currently cannot exclude the possibility of different GB histopathological subtypes affecting experimental responses.

The traditional two-dimensional (2D) monolayer cell culture system used in my studies does not reflect the in vivo 3D microenvironments of these GB cells. Matrix-based 3D in vitro cell culture systems have been shown to better reflect physiologically relevant in vivo condition and cell responses. 3D-cultured cells show improved interactions between cells and –ECM, with cell structures being more similar to the in vivo scenario (Edmondson et al. 2014, Placone et al. 2015). I plan to use 3D culture experiments as the next step to determine the response to drug treatments of patient GB cells. While I have successfully established orthotopic xenografts of the glioma cell line U251 in mouse brain the use of primary GB cells is more challenging, expensive and very time-consuming, making it a less feasible approach for routine experimental use.

GB invasiveness involves and facilitates the degradation of ECM barrier to increase matrix/ tissue invasion. Brain ECM consists of proteoglycans (i.e. aggrecan, brevican, and neurocan), glycoproteins (i.e. tenascin-C, -R, and -X), and fibrous glycoproteins (i.e. collagen, fibronectin, and laminin) (Novak and Kaye 2000, Cuddapah et al. 2014). We showed that RXFP1 activation enhances cathepsin B secretion and this promotes the invasion of patient GB cells into a laminin matrix. Cathepsin B is a potent lysosomal protease which, *in vivo*, is secreted into extracellular space to degrade various ECM component. Laminin is not only substrate for cathepsin B. Aggregan, tenascin C, collagen II, IV, and fibronectin are also degraded by cathepsin B (Fonovic and Turk 2014). Thus, it remains to be shown what matrix components are most vulnerable to RXFP1-cathepsin B induced ECM degradation to facilitate GB cell invasion. MMPs are matrix metalloproteinases able to degrade ECM (Jablonska-Trypuc et al. 2016). RXFP1 activation was shown to regulate tumor cell migration and invasion via MMP-1, 2, 3, 9, and 14 activities in breast and thyroid cancer (Binder et al. 2002, Bialek et al. 2011). The role of the activated RXFP1 in MMP-mediated brain matrix degradation is currently unexplored and may be an important mechanism involved in enhancing GB cell migration and brain tissue invasion.

This study provides first evidence for a new role of RXFP1 as an enhancer of cell migration and invasion of GB. RXFP1-RLN2 system has been ahown to enhance cell invasion and migration in breast, thyroid, prostate cancer (Hombach-Klonisch et al. 2006, Radestock et al. 2008, Feng et al. 2009). However, less evidence supports a role for RXFP1 and RLN2 in cancer progression or clinal outcome. High expression of RLN2 was dectected in recurrent prostate cancer tissues (Feng et al. 2007). Suppression of RXFP1

expression decreased tumor growth *in vivo* and markedly reduced cell proliferation and metastatsis in PC-3 prostate cancer xenograft mouse model (Feng et al. 2009). Further studies correlating the level of RXFP1 and CTRP8 expression with GB progression may reveal either or both factors as pronostic marker(s) in GB patients. To address this question, I intend to link the motility/invasion data I have collected from patient GB cells with overall survival (OS) data from the same patients. Also, my GB cells resource contains GB cells derived from the primary and recurrence tissues of the same patient. This will allow me to compare reponsiveness to RXFP1 agonists and signaling pathways in primary and recurrent GB to assess the effect of clonal selection of the GB tumor in the same patient.

My studies have demonstrated that RXFP1 activation promotes TMZ chemoresistance which enhances BER and cell survival by reducing apoptosis. TMZ treatment selects for population of GB cells that subsequently become resistant and form fatal tumor recurrences in patients. RXFP1 inhibition may provide a possibility to inhibit signaling pathways which promote TMZ chemoresistance and invasion in GB. An emerging number of RXFP1 antagonists will hopefully allow me to address this clinically relevant issue. AT-001 is an analog of human RLN2 and contains B13K and B17K mutations of the B-chain of RLN2 which impairs receptor binding and reduces the induction of cAMP in THP-1 and HEK293-RXFP1 cells (Silvertown et al. 2007). AT-001 inhibits cell migration in MCF-7 breast cancer cells and suppresses tumor growth of prostate cancer xenograft (Hossain et al. 2010, Neschadim et al. 2014). Single treatment with AT-001 showed a 60% reduction in tumor growth of xenografts derived from PC3 androgen-independent prostate cancer cells. The combination of AT-001 with first line therapeutic drug decetaxel showed synergistic effect with a suppression of tumor growth

of up to 98% (Neschadim et al. 2014). AT-001 is not without challenges as this RLN2 mutant peptide is unlikely to cross the blood-brain-barrier. Emerging small molecules acting as partial or complete antagonists of RXFP1 may provide a more promising avenue to overcome the blood-brain-barrier and block RXFP1 signaling in GB cells.

Despite the above mentioned caveats, the data from the studies presented here have helped expand the current knowledge on the role of this new CTRP8-RXFP1 system in GB. My results have established novel roles of RXFP1 signaling and functions in human GB. As for its role in chemoresistance, future research will reveal whether RXFP1 has similar roles in solid tumors other than GB.

4.5 Conclusion

My work has unveiled the CTRP8-RXFP1 system as a novel receptor signaling pathway and STAT3 as a crucial mediator that can promote the survival of GB cells when exposed to TMZ **(Figure 4.1).** I identified key molecular factors as that contribute to the function of HMGA2 in GB cells. My concept of "DOV priming" to sensitize GB cells towards TMZ actions may provide a new therapeutic strategy for improved TMZ efficacy in GB patients. This work also provides rationale for targeting the CTRP8-RXFP1-STAT3-LIN28-Let-7-HMGA2 axis. The recent discovery of a LIN28 targeting small molecule compound may offer a more specific strategy to target $LIN28^{+}$/$HMGA2^{+}$ GB stem/progenitor cells with less off-target effects (Roos et al. 2016). Other therapeutic avenues may include the development of peptide or small molecules capable of crossing the BBB and blocking CTRP8 receptor binding and low-toxicity RXFP1 antagonists (Xiao et al. 2010, Chen et al. 2013, Xiao et al. 2013). The results from this work provide a scientific rational for a future use of novel RXFP1 antagonists glioblastoma.

Figure 4.1 A schematic summary diagram

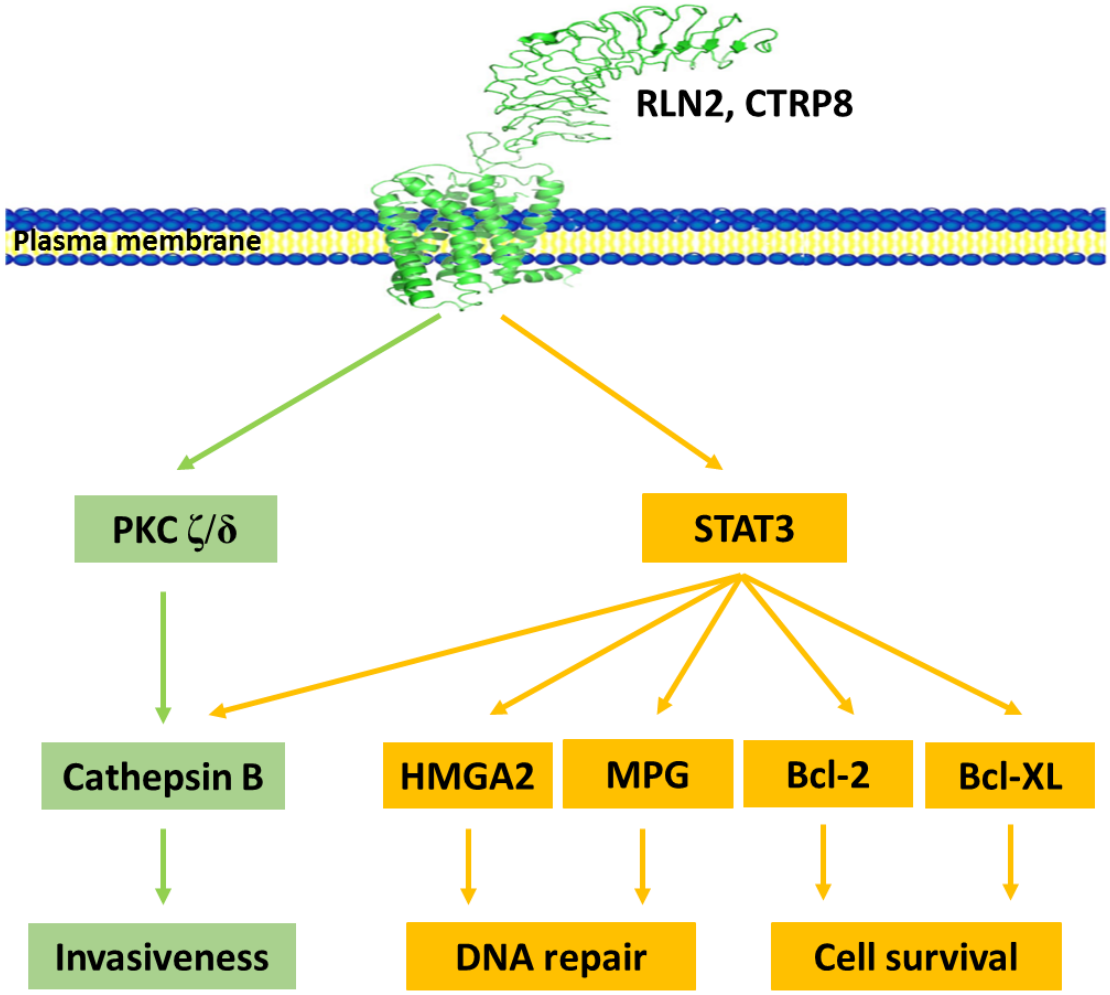

Figure 4.1 A schematic diagram demonstrates two signaling pathways, PKCζ/δ and STAT3, as target of RXFP1 activation in GB cells. I identified role of PKCζ/δ and STAT3 caused the increased production/secretion of cathepsin B and promoted GB invasiveness. Moreover, STAT3 signaling regulates BER proteins, MPG and HMGA2, and anti-apoptotic molecules, Bcl-2 and Bcl-XL, to protect GB cells from TMZ-induced DNA damage and enhance cell survival.

CHAPTER 5: REFERENCES

Abdullah, L. N., and E. K. Chow. 2013. Mechanisms of chemoresistance in cancer stem cells. Clin Transl Med 2: 3.

Agnihotri, S., A. S. Gajadhar, C. Ternamian, T. Gorlia, K. L. Diefes, P. S. Mischel, J. Kelly, G. McGown, M. Thorncroft, B. L. Carlson, J. N. Sarkaria, G. P. Margison, K. Aldape, C. Hawkins, M. Hegi, and A. Guha. 2012. Alkylpurine-DNA-N-glycosylase confers resistance to temozolomide in xenograft models of glioblastoma multiforme and is associated with poor survival in patients. The Journal of clinical investigation 122: 253-266.

Agnihotri, S., K. Burrell, P. Buczkowicz, M. Remke, B. Golbourn, Y. Chornenkyy, A. Gajadhar, N. A. Fernandez, I. D. Clarke, M. S. Barszczyk, S. Pajovic, C. Ternamian, R. Head, N. Sabha, R. W. Sobol, M. D. Taylor, J. T. Rutka, C. Jones, P. B. Dirks, G. Zadeh, and C. Hawkins. 2014. ATM regulates 3-methylpurine-DNA glycosylase and promotes therapeutic resistance to alkylating agents. Cancer Discov 4: 1198-1213.

Ahmad, N., W. Wang, R. Nair, and S. Kapila. 2012. Relaxin induces matrix-metalloproteinases-9 and -13 via RXFP1: induction of MMP-9 involves the PI3K, ERK, Akt and PKC-zeta pathways. Mol Cell Endocrinol 363: 46-61.

Akai, T., Y. Ueda, Y. Sasagawa, T. Hamada, T. Date, S. Katsuda, H. Iizuka, Y. Okada, and K. Chada. 2004. High mobility group I-C protein in astrocytoma and glioblastoma. Pathol Res Pract 200: 619-624.

Akiyama, H., S. Furukawa, S. Wakisaka, and T. Maeda. 2009. Elevated expression of CTRP3/cartducin contributes to promotion of osteosarcoma cell proliferation. Oncology reports 21: 1477-1481.

Alam, M., R. Ahmad, H. Rajabi, and D. Kufe. 2015. MUC1-C Induces the LIN28B-->LET-7-->HMGA2 Axis to Regulate Self-Renewal in NSCLC. Molecular cancer research : MCR 13: 449-460.

Alonso, N., R. Guillen, J. W. Chambers, and F. Leng. 2015. A rapid and sensitive high-throughput screening method to identify compounds targeting protein-nucleic acids interactions. Nucleic Acids Res 43: e52.

Anand-Ivell, R., and R. Ivell. 2014. Regulation of the reproductive cycle and early pregnancy by relaxin family peptides. Mol Cell Endocrinol 382: 472-479.

Anand, A., and K. Chada. 2000. In vivo modulation of Hmgic reduces obesity. Nat Genet 24: 377-380.

Appin, C. L., and D. J. Brat. 2014. Molecular genetics of gliomas. Cancer J 20: 66-72.

Aziz, M. H., B. B. Hafeez, J. M. Sand, D. B. Pierce, S. W. Aziz, N. E. Dreckschmidt, and A. K. Verma. 2010. Protein kinase Cvarepsilon mediates Stat3Ser727 phosphorylation, Stat3-regulated gene expression, and cell invasion in various human cancer cell lines through integration with MAPK cascade (RAF-1, MEK1/2, and ERK1/2). Oncogene 29: 3100-3109.

Baker, S. D., M. Wirth, P. Statkevich, P. Reidenberg, K. Alton, S. E. Sartorius, M. Dugan, D. Cutler, V. Batra, L. B. Grochow, R. C. Donehower, and E. K. Rowinsky. 1999. Absorption, metabolism, and excretion of 14C-temozolomide following oral administration to patients with advanced cancer. Clinical cancer research : an official journal of the American Association for Cancer Research 5: 309-317.

Banerjee, S., J. N. Byrd, S. M. Gianino, S. E. Harpstrite, F. J. Rodriguez, R. G. Tuskan, K. M. Reilly, D. R. Piwnica-Worms, and D. H. Gutmann. 2010. The neurofibromatosis type 1 tumor suppressor controls cell growth by regulating signal transducer and activator of transcription-3 activity in vitro and in vivo. Cancer Res 70: 1356-1366.

Banga, A., A. M. Bodles, N. Rasouli, G. Ranganathan, P. A. Kern, and R. J. Owens. 2008. Calcium is involved in formation of high molecular weight adiponectin. Metab Syndr Relat Disord 6: 103-111.

Bani-Sacchi, T., M. Bigazzi, D. Bani, P. F. Mannaioni, and E. Masini. 1995. Relaxin-induced increased coronary flow through stimulation of nitric oxide production. British journal of pharmacology 116: 1589-1594.

Bani, D., A. Riva, M. Bigazzi, and T. Bani Sacchi. 1994. Differentiation of breast cancer cells in vitro is promoted by the concurrent influence of myoepithelial cells and relaxin. British journal of cancer 70: 900-904.

Bani, D., E. Masini, M. G. Bello, M. Bigazzi, and T. B. Sacchi. 1995. Relaxin activates the L-arginine-nitric oxide pathway in human breast cancer cells. Cancer Res 55: 5272-5275.

Bani, D., E. Masini, M. G. Bello, M. Bigazzi, and T. B. Sacchi. 1998. Relaxin protects against myocardial injury caused by ischemia and reperfusion in rat heart. The American journal of pathology 152: 1367-1376.

Bani, G., T. Bani Sacchi, M. Bigazzi, and S. Bianchi. 1988. Effects of relaxin on the microvasculature of mouse mammary gland. Histol Histopathol 3: 337-343.

Bartsch, O., B. Bartlick, and R. Ivell. 2004. Phosphodiesterase 4 inhibition synergizes with relaxin signaling to promote decidualization of human endometrial stromal cells. J Clin Endocrinol Metab 89: 324-334.

Bathgate, R. A., R. Ivell, B. M. Sanborn, O. D. Sherwood, and R. J. Summers. 2006. International Union of Pharmacology LVII: recommendations for the nomenclature of receptors for relaxin family peptides. Pharmacol Rev 58: 7-31.

Bathgate, R. A., M. L. Halls, E. T. van der Westhuizen, G. E. Callander, M. Kocan, and R. J. Summers. 2013. Relaxin family peptides and their receptors. Physiological reviews 93: 405-480.

Battista, S., V. Fidanza, M. Fedele, A. J. Klein-Szanto, E. Outwater, H. Brunner, M. Santoro, C. M. Croce, and A. Fusco. 1999. The expression of a truncated HMGI-C gene induces gigantism associated with lipomatosis. Cancer Res 59: 4793-4797.

Baysan, M., S. Bozdag, M. C. Cam, S. Kotliarova, S. Ahn, J. Walling, J. K. Killian, H. Stevenson, P. Meltzer, and H. A. Fine. 2012. G-cimp status prediction of glioblastoma samples using mRNA expression data. PloS one 7: e47839.

Belge, G., A. Meyer, M. Klemke, K. Burchardt, C. Stern, W. Wosniok, S. Loeschke, and J. Bullerdiek. 2008. Upregulation of HMGA2 in thyroid carcinomas: a novel molecular marker to distinguish between benign and malignant follicular neoplasias. Genes Chromosomes Cancer 47: 56-63.

Bennett, R. G., D. G. Heimann, and D. J. Tuma. 2009. Relaxin reduces fibrosis in models of progressive and established hepatic fibrosis. Annals of the New York Academy of Sciences 1160: 348-349.

Berube, N. G., X. H. Swanson, M. J. Bertram, J. D. Kittle, V. Didenko, D. S. Baskin, J. R. Smith, and O. M. Pereira-Smith. 1999. Cloning and characterization of CRF, a novel C1q-related factor, expressed in areas of the brain involved in motor function. Brain Res Mol Brain Res 63: 233-240.

Bhat, K. P., K. L. Salazar, V. Balasubramaniyan, K. Wani, L. Heathcock, F. Hollingsworth, J. D. James, J. Gumin, K. L. Diefes, S. H. Kim, A. Turski, Y. Azodi, Y. Yang, T. Doucette, H. Colman, E. P. Sulman, F. F. Lang, G. Rao, S. Copray, B. D. Vaillant, and K. D. Aldape. 2011. The transcriptional coactivator TAZ regulates mesenchymal differentiation in malignant glioma. Genes Dev 25: 2594-2609.

Bialek, J., U. Kunanuvat, S. Hombach-Klonisch, A. Spens, J. Stetefeld, K. Sunley, D. Lippert, J. A. Wilkins, C. Hoang-Vu, and T. Klonisch. 2011. Relaxin enhances the collagenolytic activity and in vitro invasiveness by upregulating matrix

metalloproteinases in human thyroid carcinoma cells. Molecular cancer research : MCR 9: 673-687.

Bigazzi, M., M. L. Brandi, G. Bani, and T. B. Sacchi. 1992. Relaxin influences the growth of MCF-7 breast cancer cells. Mitogenic and antimitogenic action depends on peptide concentration. Cancer 70: 639-643.

Bigazzi, M., A. Del Mese, F. Petrucci, R. Casali, and G. P. Novelli. 1986. The local administration of relaxin induces changes in the microcirculation of the rat mesocaecum. Acta Endocrinol (Copenh) 112: 296-299.

Binder, C., T. Hagemann, B. Husen, M. Schulz, and A. Einspanier. 2002. Relaxin enhances in-vitro invasiveness of breast cancer cell lines by up-regulation of matrix metalloproteases. Molecular human reproduction 8: 789-796.

Binder, C., E. Chuang, C. Habla, A. Bleckmann, M. Schulz, R. Bathgate, and A. Einspanier. 2014. Relaxins enhance growth of spontaneous murine breast cancers as well as metastatic colonization of the brain. Clin Exp Metastasis 31: 57-65.

Blankenship, T., D. R. Stewart, K. Benirschke, B. King, and B. L. Lasley. 1994. Immunocytochemical localization of nonluteal ovarian relaxin. J Reprod Med 39: 235-240.

Bobola, M. S., D. D. Kolstoe, A. Blank, M. C. Chamberlain, and J. R. Silber. 2012. Repair of 3-methyladenine and abasic sites by base excision repair mediates glioblastoma resistance to temozolomide. Front Oncol 2: 176.

Boccalini, G., C. Sassoli, L. Formigli, D. Bani, and S. Nistri. 2015. Relaxin protects cardiac muscle cells from hypoxia/reoxygenation injury: involvement of the Notch-1 pathway. FASEB journal : official publication of the Federation of American Societies for Experimental Biology 29: 239-249.

Bond, C. P., L. J. Parry, C. S. Samuel, H. M. Gehring, F. L. Lederman, P. A. Rogers, and R. J. Summers. 2004. Increased expression of the relaxin receptor (LGR7) in human endometrium during the secretory phase of the menstrual cycle. J Clin Endocrinol Metab 89: 3477-3485.

Brennan, C. W., R. G. Verhaak, A. McKenna, B. Campos, H. Noushmehr, S. R. Salama, S. Zheng, D. Chakravarty, J. Z. Sanborn, S. H. Berman, R. Beroukhim, B. Bernard, C. J. Wu, G. Genovese, I. Shmulevich, J. Barnholtz-Sloan, L. Zou, R. Vegesna, S. A. Shukla, G. Ciriello, W. K. Yung, W. Zhang, C. Sougnez, T. Mikkelsen, K. Aldape, D. D. Bigner, E. G. Van Meir, M. Prados, A. Sloan, K. L. Black, J. Eschbacher, G. Finocchiaro, W. Friedman, D. W. Andrews, A. Guha, M. Iacocca, B. P. O'Neill, G. Foltz, J. Myers, D. J. Weisenberger, R. Penny, R.

Kucherlapati, C. M. Perou, D. N. Hayes, R. Gibbs, M. Marra, G. B. Mills, E. Lander, P. Spellman, R. Wilson, C. Sander, J. Weinstein, M. Meyerson, S. Gabriel, P. W. Laird, D. Haussler, G. Getz, L. Chin, and T. R. Network. 2013. The somatic genomic landscape of glioblastoma. Cell 155: 462-477.

Bryant-Greenwood, G. D., E. M. Rutanen, S. Partanen, T. K. Coelho, and S. Y. Yamamoto. 1993. Sequential appearance of relaxin, prolactin and IGFBP-1 during growth and differentiation of the human endometrium. Mol Cell Endocrinol 95: 23-29.

Buck, M. R., D. G. Karustis, N. A. Day, K. V. Honn, and B. F. Sloane. 1992. Degradation of extracellular-matrix proteins by human cathepsin B from normal and tumour tissues. The Biochemical journal 282 (Pt 1): 273-278.

Burazin, T. C., K. J. Johnson, S. Ma, R. A. Bathgate, G. W. Tregear, and A. L. Gundlach. 2005. Localization of LGR7 (relaxin receptor) mRNA and protein in rat forebrain: correlation with relaxin binding site distribution. Annals of the New York Academy of Sciences 1041: 205-210.

Busch, B., N. Bley, S. Muller, M. Glass, D. Misiak, M. Lederer, M. Vetter, H. G. Strauss, C. Thomssen, and S. Huttelmaier. 2016. The oncogenic triangle of HMGA2, LIN28B and IGF2BP1 antagonizes tumor-suppressive actions of the let-7 family. Nucleic Acids Res 44: 3845-3864.

Butler, A. M., M. L. Scotti Buzhardt, S. Li, K. E. Smith, A. P. Fields, and N. R. Murray. 2013. Protein kinase C zeta regulates human pancreatic cancer cell transformed growth and invasion through a STAT3-dependent mechanism. PloS one 8: e72061.

Butler, A. M., M. L. Scotti Buzhardt, E. Erdogan, S. Li, K. S. Inman, A. P. Fields, and N. R. Murray. 2015. A small molecule inhibitor of atypical protein kinase C signaling inhibits pancreatic cancer cell transformed growth and invasion. Oncotarget 6: 15297-15310.

Byerly, M. S., P. S. Petersen, S. Ramamurthy, M. M. Seldin, X. Lei, E. Provost, Z. Wei, G. V. Ronnett, and G. W. Wong. 2014. C1q/TNF-related protein 4 (CTRP4) is a unique secreted protein with two tandem C1q domains that functions in the hypothalamus to modulate food intake and body weight. The Journal of biological chemistry 289: 4055-4069.

Cahill, D. P., K. K. Levine, R. A. Betensky, P. J. Codd, C. A. Romany, L. B. Reavie, T. T. Batchelor, P. A. Futreal, M. R. Stratton, W. T. Curry, A. J. Iafrate, and D. N. Louis. 2007. Loss of the mismatch repair protein MSH6 in human glioblastomas is associated with tumor progression during temozolomide treatment. Clinical cancer research : an official journal of the American Association for Cancer Research 13: 2038-2045.

Cai, J., G. Shen, S. Liu, and Q. Meng. 2016. Downregulation of HMGA2 inhibits cellular proliferation and invasion, improves cellular apoptosis in prostate cancer. Tumour Biol 37: 699-707.

Califano, D., S. Pignata, N. S. Losito, A. Ottaiano, S. Greggi, V. De Simone, S. Cecere, C. Aiello, F. Esposito, A. Fusco, and G. Chiappetta. 2014. High HMGA2 expression and high body mass index negatively affect the prognosis of patients with ovarian cancer. J Cell Physiol 229: 53-59.

Call, J. A., S. G. Eckhardt, and D. R. Camidge. 2008. Targeted manipulation of apoptosis in cancer treatment. The Lancet Oncology 9: 1002-1011.

Callander, G. E., W. G. Thomas, and R. A. Bathgate. 2009. Prolonged RXFP1 and RXFP2 signaling can be explained by poor internalization and a lack of beta-arrestin recruitment. Am J Physiol Cell Physiol 296: C1058-1066.

Carrasco-Garcia, E., M. Saceda, and I. Martinez-Lacaci. 2014. Role of receptor tyrosine kinases and their ligands in glioblastoma. Cells 3: 199-235.

Carrell, D. T., C. M. Peterson, and R. L. Urry. 1995. The binding of recombinant human relaxin to human spermatozoa. Endocr Res 21: 697-707.

Castrini, A. I., V. Carubelli, V. Lazzarini, I. Bonadei, C. Lombardi, and M. Metra. 2015. Serelaxin a novel treatment for acute heart failure. Expert review of clinical pharmacology 8: 549-557.

Cerda, S. R., P. W. Turk, A. D. Thor, and S. A. Weitzman. 1998. Altered expression of the DNA repair protein, N-methylpurine-DNA glycosylase (MPG) in breast cancer. FEBS Lett 431: 12-18.

Chen, C. Z., N. Southall, J. Xiao, J. J. Marugan, M. Ferrer, X. Hu, R. E. Jones, S. Feng, I. U. Agoulnik, W. Zheng, and A. I. Agoulnik. 2013. Identification of small-molecule agonists of human relaxin family receptor 1 (RXFP1) by using a homogenous cell-based cAMP assay. J Biomol Screen 18: 670-677.

Chen, J., Q. Qiu, P. N. Lohstroh, J. W. Overstreet, and B. L. Lasley. 2003. Hormonal characteristics in the early luteal phase of conceptive and nonconceptive menstrual cycles. J Soc Gynecol Investig 10: 27-31.

Chen, K. F., H. L. Chen, C. Y. Liu, W. T. Tai, K. Ichikawa, P. J. Chen, and A. L. Cheng. 2012. Dovitinib sensitizes hepatocellular carcinoma cells to TRAIL and tigatuzumab, a novel anti-DR5 antibody, through SHP-1-dependent inhibition of STAT3. Biochem Pharmacol 83: 769-777.

Chen, K. J., Y. Hou, K. Wang, J. Li, Y. Xia, X. Y. Yang, G. Lv, X. L. Xing, and F. Shen. 2014. Reexpression of Let-7g microRNA inhibits the proliferation and migration via K-Ras/HMGA2/snail axis in hepatocellular carcinoma. Biomed Res Int 2014: 742417.

Chen, R. J., Y. S. Ho, H. R. Guo, and Y. J. Wang. 2008. Rapid activation of Stat3 and ERK1/2 by nicotine modulates cell proliferation in human bladder cancer cells. Toxicological sciences : an official journal of the Society of Toxicology 104: 283-293.

Chiappetta, G., A. Ferraro, E. Vuttariello, M. Monaco, F. Galdiero, V. De Simone, D. Califano, P. Pallante, G. Botti, L. Pezzullo, G. M. Pierantoni, M. Santoro, and A. Fusco. 2008. HMGA2 mRNA expression correlates with the malignant phenotype in human thyroid neoplasias. Eur J Cancer 44: 1015-1021.

Chieffi, P., S. Battista, M. Barchi, S. Di Agostino, G. M. Pierantoni, M. Fedele, L. Chiariotti, D. Tramontano, and A. Fusco. 2002. HMGA1 and HMGA2 protein expression in mouse spermatogenesis. Oncogene 21: 3644-3650.

Chiou, G. Y., C. S. Chien, M. L. Wang, M. T. Chen, Y. P. Yang, Y. L. Yu, Y. Chien, Y. C. Chang, C. C. Shen, C. C. Chio, K. H. Lu, H. I. Ma, K. H. Chen, D. M. Liu, S. A. Miller, Y. W. Chen, P. I. Huang, Y. H. Shih, M. C. Hung, and S. H. Chiou. 2013. Epigenetic regulation of the miR142-3p/interleukin-6 circuit in glioblastoma. Mol Cell 52: 693-706.

Christmann, M., B. Verbeek, W. P. Roos, and B. Kaina. 2011. O(6)-Methylguanine-DNA methyltransferase (MGMT) in normal tissues and tumors: enzyme activity, promoter methylation and immunohistochemistry. Biochimica et biophysica acta 1816: 179-190.

Clay, M. R., M. Tabor, J. H. Owen, T. E. Carey, C. R. Bradford, G. T. Wolf, M. S. Wicha, and M. E. Prince. 2010. Single-marker identification of head and neck squamous cell carcinoma cancer stem cells with aldehyde dehydrogenase. Head Neck 32: 1195-1201.

Cleynen, I., and W. J. Van de Ven. 2008. The HMGA proteins: a myriad of functions (Review). International journal of oncology 32: 289-305.

Cohen, M. H., J. R. Johnson, and R. Pazdur. 2005. Food and Drug Administration Drug approval summary: temozolomide plus radiation therapy for the treatment of newly diagnosed glioblastoma multiforme. Clinical cancer research : an official journal of the American Association for Cancer Research 11: 6767-6771.

Cohly, H., J. Stephens, A. Markhov, M. Angel, W. Campbell, K. Ndebele, and J. Jenkins. 2001. Cell culture conditions affect LPS inducibility of the inflammatory mediators in J774A.1 murine macrophages. Immunological investigations 30: 1-15.

Conrad, K. P. 2004. Mechanisms of renal vasodilation and hyperfiltration during pregnancy. J Soc Gynecol Investig 11: 438-448.

Conrad, K. P., and J. Novak. 2004. Emerging role of relaxin in renal and cardiovascular function. Am J Physiol Regul Integr Comp Physiol 287: R250-261.

Copley, M. R., S. Babovic, C. Benz, D. J. Knapp, P. A. Beer, D. G. Kent, S. Wohrer, D. Q. Treloar, C. Day, K. Rowe, H. Mader, F. Kuchenbauer, R. K. Humphries, and C. J. Eaves. 2013. The Lin28b-let-7-Hmga2 axis determines the higher self-renewal potential of fetal haematopoietic stem cells. Nat Cell Biol 15: 916-925.

Cuddapah, V. A., S. Robel, S. Watkins, and H. Sontheimer. 2014. A neurocentric perspective on glioma invasion. Nature reviews. Neuroscience 15: 455-465.

Danussi, C., U. D. Akavia, F. Niola, A. Jovic, A. Lasorella, D. Pe'er, and A. Iavarone. 2013. RHPN2 drives mesenchymal transformation in malignant glioma by triggering RhoA activation. Cancer Res 73: 5140-5150.

Das, A., N. L. Banik, S. J. Patel, and S. K. Ray. 2004. Dexamethasone protected human glioblastoma U87MG cells from temozolomide induced apoptosis by maintaining Bax:Bcl-2 ratio and preventing proteolytic activities. Mol Cancer 3: 36.

Debrah, D. O., K. P. Conrad, L. A. Danielson, and S. G. Shroff. 2005. Effects of relaxin on systemic arterial hemodynamics and mechanical properties in conscious rats: sex dependency and dose response. J Appl Physiol (1985) 98: 1013-1020.

Debrah, D. O., J. Novak, J. E. Matthews, R. J. Ramirez, S. G. Shroff, and K. P. Conrad. 2006. Relaxin is essential for systemic vasodilation and increased global arterial compliance during early pregnancy in conscious rats. Endocrinology 147: 5126-5131.

Demchik, L. L., M. Sameni, K. Nelson, T. Mikkelsen, and B. F. Sloane. 1999. Cathepsin B and glioma invasion. Int J Dev Neurosci 17: 483-494.

Di Agostino, S., M. Fedele, P. Chieffi, A. Fusco, P. Rossi, R. Geremia, and C. Sette. 2004. Phosphorylation of high-mobility group protein A2 by Nek2 kinase during the first meiotic division in mouse spermatocytes. Mol Biol Cell 15: 1224-1232.

Di Fazio, P., R. Montalbano, D. Neureiter, B. Alinger, A. Schmidt, A. L. Merkel, K. Quint, and M. Ocker. 2012. Downregulation of HMGA2 by the pan-deacetylase

inhibitor panobinostat is dependent on hsa-let-7b expression in liver cancer cell lines. Experimental cell research 318: 1832-1843.

Drablos, F., E. Feyzi, P. A. Aas, C. B. Vaagbo, B. Kavli, M. S. Bratlie, J. Pena-Diaz, M. Otterlei, G. Slupphaug, and H. E. Krokan. 2004. Alkylation damage in DNA and RNA--repair mechanisms and medical significance. DNA Repair (Amst) 3: 1389-1407.

Droge, P., and C. A. Davey. 2008. Do cells let-7 determine stemness? Cell Stem Cell 2: 8-9.

Dschietzig, T., C. Bartsch, C. Richter, M. Laule, G. Baumann, and K. Stangl. 2003. Relaxin, a pregnancy hormone, is a functional endothelin-1 antagonist: attenuation of endothelin-1-mediated vasoconstriction by stimulation of endothelin type-B receptor expression via ERK-1/2 and nuclear factor-kappaB. Circ Res 92: 32-40.

Dschietzig, T., S. Teichman, E. Unemori, S. Wood, J. Boehmer, C. Richter, G. Baumann, and K. Stangl. 2009. Intravenous recombinant human relaxin in compensated heart failure: a safety, tolerability, and pharmacodynamic trial. J Card Fail 15: 182-190.

Du, X. J., Q. Xu, E. Lekgabe, X. M. Gao, H. Kiriazis, X. L. Moore, A. M. Dart, G. W. Tregear, R. A. Bathgate, and C. S. Samuel. 2009. Reversal of cardiac fibrosis and related dysfunction by relaxin. Annals of the New York Academy of Sciences 1160: 278-284.

Dunn, G. P., M. L. Rinne, J. Wykosky, G. Genovese, S. N. Quayle, I. F. Dunn, P. K. Agarwalla, M. G. Chheda, B. Campos, A. Wang, C. Brennan, K. L. Ligon, F. Furnari, W. K. Cavenee, R. A. Depinho, L. Chin, and W. C. Hahn. 2012. Emerging insights into the molecular and cellular basis of glioblastoma. Genes Dev 26: 756-784.

Dunn, J., A. Baborie, F. Alam, K. Joyce, M. Moxham, R. Sibson, D. Crooks, D. Husband, A. Shenoy, A. Brodbelt, H. Wong, T. Liloglou, B. Haylock, and C. Walker. 2009. Extent of MGMT promoter methylation correlates with outcome in glioblastomas given temozolomide and radiotherapy. British journal of cancer 101: 124-131.

Eddie, L. W., F. Martinez, D. L. Healy, B. Sutton, R. J. Bell, and G. W. Tregear. 1990. Relaxin in sera during the luteal phase of in-vitro fertilization cycles. Br J Obstet Gynaecol 97: 215-220.

Edmondson, R., J. J. Broglie, A. F. Adcock, and L. Yang. 2014. Three-dimensional cell culture systems and their applications in drug discovery and cell-based biosensors. Assay and drug development technologies 12: 207-218.

Eeckhout, Y., and G. Vaes. 1977. Further studies on the activation of procollagenase, the latent precursor of bone collagenase. Effects of lysosomal cathepsin B, plasmin and kallikrein, and spontaneous activation. The Biochemical journal 166: 21-31.

Einspanier, A., D. Muller, J. Lubberstedt, O. Bartsch, A. Jurdzinski, K. Fuhrmann, and R. Ivell. 2001. Characterization of relaxin binding in the uterus of the marmoset monkey. Molecular human reproduction 7: 963-970.

Einspanier, A., K. Lieder, B. Husen, K. Ebert, S. Lier, R. Einspanier, E. Unemori, and M. Kemper. 2009. Relaxin supports implantation and early pregnancy in the marmoset monkey. Annals of the New York Academy of Sciences 1160: 140-146.

Eldridge-White, R., R. A. Easter, D. M. Heaton, M. B. O'Day, G. C. Petersen, R. D. Shanks, M. K. Tarbell, and O. D. Sherwood. 1989. Hormonal control of the cervix in pregnant gilts. I. Changes in the physical properties of the cervix correlate temporally with elevated serum levels of estrogen and relaxin. Endocrinology 125: 2996-3003.

Elkholi, R., T. T. Renault, M. N. Serasinghe, and J. E. Chipuk. 2014. Putting the pieces together: How is the mitochondrial pathway of apoptosis regulated in cancer and chemotherapy? Cancer Metab 2: 16.

Esmailzadeh, S., B. Mansoori, A. Mohammadi, D. Shanehbandi, and B. Baradaran. 2016. siRNA-Mediated Silencing of HMGA2 Induces Apoptosis and Cell Cycle Arrest in Human Colorectal Carcinoma. J Gastrointest Cancer.

Fan, C., Y. Lin, Y. Mao, Z. Huang, A. Y. Liu, H. Ma, D. Yu, A. Maitikabili, H. Xiao, C. Zhang, F. Liu, Q. Luo, and G. Ouyang. 2016. MicroRNA-543 suppresses colorectal cancer growth and metastasis by targeting KRAS, MTA1 and HMGA2. Oncotarget 7: 21825-21839.

Fan, C. H., W. L. Liu, H. Cao, C. Wen, L. Chen, and G. Jiang. 2013. O6-methylguanine DNA methyltransferase as a promising target for the treatment of temozolomide-resistant gliomas. Cell death & disease 4: e876.

Fan, L. C., C. W. Shiau, W. T. Tai, M. H. Hung, P. Y. Chu, F. S. Hsieh, H. Lin, H. C. Yu, and K. F. Chen. 2015. SHP-1 is a negative regulator of epithelial-mesenchymal transition in hepatocellular carcinoma. Oncogene 34: 5252-5263.

Fedele, M., and A. Fusco. 2010. HMGA and cancer. Biochimica et biophysica acta 1799: 48-54.

Fei, D. T., M. C. Gross, J. L. Lofgren, M. Mora-Worms, and A. B. Chen. 1990. Cyclic AMP response to recombinant human relaxin by cultured human endometrial

cells--a specific and high throughput in vitro bioassay. Biochem Biophys Res Commun 170: 214-222.

Feng, C., V. Neumeister, W. Ma, J. Xu, L. Lu, J. Bordeaux, N. J. Maihle, D. L. Rimm, and Y. Huang. 2012. Lin28 regulates HER2 and promotes malignancy through multiple mechanisms. Cell cycle 11: 2486-2494.

Feng, S., and A. I. Agoulnik. 2011. Expression of LDL-A module of relaxin receptor in prostate cancer cells inhibits tumorigenesis. International journal of oncology 39: 1559-1565.

Feng, S., I. U. Agoulnik, Z. Li, H. D. Han, G. Lopez-Berestein, A. Sood, M. M. Ittmann, and A. I. Agoulnik. 2009. Relaxin/RXFP1 signaling in prostate cancer progression. Annals of the New York Academy of Sciences 1160: 379-380.

Feng, S., I. U. Agoulnik, N. V. Bogatcheva, A. A. Kamat, B. Kwabi-Addo, R. Li, G. Ayala, M. M. Ittmann, and A. I. Agoulnik. 2007. Relaxin promotes prostate cancer progression. Clinical cancer research : an official journal of the American Association for Cancer Research 13: 1695-1702.

Feng, S., I. U. Agoulnik, A. Truong, Z. Li, C. J. Creighton, E. M. Kaftanovskaya, R. Pereira, H. D. Han, G. Lopez-Berestein, T. Klonisch, M. M. Ittmann, A. K. Sood, and A. I. Agoulnik. 2010. Suppression of relaxin receptor RXFP1 decreases prostate cancer growth and metastasis. Endocrine-related cancer 17: 1021-1033.

Fiandalo, M. V., and N. Kyprianou. 2012. Caspase control: protagonists of cancer cell apoptosis. Exp Oncol 34: 165-175.

Fillmore, H. L., T. E. VanMeter, and W. C. Broaddus. 2001. Membrane-type matrix metalloproteinases (MT-MMPs): expression and function during glioma invasion. J Neurooncol 53: 187-202.

Filonzi, M., L. C. Cardoso, M. T. Pimenta, D. B. Queiroz, M. C. Avellar, C. S. Porto, and M. F. Lazari. 2007. Relaxin family peptide receptors Rxfp1 and Rxfp2: mapping of the mRNA and protein distribution in the reproductive tract of the male rat. Reprod Biol Endocrinol 5: 29.

Fishel, M. L., Y. He, M. L. Smith, and M. R. Kelley. 2007. Manipulation of base excision repair to sensitize ovarian cancer cells to alkylating agent temozolomide. Clinical cancer research : an official journal of the American Association for Cancer Research 13: 260-267.

Fisher, C., C. Berry, L. Blue, J. J. Morton, and J. McMurray. 2003. N-terminal pro B type natriuretic peptide, but not the new putative cardiac hormone relaxin, predicts prognosis in patients with chronic heart failure. Heart 89: 879-881.

Fonovic, M., and B. Turk. 2014. Cysteine cathepsins and extracellular matrix degradation. Biochimica et biophysica acta 1840: 2560-2570.

Frattini, V., V. Trifonov, J. M. Chan, A. Castano, M. Lia, F. Abate, S. T. Keir, A. X. Ji, P. Zoppoli, F. Niola, C. Danussi, I. Dolgalev, P. Porrati, S. Pellegatta, A. Heguy, G. Gupta, D. J. Pisapia, P. Canoll, J. N. Bruce, R. E. McLendon, H. Yan, K. Aldape, G. Finocchiaro, T. Mikkelsen, G. G. Prive, D. D. Bigner, A. Lasorella, R. Rabadan, and A. Iavarone. 2013. The integrated landscape of driver genomic alterations in glioblastoma. Nat Genet 45: 1141-1149.

Friedl, P., and K. Wolf. 2003. Tumour-cell invasion and migration: diversity and escape mechanisms. Nature reviews. Cancer 3: 362-374.

Fukushima, T., H. Takeshima, and H. Kataoka. 2009. Anti-glioma therapy with temozolomide and status of the DNA-repair gene MGMT. Anticancer research 29: 4845-4854.

Fulda, S., and K. Debatin. 2006. Extrinsic versus intrinsic apoptosis pathways in anticancer chemotherapy. Oncogene 25: 4798-4811.

Furnari, F. B., T. Fenton, R. M. Bachoo, A. Mukasa, J. M. Stommel, A. Stegh, W. C. Hahn, K. L. Ligon, D. N. Louis, C. Brennan, L. Chin, R. A. DePinho, and W. K. Cavenee. 2007. Malignant astrocytic glioma: genetics, biology, and paths to treatment. Genes Dev 21: 2683-2710.

Fusco, A., and M. Fedele. 2007. Roles of HMGA proteins in cancer. Nat Rev Cancer 7: 899-910.

Gadji, M., A. M. Crous, D. Fortin, J. Krcek, M. Torchia, S. Mai, R. Drouin, and T. Klonisch. 2009. EGF receptor inhibitors in the treatment of glioblastoma multiform: old clinical allies and newly emerging therapeutic concepts. Eur J Pharmacol 625: 23-30.

Gan, H. K., A. N. Cvrljevic, and T. G. Johns. 2013. The epidermal growth factor receptor variant III (EGFRvIII): where wild things are altered. FEBS J 280: 5350-5370.

Gartsbein, M., A. Alt, K. Hashimoto, K. Nakajima, T. Kuroki, and T. Tennenbaum. 2006. The role of protein kinase C delta activation and STAT3 Ser727 phosphorylation in insulin-induced keratinocyte proliferation. J Cell Sci 119: 470-481.

Ghai, R., P. Waters, L. T. Roumenina, M. Gadjeva, M. S. Kojouharova, K. B. Reid, R. B. Sim, and U. Kishore. 2007. C1q and its growing family. Immunobiology 212: 253-266.

Ghavami, S., M. Hashemi, S. R. Ande, B. Yeganeh, W. Xiao, M. Eshraghi, C. J. Bus, K. Kadkhoda, E. Wiechec, and A. J. Halayko. 2009a. Apoptosis and cancer: mutations within caspase genes. Journal of medical genetics 46: 497-510.

Ghavami, S., M. Hashemi, S. R. Ande, B. Yeganeh, W. Xiao, M. Eshraghi, C. J. Bus, K. Kadkhoda, E. Wiechec, A. J. Halayko, and M. Los. 2009b. Apoptosis and cancer: mutations within caspase genes. J Med Genet 46: 497-510.

Gielen, P. R., Q. Aftab, N. Ma, V. C. Chen, X. Hong, S. Lozinsky, C. C. Naus, and W. C. Sin. 2013. Connexin43 confers Temozolomide resistance in human glioma cells by modulating the mitochondrial apoptosis pathway. Neuropharmacology 75: 539-548.

Glogowska, A., U. Kunanuvat, J. Stetefeld, T. R. Patel, T. Thanasupawat, J. Krcek, E. Weber, G. W. Wong, M. R. Del Bigio, C. Hoang-Vu, S. Hombach-Klonisch, and T. Klonisch. 2013. C1q-tumour necrosis factor-related protein 8 (CTRP8) is a novel interaction partner of relaxin receptor RXFP1 in human brain cancer cells. The Journal of pathology 231: 466-479.

Goellner, E. M., B. Grimme, A. R. Brown, Y. C. Lin, X. H. Wang, K. F. Sugrue, L. Mitchell, R. N. Trivedi, J. B. Tang, and R. W. Sobol. 2011. Overcoming temozolomide resistance in glioblastoma via dual inhibition of NAD+ biosynthesis and base excision repair. Cancer Res 71: 2308-2317.

Goldsmith, L. T., G. Weiss, S. Palejwala, T. M. Plant, A. Wojtczuk, W. C. Lambert, N. Ammur, D. Heller, J. H. Skurnick, D. Edwards, and D. M. Cole. 2004. Relaxin regulation of endometrial structure and function in the rhesus monkey. Proc Natl Acad Sci U S A 101: 4685-4689.

Graham, C. A., and T. F. Cloughesy. 2004. Brain tumor treatment: chemotherapy and other new developments. Seminars in oncology nursing 20: 260-272.

Grossman, J., and W. H. Frishman. 2010. Relaxin: a new approach for the treatment of acute congestive heart failure. Cardiology in review 18: 305-312.

Guan, X., J. Vengoechea, S. Zheng, A. E. Sloan, Y. Chen, D. J. Brat, B. P. O'Neill, J. de Groot, S. Yust-Katz, W. K. Yung, M. L. Cohen, K. D. Aldape, S. Rosenfeld, R. G. Verhaak, and J. S. Barnholtz-Sloan. 2014. Molecular subtypes of glioblastoma are relevant to lower grade glioma. PloS one 9: e91216.

Guensberg, P., V. Wacheck, T. Lucas, B. Monia, H. Pehamberger, H. G. Eichler, and B. Jansen. 2002. Bcl-xL antisense oligonucleotides chemosensitize human glioblastoma cells. Chemotherapy 48: 189-195.

Guo, L., C. Chen, M. Shi, F. Wang, X. Chen, D. Diao, M. Hu, M. Yu, L. Qian, and N. Guo. 2013. Stat3-coordinated Lin-28-let-7-HMGA2 and miR-200-ZEB1 circuits initiate and maintain oncostatin M-driven epithelial-mesenchymal transition. Oncogene 32: 5272-5282.

Gurney, J. G., and N. Kadan-Lottick. 2001. Brain and other central nervous system tumors: rates, trends, and epidemiology. Curr Opin Oncol 13: 160-166.

Hall, K. 1960. Modification by relaxin of the response of the reproductive tract of mice to oestradiol and progesterone. J Endocrinol 20: 355-364.

Halls, M. L., and D. M. Cooper. 2010. Sub-picomolar relaxin signalling by a pre-assembled RXFP1, AKAP79, AC2, beta-arrestin 2, PDE4D3 complex. EMBO J 29: 2772-2787.

Halls, M. L., R. A. Bathgate, and R. J. Summers. 2006. Relaxin family peptide receptors RXFP1 and RXFP2 modulate cAMP signaling by distinct mechanisms. Molecular pharmacology 70: 214-226.

Halls, M. L., R. A. Bathgate, and R. J. Summers. 2007. Comparison of signaling pathways activated by the relaxin family peptide receptors, RXFP1 and RXFP2, using reporter genes. The Journal of pharmacology and experimental therapeutics 320: 281-290.

Halls, M. L., R. A. Bathgate, S. W. Sutton, T. B. Dschietzig, and R. J. Summers. 2015. International Union of Basic and Clinical Pharmacology. XCV. Recent advances in the understanding of the pharmacology and biological roles of relaxin family peptide receptors 1-4, the receptors for relaxin family peptides. Pharmacol Rev 67: 389-440.

Halls, M. L., E. T. van der Westhuizen, J. D. Wade, B. A. Evans, R. A. Bathgate, and R. J. Summers. 2009. Relaxin family peptide receptor (RXFP1) coupling to G(alpha)i3 involves the C-terminal Arg752 and localization within membrane Raft Microdomains. Molecular pharmacology 75: 415-428.

Hammond, S. M., and N. E. Sharpless. 2008. HMGA2, microRNAs, and stem cell aging. Cell 135: 1013-1016.

Han, J., and Q. Chen. 2015. MiR-16 modulate temozolomide resistance by regulating BCL-2 in human glioma cells. Int J Clin Exp Pathol 8: 12698-12707.

Han, T. J., B. J. Cho, E. J. Choi, D. H. Kim, S. H. Song, S. H. Paek, and I. A. Kim. 2016. Inhibition of STAT3 enhances the radiosensitizing effect of temozolomide in glioblastoma cells in vitro and in vivo. J Neurooncol 130: 89-98.

Hansen, W. K., and M. R. Kelley. 2000. Review of mammalian DNA repair and translational implications. The Journal of pharmacology and experimental therapeutics 295: 1-9.

Hasinoff, B. B., X. Wu, J. L. Nitiss, R. Kanagasabai, and J. C. Yalowich. 2012. The anticancer multi-kinase inhibitor dovitinib also targets topoisomerase I and topoisomerase II. Biochem Pharmacol 84: 1617-1626.

Hayward, C., X. Shu, A. V. Cideciyan, A. Lennon, P. Barran, S. Zareparsi, L. Sawyer, G. Hendry, B. Dhillon, A. H. Milam, P. J. Luthert, A. Swaroop, N. D. Hastie, S. G. Jacobson, and A. F. Wright. 2003. Mutation in a short-chain collagen gene, CTRP5, results in extracellular deposit formation in late-onset retinal degeneration: a genetic model for age-related macular degeneration. Hum Mol Genet 12: 2657-2667.

Heeg, M. H., M. J. Koziolek, R. Vasko, L. Schaefer, K. Sharma, G. A. Muller, and F. Strutz. 2005. The antifibrotic effects of relaxin in human renal fibroblasts are mediated in part by inhibition of the Smad2 pathway. Kidney Int 68: 96-109.

Hegi, M. E., L. Liu, J. G. Herman, R. Stupp, W. Wick, M. Weller, M. P. Mehta, and M. R. Gilbert. 2008. Correlation of O6-methylguanine methyltransferase (MGMT) promoter methylation with clinical outcomes in glioblastoma and clinical strategies to modulate MGMT activity. J Clin Oncol 26: 4189-4199.

Hegi, M. E., A. C. Diserens, T. Gorlia, M. F. Hamou, N. de Tribolet, M. Weller, J. M. Kros, J. A. Hainfellner, W. Mason, L. Mariani, J. E. Bromberg, P. Hau, R. O. Mirimanoff, J. G. Cairncross, R. C. Janzer, and R. Stupp. 2005. MGMT gene silencing and benefit from temozolomide in glioblastoma. The New England journal of medicine 352: 997-1003.

Hellsten, R., M. Johansson, A. Dahlman, O. Sterner, and A. Bjartell. 2011. Galiellalactone inhibits stem cell-like ALDH-positive prostate cancer cells. PloS one 6: e22118.

Hewitson, T. D., W. Y. Ho, and C. S. Samuel. 2010. Antifibrotic properties of relaxin: in vivo mechanism of action in experimental renal tubulointerstitial fibrosis. Endocrinology 151: 4938-4948.

Hickman, M. J., and L. D. Samson. 1999. Role of DNA mismatch repair and p53 in signaling induction of apoptosis by alkylating agents. Proc Natl Acad Sci U S A 96: 10764-10769.

Holland, E. C. 2000. Glioblastoma multiforme: the terminator. Proc Natl Acad Sci U S A 97: 6242-6244.

Hombach-Klonisch, S., J. Buchmann, S. Sarun, B. Fischer, and T. Klonisch. 2000. Relaxin-like factor (RLF) is differentially expressed in the normal and neoplastic human mammary gland. Cancer 89: 2161-2168.

Hombach-Klonisch, S., J. Bialek, B. Trojanowicz, E. Weber, H. J. Holzhausen, J. D. Silvertown, A. J. Summerlee, H. Dralle, C. Hoang-Vu, and T. Klonisch. 2006. Relaxin enhances the oncogenic potential of human thyroid carcinoma cells. The American journal of pathology 169: 617-632.

Hombach-Klonisch, S., J. Bialek, Y. Radestock, A. Truong, A. I. Agoulnik, B. Fiebig, C. Willing, E. Weber, C. Hoang-Vu, and T. Klonisch. 2010. INSL3 has tumor-promoting activity in thyroid cancer. International journal of cancer 127: 521-531.

Hopkins, E. J., S. Layfield, T. Ferraro, R. A. Bathgate, and P. R. Gooley. 2007. The NMR solution structure of the relaxin (RXFP1) receptor lipoprotein receptor class A module and identification of key residues in the N-terminal region of the module that mediate receptor activation. The Journal of biological chemistry 282: 4172-4184.

Hossain, M. A., C. S. Samuel, C. Binder, T. D. Hewitson, G. W. Tregear, J. D. Wade, and R. A. Bathgate. 2010. The chemically synthesized human relaxin-2 analog, B-R13/17K H2, is an RXFP1 antagonist. Amino acids 39: 409-416.

Hossain, M. A., K. J. Rosengren, L. M. Haugaard-Jonsson, S. Zhang, S. Layfield, T. Ferraro, N. L. Daly, G. W. Tregear, J. D. Wade, and R. A. Bathgate. 2008. The A-chain of human relaxin family peptides has distinct roles in the binding and activation of the different relaxin family peptide receptors. The Journal of biological chemistry 283: 17287-17297.

Hou, L. C., A. Veeravagu, A. R. Hsu, and V. C. Tse. 2006. Recurrent glioblastoma multiforme: a review of natural history and management options. Neurosurg Focus 20: E5.

Huang, C. Y., W. T. Tai, S. Y. Wu, C. T. Shih, M. H. Chen, M. H. Tsai, C. W. Kuo, C. W. Shiau, M. H. Hung, and K. F. Chen. 2016. Dovitinib Acts As a Novel Radiosensitizer in Hepatocellular Carcinoma by Targeting SHP-1/STAT3 Signaling. Int J Radiat Oncol Biol Phys 95: 761-771.

Huse, J. T., E. L. Diamond, L. Wang, and M. K. Rosenblum. 2015. Mixed glioma with molecular features of composite oligodendroglioma and astrocytoma: a true "oligoastrocytoma"? Acta neuropathologica 129: 151-153.

Huso, T. H., and L. M. Resar. 2014. The high mobility group A1 molecular switch: turning on cancer - can we turn it off? Expert Opin Ther Targets 18: 541-553.

Innamorati, G., E. Bianchi, and M. I. Whang. 2006. An intracellular role for the C1q-globular domain. Cell Signal 18: 761-770.

Iranpour, M., A. R. Moghadam, M. Yazdi, S. R. Ande, J. Alizadeh, E. Wiechec, R. Lindsay, M. Drebot, K. M. Coombs, and S. Ghavami. 2016. Apoptosis, autophagy and unfolded protein response pathways in Arbovirus replication and pathogenesis. Expert Rev Mol Med 18: e1.

Ivell, R., M. Kotula-Balak, D. Glynn, K. Heng, and R. Anand-Ivell. 2011. Relaxin family peptides in the male reproductive system--a critical appraisal. Molecular human reproduction 17: 71-84.

Iyama, T., and D. M. Wilson, 3rd. 2013. DNA repair mechanisms in dividing and non-dividing cells. DNA Repair (Amst) 12: 620-636.

Jablonska-Trypuc, A., M. Matejczyk, and S. Rosochacki. 2016. Matrix metalloproteinases (MMPs), the main extracellular matrix (ECM) enzymes in collagen degradation, as a target for anticancer drugs. Journal of enzyme inhibition and medicinal chemistry 31: 177-183.

Jaiswal, A. S., S. Banerjee, H. Panda, C. D. Bulkin, T. Izumi, F. H. Sarkar, D. A. Ostrov, and S. Narayan. 2009. A novel inhibitor of DNA polymerase beta enhances the ability of temozolomide to impair the growth of colon cancer cells. Molecular cancer research : MCR 7: 1973-1983.

Jonas, S., and E. Izaurralde. 2015. Towards a molecular understanding of microRNA-mediated gene silencing. Nat Rev Genet 16: 421-433.

Jovcevska, I., N. Kocevar, and R. Komel. 2013. Glioma and glioblastoma - how much do we (not) know? Mol Clin Oncol 1: 935-941.

Kaftanovskaya, E. M., Z. Huang, C. Lopez, K. Conrad, and A. I. Agoulnik. 2015. Conditional deletion of the relaxin receptor gene in cells of smooth muscle lineage affects lower reproductive tract in pregnant mice. Biology of reproduction 92: 91.

Kaina, B., G. P. Margison, and M. Christmann. 2010. Targeting O(6)-methylguanine-DNA methyltransferase with specific inhibitors as a strategy in cancer therapy. Cell Mol Life Sci 67: 3663-3681.

Kaina, B., M. Christmann, S. Naumann, and W. P. Roos. 2007. MGMT: key node in the battle against genotoxicity, carcinogenicity and apoptosis induced by alkylating agents. DNA Repair (Amst) 6: 1079-1099.

Kalluri, R., and R. A. Weinberg. 2009. The basics of epithelial-mesenchymal transition. The Journal of clinical investigation 119: 1420-1428.

Kang, Y. K., C. Yoo, B. Y. Ryoo, J. J. Lee, E. Tan, I. Park, J. H. Park, Y. J. Choi, J. Jo, J. S. Ryu, and M. H. Ryu. 2013. Phase II study of dovitinib in patients with metastatic and/or unresectable gastrointestinal stromal tumours after failure of imatinib and sunitinib. British journal of cancer 109: 2309-2315.

Kao, C. Y., P. M. Yang, M. H. Wu, C. C. Huang, Y. C. Lee, and K. H. Lee. 2016. Heat shock protein 90 is involved in the regulation of HMGA2-driven growth and epithelial-to-mesenchymal transition of colorectal cancer cells. PeerJ 4: e1683.

Kaur, H., M. Hutt-Cabezas, M. F. Weingart, J. Xu, Y. Kuwahara, A. Erdreich-Epstein, B. E. Weissman, C. G. Eberhart, and E. H. Raabe. 2015. The chromatin-modifying protein HMGA2 promotes atypical teratoid/rhabdoid cell tumorigenicity. J Neuropathol Exp Neurol 74: 177-185.

Kaur, H., S. Z. Ali, L. Huey, M. Hutt-Cabezas, I. Taylor, X. G. Mao, M. Weingart, Q. Chu, F. J. Rodriguez, C. G. Eberhart, and E. H. Raabe. 2016. The transcriptional modulator HMGA2 promotes stemness and tumorigenicity in glioblastoma. Cancer letters 377: 55-64.

Kern, A., A. I. Agoulnik, and G. D. Bryant-Greenwood. 2007. The low-density lipoprotein class A module of the relaxin receptor (leucine-rich repeat containing G-protein coupled receptor 7): its role in signaling and trafficking to the cell membrane. Endocrinology 148: 1181-1194.

Kern, A., D. Hubbard, A. Amano, and G. D. Bryant-Greenwood. 2008. Cloning, expression, and functional characterization of relaxin receptor (leucine-rich repeat-containing g protein-coupled receptor 7) splice variants from human fetal membranes. Endocrinology 149: 1277-1294.

Kim, J. E., M. Patel, J. Ruzevick, C. M. Jackson, and M. Lim. 2014. STAT3 Activation in Glioblastoma: Biochemical and Therapeutic Implications. Cancers (Basel) 6: 376-395.

Kim, Y. J., and D. M. Wilson, 3rd. 2012. Overview of base excision repair biochemistry. Curr Mol Pharmacol 5: 3-13.

King, C. E., L. Wang, R. Winograd, B. B. Madison, P. S. Mongroo, C. N. Johnstone, and A. K. Rustgi. 2011. LIN28B fosters colon cancer migration, invasion and transformation through let-7-dependent and -independent mechanisms. Oncogene 30: 4185-4193.

Kishore, U., C. Gaboriaud, P. Waters, A. K. Shrive, T. J. Greenhough, K. B. Reid, R. B. Sim, and G. J. Arlaud. 2004. C1q and tumor necrosis factor superfamily: modularity and versatility. Trends Immunol 25: 551-561.

Klonisch, T., J. Bialek, Y. Radestock, C. Hoang-Vu, and S. Hombach-Klonisch. 2007. Relaxin-like ligand-receptor systems are autocrine/paracrine effectors in tumor cells and modulate cancer progression and tissue invasiveness. Adv Exp Med Biol 612: 104-118.

Klonisch, T., A. Glogowska, T. Thanasupawat, M. Burg, J. Krcek, M. Pitz, A. Jaggupilli, P. Chelikani, G. W. Wong, and S. Hombach-Klonisch. 2016. Structural commonality of C1q TNF-related proteins and their potential to activate relaxin/insulin-like family peptide receptor 1 signalling pathways in cancer cells. British journal of pharmacology.

Klonisch, T., H. Muller-Huesmann, M. Riedel, A. Kehlen, J. Bialek, Y. Radestock, H. J. Holzhausen, K. Steger, M. Ludwig, W. Weidner, C. Hoang-Vu, and S. Hombach-Klonisch. 2005. INSL3 in the benign hyperplastic and neoplastic human prostate gland. International journal of oncology 27: 307-315.

Knizhnik, A. V., W. P. Roos, T. Nikolova, S. Quiros, K. H. Tomaszowski, M. Christmann, and B. Kaina. 2013. Survival and death strategies in glioma cells: autophagy, senescence and apoptosis triggered by a single type of temozolomide-induced DNA damage. PloS one 8: e55665.

Koh, M., J. C. Lee, C. Min, and A. Moon. 2013. A novel metformin derivative, HL010183, inhibits proliferation and invasion of triple-negative breast cancer cells. Bioorganic & medicinal chemistry 21: 2305-2313.

Kohsaka, S., L. Wang, K. Yachi, R. Mahabir, T. Narita, T. Itoh, M. Tanino, T. Kimura, H. Nishihara, and S. Tanaka. 2012. STAT3 inhibition overcomes temozolomide resistance in glioblastoma by downregulating MGMT expression. Mol Cancer Ther 11: 1289-1299.

Kong, R. C., P. J. Shilling, D. K. Lobb, P. R. Gooley, and R. A. Bathgate. 2010. Membrane receptors: structure and function of the relaxin family peptide receptors. Mol Cell Endocrinol 320: 1-15.

Kontos, C. K., M. I. Christodoulou, and A. Scorilas. 2014. Apoptosis-related BCL2-family members: Key players in chemotherapy. Anticancer Agents Med Chem 14: 353-374.

Krex, D., B. Klink, C. Hartmann, A. von Deimling, T. Pietsch, M. Simon, M. Sabel, J. P. Steinbach, O. Heese, G. Reifenberger, M. Weller, G. Schackert, and N. German Glioma. 2007. Long-term survival with glioblastoma multiforme. Brain 130: 2596-2606.

Krusche, C. A., T. Kroll, H. M. Beier, and I. Classen-Linke. 2007. Expression of leucine-rich repeat-containing G-protein-coupled receptors in the human cyclic endometrium. Fertil Steril 87: 1428-1437.

Lah, T. T., and J. Kos. 1998. Cysteine proteinases in cancer progression and their clinical relevance for prognosis. Biol Chem 379: 125-130.

Lee, E. S., K. K. Ko, Y. A. Joe, S. G. Kang, and Y. K. Hong. 2011. Inhibition of STAT3 reverses drug resistance acquired in temozolomide-resistant human glioma cells. Oncol Lett 2: 115-121.

Lee, H., J. Deng, M. Kujawski, C. Yang, Y. Liu, A. Herrmann, M. Kortylewski, D. Horne, G. Somlo, S. Forman, R. Jove, and H. Yu. 2010. STAT3-induced S1PR1 expression is crucial for persistent STAT3 activation in tumors. Nat Med 16: 1421-1428.

Lee, H. Y., S. Zhao, P. A. Fields, and O. D. Sherwood. 2005a. The extent to which relaxin promotes proliferation and inhibits apoptosis of cervical epithelial and stromal cells is greatest during late pregnancy in rats. Endocrinology 146: 511-518.

Lee, J. H., S. Q. Koh, S. Guadagna, P. T. Francis, M. M. Esiri, C. P. Chen, P. T. Wong, G. S. Dawe, and M. K. Lai. 2016. Altered relaxin family receptors RXFP1 and RXFP3 in the neocortex of depressed Alzheimer's disease patients. Psychopharmacology (Berl) 233: 591-598.

Lee, Y. H., S. Nair, E. Rousseau, D. B. Allison, G. P. Page, P. A. Tataranni, C. Bogardus, and P. A. Permana. 2005b. Microarray profiling of isolated abdominal subcutaneous adipocytes from obese vs non-obese Pima Indians: increased expression of inflammation-related genes. Diabetologia 48: 1776-1783.

Lee, Y. S., and A. Dutta. 2007. The tumor suppressor microRNA let-7 represses the HMGA2 oncogene. Genes Dev 21: 1025-1030.

Lessing, J. B., S. H. Brenner, C. Schoenfeld, L. T. Goldsmith, R. D. Amelar, L. Dubin, and G. Weiss. 1985. The effect of relaxin on the motility of sperm in freshly thawed human semen. Fertil Steril 44: 406-409.

Levicar, N., R. K. Nuttall, and T. T. Lah. 2003a. Proteases in brain tumour progression. Acta Neurochir (Wien) 145: 825-838.

Levicar, N., R. A. Dewey, E. Daley, T. E. Bates, D. Davies, J. Kos, G. J. Pilkington, and T. T. Lah. 2003b. Selective suppression of cathepsin L by antisense cDNA impairs human brain tumor cell invasion in vitro and promotes apoptosis. Cancer Gene Ther 10: 141-151.

Li, O., J. Li, and P. Droge. 2007. DNA architectural factor and proto-oncogene HMGA2 regulates key developmental genes in pluripotent human embryonic stem cells. FEBS Lett 581: 3533-3537.

Li, O., D. Vasudevan, C. A. Davey, and P. Droge. 2006. High-level expression of DNA architectural factor HMGA2 and its association with nucleosomes in human embryonic stem cells. Genesis 44: 523-529.

Li, Q., L. Wang, W. Tan, Z. Peng, Y. Luo, Y. Zhang, G. Zhang, D. Na, P. Jin, T. Shi, D. Ma, and L. Wang. 2011. Identification of C1qTNF-related protein 4 as a potential cytokine that stimulates the STAT3 and NF-kappaB pathways and promotes cell survival in human cancer cells. Cancer letters 308: 203-214.

Li, Y., X. Zhang, D. Chen, and C. Ma. 2016. Let-7a suppresses glioma cell proliferation and invasion through TGF-beta/Smad3 signaling pathway by targeting HMGA2. Tumour Biol 37: 8107-8119.

Li, Y., Z. Zhao, C. Xu, Z. Zhou, Z. Zhu, and T. You. 2014. HMGA2 induces transcription factor Slug expression to promote epithelial-to-mesenchymal transition and contributes to colon cancer progression. Cancer letters 355: 130-140.

Ligon, A. H., S. D. Moore, M. A. Parisi, M. E. Mealiffe, D. J. Harris, H. L. Ferguson, B. J. Quade, and C. C. Morton. 2005. Constitutional rearrangement of the architectural factor HMGA2: a novel human phenotype including overgrowth and lipomas. Am J Hum Genet 76: 340-348.

Lin, C. K., J. S. Jin, C. P. Yu, and W. C. Tsai. 2011. Expression of LGR8 and related biomarkers in hepatocellular carcinoma: correlation with clinicopathological parameters. The Chinese journal of physiology 54: 161-168.

Lin, Y., A. Y. Liu, C. Fan, H. Zheng, Y. Li, C. Zhang, S. Wu, D. Yu, Z. Huang, F. Liu, Q. Luo, C. J. Yang, and G. Ouyang. 2015. MicroRNA-33b Inhibits Breast Cancer Metastasis by Targeting HMGA2, SALL4 and Twist1. Sci Rep 5: 9995.

Liotta, L. A., P. S. Steeg, and W. G. Stetler-Stevenson. 1991. Cancer metastasis and angiogenesis: an imbalance of positive and negative regulation. Cell 64: 327-336.

Litherland, G. J., M. S. Elias, W. Hui, C. D. Macdonald, J. B. Catterall, M. J. Barter, M. J. Farren, M. Jefferson, and A. D. Rowan. 2010. Protein kinase C isoforms zeta and iota mediate collagenase expression and cartilage destruction via STAT3- and ERK-dependent c-fos induction. The Journal of biological chemistry 285: 22414-22425.

Liu, B., B. Pang, X. Hou, H. Fan, N. Liang, S. Zheng, B. Feng, W. Liu, H. Guo, S. Xu, and Q. Pang. 2014. Expression of high-mobility group AT-hook protein 2 and its prognostic significance in malignant gliomas. Hum Pathol 45: 1752-1758.

Liu, C., Y. Tu, J. Yuan, X. Mao, S. He, L. Wang, G. Fu, J. Zong, and Y. Zhang. 2012. Aberrant expression of N-methylpurine-DNA glycosylase influences patient survival in malignant gliomas. J Biomed Biotechnol 2012: 760679.

Liu, Y., H. Li, J. Feng, X. Cui, W. Huang, Y. Li, F. Su, Q. Liu, J. Zhu, X. Lv, J. Chen, D. Huang, and F. Yu. 2013. Lin28 induces epithelial-to-mesenchymal transition and stemness via downregulation of let-7a in breast cancer cells. PloS one 8: e83083.

Liu, Y., S. Shete, C. J. Etzel, M. Scheurer, G. Alexiou, G. Armstrong, S. Tsavachidis, F. W. Liang, M. Gilbert, K. Aldape, T. Armstrong, R. Houlston, F. Hosking, L. Robertson, Y. Xiao, J. Wiencke, M. Wrensch, U. Andersson, B. S. Melin, and M. Bondy. 2010. Polymorphisms of LIG4, BTBD2, HMGA2, and RTEL1 genes involved in the double-strand break repair pathway predict glioblastoma survival. J Clin Oncol 28: 2467-2474.

Louis, D. N., A. Perry, G. Reifenberger, A. von Deimling, D. Figarella-Branger, W. K. Cavenee, H. Ohgaki, O. D. Wiestler, P. Kleihues, and D. W. Ellison. 2016. The 2016 World Health Organization Classification of Tumors of the Central Nervous System: a summary. Acta neuropathologica 131: 803-820.

Loumaye, E., S. De Cooman, and K. Thomas. 1980. Immunoreactive relaxin-like substance in human seminal plasma. J Clin Endocrinol Metab 50: 1142-1143.

Luna, J. J., A. Riesewijk, J. A. Horcajadas, R. Van Os Rd, F. Dominguez, S. Mosselman, A. Pellicer, and C. Simon. 2004. Gene expression pattern and immunoreactive protein localization of LGR7 receptor in human endometrium throughout the menstrual cycle. Molecular human reproduction 10: 85-90.

Luo, Y., W. Li, and H. Liao. 2013. HMGA2 induces epithelial-to-mesenchymal transition in human hepatocellular carcinoma cells. Oncol Lett 5: 1353-1356.

Lv, K., L. Liu, L. Wang, J. Yu, X. Liu, Y. Cheng, M. Dong, R. Teng, L. Wu, P. Fu, W. Deng, W. Hu, and L. Teng. 2012. Lin28 mediates paclitaxel resistance by modulating p21, Rb and Let-7a miRNA in breast cancer cells. PloS one 7: e40008.

Ma, J., H. Huang, Z. Han, C. Zhu, and B. Yue. 2015. RLN2 Is a Positive Regulator of AKT-2-Induced Gene Expression Required for Osteosarcoma Cells Invasion and Chemoresistance. Biomed Res Int 2015: 147468.

Ma, S., B. Roozendaal, T. C. Burazin, G. W. Tregear, J. L. McGaugh, and A. L. Gundlach. 2005. Relaxin receptor activation in the basolateral amygdala impairs memory consolidation. Eur J Neurosci 22: 2117-2122.

Ma, S., K. W. Chan, T. K. Lee, K. H. Tang, J. Y. Wo, B. J. Zheng, and X. Y. Guan. 2008. Aldehyde dehydrogenase discriminates the CD133 liver cancer stem cell populations. Molecular cancer research : MCR 6: 1146-1153.

MacLennan, A. H., and P. Grant. 1991. Human relaxin. In vitro response of human and pig myometrium. J Reprod Med 36: 630-634.

MacLennan, A. H., P. Grant, D. Ness, and A. Down. 1986. Effect of porcine relaxin and progesterone on rat, pig and human myometrial activity in vitro. J Reprod Med 31: 43-49.

Madison, B. B., Q. Liu, X. Zhong, C. M. Hahn, N. Lin, M. J. Emmett, B. Z. Stanger, J. S. Lee, and A. K. Rustgi. 2013. LIN28B promotes growth and tumorigenesis of the intestinal epithelium via Let-7. Genes Dev 27: 2233-2245.

Mansoori, B., A. Mohammadi, S. Goldar, D. Shanehbandi, L. Mohammadnejad, E. Baghbani, T. Kazemi, S. Kachalaki, and B. Baradaran. 2016. Silencing of High Mobility Group Isoform I-C (HMGI-C) Enhances Paclitaxel Chemosensitivity in Breast Adenocarcinoma Cells (MDA-MB-468). Adv Pharm Bull 6: 171-177.

Mao, X. G., M. Hutt-Cabezas, B. A. Orr, M. Weingart, I. Taylor, A. K. Rajan, Y. Odia, U. Kahlert, J. Maciaczyk, G. Nikkhah, C. G. Eberhart, and E. H. Raabe. 2013. LIN28A facilitates the transformation of human neural stem cells and promotes glioblastoma tumorigenesis through a pro-invasive genetic program. Oncotarget 4: 1050-1064.

Marshall, S. A., S. N. Senadheera, L. J. Parry, and J. E. Girling. 2016. The Role of Relaxin in Normal and Abnormal Uterine Function During the Menstrual Cycle and Early Pregnancy. Reprod Sci.

McKinley, M. J., A. M. Allen, P. Burns, L. M. Colvill, and B. J. Oldfield. 1998. Interaction of circulating hormones with the brain: the roles of the subfornical organ and the organum vasculosum of the lamina terminalis. Clin Exp Pharmacol Physiol Suppl 25: S61-67.

McKinley, M. J., P. Burns, L. M. Colvill, B. J. Oldfield, J. D. Wade, R. S. Weisinger, and G. W. Tregear. 1997. Distribution of Fos immunoreactivity in the lamina terminalis and hypothalamus induced by centrally administered relaxin in conscious rats. J Neuroendocrinol 9: 431-437.

Messaoudi, K., A. Clavreul, and F. Lagarce. 2015. Toward an effective strategy in glioblastoma treatment. Part I: resistance mechanisms and strategies to overcome resistance of glioblastoma to temozolomide. Drug Discov Today 20: 899-905.

Miah, A. G., U. Salma, K. Hamano, and K. Schellander. 2015. Physiological roles of relaxin in prefertilizing activities of spermatozoa. Anim Reprod Sci 161: 1-15.

Miao, Y., T. Cui, F. Leng, and W. D. Wilson. 2008. Inhibition of high-mobility-group A2 protein binding to DNA by netropsin: a biosensor-surface plasmon resonance assay. Anal Biochem 374: 7-15.

Mikkelsen, T., P. S. Yan, K. L. Ho, M. Sameni, B. F. Sloane, and M. L. Rosenblum. 1995. Immunolocalization of cathepsin B in human glioma: implications for tumor invasion and angiogenesis. J Neurosurg 83: 285-290.

Min, X., B. Lemon, J. Tang, Q. Liu, R. Zhang, N. Walker, Y. Li, and Z. Wang. 2012. Crystal structure of a single-chain trimer of human adiponectin globular domain. FEBS Lett 586: 912-917.

Miyata, H., T. Ashizawa, A. Iizuka, R. Kondou, C. Nonomura, T. Sugino, K. Urakami, A. Asai, N. Hayashi, K. Mitsuya, Y. Nakasu, K. Yamaguchi, and Y. Akiyama. 2017. Combination of a STAT3 Inhibitor and an mTOR Inhibitor Against a Temozolomide-resistant Glioblastoma Cell Line. Cancer genomics & proteomics 14: 83-91.

Montaldi, A. P., and E. T. Sakamoto-Hojo. 2013. Methoxyamine sensitizes the resistant glioblastoma T98G cell line to the alkylating agent temozolomide. Clin Exp Med 13: 279-288.

Mookerjee, I., T. D. Hewitson, M. L. Halls, R. J. Summers, M. L. Mathai, R. A. Bathgate, G. W. Tregear, and C. S. Samuel. 2009. Relaxin inhibits renal myofibroblast differentiation via RXFP1, the nitric oxide pathway, and Smad2. FASEB journal : official publication of the Federation of American Societies for Experimental Biology 23: 1219-1229.

Moore, X. L., S. L. Tan, C. Y. Lo, L. Fang, Y. D. Su, X. M. Gao, E. A. Woodcock, R. J. Summers, G. W. Tregear, R. A. Bathgate, and X. J. Du. 2007. Relaxin antagonizes hypertrophy and apoptosis in neonatal rat cardiomyocytes. Endocrinology 148: 1582-1589.

Moreb, J. S., H. V. Baker, L. J. Chang, M. Amaya, M. C. Lopez, B. Ostmark, and W. Chou. 2008. ALDH isozymes downregulation affects cell growth, cell motility and gene expression in lung cancer cells. Mol Cancer 7: 87.

Morishita, A., M. R. Zaidi, A. Mitoro, D. Sankarasharma, M. Szabolcs, Y. Okada, J. D'Armiento, and K. Chada. 2013. HMGA2 is a driver of tumor metastasis. Cancer Res 73: 4289-4299.

Motzer, R. J., C. Porta, N. J. Vogelzang, C. N. Sternberg, C. Szczylik, J. Zolnierek, C. Kollmannsberger, S. Y. Rha, G. A. Bjarnason, B. Melichar, U. De Giorgi, V. Grunwald, I. D. Davis, J. L. Lee, E. Esteban, G. Urbanowitz, C. Cai, M. Squires, M. Marker, M. M. Shi, and B. Escudier. 2014. Dovitinib versus sorafenib for third-line targeted treatment of patients with metastatic renal cell carcinoma: an open-label, randomised phase 3 trial. The Lancet. Oncology 15: 286-296.

Muda, M., C. He, P. G. Martini, T. Ferraro, S. Layfield, D. Taylor, C. Chevrier, R. Schweickhardt, C. Kelton, P. L. Ryan, and R. A. Bathgate. 2005. Splice variants of the relaxin and INSL3 receptors reveal unanticipated molecular complexity. Molecular human reproduction 11: 591-600.

Nakada, M., H. Nakamura, E. Ikeda, N. Fujimoto, J. Yamashita, H. Sato, M. Seiki, and Y. Okada. 1999. Expression and tissue localization of membrane-type 1, 2, and 3 matrix metalloproteinases in human astrocytic tumors. The American journal of pathology 154: 417-428.

Naskar, S., K. Datta, A. Mitra, K. Pathak, R. Datta, T. Bansal, and S. Sarkar. 2014. Differential and conditional activation of PKC-isoforms dictates cardiac adaptation during physiological to pathological hypertrophy. PloS one 9: e104711.

Natarajan, S., S. Hombach-Klonisch, P. Droge, and T. Klonisch. 2013. HMGA2 inhibits apoptosis through interaction with ATR-CHK1 signaling complex in human cancer cells. Neoplasia 15: 263-280.

Neschadim, A., L. B. Pritzker, K. P. Pritzker, D. R. Branch, A. J. Summerlee, J. Trachtenberg, and J. D. Silvertown. 2014. Relaxin receptor antagonist AT-001 synergizes with docetaxel in androgen-independent prostate xenografts. Endocrine-related cancer 21: 459-471.

Nguyen, B. T., and C. W. Dessauer. 2005. Relaxin stimulates protein kinase C zeta translocation: requirement for cyclic adenosine 3',5'-monophosphate production. Mol Endocrinol 19: 1012-1023.

Nguyen, L. H., and H. Zhu. 2015. Lin28 and let-7 in cell metabolism and cancer. Transl Pediatr 4: 4-11.

Nguyen, S. A., O. D. Stechishin, H. A. Luchman, X. Q. Lun, D. L. Senger, S. M. Robbins, J. G. Cairncross, and S. Weiss. 2014. Novel MSH6 mutations in treatment-naive glioblastoma and anaplastic oligodendroglioma contribute to temozolomide resistance independently of MGMT promoter methylation. Clinical cancer research : an official journal of the American Association for Cancer Research 20: 4894-4903.

Nishino, J., I. Kim, K. Chada, and S. J. Morrison. 2008. Hmga2 promotes neural stem cell self-renewal in young but not old mice by reducing p16Ink4a and p19Arf Expression. Cell 135: 227-239.

Nistri, S., and D. Bani. 2003. Relaxin receptors and nitric oxide synthases: search for the missing link. Reprod Biol Endocrinol 1: 5.

Nistri, S., L. Cinci, A. M. Perna, E. Masini, R. Mastroianni, and D. Bani. 2008. Relaxin induces mast cell inhibition and reduces ventricular arrhythmias in a swine model of acute myocardial infarction. Pharmacol Res 57: 43-48.

Noushmehr, H., D. J. Weisenberger, K. Diefes, H. S. Phillips, K. Pujara, B. P. Berman, F. Pan, C. E. Pelloski, E. P. Sulman, K. P. Bhat, R. G. Verhaak, K. A. Hoadley, D. N. Hayes, C. M. Perou, H. K. Schmidt, L. Ding, R. K. Wilson, D. Van Den Berg, H. Shen, H. Bengtsson, P. Neuvial, L. M. Cope, J. Buckley, J. G. Herman, S. B. Baylin, P. W. Laird, K. Aldape, and N. Cancer Genome Atlas Research. 2010. Identification of a CpG island methylator phenotype that defines a distinct subgroup of glioma. Cancer Cell 17: 510-522.

Novak, U., and A. H. Kaye. 2000. Extracellular matrix and the brain: components and function. Journal of clinical neuroscience : official journal of the Neurosurgical Society of Australasia 7: 280-290.

Ohgaki, H., and P. Kleihues. 2005. Population-based studies on incidence, survival rates, and genetic alterations in astrocytic and oligodendroglial gliomas. J Neuropathol Exp Neurol 64: 479-489.

Ohgaki, H., and P. Kleihues. 2007. Genetic pathways to primary and secondary glioblastoma. The American journal of pathology 170: 1445-1453.

Ohgaki, H., and P. Kleihues. 2009. Genetic alterations and signaling pathways in the evolution of gliomas. Cancer Sci 100: 2235-2241.

Ohgaki, H., and P. Kleihues. 2013. The definition of primary and secondary glioblastoma. Clinical cancer research : an official journal of the American Association for Cancer Research 19: 764-772.

Ostrom, Q. T., H. Gittleman, J. Fulop, M. Liu, R. Blanda, C. Kromer, Y. Wolinsky, C. Kruchko, and J. S. Barnholtz-Sloan. 2015. CBTRUS Statistical Report: Primary Brain and Central Nervous System Tumors Diagnosed in the United States in 2008-2012. Neuro Oncol 17 Suppl 4: iv1-iv62.

Ouedraogo, Z. G., J. Biau, J. L. Kemeny, L. Morel, P. Verrelle, and E. Chautard. 2016. Role of STAT3 in Genesis and Progression of Human Malignant Gliomas. Molecular neurobiology.

Ozturk, N., I. Singh, A. Mehta, T. Braun, and G. Barreto. 2014. HMGA proteins as modulators of chromatin structure during transcriptional activation. Front Cell Dev Biol 2: 5.

Pagenstecher, A., E. M. Wussler, G. Opdenakker, B. Volk, and I. L. Campbell. 2001. Distinct expression patterns and levels of enzymatic activity of matrix metalloproteinases and their inhibitors in primary brain tumors. J Neuropathol Exp Neurol 60: 598-612.

Palmieri, D., T. Valentino, D. D'Angelo, I. De Martino, I. Postiglione, R. Pacelli, C. M. Croce, M. Fedele, and A. Fusco. 2011. HMGA proteins promote ATM expression and enhance cancer cell resistance to genotoxic agents. Oncogene 30: 3024-3035.

Park, J. I., J. Semyonov, W. Yi, C. L. Chang, and S. Y. Hsu. 2008. Regulation of receptor signaling by relaxin A chain motifs: derivation of pan-specific and LGR7-specific human relaxin analogs. The Journal of biological chemistry 283: 32099-32109.

Parsons, D. W., S. Jones, X. Zhang, J. C. Lin, R. J. Leary, P. Angenendt, P. Mankoo, H. Carter, I. M. Siu, G. L. Gallia, A. Olivi, R. McLendon, B. A. Rasheed, S. Keir, T. Nikolskaya, Y. Nikolsky, D. A. Busam, H. Tekleab, L. A. Diaz, Jr., J. Hartigan, D. R. Smith, R. L. Strausberg, S. K. Marie, S. M. Shinjo, H. Yan, G. J. Riggins, D. D. Bigner, R. Karchin, N. Papadopoulos, G. Parmigiani, B. Vogelstein, V. E. Velculescu, and K. W. Kinzler. 2008. An integrated genomic analysis of human glioblastoma multiforme. Science 321: 1807-1812.

Paw, I., R. C. Carpenter, K. Watabe, W. Debinski, and H. W. Lo. 2015. Mechanisms regulating glioma invasion. Cancer letters 362: 1-7.

Peter, S., H. Yu, R. Ivanyi-Nagy, and P. Droge. 2016. Cell-based high-throughput compound screening reveals functional interaction between oncofetal HMGA2 and topoisomerase I. Nucleic Acids Res.

Peterson, J. M., Z. Wei, and G. W. Wong. 2009. CTRP8 and CTRP9B are novel proteins that hetero-oligomerize with C1q/TNF family members. Biochem Biophys Res Commun 388: 360-365.

Pfannkuche, K., H. Summer, O. Li, J. Hescheler, and P. Droge. 2009. The high mobility group protein HMGA2: a co-regulator of chromatin structure and pluripotency in stem cells? Stem Cell Rev 5: 224-230.

Phillips, H. S., S. Kharbanda, R. Chen, W. F. Forrest, R. H. Soriano, T. D. Wu, A. Misra, J. M. Nigro, H. Colman, L. Soroceanu, P. M. Williams, Z. Modrusan, B. G. Feuerstein, and K. Aldape. 2006. Molecular subclasses of high-grade glioma predict prognosis, delineate a pattern of disease progression, and resemble stages in neurogenesis. Cancer Cell 9: 157-173.

Pini, A., R. Shemesh, C. S. Samuel, R. A. Bathgate, A. Zauberman, C. Hermesh, A. Wool, D. Bani, and G. Rotman. 2010. Prevention of bleomycin-induced pulmonary fibrosis by a novel antifibrotic peptide with relaxin-like activity. The Journal of pharmacology and experimental therapeutics 335: 589-599.

Placone, A. L., P. M. McGuiggan, D. E. Bergles, H. Guerrero-Cazares, A. Quinones-Hinojosa, and P. C. Searson. 2015. Human astrocytes develop physiological morphology and remain quiescent in a novel 3D matrix. Biomaterials 42: 134-143.

Ponikowski, P., M. Metra, J. R. Teerlink, E. Unemori, G. M. Felker, A. A. Voors, G. Filippatos, B. Greenberg, S. L. Teichman, T. Severin, G. Mueller-Velten, G. Cotter, and B. A. Davison. 2012. Design of the RELAXin in acute heart failure study. American heart journal 163: 149-155 e141.

Portnow, J., B. Badie, M. Chen, A. Liu, S. Blanchard, and T. W. Synold. 2009. The neuropharmacokinetics of temozolomide in patients with resectable brain tumors: potential implications for the current approach to chemoradiation. Clin Cancer Res 15: 7092-7098.

Qin, R., J. Zhou, C. Chen, T. Xu, Y. Yan, Y. Ma, Z. Zheng, Y. Shen, Y. Lu, D. Fu, and J. Chen. 2014. LIN28 is involved in glioma carcinogenesis and predicts outcomes of glioblastoma multiforme patients. PLoS One 9: e86446.

Quattrone, S., L. Chiappini, G. Scapagnini, B. Bigazzi, and D. Bani. 2004. Relaxin potentiates the expression of inducible nitric oxide synthase by endothelial cells from human umbilical vein in in vitro culture. Molecular human reproduction 10: 325-330.

Quiros, S., W. P. Roos, and B. Kaina. 2010. Processing of O6-methylguanine into DNA double-strand breaks requires two rounds of replication whereas apoptosis is also induced in subsequent cell cycles. Cell cycle 9: 168-178.

Radestock, Y., C. Hoang-Vu, and S. Hombach-Klonisch. 2008. Relaxin reduces xenograft tumour growth of human MDA-MB-231 breast cancer cells. Breast cancer research : BCR 10: R71.

Radestock, Y., C. Willing, A. Kehlen, C. Hoang-Vu, and S. Hombach-Klonisch. 2010. Relaxin enhances S100A4 and promotes growth of human thyroid carcinoma cell xenografts. Molecular cancer research : MCR 8: 494-506.

Rao, J. S. 2003. Molecular mechanisms of glioma invasiveness: the role of proteases. Nature reviews. Cancer 3: 489-501.

Rashedi, I., S. Panigrahi, P. Ezzati, S. Ghavami, and M. Los. 2007. Autoimmunity and apoptosis--therapeutic implications. Current medicinal chemistry 14: 3139-3151.

Rempel, S. A., M. L. Rosenblum, T. Mikkelsen, P. S. Yan, K. D. Ellis, W. A. Golembieski, M. Sameni, J. Rozhin, G. Ziegler, and B. F. Sloane. 1994. Cathepsin B expression and localization in glioma progression and invasion. Cancer Res 54: 6027-6031.

Resar, L. M. 2010. The high mobility group A1 gene: transforming inflammatory signals into cancer? Cancer Res 70: 436-439.

Ressl, S., B. K. Vu, S. Vivona, D. C. Martinelli, T. C. Sudhof, and A. T. Brunger. 2015. Structures of C1q-like proteins reveal unique features among the C1q/TNF superfamily. Structure 23: 688-699.

Ricard, D., A. Idbaih, F. Ducray, M. Lahutte, K. Hoang-Xuan, and J. Y. Delattre. 2012. Primary brain tumours in adults. Lancet 379: 1984-1996.

Riccardi, C., and I. Nicoletti. 2006. Analysis of apoptosis by propidium iodide staining and flow cytometry. Nature protocols 1: 1458-1461.

Rinne, M., D. Caldwell, and M. R. Kelley. 2004. Transient adenoviral N-methylpurine DNA glycosylase overexpression imparts chemotherapeutic sensitivity to human breast cancer cells. Mol Cancer Ther 3: 955-967.

Roos, M., U. Pradere, R. P. Ngondo, A. Behera, S. Allegrini, G. Civenni, J. A. Zagalak, J. R. Marchand, M. Menzi, H. Towbin, J. Scheuermann, D. Neri, A. Caflisch, C. V. Catapano, C. Ciaudo, and J. Hall. 2016. A Small-Molecule Inhibitor of Lin28. ACS Chem Biol 11: 2773-2781.

Roos, W. P., L. F. Batista, S. C. Naumann, W. Wick, M. Weller, C. F. Menck, and B. Kaina. 2007. Apoptosis in malignant glioma cells triggered by the temozolomide-induced DNA lesion O6-methylguanine. Oncogene 26: 186-197.

Rosse, C., M. Linch, S. Kermorgant, A. J. Cameron, K. Boeckeler, and P. J. Parker. 2010. PKC and the control of localized signal dynamics. Nature reviews. Molecular cell biology 11: 103-112.

Rowe, R. G., L. D. Wang, S. Coma, A. Han, R. Mathieu, D. S. Pearson, S. Ross, P. Sousa, P. T. Nguyen, A. Rodriguez, A. J. Wagers, and G. Q. Daley. 2016. Developmental regulation of myeloerythroid progenitor function by the Lin28b-let-7-Hmga2 axis. J Exp Med 213: 1497-1512.

Sacchi, T. B., D. Bani, M. L. Brandi, A. Falchetti, and M. Bigazzi. 1994. Relaxin influences growth, differentiation and cell-cell adhesion of human breast-cancer cells in culture. International journal of cancer 57: 129-134.

Samuel, C. S., E. D. Lekgabe, and I. Mookerjee. 2007. The effects of relaxin on extracellular matrix remodeling in health and fibrotic disease. Adv Exp Med Biol 612: 88-103.

Samuel, C. S., S. G. Royce, T. D. Hewitson, K. M. Denton, T. E. Cooney, and R. G. Bennett. 2016. Anti-fibrotic actions of relaxin. British journal of pharmacology.

Samuel, C. S., S. G. Royce, B. Chen, H. Cao, J. A. Gossen, G. W. Tregear, and M. L. Tang. 2009. Relaxin family peptide receptor-1 protects against airway fibrosis during homeostasis but not against fibrosis associated with chronic allergic airways disease. Endocrinology 150: 1495-1502.

Samuel, C. S., S. Cendrawan, X. M. Gao, Z. Ming, C. Zhao, H. Kiriazis, Q. Xu, G. W. Tregear, R. A. Bathgate, and X. J. Du. 2011. Relaxin remodels fibrotic healing following myocardial infarction. Lab Invest 91: 675-690.

Sarkaria, J. N., G. J. Kitange, C. D. James, R. Plummer, H. Calvert, M. Weller, and W. Wick. 2008. Mechanisms of chemoresistance to alkylating agents in malignant glioma. Clinical cancer research : an official journal of the American Association for Cancer Research 14: 2900-2908.

Sarwar, M., X. J. Du, T. B. Dschietzig, and R. J. Summers. 2016. The actions of relaxin on the human cardiovascular system. British journal of pharmacology.

Sarwar, M., C. S. Samuel, R. A. Bathgate, D. R. Stewart, and R. J. Summers. 2015. Serelaxin-mediated signal transduction in human vascular cells: bell-shaped concentration-response curves reflect differential coupling to G proteins. British journal of pharmacology 172: 1005-1019.

Schafer, N., G. H. Gielen, S. Kebir, A. Wieland, A. Till, F. Mack, C. Schaub, T. Tzaridis, R. Reinartz, M. Niessen, R. Fimmers, M. Simon, C. Coch, C. Fuhrmann, U. Herrlinger, B. Scheffler, and M. Glas. 2016. Phase I trial of dovitinib (TKI258) in recurrent glioblastoma. J Cancer Res Clin Oncol.

Schaffler, A., and C. Buechler. 2012. CTRP family: linking immunity to metabolism. Trends Endocrinol Metab 23: 194-204.

Schouten, L. J., J. Rutten, H. A. Huveneers, and A. Twijnstra. 2002. Incidence of brain metastases in a cohort of patients with carcinoma of the breast, colon, kidney, and lung and melanoma. Cancer 94: 2698-2705.

Schwarm, F. P., F. Uhle, A. Schanzer, T. Acker, M. Stein, M. H. Reinges, C. Weischer, M. A. Weigand, E. Uhl, and M. A. Kolodziej. 2016. High-mobility group AT-hook protein 2 expression and its prognostic significance in MGMT methylated and unmethylated glioblastoma. International journal of oncology 48: 1485-1492.

Scott, D. J., G. W. Tregear, and R. A. Bathgate. 2005. LGR7-truncate is a splice variant of the relaxin receptor LGR7 and is a relaxin antagonist in vitro. Annals of the New York Academy of Sciences 1041: 22-26.

Scott, D. J., S. Layfield, Y. Yan, S. Sudo, A. J. Hsueh, G. W. Tregear, and R. A. Bathgate. 2006. Characterization of novel splice variants of LGR7 and LGR8 reveals that receptor signaling is mediated by their unique low density lipoprotein class A modules. The Journal of biological chemistry 281: 34942-34954.

Seldin, M. M., S. Y. Tan, and G. W. Wong. 2014. Metabolic function of the CTRP family of hormones. Rev Endocr Metab Disord 15: 111-123.

Seldin, M. M., J. M. Peterson, M. S. Byerly, Z. Wei, and G. W. Wong. 2012. Myonectin (CTRP15), a novel myokine that links skeletal muscle to systemic lipid homeostasis. The Journal of biological chemistry 287: 11968-11980.

Sethi, A., S. Bruell, N. Patil, M. A. Hossain, D. J. Scott, E. J. Petrie, R. A. Bathgate, and P. R. Gooley. 2016. The complex binding mode of the peptide hormone H2 relaxin to its receptor RXFP1. Nat Commun 7: 11344.

Shapiro, L., and P. E. Scherer. 1998. The crystal structure of a complement-1q family protein suggests an evolutionary link to tumor necrosis factor. Curr Biol 8: 335-338.

Sharma, A., K. Singh, and A. Almasan. 2012. Histone H2AX phosphorylation: a marker for DNA damage. Methods in molecular biology 920: 613-626.

Shemesh, R., C. Hermesh, A. Toporik, Z. Levine, A. Novik, A. Wool, Y. Kliger, A. Rosenberg, R. A. Bathgate, and Y. Cohen. 2009. Activation of relaxin-related receptors by short, linear peptides derived from a collagen-containing precursor. Ann N Y Acad Sci 1160: 78-86.

Shemesh, R., A. Toporik, Z. Levine, I. Hecht, G. Rotman, A. Wool, D. Dahary, E. Gofer, Y. Kliger, M. A. Soffer, A. Rosenberg, D. Eshel, and Y. Cohen. 2008. Discovery and validation of novel peptide agonists for G-protein-coupled receptors. J Biol Chem 283: 34643-34649.

Sherwood, O. D. 2004. Relaxin's physiological roles and other diverse actions. Endocr Rev 25: 205-234.

Sherwood, O. D., V. E. Crnekovic, W. L. Gordon, and J. E. Rutherford. 1980. Radioimmunoassay of relaxin throughout pregnancy and during parturition in the rat. Endocrinology 107: 691-698.

Shi, L., J. Chen, J. Yang, T. Pan, S. Zhang, and Z. Wang. 2010. MiR-21 protected human glioblastoma U87MG cells from chemotherapeutic drug temozolomide induced apoptosis by decreasing Bax/Bcl-2 ratio and caspase-3 activity. Brain Res 1352: 255-264.

Shi, Z., X. Li, D. Wu, R. Tang, R. Chen, S. Xue, and X. Sun. 2016a. Silencing of HMGA2 suppresses cellular proliferation, migration, invasion, and epithelial-mesenchymal transition in bladder cancer. Tumour Biol 37: 7515-7523.

Shi, Z., D. Wu, R. Tang, X. Li, R. Chen, S. Xue, C. Zhang, and X. Sun. 2016b. Silencing of HMGA2 promotes apoptosis and inhibits migration and invasion of prostate cancer cells. J Biosci 41: 229-236.

Shirota, K., K. Tateishi, T. Koji, Y. Hishikawa, T. Hachisuga, M. Kuroki, and T. Kawarabayashi. 2005. Early human preantral follicles have relaxin and relaxin receptor (LGR7), and relaxin promotes their development. J Clin Endocrinol Metab 90: 516-521.

Shyh-Chang, N., and G. Q. Daley. 2013. Lin28: primal regulator of growth and metabolism in stem cells. Cell Stem Cell 12: 395-406.

Silber, J. R., M. S. Bobola, A. Blank, and M. C. Chamberlain. 2012. O(6)-methylguanine-DNA methyltransferase in glioma therapy: promise and problems. Biochimica et biophysica acta 1826: 71-82.

Silber, J. R., M. S. Bobola, A. Blank, K. D. Schoeler, P. D. Haroldson, M. B. Huynh, and D. D. Kolstoe. 2002. The apurinic/apyrimidinic endonuclease activity of Ape1/Ref-1 contributes to human glioma cell resistance to alkylating agents and is elevated by oxidative stress. Clinical cancer research : an official journal of the American Association for Cancer Research 8: 3008-3018.

Silvertown, J. D., A. J. Summerlee, and T. Klonisch. 2003. Relaxin-like peptides in cancer. International journal of cancer 107: 513-519.

Silvertown, J. D., J. C. Symes, A. Neschadim, T. Nonaka, J. C. Kao, A. J. Summerlee, and J. A. Medin. 2007. Analog of H2 relaxin exhibits antagonistic properties and impairs prostate tumor growth. FASEB journal : official publication of the Federation of American Societies for Experimental Biology 21: 754-765.

Soh, Y. M., A. Tiwari, M. Mahendroo, K. P. Conrad, and L. J. Parry. 2012. Relaxin regulates hyaluronan synthesis and aquaporins in the cervix of late pregnant mice. Endocrinology 153: 6054-6064.

Sohn, T. J., N. K. Kim, H. J. An, J. J. Ko, T. R. Hahn, D. Oh, S. G. Lee, R. Roy, K. Y. Cha, and Y. K. Oh. 2001. Gene amplification and expression of the DNA repair enzyme, N-methylpurine-DNA glycosylase (MPG) in HPV-infected cervical neoplasias. Anticancer research 21: 2405-2411.

Spiegl-Kreinecker, S., C. Pirker, M. Filipits, D. Lotsch, J. Buchroithner, J. Pichler, R. Silye, S. Weis, M. Micksche, J. Fischer, and W. Berger. 2010. O6-Methylguanine DNA methyltransferase protein expression in tumor cells predicts outcome of temozolomide therapy in glioblastoma patients. Neuro Oncol 12: 28-36.

Steed, T. C., J. M. Treiber, K. Patel, V. Ramakrishnan, A. Merk, A. R. Smith, B. S. Carter, A. M. Dale, L. M. Chow, and C. C. Chen. 2016. Differential localization of glioblastoma subtype: implications on glioblastoma pathogenesis. Oncotarget 7: 24899-24907.

Steinberg, S. F. 2008. Structural basis of protein kinase C isoform function. Physiological reviews 88: 1341-1378.

Stewart, D. R., A. C. Celniker, C. A. Taylor, Jr., J. R. Cragun, J. W. Overstreet, and B. L. Lasley. 1990. Relaxin in the peri-implantation period. J Clin Endocrinol Metab 70: 1771-1773.

Strojnik, T., T. Smigoc, and T. T. Lah. 2014. Prognostic value of erythrocyte sedimentation rate and C-reactive protein in the blood of patients with glioma. Anticancer research 34: 339-347.

Stupp, R., M. E. Hegi, W. P. Mason, M. J. van den Bent, M. J. Taphoorn, R. C. Janzer, S. K. Ludwin, A. Allgeier, B. Fisher, K. Belanger, P. Hau, A. A. Brandes, J. Gijtenbeek, C. Marosi, C. J. Vecht, K. Mokhtari, P. Wesseling, S. Villa, E. Eisenhauer, T. Gorlia, M. Weller, D. Lacombe, J. G. Cairncross, R. O. Mirimanoff, R. European Organisation for, T. Treatment of Cancer Brain, G. Radiation Oncology, and G. National Cancer Institute of Canada Clinical Trials. 2009. Effects of radiotherapy with concomitant and adjuvant temozolomide versus radiotherapy alone on survival in glioblastoma in a randomised phase III study: 5-year analysis of the EORTC-NCIC trial. Lancet Oncol 10: 459-466.

Summer, H., O. Li, Q. Bao, L. Zhan, S. Peter, P. Sathiyanathan, D. Henderson, T. Klonisch, S. D. Goodman, and P. Droge. 2009. HMGA2 exhibits dRP/AP site cleavage activity and protects cancer cells from DNA-damage-induced cytotoxicity during chemotherapy. Nucleic Acids Res 37: 4371-4384.

Summers, R. J. 2012. Themed section: molecular pharmacology of GPCRs. British journal of pharmacology 165: 1609-1612.

Sunn, N., M. J. McKinley, and B. J. Oldfield. 2001. Identification of efferent neural pathways from the lamina terminalis activated by blood-borne relaxin. J Neuroendocrinol 13: 432-437.

Sunn, N., M. Egli, T. C. Burazin, P. Burns, L. Colvill, P. Davern, D. A. Denton, B. J. Oldfield, R. S. Weisinger, M. Rauch, H. A. Schmid, and M. J. McKinley. 2002. Circulating relaxin acts on subfornical organ neurons to stimulate water drinking in the rat. Proc Natl Acad Sci U S A 99: 1701-1706.

Svendsen, A. M., A. Zalesko, J. Konig, M. Vrecl, A. Heding, J. B. Kristensen, J. D. Wade, R. A. Bathgate, P. De Meyts, and J. Nohr. 2008. Negative cooperativity in H2 relaxin binding to a dimeric relaxin family peptide receptor 1. Mol Cell Endocrinol 296: 10-17.

Svilar, D., C. Vens, and R. W. Sobol. 2012. Quantitative, real-time analysis of base excision repair activity in cell lysates utilizing lesion-specific molecular beacons. J Vis Exp: e4168.

Tai, W. T., A. L. Cheng, C. W. Shiau, C. Y. Liu, C. H. Ko, M. W. Lin, P. J. Chen, and K. F. Chen. 2012. Dovitinib induces apoptosis and overcomes sorafenib resistance in hepatocellular carcinoma through SHP-1-mediated inhibition of STAT3. Mol Cancer Ther 11: 452-463.

Tait, S. W., and D. R. Green. 2010. Mitochondria and cell death: outer membrane permeabilization and beyond. Nature reviews. Molecular cell biology 11: 621-632.

Takematsu, E., K. Cho, J. Hieda, M. Nakai, K. Katsumata, K. Okada, M. Niinomi, and N. Matsushita. 2016. Adhesive strength of bioactive oxide layers fabricated on TNTZ alloy by three different alkali-solution treatments. J Mech Behav Biomed Mater 61: 174-181.

Takeuchi, T., Y. Adachi, and T. Nagayama. 2011. Expression of a secretory protein C1qTNF6, a C1qTNF family member, in hepatocellular carcinoma. Anal Cell Pathol (Amst) 34: 113-121.

Tan, E. J., S. Thuault, L. Caja, T. Carletti, C. H. Heldin, and A. Moustakas. 2012. Regulation of transcription factor Twist expression by the DNA architectural protein high mobility group A2 during epithelial-to-mesenchymal transition. The Journal of biological chemistry 287: 7134-7145.

Tan, J., J. R. Tedrow, J. A. Dutta, B. Juan-Guardela, M. Nouraie, Y. Chu, H. Trejo Bittar, K. Ramani, P. S. Biswas, K. L. Veraldi, N. Kaminski, Y. Zhang, and D. J. Kass. 2016. Expression of RXFP1 is Decreased in Idiopathic Pulmonary Fibrosis: Implications for Relaxin-Based Therapies. Am J Respir Crit Care Med.

Tanaka, M., Y. Watanabe, and K. Yoshimoto. 2009. Regulation of relaxin 3 gene expression via cAMP-PKA in a neuroblastoma cell line. J Neurosci Res 87: 820-829.

Tang, J. B., D. Svilar, R. N. Trivedi, X. H. Wang, E. M. Goellner, B. Moore, R. L. Hamilton, L. A. Banze, A. R. Brown, and R. W. Sobol. 2011. N-methylpurine DNA glycosylase and DNA polymerase beta modulate BER inhibitor potentiation of glioma cells to temozolomide. Neuro Oncol 13: 471-486.

Tang, M. L., C. S. Samuel, and S. G. Royce. 2009. Role of relaxin in regulation of fibrosis in the lung. Annals of the New York Academy of Sciences 1160: 342-347.

Tashima, L. S., G. Mazoujian, and G. D. Bryant-Greenwood. 1994. Human relaxins in normal, benign and neoplastic breast tissue. J Mol Endocrinol 12: 351-364.

Teichman, S. L., E. Unemori, T. Dschietzig, K. Conrad, A. A. Voors, J. R. Teerlink, G. M. Felker, M. Metra, and G. Cotter. 2009. Relaxin, a pleiotropic vasodilator for the treatment of heart failure. Heart Fail Rev 14: 321-329.

Thanasupawat, T., A. Glogowska, M. Burg, G. W. Wong, C. Hoang-Vu, S. Hombach-Klonisch, and T. Klonisch. 2015. RXFP1 is Targeted by Complement C1q Tumor Necrosis Factor-Related Factor 8 in Brain Cancer. Frontiers in endocrinology 6: 127.

Thuault, S., U. Valcourt, M. Petersen, G. Manfioletti, C. H. Heldin, and A. Moustakas. 2006. Transforming growth factor-beta employs HMGA2 to elicit epithelial-mesenchymal transition. J Cell Biol 174: 175-183.

Thuault, S., E. J. Tan, H. Peinado, A. Cano, C. H. Heldin, and A. Moustakas. 2008. HMGA2 and Smads co-regulate SNAIL1 expression during induction of epithelial-to-mesenchymal transition. The Journal of biological chemistry 283: 33437-33446.

Trivedi, R. N., X. H. Wang, E. Jelezcova, E. M. Goellner, J. B. Tang, and R. W. Sobol. 2008. Human methyl purine DNA glycosylase and DNA polymerase beta expression collectively predict sensitivity to temozolomide. Molecular pharmacology 74: 505-516.

Tu, X., and K. Palczewski. 2012. Crystal structure of the globular domain of C1QTNF5: Implications for late-onset retinal macular degeneration. J Struct Biol 180: 439-446.

Tu, X., and K. Palczewski. 2014. The macular degeneration-linked C1QTNF5 (S163) mutation causes higher-order structural rearrangements. J Struct Biol 186: 86-94.

Ucar, D., C. R. Cogle, J. R. Zucali, B. Ostmark, E. W. Scott, R. Zori, B. A. Gray, and J. S. Moreb. 2009. Aldehyde dehydrogenase activity as a functional marker for lung cancer. Chem Biol Interact 178: 48-55.

Ujifuku, K., N. Mitsutake, S. Takakura, M. Matsuse, V. Saenko, K. Suzuki, K. Hayashi, T. Matsuo, K. Kamada, I. Nagata, and S. Yamashita. 2010. miR-195, miR-455-3p and miR-10a(*) are implicated in acquired temozolomide resistance in glioblastoma multiforme cells. Cancer letters 296: 241-248.

Unemori, E. N., and E. P. Amento. 1990. Relaxin modulates synthesis and secretion of procollagenase and collagen by human dermal fibroblasts. The Journal of biological chemistry 265: 10681-10685.

Unemori, E. N., L. B. Pickford, A. L. Salles, C. E. Piercy, B. H. Grove, M. E. Erikson, and E. P. Amento. 1996. Relaxin induces an extracellular matrix-degrading

phenotype in human lung fibroblasts in vitro and inhibits lung fibrosis in a murine model in vivo. The Journal of clinical investigation 98: 2739-2745.

Unemori, E. N., M. E. Erikson, S. E. Rocco, K. M. Sutherland, D. A. Parsell, J. Mak, and B. H. Grove. 1999. Relaxin stimulates expression of vascular endothelial growth factor in normal human endometrial cells in vitro and is associated with menometrorrhagia in women. Hum Reprod 14: 800-806.

Uno, M., S. M. Oba-Shinjo, A. A. Camargo, R. P. Moura, P. H. Aguiar, H. N. Cabrera, M. Begnami, S. Rosemberg, M. J. Teixeira, and S. K. Marie. 2011. Correlation of MGMT promoter methylation status with gene and protein expression levels in glioblastoma. Clinics (Sao Paulo) 66: 1747-1755.

Urtreger, A. J., M. G. Kazanietz, and E. D. Bal de Kier Joffe. 2012. Contribution of individual PKC isoforms to breast cancer progression. IUBMB life 64: 18-26.

VanMeter, T. E., H. K. Rooprai, M. M. Kibble, H. L. Fillmore, W. C. Broaddus, and G. J. Pilkington. 2001. The role of matrix metalloproteinase genes in glioma invasion: co-dependent and interactive proteolysis. J Neurooncol 53: 213-235.

Verbeek, B., T. D. Southgate, D. E. Gilham, and G. P. Margison. 2008. O6-Methylguanine-DNA methyltransferase inactivation and chemotherapy. Br Med Bull 85: 17-33.

Verhaak, R. G., K. A. Hoadley, E. Purdom, V. Wang, Y. Qi, M. D. Wilkerson, C. R. Miller, L. Ding, T. Golub, J. P. Mesirov, G. Alexe, M. Lawrence, M. O'Kelly, P. Tamayo, B. A. Weir, S. Gabriel, W. Winckler, S. Gupta, L. Jakkula, H. S. Feiler, J. G. Hodgson, C. D. James, J. N. Sarkaria, C. Brennan, A. Kahn, P. T. Spellman, R. K. Wilson, T. P. Speed, J. W. Gray, M. Meyerson, G. Getz, C. M. Perou, D. N. Hayes, and N. Cancer Genome Atlas Research. 2010. Integrated genomic analysis identifies clinically relevant subtypes of glioblastoma characterized by abnormalities in PDGFRA, IDH1, EGFR, and NF1. Cancer Cell 17: 98-110.

Vinall, R. L., C. M. Mahaffey, R. R. Davis, Z. Luo, R. Gandour-Edwards, P. M. Ghosh, C. G. Tepper, and R. W. de Vere White. 2011. Dual blockade of PKA and NF-kappaB inhibits H2 relaxin-mediated castrate-resistant growth of prostate cancer sublines and induces apoptosis. Horm Cancer 2: 224-238.

Viswanathan, S. R., J. T. Powers, W. Einhorn, Y. Hoshida, T. L. Ng, S. Toffanin, M. O'Sullivan, J. Lu, L. A. Phillips, V. L. Lockhart, S. P. Shah, P. S. Tanwar, C. H. Mermel, R. Beroukhim, M. Azam, J. Teixeira, M. Meyerson, T. P. Hughes, J. M. Llovet, J. Radich, C. G. Mullighan, T. R. Golub, P. H. Sorensen, and G. Q. Daley. 2009. Lin28 promotes transformation and is associated with advanced human malignancies. Nat Genet 41: 843-848.

Wallace, S. S. 2014. Base excision repair: a critical player in many games. DNA Repair (Amst) 19: 14-26.

Wallerstedt, E., U. Smith, and C. X. Andersson. 2010. Protein kinase C-delta is involved in the inflammatory effect of IL-6 in mouse adipose cells. Diabetologia 53: 946-954.

Wang, C., C. Gao, J. L. Zhuang, C. Ding, and Y. Wang. 2012. A combined approach identifies three mRNAs that are down-regulated by microRNA-29b and promote invasion ability in the breast cancer cell line MCF-7. J Cancer Res Clin Oncol 138: 2127-2136.

Wang, D., Z. Y. Zhong, Q. H. Zhang, Z. P. Li, and M. R. Kelley. 2006. [Effect of adenoviral N-methylpurine DNA glycosylase overexpression on chemosensitivity of human osteosarcoma cells]. Zhonghua Bing Li Xue Za Zhi 35: 352-356.

Wang, L., Z. Liu, L. Duan, B. Ma, and Z. Sun. 2015. [C1q tumor necrosis factor-related protein 6 (CTRP6) inhibits the proliferation and migration of ovarian cancer cells]. Xi Bao Yu Fen Zi Mian Yi Xue Za Zhi 31: 1664-1668.

Wang, X., X. Liu, A. Y. Li, L. Chen, L. Lai, H. H. Lin, S. Hu, L. Yao, J. Peng, S. Loera, L. Xue, B. Zhou, L. Zhou, S. Zheng, P. Chu, S. Zhang, D. K. Ann, and Y. Yen. 2011. Overexpression of HMGA2 promotes metastasis and impacts survival of colorectal cancers. Clinical cancer research : an official journal of the American Association for Cancer Research 17: 2570-2580.

Watanabe, S., Y. Ueda, S. Akaboshi, Y. Hino, Y. Sekita, and M. Nakao. 2009. HMGA2 maintains oncogenic RAS-induced epithelial-mesenchymal transition in human pancreatic cancer cells. The American journal of pathology 174: 854-868.

Way, S. A., and G. Leng. 1992. Relaxin increases the firing rate of supraoptic neurones and increases oxytocin secretion in the rat. J Endocrinol 132: 149-158.

Wei, Z., J. M. Peterson, and G. W. Wong. 2011. Metabolic regulation by C1q/TNF-related protein-13 (CTRP13): activation OF AMP-activated protein kinase and suppression of fatty acid-induced JNK signaling. The Journal of biological chemistry 286: 15652-15665.

Wei, Z., X. Lei, M. M. Seldin, and G. W. Wong. 2012. Endopeptidase cleavage generates a functionally distinct isoform of C1q/tumor necrosis factor-related protein-12 (CTRP12) with an altered oligomeric state and signaling specificity. The Journal of biological chemistry 287: 35804-35814.

Wei, Z., M. M. Seldin, N. Natarajan, D. C. Djemal, J. M. Peterson, and G. W. Wong. 2013. C1q/tumor necrosis factor-related protein 11 (CTRP11), a novel adipose stroma-derived regulator of adipogenesis. The Journal of biological chemistry 288: 10214-10229.

Weingart, M. F., J. J. Roth, M. Hutt-Cabezas, T. M. Busse, H. Kaur, A. Price, R. Maynard, J. Rubens, I. Taylor, X. G. Mao, J. Xu, Y. Kuwahara, S. J. Allen, A. Erdreich-Epstein, B. E. Weissman, B. A. Orr, C. G. Eberhart, J. A. Biegel, and E. H. Raabe. 2015. Disrupting LIN28 in atypical teratoid rhabdoid tumors reveals the importance of the mitogen activated protein kinase pathway as a therapeutic target. Oncotarget 6: 3165-3177.

Wen, P. Y., and S. Kesari. 2008. Malignant gliomas in adults. The New England journal of medicine 359: 492-507.

Wend, P., S. Runke, K. Wend, B. Anchondo, M. Yesayan, M. Jardon, N. Hardie, C. Loddenkemper, I. Ulasov, M. S. Lesniak, R. Wolsky, L. A. Bentolila, S. G. Grant, D. Elashoff, S. Lehr, J. J. Latimer, S. Bose, H. Sattar, S. A. Krum, and G. A. Miranda-Carboni. 2013. WNT10B/beta-catenin signalling induces HMGA2 and proliferation in metastatic triple-negative breast cancer. EMBO molecular medicine 5: 264-279.

Wong, G. W., J. Wang, C. Hug, T. S. Tsao, and H. F. Lodish. 2004. A family of Acrp30/adiponectin structural and functional paralogs. Proc Natl Acad Sci U S A 101: 10302-10307.

Wong, G. W., S. A. Krawczyk, C. Kitidis-Mitrokostas, T. Revett, R. Gimeno, and H. F. Lodish. 2008. Molecular, biochemical and functional characterizations of C1q/TNF family members: adipose-tissue-selective expression patterns, regulation by PPAR-gamma agonist, cysteine-mediated oligomerizations, combinatorial associations and metabolic functions. The Biochemical journal 416: 161-177.

Wong, G. W., S. A. Krawczyk, C. Kitidis-Mitrokostas, G. Ge, E. Spooner, C. Hug, R. Gimeno, and H. F. Lodish. 2009. Identification and characterization of CTRP9, a novel secreted glycoprotein, from adipose tissue that reduces serum glucose in mice and forms heterotrimers with adiponectin. FASEB journal : official publication of the Federation of American Societies for Experimental Biology 23: 241-258.

Wu, H., Y. Liang, L. Shen, and L. Shen. 2016a. MicroRNA-204 modulates colorectal cancer cell sensitivity in response to 5-fluorouracil-based treatment by targeting high mobility group protein A2. Biol Open 5: 563-570.

Wu, J., S. Li, W. Jia, H. Deng, K. Chen, L. Zhu, F. Yu, and F. Su. 2015a. Reduced Let-7a Is Associated with Chemoresistance in Primary Breast Cancer. PloS one 10: e0133643.

Wu, J., S. Zhang, J. Shan, Z. Hu, X. Liu, L. Chen, X. Ren, L. Yao, H. Sheng, L. Li, D. Ann, Y. Yen, J. Wang, and X. Wang. 2016b. Elevated HMGA2 expression is associated with cancer aggressiveness and predicts poor outcome in breast cancer. Cancer letters 376: 284-292.

Wu, Z., M. Eguchi-Ishimae, C. Yagi, H. Iwabuki, W. Gao, H. Tauchi, T. Inukai, K. Sugita, E. Ishii, and M. Eguchi. 2015b. HMGA2 as a potential molecular target in KMT2A-AFF1-positive infant acute lymphoblastic leukaemia. Br J Haematol 171: 818-829.

Wu, Z. Y., S. M. Wang, Z. H. Chen, S. X. Huv, K. Huang, B. J. Huang, J. L. Du, C. M. Huang, L. Peng, Z. X. Jian, and G. Zhao. 2015c. MiR-204 regulates HMGA2 expression and inhibits cell proliferation in human thyroid cancer. Cancer Biomark 15: 535-542.

Wurstle, M. L., E. Zink, J. H. Prehn, and M. Rehm. 2014. From computational modelling of the intrinsic apoptosis pathway to a systems-based analysis of chemotherapy resistance: achievements, perspectives and challenges in systems medicine. Cell Death Dis 5: e1258.

Xiao, J., C. Z. Chen, Z. Huang, I. U. Agoulnik, M. Ferrer, N. Southall, X. Hu, W. Zheng, A. I. Agoulnik, and J. J. Marugan. 2010. Discovery, optimization, and biological activity of the first potent and selective small-molecule agonist series of human relaxin receptor 1 (RXFP1), Probe Reports from the NIH Molecular Libraries Program, Bethesda (MD).

Xiao, J., Z. Huang, C. Z. Chen, I. U. Agoulnik, N. Southall, X. Hu, R. E. Jones, M. Ferrer, W. Zheng, A. I. Agoulnik, and J. J. Marugan. 2013. Identification and optimization of small-molecule agonists of the human relaxin hormone receptor RXFP1. Nat Commun 4: 1953.

Xipell, E., T. Aragon, N. Martinez-Velez, B. Vera, M. A. Idoate, J. J. Martinez-Irujo, A. G. Garzon, M. Gonzalez-Huarriz, A. M. Acanda, C. Jones, F. F. Lang, J. Fueyo, C. Gomez-Manzano, and M. M. Alonso. 2016. Endoplasmic reticulum stress-inducing drugs sensitize glioma cells to temozolomide through downregulation of MGMT, MPG, and Rad51. Neuro Oncol 18: 1109-1119.

Yan, H., D. W. Parsons, G. Jin, R. McLendon, B. A. Rasheed, W. Yuan, I. Kos, I. Batinic-Haberle, S. Jones, G. J. Riggins, H. Friedman, A. Friedman, D. Reardon, J. Herndon, K. W. Kinzler, V. E. Velculescu, B. Vogelstein, and D. D. Bigner. 2009. IDH1 and IDH2 mutations in gliomas. The New England journal of medicine 360: 765-773.

Yang, E., J. Cisowski, N. Nguyen, K. O'Callaghan, J. Xu, A. Agarwal, A. Kuliopulos, and L. Covic. 2016. Dysregulated protease activated receptor 1 (PAR1) promotes metastatic phenotype in breast cancer through HMGA2. Oncogene 35: 1529-1540.

Yang, S. H., K. S. Lee, H. J. Yang, B. H. Jeon, Y. S. Lee, S. W. Nam, D. S. Chung, S. W. Lee, and Y. K. Hong. 2012. O(6)-methylguanine-DNA-methyltransferase promoter methylation assessment by microdissection-assisted methylation-specific PCR and high resolution melting analysis in patients with glioblastomas. J Neurooncol 106: 243-250.

Yao, L., A. I. Agoulnik, P. S. Cooke, D. D. Meling, and O. D. Sherwood. 2008. Relaxin acts on stromal cells to promote epithelial and stromal proliferation and inhibit apoptosis in the mouse cervix and vagina. Endocrinology 149: 2072-2079.

Yao, L., A. I. Agoulnik, P. S. Cooke, D. D. Meling, and O. D. Sherwood. 2009. Relative roles of the epithelial and stromal tissue compartment(s) in mediating the actions of relaxin and estrogen on cell proliferation and apoptosis in the mouse lower reproductive tract. Annals of the New York Academy of Sciences 1160: 121-129.

Ye, X., and R. A. Weinberg. 2015. Epithelial-Mesenchymal Plasticity: A Central Regulator of Cancer Progression. Trends Cell Biol 25: 675-686.

Yeganeh, B., A. R. Moghadam, A. T. Tran, M. N. Rahim, S. R. Ande, M. Hashemi, K. M. Coombs, and S. Ghavami. 2013. Asthma and Influenza Virus Infection: Focusing on Cell Death and Stress Pathways in Influenza Virus Replication. Iranian Journal of Allergy, Asthma and Immunology 12: 1-17.

Yip, S., J. Miao, D. P. Cahill, A. J. Iafrate, K. Aldape, C. L. Nutt, and D. N. Louis. 2009. MSH6 mutations arise in glioblastomas during temozolomide therapy and mediate temozolomide resistance. Clinical cancer research : an official journal of the American Association for Cancer Research 15: 4622-4629.

Yoshimoto, K., M. Mizoguchi, N. Hata, H. Murata, R. Hatae, T. Amano, A. Nakamizo, and T. Sasaki. 2012. Complex DNA repair pathways as possible therapeutic targets to overcome temozolomide resistance in glioblastoma. Front Oncol 2: 186.

Zha, L., J. Zhang, W. Tang, N. Zhang, M. He, Y. Guo, and Z. Wang. 2013. HMGA2 elicits EMT by activating the Wnt/beta-catenin pathway in gastric cancer. Dig Dis Sci 58: 724-733.

Zhang, J., M. F. Stevens, and T. D. Bradshaw. 2012. Temozolomide: mechanisms of action, repair and resistance. Curr Mol Pharmacol 5: 102-114.

Zhang, J., L. Han, A. Zhang, Y. Wang, X. Yue, Y. You, P. Pu, and C. Kang. 2010. AKT2 expression is associated with glioma malignant progression and required for cell survival and invasion. Oncology reports 24: 65-72.

Zhang, P., C. Huang, C. Fu, Y. Tian, Y. Hu, B. Wang, A. Strasner, Y. Song, and E. Song. 2015. Cordycepin (3'-deoxyadenosine) suppressed HMGA2, Twist1 and ZEB1-dependent melanoma invasion and metastasis by targeting miR-33b. Oncotarget 6: 9834-9853.

Zhang, Q., S. H. Liu, M. Erikson, M. Lewis, and E. Unemori. 2002. Relaxin activates the MAP kinase pathway in human endometrial stromal cells. Journal of cellular biochemistry 85: 536-544.

Zhao, S., M. J. Kuenzi, and O. D. Sherwood. 1996. Monoclonal antibodies specific for rat relaxin. IX. Evidence that endogenous relaxin promotes growth of the vagina during the second half of pregnancy in rats. Endocrinology 137: 425-430.

Zhao, S., P. A. Fields, and O. D. Sherwood. 2001. Evidence that relaxin inhibits apoptosis in the cervix and the vagina during the second half of pregnancy in the rat. Endocrinology 142: 2221-2229.

Zhong, X., X. Liu, Y. Li, M. Cheng, W. Wang, K. Tian, L. Mu, T. Zeng, Y. Liu, X. Jiang, L. Yu, L. Gao, and Y. Zhou. 2016a. HMGA2 sustains self-renewal and invasiveness of glioma-initiating cells. Oncotarget 7: 44365-44380.

Zhong, X., X. Liu, Y. Li, M. Cheng, W. Wang, K. Tian, L. Mu, T. Zeng, Y. Liu, X. Jiang, L. Yu, L. Gao, and Y. Zhou. 2016b. HMGA2 sustains self-renewal and invasiveness of glioma-initiating cells. Oncotarget.

Zhong, Z., Z. Wen, and J. E. Darnell, Jr. 1994. Stat3: a STAT family member activated by tyrosine phosphorylation in response to epidermal growth factor and interleukin-6. Science 264: 95-98.

Zhou, X., K. F. Benson, H. R. Ashar, and K. Chada. 1995. Mutation responsible for the mouse pygmy phenotype in the developmentally regulated factor HMGI-C. Nature 376: 771-774.

Zhou, X., X. Chen, J. J. Cai, L. Z. Chen, Y. S. Gong, L. X. Wang, Z. Gao, H. Q. Zhang, W. J. Huang, and H. Zhou. 2015. Relaxin inhibits cardiac fibrosis and endothelial-mesenchymal transition via the Notch pathway. Drug Des Devel Ther 9: 4599-4611.

Zhuang, L., C. S. Lee, R. A. Scolyer, S. W. McCarthy, X. D. Zhang, J. F. Thompson, and P. Hersey. 2007. Mcl-1, Bcl-XL and Stat3 expression are associated with progression of melanoma whereas Bcl-2, AP-2 and MITF levels decrease during progression of melanoma. Mod Pathol 20: 416-426.

APPENDIX

JOHN WILEY AND SONS LICENSE TERMS AND CONDITIONS

Apr 18, 2017

This Agreement between Thatchawan Thanasupawat ("You") and John Wiley and Sons ("John Wiley and Sons") consists of your license details and the terms and conditions provided by John Wiley and Sons and Copyright Clearance Center.

License Number	4092200990663
License date	
Licensed Content Publisher	John Wiley and Sons
Licensed Content Publication	Journal of Pathology
Licensed Content Title	C1q-tumour necrosis factor-related protein 8 (CTRP8) is a novel interaction partner of relaxin receptor RXFP1 in human brain cancer cells
Licensed Content Author	Aleksandra Glogowska,Usakorn Kunanuvat,Jörg Stetefeld,Trushar R Patel,Thatchawan Thanasupawat,Jerry Krcek,Ekkehard Weber,G William Wong,Marc R Del Bigio,Cuong Hoang-Vu,Sabine Hombach-Klonisch,Thomas Klonisch
Licensed Content Date	Nov 12, 2013
Licensed Content Pages	14
Type of use	Dissertation/Thesis
Requestor type	Author of this Wiley article
Format	Print and electronic
Portion	Figure/table
Number of figures/tables	6
Original Wiley figure/table number(s)	Figure 1, 2, 4, 7, 8, 10
Will you be translating?	No
Title of your thesis / dissertation	Functional role of C1Q-TNF related peptide 8 (CTRP8)-binding RXFP1 in brain tumors
Expected completion date	Oct 2017
Expected size (number of pages)	200
Requestor Location	Thatchawan Thanasupawat [redacted] Winnipeg, MB [redacted] Canada Attn: Thatchawan Thanasupawat
Publisher Tax ID	EU826007151
Billing Type	Invoice
Billing Address	Thatchawan Thanasupawat [redacted]

Winnipeg, MB [redacted]
Canada
Attn: Thatchawan Thanasupawat

Total 0.00 USD

Terms and Conditions

TERMS AND CONDITIONS

This copyrighted material is owned by or exclusively licensed to John Wiley & Sons, Inc. or one of its group companies (each a"Wiley Company") or handled on behalf of a society with which a Wiley Company has exclusive publishing rights in relation to a particular work (collectively "WILEY"). By clicking "accept" in connection with completing this licensing transaction, you agree that the following terms and conditions apply to this transaction (along with the billing and payment terms and conditions established by the Copyright Clearance Center Inc., ("CCC's Billing and Payment terms and conditions"), at the time that you opened your RightsLink account (these are available at any time at http://myaccount.copyright.com).

Terms and Conditions

- The materials you have requested permission to reproduce or reuse (the "Wiley Materials") are protected by copyright.

- You are hereby granted a personal, non-exclusive, non-sub licensable (on a stand-alone basis), non-transferable, worldwide, limited license to reproduce the Wiley Materials for the purpose specified in the licensing process. This license, **and any CONTENT (PDF or image file) purchased as part of your order**, is for a one-time use only and limited to any maximum distribution number specified in the license. The first instance of republication or reuse granted by this license must be completed within two years of the date of the grant of this license (although copies prepared before the end date may be distributed thereafter). The Wiley Materials shall not be used in any other manner or for any other purpose, beyond what is granted in the license. Permission is granted subject to an appropriate acknowledgement given to the author, title of the material/book/journal and the publisher. You shall also duplicate the copyright notice that appears in the Wiley publication in your use of the Wiley Material. Permission is also granted on the understanding that nowhere in the text is a previously published source acknowledged for all or part of this Wiley Material. Any third party

content is expressly excluded from this permission.

- With respect to the Wiley Materials, all rights are reserved. Except as expressly granted by the terms of the license, no part of the Wiley Materials may be copied, modified, adapted (except for minor reformatting required by the new Publication), translated, reproduced, transferred or distributed, in any form or by any means, and no derivative works may be made based on the Wiley Materials without the prior permission of the respective copyright owner.**For STM Signatory Publishers clearing permission under the terms of the STM Permissions Guidelines only, the terms of the license are extended to include subsequent editions and for editions in other languages, provided such editions are for the work as a whole in situ and does not involve the separate exploitation of the permitted figures or extracts,** You may not alter, remove or suppress in any manner any copyright, trademark or other notices displayed by the Wiley Materials. You may not license, rent, sell, loan, lease, pledge, offer as security, transfer or assign the Wiley Materials on a stand-alone basis, or any of the rights granted to you hereunder to any other person.

- The Wiley Materials and all of the intellectual property rights therein shall at all times remain the exclusive property of John Wiley & Sons Inc, the Wiley Companies, or their respective licensors, and your interest therein is only that of having possession of and the right to reproduce the Wiley Materials pursuant to Section 2 herein during the continuance of this Agreement. You agree that you own no right, title or interest in or to the Wiley Materials or any of the intellectual property rights therein. You shall have no rights hereunder other than the license as provided for above in Section 2. No right, license or interest to any trademark, trade name, service mark or other branding ("Marks") of WILEY or its licensors is granted hereunder, and you agree that you shall not assert any such right, license or interest with respect thereto

- NEITHER WILEY NOR ITS LICENSORS MAKES ANY WARRANTY OR REPRESENTATION OF ANY KIND TO YOU OR ANY THIRD PARTY, EXPRESS, IMPLIED OR STATUTORY, WITH RESPECT TO THE MATERIALS OR THE ACCURACY OF ANY INFORMATION CONTAINED IN THE MATERIALS, INCLUDING, WITHOUT LIMITATION, ANY IMPLIED WARRANTY OF MERCHANTABILITY, ACCURACY,

SATISFACTORY QUALITY, FITNESS FOR A PARTICULAR PURPOSE, USABILITY, INTEGRATION OR NON-INFRINGEMENT AND ALL SUCH WARRANTIES ARE HEREBY EXCLUDED BY WILEY AND ITS LICENSORS AND WAIVED BY YOU.

- WILEY shall have the right to terminate this Agreement immediately upon breach of this Agreement by you.

- You shall indemnify, defend and hold harmless WILEY, its Licensors and their respective directors, officers, agents and employees, from and against any actual or threatened claims, demands, causes of action or proceedings arising from any breach of this Agreement by you.

- IN NO EVENT SHALL WILEY OR ITS LICENSORS BE LIABLE TO YOU OR ANY OTHER PARTY OR ANY OTHER PERSON OR ENTITY FOR ANY SPECIAL, CONSEQUENTIAL, INCIDENTAL, INDIRECT, EXEMPLARY OR PUNITIVE DAMAGES, HOWEVER CAUSED, ARISING OUT OF OR IN CONNECTION WITH THE DOWNLOADING, PROVISIONING, VIEWING OR USE OF THE MATERIALS REGARDLESS OF THE FORM OF ACTION, WHETHER FOR BREACH OF CONTRACT, BREACH OF WARRANTY, TORT, NEGLIGENCE, INFRINGEMENT OR OTHERWISE (INCLUDING, WITHOUT LIMITATION, DAMAGES BASED ON LOSS OF PROFITS, DATA, FILES, USE, BUSINESS OPPORTUNITY OR CLAIMS OF THIRD PARTIES), AND WHETHER OR NOT THE PARTY HAS BEEN ADVISED OF THE POSSIBILITY OF SUCH DAMAGES. THIS LIMITATION SHALL APPLY NOTWITHSTANDING ANY FAILURE OF ESSENTIAL PURPOSE OF ANY LIMITED REMEDY PROVIDED HEREIN.

- Should any provision of this Agreement be held by a court of competent jurisdiction to be illegal, invalid, or unenforceable, that provision shall be deemed amended to achieve as nearly as possible the same economic effect as the original provision, and the legality, validity and enforceability of the remaining provisions of this Agreement shall not be affected or impaired thereby.

- The failure of either party to enforce any term or condition of this Agreement shall not constitute a waiver of either party's right to

enforce each and every term and condition of this Agreement. No breach under this agreement shall be deemed waived or excused by either party unless such waiver or consent is in writing signed by the party granting such waiver or consent. The waiver by or consent of a party to a breach of any provision of this Agreement shall not operate or be construed as a waiver of or consent to any other or subsequent breach by such other party.

- This Agreement may not be assigned (including by operation of law or otherwise) by you without WILEY's prior written consent.
- Any fee required for this permission shall be non-refundable after thirty (30) days from receipt by the CCC.
- These terms and conditions together with CCC's Billing and Payment terms and conditions (which are incorporated herein) form the entire agreement between you and WILEY concerning this licensing transaction and (in the absence of fraud) supersedes all prior agreements and representations of the parties, oral or written. This Agreement may not be amended except in writing signed by both parties. This Agreement shall be binding upon and inure to the benefit of the parties' successors, legal representatives, and authorized assigns.
- In the event of any conflict between your obligations established by these terms and conditions and those established by CCC's Billing and Payment terms and conditions, these terms and conditions shall prevail.
- WILEY expressly reserves all rights not specifically granted in the combination of (i) the license details provided by you and accepted in the course of this licensing transaction, (ii) these terms and conditions and (iii) CCC's Billing and Payment terms and conditions.
- This Agreement will be void if the Type of Use, Format, Circulation, or Requestor Type was misrepresented during the licensing process.
- This Agreement shall be governed by and construed in accordance with the laws of the State of New York, USA, without regards to such state's conflict of law rules. Any legal action, suit or proceeding arising out of or relating to these Terms and Conditions or the breach thereof shall be instituted in a court of competent jurisdiction in New

York County in the State of New York in the United States of America and each party hereby consents and submits to the personal jurisdiction of such court, waives any objection to venue in such court and consents to service of process by registered or certified mail, return receipt requested, at the last known address of such party.

WILEY OPEN ACCESS TERMS AND CONDITIONS

Wiley Publishes Open Access Articles in fully Open Access Journals and in Subscription journals offering Online Open. Although most of the fully Open Access journals publish open access articles under the terms of the Creative Commons Attribution (CC BY) License only, the subscription journals and a few of the Open Access Journals offer a choice of Creative Commons Licenses. The license type is clearly identified on the article.

The Creative Commons Attribution License

The Creative Commons Attribution License (CC-BY) allows users to copy, distribute and transmit an article, adapt the article and make commercial use of the article. The CC-BY license permits commercial and non-

Creative Commons Attribution Non-Commercial License

The Creative Commons Attribution Non-Commercial (CC-BY-NC)License permits use, distribution and reproduction in any medium, provided the original work is properly cited and is not used for commercial purposes.(see below)

Creative Commons Attribution-Non-Commercial-NoDerivs License

The Creative Commons Attribution Non-Commercial-NoDerivs License (CC-BY-NC-ND) permits use, distribution and reproduction in any medium, provided the original work is properly cited, is not used for commercial purposes and no modifications or adaptations are made. (see below)

Use by commercial "for-profit" organizations

Use of Wiley Open Access articles for commercial, promotional, or marketing purposes requires further explicit permission from Wiley and will be subject to a fee.

Further details can be found on Wiley Online Library http://olabout.wiley.com/WileyCDA/Section/id-410895.html

Other Terms and Conditions:

v1.10 Last updated September 2015

Questions? customercare@copyright.com or +1-855-239-3415 (toll free in the US) or +1-978-646-2777.

JOHN WILEY AND SONS LICENSE TERMS AND CONDITIONS

Apr 18, 2017

This Agreement between Thatchawan Thanasupawat ("You") and John Wiley and Sons ("John Wiley and Sons") consists of your license details and the terms and conditions provided by John Wiley and Sons and Copyright Clearance Center.

License Number	4090011439494
License date	
Licensed Content Publisher	John Wiley and Sons
Licensed Content Publication	Annals of the New York Academy of Sciences
Licensed Content Title	Mechanisms of Relaxin Receptor (LGR7/RXFP1) Expression and Function
Licensed Content Author	András Kern,Gillian D. Bryant-Greenwood
Licensed Content Date	Apr 10, 2009
Licensed Content Pages	7
Type of use	Dissertation/Thesis
Requestor type	University/Academic
Format	Print and electronic
Portion	Figure/table
Number of figures/tables	1
Original Wiley figure/table number(s)	table 1
Will you be translating?	No
Title of your thesis / dissertation	Functional role of C1Q-TNF related peptide 8 (CTRP8)-binding RXFP1 in brain tumors
Expected completion date	Oct 2017
Expected size (number of pages)	200
Requestor Location	Thatchawan Thanasupawat [redacted] Winnipeg, MB [redacted] Canada Attn: Thatchawan Thanasupawat
Publisher Tax ID	EU826007151
Billing Type	Invoice
Billing Address	Thatchawan Thanasupawat [redacted] Winnipeg, MB [redacted]

Canada
Attn: Thatchawan Thanasupawat

Total 0.00 USD

Terms and Conditions

TERMS AND CONDITIONS

This copyrighted material is owned by or exclusively licensed to John Wiley & Sons, Inc. or one of its group companies (each a"Wiley Company") or handled on behalf of a society with which a Wiley Company has exclusive publishing rights in relation to a particular work (collectively "WILEY"). By clicking "accept" in connection with completing this licensing transaction, you agree that the following terms and conditions apply to this transaction (along with the billing and payment terms and conditions established by the Copyright Clearance Center Inc., ("CCC's Billing and Payment terms and conditions"), at the time that you opened your RightsLink account (these are available at any time at http://myaccount.copyright.com).

Terms and Conditions

- The materials you have requested permission to reproduce or reuse (the "Wiley Materials") are protected by copyright.

- You are hereby granted a personal, non-exclusive, non-sub licensable (on a stand-alone basis), non-transferable, worldwide, limited license to reproduce the Wiley Materials for the purpose specified in the licensing process. This license, **and any CONTENT (PDF or image file) purchased as part of your order**, is for a one-time use only and limited to any maximum distribution number specified in the license. The first instance of republication or reuse granted by this license must be completed within two years of the date of the grant of this license (although copies prepared before the end date may be distributed thereafter). The Wiley Materials shall not be used in any other manner or for any other purpose, beyond what is granted in the license. Permission is granted subject to an appropriate acknowledgement given to the author, title of the material/book/journal and the publisher. You shall also duplicate the copyright notice that appears in the Wiley publication in your use of the Wiley Material. Permission is also granted on the understanding that nowhere in the text is a previously published source acknowledged for all or part of this Wiley Material. Any third party content is expressly excluded from this permission.

- With respect to the Wiley Materials, all rights are reserved. Except as expressly granted by the terms of the license, no part of the Wiley Materials may be copied, modified, adapted (except for minor reformatting required by the new Publication), translated, reproduced, transferred or distributed, in any form or by any means, and no derivative works may be made based on the Wiley Materials without the prior permission of the respective copyright owner.**For STM Signatory Publishers clearing permission under the terms of the STM Permissions Guidelines only, the terms of the license are extended to include subsequent editions and for editions in other languages, provided such editions are for the work as a whole in situ and does not involve the separate exploitation of the permitted figures or extracts,** You may not alter, remove or suppress in any manner any copyright, trademark or other notices displayed by the Wiley Materials. You may not license, rent, sell, loan, lease, pledge, offer as security, transfer or assign the Wiley Materials on a stand-alone basis, or any of the rights granted to you hereunder to any other person.

- The Wiley Materials and all of the intellectual property rights therein shall at all times remain the exclusive property of John Wiley & Sons Inc, the Wiley Companies, or their respective licensors, and your interest therein is only that of having possession of and the right to reproduce the Wiley Materials pursuant to Section 2 herein during the continuance of this Agreement. You agree that you own no right, title or interest in or to the Wiley Materials or any of the intellectual property rights therein. You shall have no rights hereunder other than the license as provided for above in Section 2. No right, license or interest to any trademark, trade name, service mark or other branding ("Marks") of WILEY or its licensors is granted hereunder, and you agree that you shall not assert any such right, license or interest with respect thereto

- NEITHER WILEY NOR ITS LICENSORS MAKES ANY WARRANTY OR REPRESENTATION OF ANY KIND TO YOU OR ANY THIRD PARTY, EXPRESS, IMPLIED OR STATUTORY, WITH RESPECT TO THE MATERIALS OR THE ACCURACY OF ANY INFORMATION CONTAINED IN THE MATERIALS, INCLUDING, WITHOUT LIMITATION, ANY IMPLIED WARRANTY OF MERCHANTABILITY, ACCURACY, SATISFACTORY QUALITY, FITNESS FOR A PARTICULAR PURPOSE, USABILITY, INTEGRATION OR NON-

INFRINGEMENT AND ALL SUCH WARRANTIES ARE HEREBY EXCLUDED BY WILEY AND ITS LICENSORS AND WAIVED BY YOU.

- WILEY shall have the right to terminate this Agreement immediately upon breach of this Agreement by you.
- You shall indemnify, defend and hold harmless WILEY, its Licensors and their respective directors, officers, agents and employees, from and against any actual or threatened claims, demands, causes of action or proceedings arising from any breach of this Agreement by you.
- IN NO EVENT SHALL WILEY OR ITS LICENSORS BE LIABLE TO YOU OR ANY OTHER PARTY OR ANY OTHER PERSON OR ENTITY FOR ANY SPECIAL, CONSEQUENTIAL, INCIDENTAL, INDIRECT, EXEMPLARY OR PUNITIVE DAMAGES, HOWEVER CAUSED, ARISING OUT OF OR IN CONNECTION WITH THE DOWNLOADING, PROVISIONING, VIEWING OR USE OF THE MATERIALS REGARDLESS OF THE FORM OF ACTION, WHETHER FOR BREACH OF CONTRACT, BREACH OF WARRANTY, TORT, NEGLIGENCE, INFRINGEMENT OR OTHERWISE (INCLUDING, WITHOUT LIMITATION, DAMAGES BASED ON LOSS OF PROFITS, DATA, FILES, USE, BUSINESS OPPORTUNITY OR CLAIMS OF THIRD PARTIES), AND WHETHER OR NOT THE PARTY HAS BEEN ADVISED OF THE POSSIBILITY OF SUCH DAMAGES. THIS LIMITATION SHALL APPLY NOTWITHSTANDING ANY FAILURE OF ESSENTIAL PURPOSE OF ANY LIMITED REMEDY PROVIDED HEREIN.
- Should any provision of this Agreement be held by a court of competent jurisdiction to be illegal, invalid, or unenforceable, that provision shall be deemed amended to achieve as nearly as possible the same economic effect as the original provision, and the legality, validity and enforceability of the remaining provisions of this Agreement shall not be affected or impaired thereby.
- The failure of either party to enforce any term or condition of this Agreement shall not constitute a waiver of either party's right to enforce each and every term and condition of this Agreement. No breach under this agreement shall be deemed waived or excused by

either party unless such waiver or consent is in writing signed by the party granting such waiver or consent. The waiver by or consent of a party to a breach of any provision of this Agreement shall not operate or be construed as a waiver of or consent to any other or subsequent breach by such other party.

- This Agreement may not be assigned (including by operation of law or otherwise) by you without WILEY's prior written consent.
- Any fee required for this permission shall be non-refundable after thirty (30) days from receipt by the CCC.
- These terms and conditions together with CCC's Billing and Payment terms and conditions (which are incorporated herein) form the entire agreement between you and WILEY concerning this licensing transaction and (in the absence of fraud) supersedes all prior agreements and representations of the parties, oral or written. This Agreement may not be amended except in writing signed by both parties. This Agreement shall be binding upon and inure to the benefit of the parties' successors, legal representatives, and authorized assigns.
- In the event of any conflict between your obligations established by these terms and conditions and those established by CCC's Billing and Payment terms and conditions, these terms and conditions shall prevail.
- WILEY expressly reserves all rights not specifically granted in the combination of (i) the license details provided by you and accepted in the course of this licensing transaction, (ii) these terms and conditions and (iii) CCC's Billing and Payment terms and conditions.
- This Agreement will be void if the Type of Use, Format, Circulation, or Requestor Type was misrepresented during the licensing process.
- This Agreement shall be governed by and construed in accordance with the laws of the State of New York, USA, without regards to such state's conflict of law rules. Any legal action, suit or proceeding arising out of or relating to these Terms and Conditions or the breach thereof shall be instituted in a court of competent jurisdiction in New York County in the State of New York in the United States of America and each party hereby consents and submits to the personal

jurisdiction of such court, waives any objection to venue in such court and consents to service of process by registered or certified mail, return receipt requested, at the last known address of such party.

WILEY OPEN ACCESS TERMS AND CONDITIONS

Wiley Publishes Open Access Articles in fully Open Access Journals and in Subscription journals offering Online Open. Although most of the fully Open Access journals publish open access articles under the terms of the Creative Commons Attribution (CC BY) License only, the subscription journals and a few of the Open Access Journals offer a choice of Creative Commons Licenses. The license type is clearly identified on the article.

The Creative Commons Attribution License

The Creative Commons Attribution License (CC-BY) allows users to copy, distribute and transmit an article, adapt the article and make commercial use of the article. The CC-BY license permits commercial and non-

Creative Commons Attribution Non-Commercial License

The Creative Commons Attribution Non-Commercial (CC-BY-NC)License permits use, distribution and reproduction in any medium, provided the original work is properly cited and is not used for commercial purposes.(see below)

Creative Commons Attribution-Non-Commercial-NoDerivs License

The Creative Commons Attribution Non-Commercial-NoDerivs License (CC-BY-NC-ND) permits use, distribution and reproduction in any medium, provided the original work is properly cited, is not used for commercial purposes and no modifications or adaptations are made. (see below)

Use by commercial "for-profit" organizations

Use of Wiley Open Access articles for commercial, promotional, or marketing purposes requires further explicit permission from Wiley and will be subject to a fee.

Further details can be found on Wiley Online Library http://olabout.wiley.com/WileyCDA/Section/id-410895.html

Other Terms and Conditions:

v1.10 Last updated September 2015

Questions? customercare@copyright.com or +1-855-239-3415 (toll free in the US) or +1-978-646-2777.

SPRINGER LICENSE
TERMS AND CONDITIONS

Apr 18, 2017

This Agreement between Thatchawan Thanasupawat ("You") and Springer ("Springer") consists of your license details and the terms and conditions provided by Springer and Copyright Clearance Center.

License Number	4090021164557
License date	
Licensed Content Publisher	Springer
Licensed Content Publication	Acta Neuropathologica
Licensed Content Title	The 2016 World Health Organization Classification of Tumors of the Central Nervous System: a summary
Licensed Content Author	David N. Louis
Licensed Content Date	Jan 1, 2016
Licensed Content Volume	131
Licensed Content Issue	6
Type of Use	Thesis/Dissertation
Portion	Figures/tables/illustrations
Number of figures/tables/illustrations	1
Author of this Springer article	No
Order reference number	
Original figure numbers	figure 1
Title of your thesis / dissertation	Functional role of C1Q-TNF related peptide 8 (CTRP8)-binding RXFP1 in brain tumors
Expected completion date	Oct 2017
Estimated size(pages)	200
Requestor Location	Thatchawan Thanasupawat [redacted] Winnipeg, MB [redacted] Canada Attn: Thatchawan Thanasupawat
Billing Type	Invoice
Billing Address	Thatchawan Thanasupawat [redacted] Winnipeg, MB [redacted] Canada Attn: Thatchawan Thanasupawat
Total	0.00 USD
Terms and Conditions	

Introduction

The publisher for this copyrighted material is Springer. By clicking "accept" in connection with completing this licensing transaction, you agree that the following terms and conditions apply to this transaction (along with the Billing and Payment terms and conditions established by Copyright Clearance Center, Inc. ("CCC"), at the time that you opened your Rightslink account and that are available at any time at http://myaccount.copyright.com).

Limited License

With reference to your request to reuse material on which Springer controls the copyright, permission is granted for the use indicated in your enquiry under the following conditions:

- Licenses are for one-time use only with a maximum distribution equal to the number stated in your request.
- Springer material represents original material which does not carry references to other sources. If the material in question appears with a credit to another source, this permission is not valid and authorization has to be obtained from the original copyright holder.
- This permission
• is non-exclusive
• is only valid if no personal rights, trademarks, or competitive products are infringed.
• explicitly excludes the right for derivatives.
- Springer does not supply original artwork or content.
- According to the format which you have selected, the following conditions apply accordingly:
• **Print and Electronic:** This License include use in electronic form provided it is password protected, on intranet, or CD-Rom/DVD or E-book/E-journal. It may not be republished in electronic open access.
• **Print:** This License excludes use in electronic form.
• **Electronic:** This License only pertains to use in electronic form provided it is password protected, on intranet, or CD-Rom/DVD or E-book/E-journal. It may not be republished in electronic open access.
For any electronic use not mentioned, please contact Springer at permissions.springer@spi-global.com.
- Although Springer controls the copyright to the material and is entitled to negotiate on rights, this license is only valid subject to courtesy information to the author (address is given in the article/chapter).
- If you are an STM Signatory or your work will be published by an STM Signatory and you are requesting to reuse figures/tables/illustrations or single text extracts, permission is granted according to STM Permissions

Guidelines: http://www.stm-assoc.org/permissions-guidelines/
For any electronic use not mentioned in the Guidelines, please contact Springer at permissions.springer@spi-global.com. If you request to reuse more content than stipulated in the STM Permissions Guidelines, you will be charged a permission fee for the excess content.
Permission is valid upon payment of the fee as indicated in the licensing process. If permission is granted free of charge on this occasion, that does not prejudice any rights we might have to charge for reproduction of our copyrighted material in the future.
-If your request is for reuse in a Thesis, permission is granted free of charge under the following conditions:
This license is valid for one-time use only for the purpose of defending your thesis and with a maximum of 100 extra copies in paper. If the thesis is going to be published, permission needs to be reobtained.
- includes use in an electronic form, provided it is an author-created version of the thesis on his/her own website and his/her university's repository, including UMI (according to the definition on the Sherpa website: http://www.sherpa.ac.uk/romeo/);
- is subject to courtesy information to the co-author or corresponding author.
Geographic Rights: Scope
Licenses may be exercised anywhere in the world.
Altering/Modifying Material: Not Permitted
Figures, tables, and illustrations may be altered minimally to serve your work. You may not alter or modify text in any manner. Abbreviations, additions, deletions and/or any other alterations shall be made only with prior written authorization of the author(s).
Reservation of Rights
Springer reserves all rights not specifically granted in the combination of (i) the license details provided by you and accepted in the course of this licensing transaction and (ii) these terms and conditions and (iii) CCC's Billing and Payment terms and conditions.
License Contingent on Payment
While you may exercise the rights licensed immediately upon issuance of the license at the end of the licensing process for the transaction, provided that you have disclosed complete and accurate details of your proposed use, no license is finally effective unless and until full payment is received from you (either by Springer or by CCC) as provided in CCC's Billing and Payment terms and conditions. If full payment is not received by the date due, then any license preliminarily granted shall be deemed automatically revoked and shall be void as if never granted. Further, in the event that you breach any of these terms and conditions or any of CCC's

Billing and Payment terms and conditions, the license is automatically revoked and shall be void as if never granted. Use of materials as described in a revoked license, as well as any use of the materials beyond the scope of an unrevoked license, may constitute copyright infringement and Springer reserves the right to take any and all action to protect its copyright in the materials.

Copyright Notice: Disclaimer

You must include the following copyright and permission notice in connection with any reproduction of the licensed material:
"Springer book/journal title, chapter/article title, volume, year of publication, page, name(s) of author(s), (original copyright notice as given in the publication in which the material was originally published)
"With permission of Springer"

In case of use of a graph or illustration, the caption of the graph or illustration must be included, as it is indicated in the original publication.

Warranties: None

Springer makes no representations or warranties with respect to the licensed material and adopts on its own behalf the limitations and disclaimers established by CCC on its behalf in its Billing and Payment terms and conditions for this licensing transaction.

Indemnity

You hereby indemnify and agree to hold harmless Springer and CCC, and their respective officers, directors, employees and agents, from and against any and all claims arising out of your use of the licensed material other than as specifically authorized pursuant to this license.

No Transfer of License

This license is personal to you and may not be sublicensed, assigned, or transferred by you without Springer's written permission.

No Amendment Except in Writing

This license may not be amended except in a writing signed by both parties (or, in the case of Springer, by CCC on Springer's behalf).

Objection to Contrary Terms

Springer hereby objects to any terms contained in any purchase order, acknowledgment, check endorsement or other writing prepared by you, which terms are inconsistent with these terms and conditions or CCC's Billing and Payment terms and conditions. These terms and conditions, together with CCC's Billing and Payment terms and conditions (which are incorporated herein), comprise the entire agreement between you and Springer (and CCC) concerning this licensing transaction. In the event of any conflict between your obligations established by these terms and conditions and those established by CCC's Billing and Payment terms and conditions, these terms and conditions shall control.

Jurisdiction

All disputes that may arise in connection with this present License, or the breach thereof, shall be settled exclusively by arbitration, to be held in the Federal Republic of Germany, in accordance with German law.

Other conditions:

V 12AUG2015

AMERICAN ASSOCIATION FOR CANCER RESEARCH LICENSE TERMS AND CONDITIONS

Apr 18, 2017

This Agreement between Thatchawan Thanasupawat ("You") and American Association for Cancer Research ("American Association for Cancer Research") consists of your license details and the terms and conditions provided by American Association for Cancer Research and Copyright Clearance Center.

License Number	4090021345640
License date	
Licensed Content Publisher	American Association for Cancer Research
Licensed Content Publication	Clinical Cancer Research
Licensed Content Title	The Definition of Primary and Secondary Glioblastoma
Licensed Content Author	Hiroko Ohgaki,Paul Kleihues
Licensed Content Date	2013-02-15
Licensed Content Volume	19
Licensed Content Issue	4
Type of Use	Thesis/Dissertation
Requestor type	academic/educational
Format	print and electronic
Portion	figures/tables/illustrations
Number of figures/tables/illustrations	1
Will you be translating?	no
Circulation	6
Territory of distribution	Worldwide
Title of your thesis / dissertation	Functional role of C1Q-TNF related peptide 8 (CTRP8)-binding RXFP1 in brain tumors
Expected completion date	Oct 2017
Estimated size (number of pages)	200
Requestor Location	Thatchawan Thanasupawat [redacted] Winnipeg, MB [redacted] Canada Attn: Thatchawan Thanasupawat
Billing Type	Invoice
Billing Address	Thatchawan Thanasupawat [redacted]

Winnipeg, MB [redacted]
Canada
Attn: Thatchawan Thanasupawat

Total 0.00 USD

Terms and Conditions

American Association for Cancer Research (AACR) Terms and Conditions

INTRODUCTION

The Publisher for this copyright material is the American Association for Cancer Research (AACR). By clicking "accept" in connection with completing this licensing transaction, you agree to the following terms and conditions applying to this transaction. You also agree to the Billing and Payment terms and conditions established by Copyright Clearance Center (CCC) at the time you opened your Rightslink account.

LIMITED LICENSE

The AACR grants exclusively to you, the User, for onetime, non-exclusive use of this material for the purpose stated in your request and used only with a maximum distribution equal to the number you identified in the permission process. Any form of republication must be completed within one year although copies made before then may be distributed thereafter and any electronic posting is limited to a period of one year. Reproduction of this material is confined to the purpose and/or media for which permission is granted. Altering or modifying this material is not permitted. However, figures and illustrations may be minimally altered or modified to serve the new work.

GEOGRAPHIC SCOPE

Licenses may be exercised as noted in the permission process

RESERVATION OF RIGHTS

The AACR reserves all rights not specifically granted in the combination of 1) the license details provided by you and accepted in the course of this licensing transaction, 2) these terms and conditions , and 3) CCC's Billing and Payment terms and conditions.

DISCLAIMER

You may obtain permission via Rightslink to use material owned by AACR. When you are requesting permission to reuse a portion for an AACR publication, it is your responsibility to examine each portion of content as published to determine whether a credit to, or copyright notice of a third party owner is published next to the item. You must obtain permission from the third party to use any material which has been reprinted with permission from the said third party. If you have not obtained permission from the third party, AACR disclaims any responsibility for the use you make of items owned by them.

LICENSE CONTINGENT ON PAYMENT

While you may exercise the rights licensed immediately upon issuance of the license at the end of the licensing process for the transaction, provided that you have disclosed complete and accurate details of your proposed use, no license is finally effective unless and until full payment is received from you, either by the publisher or by the CCC, as provided in CCC's Billing and Payment terms and conditions. If full payment is not received on a timely basis, then any license preliminarily granted shall be deemed automatically revoked and shall be void as if never granted. Further, in the event that you breach any of these terms and conditions, or any of the CCC's Billing and Payment terms and conditions, the license is automatically revoked and shall be void as if never granted. Use of materials as described in a revoked license, as well as any use of the materials beyond the scope of an unrevoked license, may constitute copyright infringement and the publisher reserves the right to take any and all action to protect its copyright in the materials.

COPYRIGHT NOTICE

You must include the following credit line in connection with your reproduction of the licensed material: "Reprinted (or adapted) from Publication Title, Copyright Year, Volume/Issue, Page Range, Author, Title of Article, with permission from AACR".

TRANSLATION

This permission is granted for non-exclusive world English rights only.

WARRANTIES

Publisher makes no representations or warranties with respect to the licensed material.

INDEMNIFICATION

You hereby indemnify and agree to hold harmless the publisher and CCC, and their respective officers, directors, employees and agents, from and against any and all claims arising out of your use of the licensed material other than as specifically authorized pursuant to this license.

REVOCATION

The AACR reserves the right to revoke a license for any reason, including but not limited to advertising and promotional uses of AACR content, third party usage and incorrect figure source attribution.

NO TRANSFER OF LICENSE

This license is personal to you and may not be sublicensed, assigned, or transferred by you to any other person without publisher's written permission.

NO AMENDMENT EXCEPT IN WRITING

This license may not be amended except in a writing signed by both parties (or, in the case of publisher, by CCC on publisher's behalf).

OBJECTION TO CONTRARY TERMS

Publishers hereby objects to any terms contained in any purchase order, acknowledgement, check endorsement or other writing prepared by you, which terms are inconsistent with these terms and conditions or CCC's Billing and Payment terms and conditions. These terms and conditions together with CCC's Billing and Payment terms and conditions (which are incorporated herein) comprise the entire agreement between you and publisher (and CCC) concerning this licensing transaction. In the event of any conflict between your obligations established by these terms and conditions, and those established by CCC's Billing and Payment terms and conditions, these terms and conditions shall control.

THESIS/DISSERTATION TERMS

If your request is to reuse an article authored by you and published by the AACR in your dissertation/thesis, your thesis may be submitted to your institution in either in print or electronic form. Should your thesis be published commercially, please reapply.

ELECTRONIC RESERVE

If this license is made in connection with a course, and the Licensed Material or any portion thereof is to be posted to a website, the website is to be password protected and made available only to the students registered for the relevant course. The permission is granted for the duration of the course. All content posted to the website must maintain the copyright information notice.

JURISDICTION

This license transaction shall be governed by and construed in accordance with the laws of Pennsylvania. You hereby agree to submit to the jurisdiction of the federal and state courts located in Pennsylvania for purposes of resolving any disputes that may arise in connection with this licensing transaction.

Other Terms and Conditions:

v1.0